CRIWI

Research Institute of Wood Industry

ITTO

International Tropical Timber Organization

Guide on Utilization of Eucalyptus and Acacia Plantations in China for Solid Wood Products

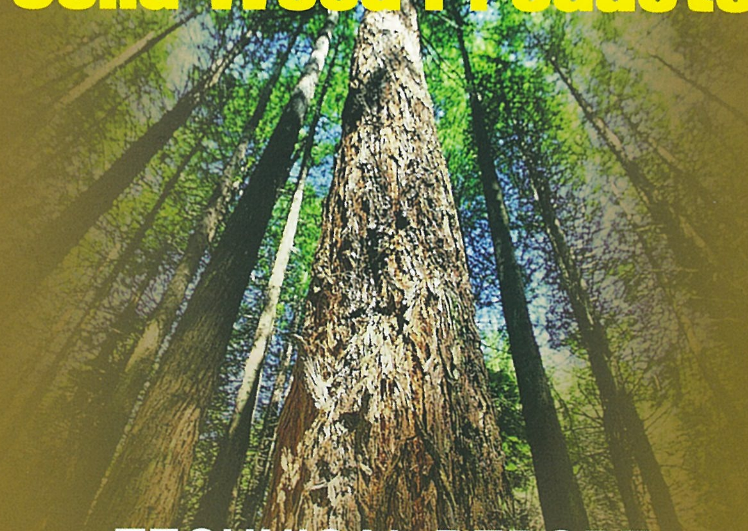

TECHNICAL REPORT

ITTO PROJECT PD 69/01 REV.2 (I)

Improved and Diversified Use of Tropical Plantation Timbers in China to Supplement Diminishing Supplies from Natural Forests

Research Institute of Wood Industry
Chinese Academy of Forestry
Sept. 2006 Beijing

CRIWI

Research Institute of Wood Industry

International Tropical Timber Organization

Guide on Utilization of Eucalyptus and Acacia Plantations in China for Solid Wood Products

TECHNICAL REPORT

ITTO PROJECT PD 69/01 REV.2 (I)

Improved and Diversified Use of Tropical Plantation Timbers in China to Supplement Diminishing Supplies from Natural Forests

Research Institute of Wood Industry

Chinese Academy of Forestry

Sept. 2006 Beijing

TABLE OF CONTENTS

I *Eucalyptus citriodora*

The information of testing materials is as Tab.1.

Tab.1 Testing materials

Tree species	Tree age (year)	Tree number	Tree height (m)		Under branch height (m)		DBH (cm)	
			Ave.	Std	Ave.	Std.	Ave.	Std
Eucalyptus citriodor	37	10	30.67	1.2455	16.57	3.1816	28.68	1.9395

1 WOOD PROPERTIES

1.1 Anatomical characteristics

Samples (2x2x1 cm) for wood anatomical section were stored in alcohol 95% : glycerine (1:1) until they sank. Transverse sections of 20μm were cut on sliding microtome, then bleached, stained with safranin, dehydrated and mounted on slides for measure anatomical properties on image analysis. Then the transverse, radial and tangential sections from each species of around 80μm were cut on the same microtome, make the samples for SEM observation and taking photos.

Prior to tracheid length measurement, the each selected growth rings were firstly separated with a chisel, then macerated in solution of acetic acid (1/3) and hydrogen peroxide 27% (2/3) for several days in 60° oven.

The measurement methods are as follows:

Measuring length and width of wood fiber and vessel element using macerated anatomical elements under fiber length measuring instrument; (2) Measuring wood fiber cell wall thickness, cell wall percentage, and tissue proportions by section method using image analysis system; (3) Measure of S_2 microfibril angle: using x-ray diffractometer.

The observation and description for macro- and micro-structure were made under the light microscope and scanning electronically microscope (SEM).

1.1.1 Tree and distribution

Evergreen a tree up to 30-40 m, 0.6-1.2 m in d.b.h., trunk straight in origin producing country. Bark grey white or light blue to light green, smooth, peeling off in long strips on old tree. It naturally distributed in C N of E Queensland in Australia. *Eucalyptus citriodora* as planted species introduced into many countries in the world. Guangdong, Guangxi, Sichuan, Zhejiang, Hunan, Yunnan etc from 60 decades in 20 century.

1.1.2 General characteristics

Sapwood yellowish brown or gray brown, distinctly differs from heartwood, width 2~3cm; ***heartwood*** dark yellowish brown or reddish brown; glossy, wood without characteristic taste & odor. ***Growth rings*** little distinct, delineated by a darker band. Wood diffuse-porous. Pores small to middle, radial or flexuous, visible to the naked eye, fairly uniformly distributed throughout the ring, with tyloses. ***Longitudinal parenchyma*** vasicentric & banded. ***Rays*** very fine to fine, visible with a hand lens; ***Ripple mark***s and ***Resin canals*** absent with visible reddish brown lines of the Kino veins.

1.1.3 *Minute anatomy* (Plane I)

Vessels in radial multiples of 2-3 & cluster, few solitary, radial or flexuous; cell wall thin to thick; tangential average diameter 120μm, max 211μm. 8(5~11) /mm^2 . Vessel element length 370 (190~560) μm, tyloses abundant, special tyloses wall thick in heartwood, some including crystals, part vessels plugging up; helical thickness absent. Simple perforation, its plate oblique. Intervessel pits ventured, alternate, round. Vasicentrics located vessels intermixing parenchyma cells, with bordered pit round and ventured. Vessel- ray pits large round, a few gash-like.

Longitudinal parenchyma vasicentric, diffuse or diffuse-aggregates. Nodular end wall of parenchyma cells inconspicuous; prismatic crystals commonly in parenchyma cells.

Fiber wall thick to very thick, 1260 (1249~1273) μm in length, with plain simple pits.

Rays unstoried, rays 9~11/mm, multiseriate rays width 2 cells, height 15~26 cells, uniseriate rays 1~16 cells. Ray tissues homogeneous uniseriate and multiseriate; parenchyma cells round or oval, some with gum. Crystal and intercellular canals absent.

The data of anatomical parameter and basic density at different heights is including to the Tab.1.1-1, the vessel distribution frequencies and tangential diameters are listed in Tab.1.1-2.

Tab.1.1-1 Anatomical parameter and basic density at different heights for *Eucalyptus citriodora*

Item	1.3m		3.3m		5.3m		7.3m	
	$\bar{x}$	δ_n	$\bar{x}$	δ_n	$\bar{x}$	δ_n	$\bar{x}$	δ_n
Fiber length (μm)	1273	26	1270	51	1251	40	1249	70
Fiber width (μm)	15.4	1.0	15.0	0.5	15.4	0.6	15.5	0.7
Fiber wall thickness (μm)	12.28	0.3355	11.84	0.5694	12.88	0.6226	12.30	0.6894
Microfibril angle (°)	9.37	0.512	9.03	0.736	9.13	0.388	9.11	0.579
Basic density (g/cm^3)	0.808	0.035	0.793	0.026	0.776	0.023	0.785	0.019

Tab.1.1-2 Vessel distribution frequencies and tangential diameters

Vessel distribution frequency (Number/mm^2)				Vessel tangential diameter (μm)			
Ave.	Std.	Max.	Min.	Ave.	Std.	Max.	Min.
7.97	2.3710	11.80	5.20	119.54	41.2107	211.01	37.20

1.2 Physical properties

1.2.1 *Moisture content of the green wood*

The moisture content data of the green wood at different tree heights and radial sites is including Tab.1.2-1 and Fig.1.2-1.

Tab.1.2-1 Moisture content of *E. citriodora* green wood at different tree heights and different radial sites (%)

Sites (from pith to bark)	Tree height (m)							
	1.3		3.3		5.3		7.3	
	Ave.	Std.	Ave.	Std.	Ave.	Std.	Ave.	Std.
1	66.25	9.81	61.44	9.56	57.83	8.33	54.73	8.65
2	58.94	5.14	54.44	8.95	57.02	11.22	49.87	7.10
3	49.08	3.56	42.05	21.26	47.71	6.76	56.81	22.97
4	44.74	3.84	42.20	11.60	42.18	8.20	42.10	5.97
5	46.60	8.18	43.45	14.76	54.88	4.39	54.20	12.03

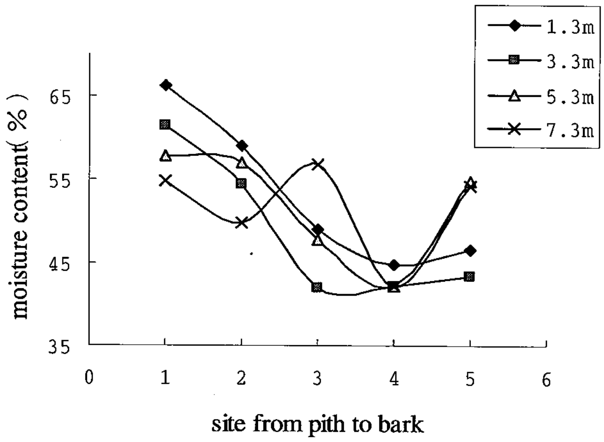

Fig.1.2-1 Variation in moisture content of E. citriodora green wood at different tree heights and different radial sites

1.2.2 Shrinkage and Density

Shrinkage is the contraction of wood caused by drying the material below the fibre saturation point (William T. Simpson, 1991). It can be divided into 3 types of shrinkage according to the direction of contraction: longitudinal, radial and tangential shrinkage. The longitudinal shrinkage is the shrinkage along the grain, the radial shrinkage and the tangential shrinkage is that across the grain in a radial or in a tangential direction. Wood density, the weight of wood per unit volume, is a very important index having a close relation with wood mechanical strength. In this study, wood air-dried density and basic density were used to describe the wood density.

The shrinkage is attributed to the dimension stability and checking problem, which causes a lot of problem for the wood utilization. In another word, it causes not only the contraction of wood in size, but also the checking and deformation resulted from the different contraction in tangential, radial and longitudinal direction. Understanding the characteristics of shrinkage has no doubt to be helpful for the wood utilization for the wood industry practice. Nowadays, studying on the characteristics of shrinkage during the losing of water is becoming one of the wood science discipline[Barber NF etc.1964; Barber, 1968; Chafe, 1986; 1987; Gu H et al., 2001]。 This study is intended to explore the shrinkage variation of acacia in different direction (North and south), different radial position and different tree height.

The trees studied were cut from Guangxi Zhuang Autonomous Region in the South China. Each trunk has been collected above the breast height and was cut every 2 meters. Then, four discs of each tree at different heights (about 1.3m, 3.3m, 5.3m and 7.3m respectively) were taken from the logs. All the discs were marked the south-north direction. For each disc, one specimen from the sapwood near the bark, one from the heartwood near pith and one from transition zone was made at the size of 2X2X2cm (Tangential X radial X longitudinal direction) for both north side and south side.

Two diagonal lines were drawn in three sections (i.e., T×R, T×L, R×L) of each specimen to locate the central point where the size was measured. The specimens were put into water until they were totally saturated and sunk in the water. The surface water was wiped off and the sizes in three directions (L, R, T) were measured. Specimens were set in the room for air-drying. After measuring the size and weight at the air-dried stage, the specimens were oven-dried and the same measurement was carried out. The shrinkage was determined according to Chinese National Standard. The air-dried density and was also calculated of both air-dried

The shrinkage coefficient was determined by the difference between shrinkage at air-dried and at oven-dried and divided by the MC at air-dried.

1.2.2.1 Shrinkage and density, and that of wood from south and north directions

The air-dried shrinkage in tangential direction (Ta), Radial direction (Ra) and volumetric shrinkage (Va), as well as the oven-dried shrinkage in tangential direction (To), Radial direction (Ro) and volumetric shrinkage (Vo) are listed in Tab.1.2-2 according to the categories of south direction, north direction and the overall. The basic density (B D) and air-dried density (A D), together with tangential shrinkage coefficient and radial shrinkage coefficient were also calculated and listed.

According to the IAWA (1989) method (the wood with an air-dried density smaller than 0.56 g/cm^3 is considered to be a small-density species, between 0.56 g/cm^3 and 0.75 g/cm^3 is considered to be a medium-density, between 0.75 g/cm^3 and 0.95 g/cm^3 is considered to be a large-density species, and bigger than 0.95 g/cm^3 is considered to be a extra-large-density species), *E. citriodora* wood has a extra large density.

According to the *CHINA WOOD* method (the wood with an air-dried tangential shrinkage smaller than 5.60% is considered to be a small-shrinkage species, between 5.60% and 7.00% is considered with a medium-shrinkage species, and bigger than 7% is considered to be a big-shrinkage species), *E. citriodora* is a big-shrinkage species, suggesting more attention should be paid on wood splitting or checking when sawing and drying.

Tab.1.2-2 The shrinkage and density of *E.citriodora* wood from south and north side

		Ta (%)	Ra (%)	Va (%)	To (%)	Ro (%)	Vo (%)	B D (g/cm^3)	A D (g/cm^3)	Co-t (%)	Co-r (%)
South	Average	7.16	5.44	12.28	10.79	8.78	19.09	0.79	1.00	0.33	0.30
	Std. dev.	0.92	1.35	1.62	1.08	1.54	2.50	0.05	0.07	0.07	0.06
	CV(%)	0.13	0.25	0.13	0.10	0.18	0.13	0.07	0.07	0.20	0.20
	Number	57	57	57	57	57	57	57	57	57	57
North	Average	7.31	5.50	12.41	10.93	9.00	19.16	0.79	1.01	0.32	0.31
	Std.	0.84	1.10	1.68	0.86	1.37	1.83	0.05	0.05	0.03	0.03
	CV(%)	0.11	0.20	0.14	0.08	0.15	0.10	0.06	0.05	0.10	0.10
	Number	59	59	59	59	59	59	59	59	59	59
Total	Average	7.24	5.47	12.35	10.86	8.89	19.13	0.79	1.00	0.33	0.31
	Std.	0.88	1.23	1.65	0.97	1.45	2.18	0.05	0.06	0.05	0.05
	CV(%)	0.12	0.22	0.13	0.09	0.16	0.11	0.06	0.06	0.16	0.16
	Number	116	116	116	116	116	116	116	116	116	116

ANOVA analysis (Tab.1.2-3) showed there was no significant difference between air-dried tangential shrinkage and air-dried radial shrinkage, suggesting that the wood from north and south could be thought has the same level in shrinkage.

Tab.1.2-3 ANOVA analysis on the shrinkage of *E. citriodora* wood from north and south

	SS	df	MS	F	P-value	F crit
Ta	0.5900	1	0.5900	0.7613	0.3848	3.9243
Ra	0.0794	1	0.0794	0.0524	0.8193	3.9243

1.2.2.2 Shrinkage and density of wood from 4 different tree heights

The shrinkage, shrinkage coefficient and density from 4 different tree heights were listed in Tab. 1.2-4.The relationship between air-dried shrinkage, basic density and tree heights were showed in Fig. 1.2-2.

ANOVA analysis (Tab.1.2-5) showed there did not exist significant air-dried radial shrinkage difference among 4 different tree heights, while existed significant difference in tangential shrinkage. This utterly agreed with the report on I-72 poplar (Lu Jianxiong etc.,2004)

Tab. 1.2-4 The shrinkage and density of *E.citriodora* wood from different heights

		Ta (%)	Ra (%)	Va (%)	To (%)	Ro (%)	Vo (%)	BD (g/cm^3)	AD (g/cm^3)	Co-t (%)	Co-r (%)
1.3m	Average	7.06	5.06	11.80	10.73	8.32	18.65	0.81	1.02	0.34	0.30
	Std. dev.	0.90	1.22	1.48	0.84	1.34	2.35	0.06	0.07	0.07	0.06
	CV(%)	0.13	0.24	0.13	0.08	0.16	0.13	0.07	0.07	0.20	0.21
	Number	30	30	30	30	30	30	30	30	30	30
3.3m	Average	7.57	5.58	12.79	11.22	9.02	19.43	0.79	1.01	0.33	0.31
	Std. dev.	0.88	1.18	1.74	0.89	1.48	1.92	0.05	0.05	0.02	0.03
	CV(%)	0.12	0.21	0.14	0.08	0.16	0.10	0.06	0.05	0.05	0.11
	Number	30	30	30	30	30	30	30	30	30	30
5.3m	Average	7.35	5.69	12.61	11.07	9.14	19.65	0.79	1.00	0.33	0.30
	Std. dev.	0.88	1.38	1.73	0.86	1.54	2.43	0.04	0.05	0.06	0.05
	CV(%)	0.12	0.24	0.14	0.08	0.17	0.12	0.05	0.05	0.18	0.17
	Number	29	29	29	29	29	29	29	29	29	29
7.3m	Average	6.94	5.57	12.17	10.38	9.12	18.76	0.77	0.98	0.31	0.32
	Std.	0.75	1.04	1.51	1.12	1.36	1.88	0.04	0.06	0.05	0.04
	CV(%)	0.11	0.19	0.12	0.11	0.15	0.10	0.06	0.06	0.16	0.12
	Number	27	27	27	27	27	27	27	27	27	27

Tab.1.2-5 ANOVA analysis on the shrinkage of *E.citriodora* wood from different heights

	SS	df	MS	F	P-value	F crit
Ta	7.0273	3	2.3424	3.2029	0.0260	2.6856
Ra	7.1437	3	2.3812	1.6101	0.1910	2.6856

Tangential and radial shrinkage had no regular pattern, while the basic density has a tendency that decreased with the increase of tree height (Fig 1.2-2).

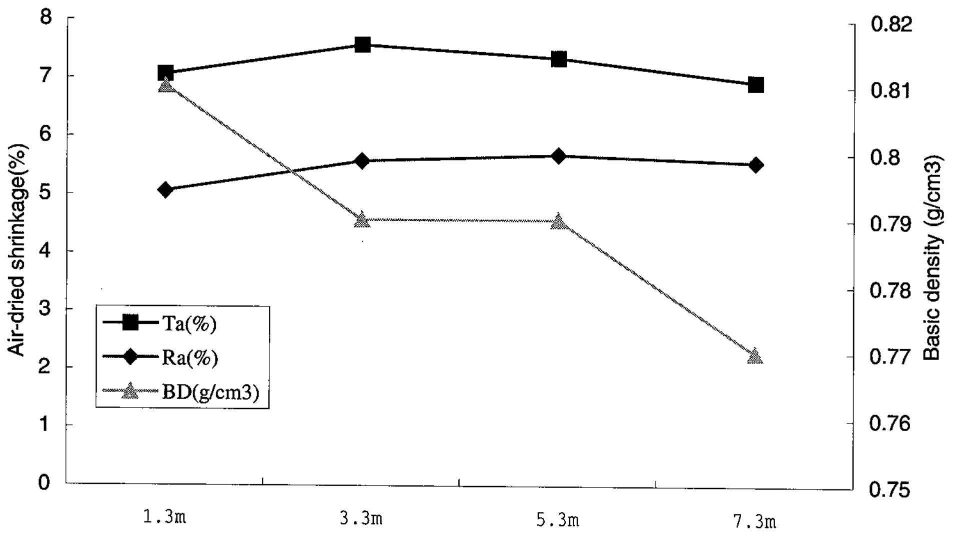

Fig.1.2-2 Relationship between air-dried shrinkage, basic density and tree heights

1.2.2.3 Shrinkage and density of wood at different radial positions

The shrinkage, shrinkage coefficient and density from 4 different tree radial positions were listed in Tab1.2-6. The relationship between air-dried shrinkage, basic density and tree heights were showed in Fig. 1.2-3

ANOVA analysis (Tab.1.2-7) showed there did not exist significant air-dried shrinkage difference in tangential direction, while the reverse was true in radial directions.

Tab. 1.2-6 The shrinkage and density of *E.citriodora* from different radial positions

		Ta	Ra	Va	To	Ro	Vo	B D	A D	Co-t	Co-r
near bark	Average	7.05	6.11	12.74	10.89	9.72	19.80	0.77	0.98	0.34	0.32
	Std. dev.	0.83	1.29	1.55	0.91	1.34	1.68	0.03	0.04	0.08	0.07
	CV(%)	0.12	0.21	0.12	0.08	0.14	0.09	0.04	0.04	0.23	0.21
	Number	40	40	40	40	40	40	40	40	40	40
transition	Average	7.29	5.43	12.39	10.86	8.92	19.18	0.84	1.06	0.33	0.32
	Std. dev.	0.79	1.11	1.67	0.81	1.34	2.20	0.03	0.03	0.01	0.03
	CV(%)	0.11	0.20	0.13	0.07	0.15	0.11	0.04	0.03	0.04	0.09
	Number	39	39	39	39	39	39	39	39	39	39
near pith	Average	7.38	4.82	11.87	10.84	7.97	18.35	0.76	0.96	0.31	0.28
	Std. dev.	1.00	0.90	1.64	1.20	1.11	2.41	0.05	0.06	0.04	0.02
	CV(%)	0.14	0.19	0.14	0.11	0.14	0.13	0.06	0.06	0.12	0.09
	Number	37	37	37	37	37	37	37	37	37	37

Tab. 1.2-7 ANOVA analysis on the shrinkage of *E.citriodora* wood from different radial positions

	SS	df	MS	F	P-value	F crit
Ta	2.233207	2	1.116603	1.455217	0.237689	3.076579
Ra	31.95154	2	15.97577	12.81888	9.61E-06	3.076579

Radial shrinkage showed a tendency that it increased from juvenile wood (near pith) to mature wood (near bark), while the reverse was true in tangential direction. The basic density in the transition zone presented the maximum value (Fig.1.2-3).

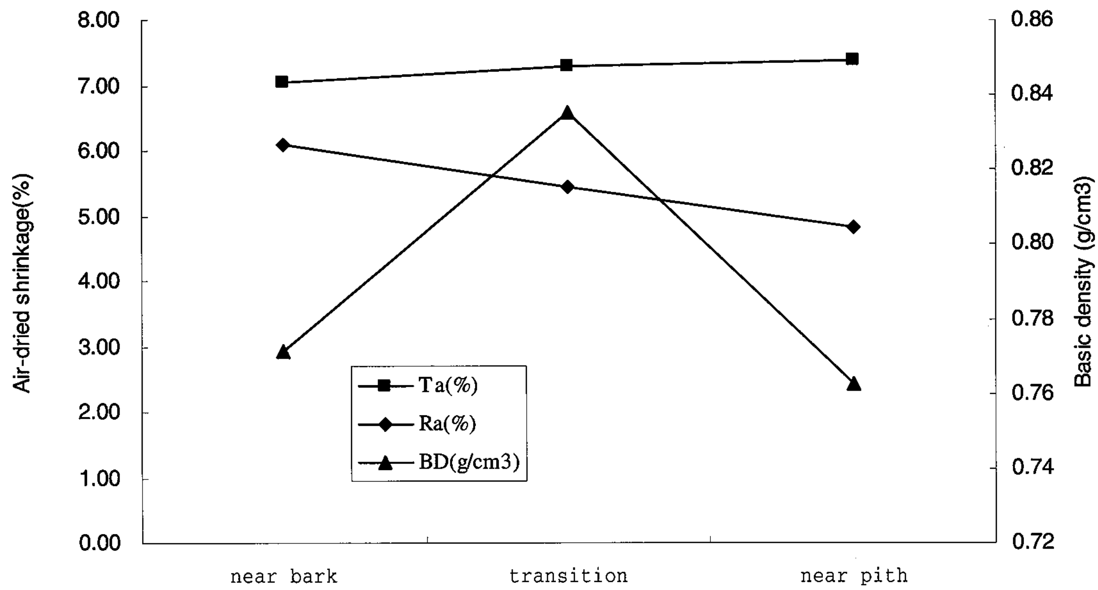

Fig.1.2-3 *E. citriodora*: relationship between air-dried shrinkage (Ta&Ra), basic density (BD) and different radial positions

1.3 Mechanical properties

The small clear wood samples of moduli of elasticity (MOE), moduli of rupture (MOR) in static bending, compression strength parallel to grain and wood density were cut in accordance with Chinese National Standards (GB 1927~1943-91). The specimens were then stored in a conditioning chamber until it reached approximately 12% moisture content. Bending, compression and wood density test were carried out in accordance with Chinese National Standard. The air-dry density was calculated by air-dried weight and volume while oven-dry density was based on oven-dried weight and volume.

Generally *Eucalyptus citriodora* wood interlocked-grain, texture fine and even, extremely heavyweight, very hard, shrinkage large, strength highly. The mechanical properties are including Tab.1.3-1 and mechanical properties data at different radial locations is listed in Tab. 1.3-2.

Tab.1.3-1 Mechanical properties data of *E. citriodora*

Locality	Density /g/cm^3		DS /%		CSPG /MPa	BS /MPa	MOE /GPa	Toughness /kJ/m^2	Hardness /N		
	BD	ADD	R	T	CSPG/MPa	BS/MPa	MOE/GPa	Toughness/kJ/m^2	E	R	T
Guangxi Dongmen		1.038			77	162	20.23	168.7			
Guangxi Yishan	0.774	0.968	0.317	0.388	64	142	18.63		8477	9016	8722
Guangdong Leizhou		0.92			80	162	31.63				

BD = basic density, ADD = air-dry density, DS = dry shrinkage, CSPG = compressive strength parallel to grain, BS = bending strength, MOE = modulus of elasticity, SSPG = shear strength parallel to grain(R), E = end, R = radial, T = tangential

Tab.1.3-2 Mechanical properties data of *E. citriodora* at different radial locations

Property	9th year			17th year			Difference	
	Sample number	Ave.	Std.	Sample number	Ave.	Std.	Absolute value	Relative value (%)
MOR (MPa)	14	146	28.2	14	161.5	22.13	15.5	10.1
MOE (MPa)	14	28051	6244	14	31631	6620	3580	12
Compressive strength (MPa)	14	75.7	9.18	14	80.1	5.81	4.4	5.65
Tensile strength (MPa)	11	15.2	51.34	11	139.2	35.76	-15	-10.2
Radial section shearing strength (MPa)	14	16.8	2.65	14	17.7	2.9	0.9	5.22
Tangential section shearing strength (MPa)	14	14.9	1.79	13	16.5	1.36	1.6	10.2
Tangential cleavage strength (N/mm)	13	25.6	2.09	14	26.5	2.67	0.9	3.45
Radial cleavage strength (N/mm)	14	22.4	2.67	14	23	2.81	0.6	2.64
Toughness (kJ/m^2)	14	—	—	14	122.7	43.46	—	—
Air dried density (g/cm^3)	14	0.84	0.08	14	0.92	0.05	0.08	9.44

1.4 Chemical properties

The chemical compositions were determined according to Chinese National Standards; the results are listed in Tab.1.4-1.

Tab.1.4-1 Chemical compositionof of *E. citriodora* (%)

wood species	Tree age (years)	M	αC	L	XY	NaOHE	BAE	CWE	HWE	A
E. citriodora	13	10.17	46.70	19.45	22.87	14.46	1.63	1.24	2.98	0.15

M—Moisture, αC—α-Cellulose, L—lignin, XY—Xylan, NaOHE—NaOH extractives, BAE—Benzene-alcohol extractives, CWE—Cold water extractives, HWE—Hot water extractives, A—Ash

The chemical composition of *E. citriodora* at different ages is including Tab.1.4-2, pH values, acid and alkaline buffering capacities are listed in Tab.1.4-3.

Tab.1.4-2 Chemical composition of *E. citriodora* at different ages (%)

Tree age (years)	M	L	XY	αC	HOC	A	CWE	HWE	NaOHE	BAE
5	—	20.27	13.79	46.09	—	0.56	3.08	4.31	16.70	1.60
6	9.99	20.03	24.03	49.49	—	0.49	2.48	4.21	15.81	1.21
13	—	19.27	22.85	—	79.95	0.44	1.38	3.22	14.24	2.39
13	—	19.39	12.71	49.85	—	0.43	2.55	3.53	14.92	1.94
13	8.66	21.41	23.42	48.16	—	0.43	2.34	4.43	15.65	2.30
13	10.17	19.45	22.37	46.70	—	0.45	1.24	2.98	14.46	1.63
13	—	24.51	22.18	43.53	—	0.45	2.15	5.52	15.91	2.91
14	—	19.56	23.80	—	81.60	0.33		3.49	14.49	1.56
15	—	21.63	23.92	47.03	—	0.33	3.27	5.18	18.59	3.30
16	14.32	26.07	15.00	47.55	—	0.46	2.40	3.97	16.80	3.15
18	10.93	21.69	23.73	47.61	—	0.42	1.78	3.51	15.87	2.49

M—Moisture, L—lignin, XY—Xylan, αC—α-Cellulose, HOC—Holocellulose, A—Ash, CWE—Cold water extractives, HWE—Hot water extractives, NaOHE—NaOH extractives, BAE—Benzene-alcohol extractives

Tab.1.4-3 pH values, acid and alkaline buffering capacities of

Wood Species	pH		Acid buffering capacity (mmol × 10^2)		Alkaline buffering capacity (mmol × 10^2)	
	Sap wood	Heart wood	Sap wood	Heart wood	Sap wood	Heart wood
E. citriodora	4.84	4.68	4.98	7.40	17.30	44.22

2 GROWTH STRESS

The research adopted CIRAD-Foret method to measure surface longitudinal growth strain (SLGS) of standing trees, the results at different orientations were listed in Tab.2-1.

Tab.2-1 Growth strain data for standing trees of *E. citriodora*

Basic density (g/cm^3)	E		W		S		N	
	$\bar{x}$	δ_n	$\bar{x}$	δ_n	$\bar{x}$	δ_n	$\bar{x}$	δ_n
0.785	636	384.5	731	256.3	763	291.6	829	352.1

3 MACHINING PROPERTIES

The logs of *E. citriodora* plantation with the age of 8 to10 years were supplied by Guangxi Chengda Wood Products Company. And its diameter was about 20~30cm. The moisture contents after kiln drying were 8 to12%. The test specimens were made based on the ASTM standard, whose dimension was 20 mm ×127 mm ×1200 mm (thickness×width×length). According to ASTM standards the test lumber should be clear and sound, which means free from all defects, including knots, stain, incipient decay, surface checks, end splits, and reaction wood.

However, for *E. citriodora* plantation wood, to thoroughly avoid all these defects is considerable difficult. The method of drawn at random was taken in order to show the real characteristics of this wood. The size for smaller samples is showed in Tab.3-1.

Tab.3-1 Smaller samples size for individual test

Individual test	Size: Thickness × Width × Length(mm)	Number
Planning	19 × 102 × 910	30
Sanding	19 × 102 × 400	30
Shaping	19 × 76 × 305	30
Boring	19 × 76 × 305	30
Mortising	19 × 76 × 305	30
Turing	19 × 19 × 305	30

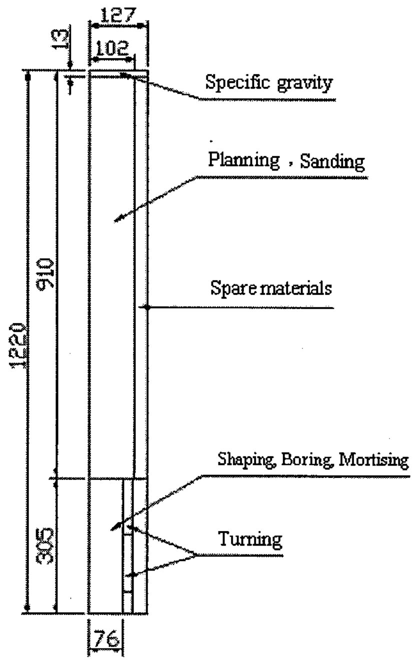

Fig.3-1 Diagram for sawing lumber into smaller samples for individual tests

3.1 Methods

3.1.1 Planning

The planning test was conducted on KUW-500F1 planer. Some adjustments of the bottom spindle allowed its cutting circle beneath the bench. The knife parameters should be stabilized. The wedge angle was 30° .The material of knife is the industry standard high-speed steel (HSS). Five treatments based on two control factors (planning thickness and feed rate) have been conducted.

Tab.3.1-1 Five treatments of planning

Treatment	Cutting thickness (mm)	KMPI	Feed velocity (m/min)
1	1.6	20	8
2	2.5	40	8
3	1.6	48	9.5
4	1.6	20	19
5	2.5	48	19

3.1.2 Sanding

WS-65 wide belt-sanding machine made by Japanese AMITE Company was used to test sanding properties. This sander has only one head and is automatic feed. The scope of feed rate is from 4.3 to 20.3m/min. 5.8m/min feed rate was used in the sanding test, while the feed rate recommend by ASTM is 6.1m/min. ASTM standard did not prescribe concrete sanding thickness. Based on China's practical production and the testing of EDVARD KARDELJ University, in this study the cutting thickness was 0.6mm. The grit of sand paper was 120.

3.1.3 Shaping

A single spindle shaper was used to test shaping properties, which was equipped with a moulding milling cutter. This hand feed shaper was made by Mudanjiang Wood Machining Factory in China and has 4 spindle rotations, of which 6 000 r/min was used in this testing. The milling cutter was produced by Chaoyang Tool Factory in Beijing.

Before shaping the specimens need to be sawn. Then make a preliminary roughing cut along the grain as soon as possible and make a 2mm deep finishing cut. However the cutting thickness recommended by ASTM was 1.6 mm.

3.1.4 Boring

Two types of bits (namely center bit and solid nose bit) were used in the boring tests. The center bit was equipped into a B13S bench borer produced by Japan. Its maximum spindle rotations was 3 000 r/min and the minimum spindle rotations was 500 r/min. The solid nose bit was equipped into a ZQ3025×5 hand feed borer, whose maximum boring diameter was 25mm.Its maximum and minimum of spindle rotation were 2 800 and 320r/min respectively.

Diameter for two types of bits was also 25 mm. The spindle rotation for B13S borer was 2 000 r/min, for ZQ3025×5 borer was 500 r/min. Although the solid nose bit is not commonly used in wood industry, it is necessary to compare different manufacturing methods for an exploring test. The bit needs to sharpen before every test. According to ASTM the rate of boring should be enough low to insure normally cut.

3.1.5 Mortising

MK312 foot feed moister produced in China was used in this test, whose maximum machining width was 20 mm. 13 mm hollow chisel recommended by ASTM was equipped on the mortising machine. According to ASTM run-thorough mortise should be processed, while the run-not thorough mortise is more commonly used in China's furniture industry. In this test two run-thorough mortises were manufactured in each specimen. The mortises should be two sides parallel to the grain and two sides perpendicular to it.

3.1.6 Turning

Turning test was conducted in Italy TS-120 wood working lathe, which is automatic feed knife. The feeding velocity for cutter block was 0-10 m/min, and returning velocity was 0-12 m/min. three spindle rotations, 2120, 3110, and 4210 r/min, could be chosen. The maximum length for work piece was 1200 mm; the maximum diameter was 200 mm.

In this test the spindle rotation speed was 3110 r/min; the feeding velocity for cutter block was 6 m/min. The material for knife was carbide. The pattern panel was equipped with the machine. The size for the pieces was 20 mm × 20 mm × 305 mm (width×thickness×length). According to ASTM, it needs to adjust the position of the knife to make turning 7.5mm thickness at the thinnest point of piece. All the pieces were processed four times. The cutting thickness for the first 3 times was 1 mm, for the last was 0.7 mm. After turning the pieces were sanding by 150-grit sandpaper.Results and discussions

3.2 Results and Discussions

3.2.1 Planning

The grade for planning quality is based on the form and quantity of defects. The planning qualities were divided into 5 grades (Excellent, Good, Fair, Poor and Very poor) by ASTM. According to ASTM standard the number of samples for excellent grade needs to be statistic. The study reveals torn grain is the main planning defect for *E. citriodora*. Grades 1 to 5 torn grain samples of *E. citriodora* were show in Fig.3.2-1.

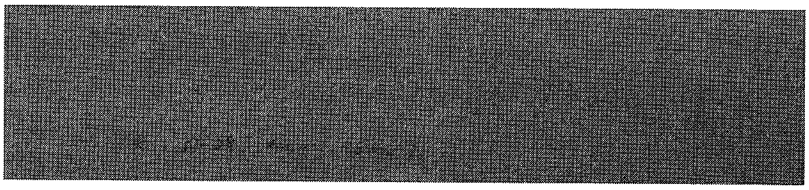

a) Grade 1

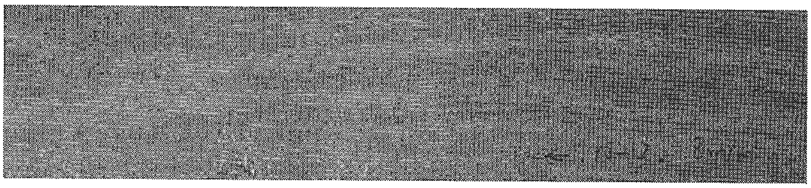

b) Grade 2

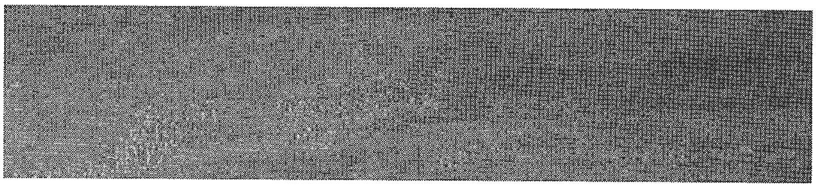

c) Grade 3

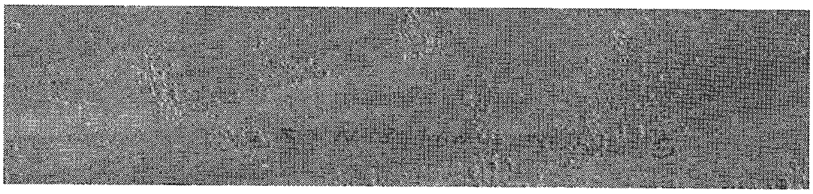

d) Grade 4

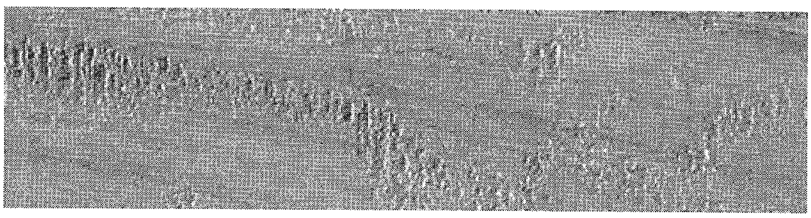

e) Grade 5

Fig.3.2-1 Grades 1 to 5 torn grain samples of *E. citriodora*

With the feed velocity decreasing, the torn grain becomes more serious. The percentage of Grade 1 and Grades1 and, 2 planning samples of *E. citriodora* planning show as Tab.3.2-2.

Tab.3.2-1 Percentage of Grade 1 and Grades1 and, 2 planning samples of *E.citriodora* planning

Cutting condition	1	2	3	4	5
Grade 1	43.3	50.0	36.7	3.3	10.0
Grades 1 and 2	76.7	73.3	66.7	40.0	43.3

Observing the position of torn grain under SEM, it shows as following figures. Obviously fiber tearing, fiber cutting and lifted tissue are the main reasons for planning defect (see Fig.3.2-2).

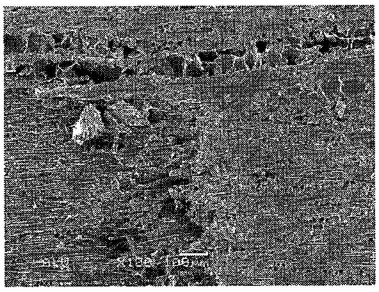

a) Defect and defect free positions

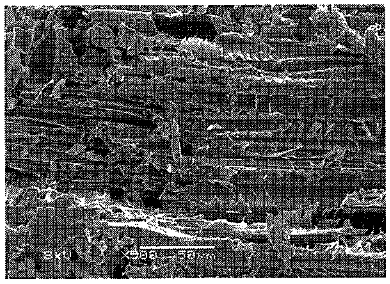

b) Fibers tearing

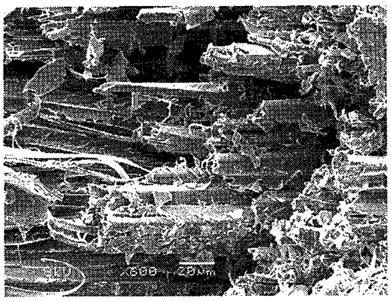

c) Fiber cutting

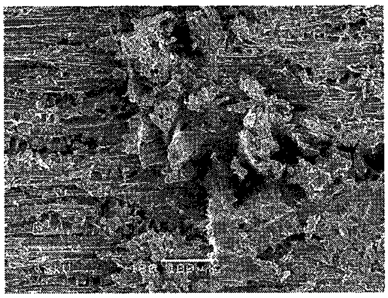

d) Lifted tissue

Fig.3.2-2 SEM observation of planning defects of *E. citriodora*

3.2.2 Sanding

The experiment result shows the planning defects can be well removed by sanding (Fig. 3.2-3). For example, the extreme planning defects produced in 19m/min can be thoroughly gotten rid of by sanding. The defects occurred nearby knots and out of straight were also lightened after sanding. Although the planning defects have been got rid of, a new kind of defect: A type defect occurred. In totally 30 pieces, there are 20 with S defect, which proportion is 66.7%.

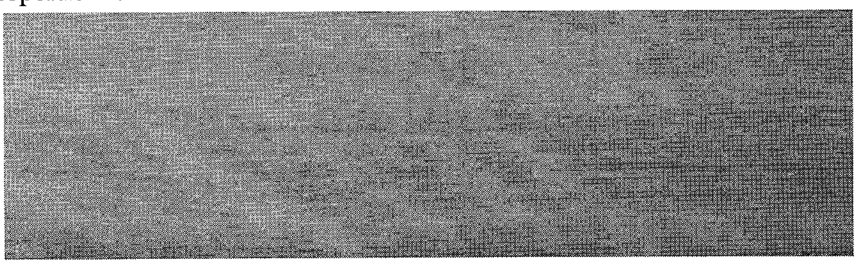

Fig.3.2-3 Sanded samples of *E. citriodora*: Type A defects

Observing the sanding samples under SEM, it shows as Fig.3.2-4. Although the surface quality after sanding is better than that after planning, it also can be seen some small wood fibers with randomly distribution on the surface (Fig.3.2-4a).

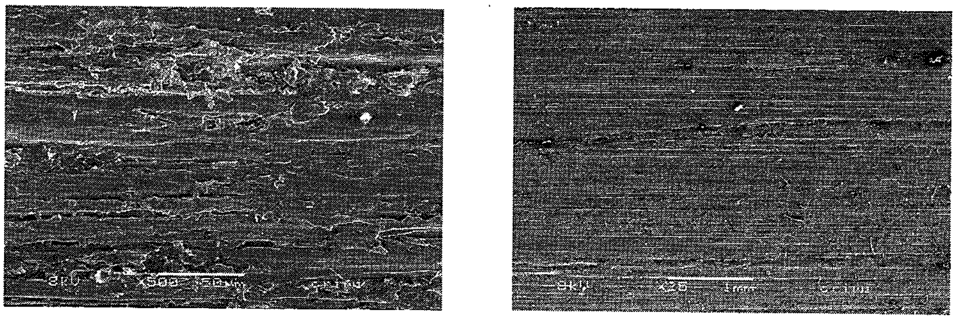

a) Grade 1 sample b) Flattened surface tissue

Fig.3.2-4 SEM observation of *E. citriodora* samples

3.2.3 Shaping

After shaping, a new type of defect-C defect was occurred on the profile with randomly distribution, which color is light. The possibly reason for C defect is high gravity and strength of *E. citriodora*. Although its severity is not serious, the quantity is considerably much. There are 6 pieces with C defect in totally 30 pieces, which proportion is 20%. 1 piece has torn grain, the proportion is 3.3%. 23 pieces are without defect, the proportion is 76.7% (Fig.3.2-5).

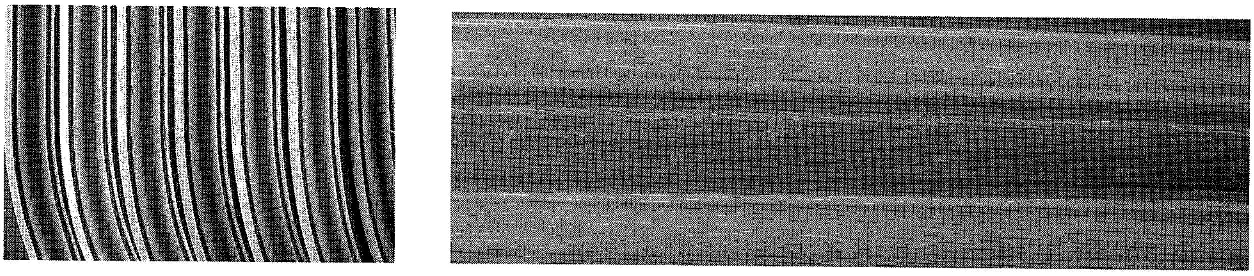

a) Grade 1 sample b) Type C defects

Fig.3.2-5 Shaping samples of *E. citriodora*

3.2.4 Boring

When using solid nose bit to boring, fuzzy grain and tearing are the main boring defects (Fig.3.2-6). There are 11 pieces with fuzzy grain and 4 with tearing. Extreme tearing can make the piece discarded. Roughness of boring hole is not well. The proportion of Grade 1 pieces is 46.7. For all the holes, the quality of top edge is better than that of bottom edge. When using center bit to boring, no piece has defect, the proportion for grade 1 pieces is high to100%.

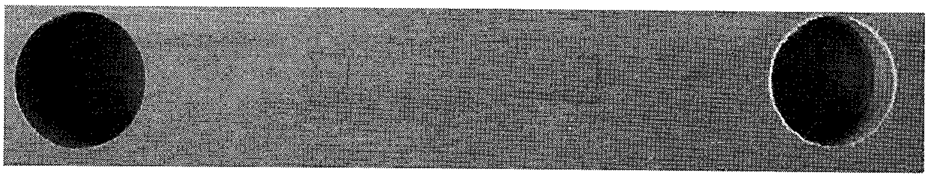

a) Upper edges of the holes in Grade 1 sample

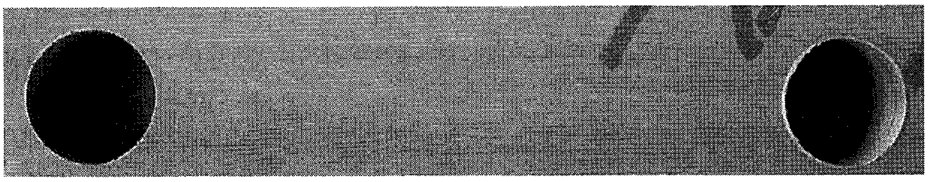

b) Bottom edges of the holes in Grade 1 sample

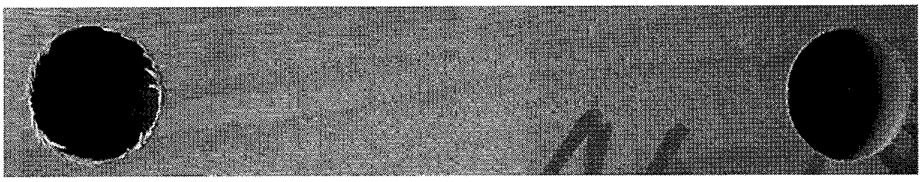

c) Fuzzy grain at bottom edge

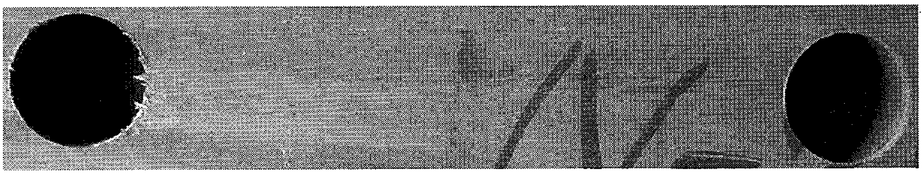

d) Tearing at bottom edge

Fig.3.2-6 Boring samples of *E. citriodora*

The left hole was bored by Solid-center bit with spur; and the right one by twist drill.

3.2.5 Mortisng

The study reveals fuzzy grain on the wall of mortising is mostly frequent defect. Almost every piece has fuzzy grain. Although its severity is not serious, fuzzy grain has a neglect influence for roughness of mortising wall (see Fig.3.2-7). It is noticeable there were no defects such as fuzzy and tearing occurrence on the top and bottom edge. The quality of top and bottom edge lies in same degree.

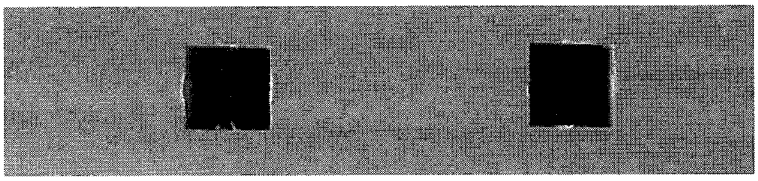

a) Top edges of the mortises in Grade 1 sample

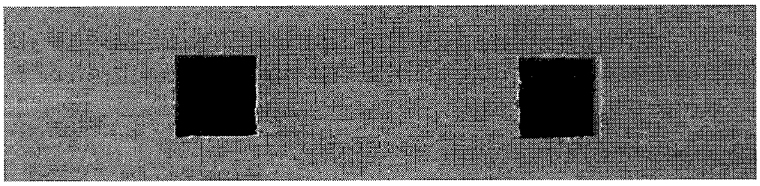

b) Bottom edges of the mortises in Grade 1 sample

Fig.3.2-7 Mortising samples of *E.citriodora*

3.2.6 Turning

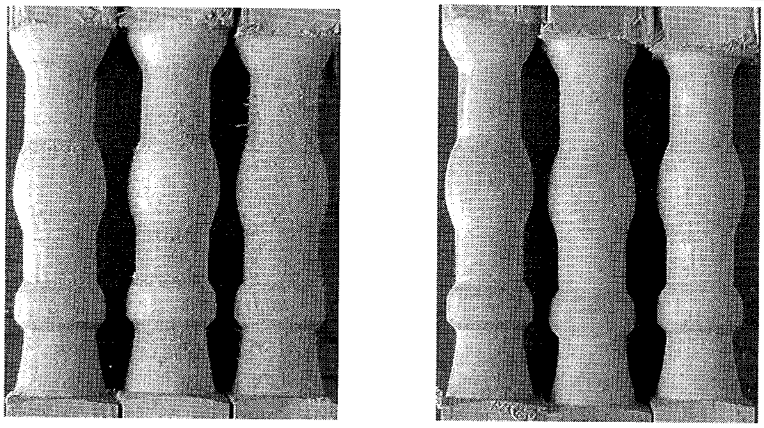

a) Before sanding b) After sanding

Fig.3.2-8 Turning samples of *E. citriodora*

After turning, the piece was been sanding with 150# sandpaper. The surface quality of piece has been greatly improved by sanding. Fuzzy grain and amount of single fiber on the pieces surface was removed by sanding (see Fig.3.2-8). However some knife marks can still be watched after sanding. There are 22 with knife marks in totally 30 pieces, the proportion is 73.3%. Only because the severity of the knife marks is light, the piece with knife marks is not degraded.

3.3 General conclusion

The statistics results for machining properties of *E. citriodora* plantation wood shows obviously that the boring (using the brad point bit) and mortising properties are the best. The shaping, turning and sanding (based on treatment 2) properties are the medium. The last is planning properties. So it can be conclude that *E. citriodora* plantation wood have a great potential for solid wood utilization.

4 SAWING TECHNIQUES

Logs were collected from DONGMEN Forest farm in Nanning, Guangxi, and 10 stems were taken. All trees were unpruned and were planted on commercial forest land. The ends of the logs were sealed with asphalt to prevent end-drying after logging. Water spraying was applied to keep them in a green condition by preventing drying degrade.

The length of each log section was from 2.00 to 2.20 meters. The taper of this species was small, so three to four sections could be harvested from each tree. The tree and log parameters are listed in Tab. 1.

Tab. 4-1 The parameters of *E. citriodora* trees and log sections

Height of tree (m)	Height under branch (m)	Age (years)	DBH (mm)	Diameter Range of log sections (mm)
30.67	16.57	37	287	180~233

Note: the height and DBH (diameter at breast height) are averaged.

The diameter of log sections refers to the Small End Diameter (SED), and bark is not included.

The equipment for the sawing consisted of a headrig band saw with a manually adjusted sizing carriage.

4.1 Strain in sawing process

The method of measuring strain is based on the method of measuring longitudinal strain (France, CIRAD-Foret Method) and instantaneous release of residue stress after drilling holes above and below gauges (M. Yoshida, T. Okuyama, 2002). The pin targets and guide for setting is displayed in Fig. 4.1-1.

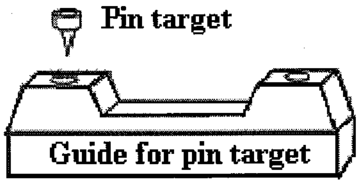

Fig. 4.1-1 Pin target and guide for measuring strain in sawing process

Height of pin target: 10mm, Internal diameter: 2.5mm, External diameter: 10mm, Distance between pin target: 45mm.

Before each sawing pass, two pin targets were placed into the existing sawn surface according to Fig.4-1.2 or in the case of the opening cut on the log side face which was to be perpendicular to the sawing surface. The distance enclosing the two pin targets was measured with a digital caliper with a precision of 0.001 mm. The head of each pin target was recessed to accept the pins and hold them in place. And their distance apart, measured before sawing and again just after the lumber containing the pin targets was sawn off. The strain changes in the longitudinal and tangential directions were then calculated using the formula:

$$strain = \frac{Da - Db}{Db} * 100\%$$

Where: Db= the dimension before the lumber is sawed off; Da= the dimension after the lumber is sawed off.

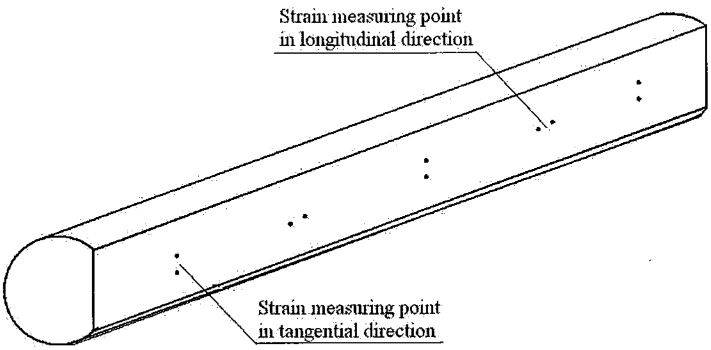

Fig. 4.1-2 Distribution of measuring point for strain change in lumber sawing

The logs were sawn using three different sawing patterns; live sawing, cant sawing and around sawing; and the strain changes were measured following the above procedure.

The strain distribution in the sawing process is analysed and displayed in Figs 4.1-2 – 4.1-3. X-coordinates show the log's position, while the number 1, 2, 3... shows the section position progressively from the bottom to the top section of the trunk. The abbreviations shown in the figures are: T—tangential, R—radial, Sap—Sapwood, Core—Core wood, Live—live sawing, Cant—cant sawing, Around—around sawing, for example, 'T_live' represents tangential direction with live sawing pattern.

The stresses are generated in newly formed wood during cell maturation in living tree. Continuous formation of growth stresses during tree growth results in an uneven distribution of residual stresses across tree stems. When logs are sawn longitudinally, the residual stresses are partially released (Crompton, 2000). And the growth stresses are presented in a random way (Tomaselli, 2000), this may resulted in the big deviation of the strain in sawing process. Fig. 4.1-3 showed the strain in the sawing process for three kinds of sawing strategies for E. citriodora. The strain in both the tangential and radial (T and R) directions is more uniform with the cant sawing strategy than that of other two strategies, The strain difference between T and R with the cant sawing strategy is small, and the absolute value of strain is close to zero (i.e. strain free), therefore it is possible to saw lumber with less sawing defect. In live sawing and the around sawing strategies, the strain fluctuation is very big, and this may result in checks and deformation of the lumber.

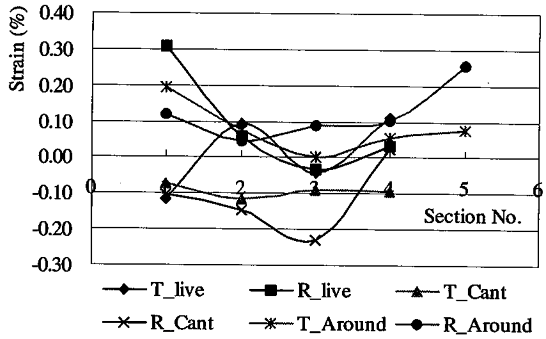

Fig. 4.1-3 Strain distribution of *E. citriodora* in tangential and radial direction

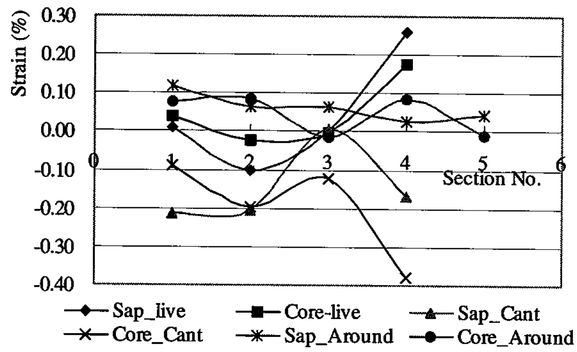

Fig. 4.1-4 Strain distribution of *E. citriodora* in longitudinal direction

From the strain changes of radial direction and tangential direction, it is almost all the strain value of radial direction is more than that in tangential direction, i.e. the radial lumber (quarter sawn lumber) is prone to defect than the tangential lumber (back sawn lumber), this may result in the end-splitting occurs in the quarter sawn lumber.

As for the longitudinal strain displayed in Fig. 4.1-4, the top section's strain changes are big, the bottom section's strain is comparatively small.

4.2 Bow Deformation

Bow deformation in sawn lumber (bending in the longitudinal direction) was recorded for each sawing strategy. The bow deformation can reflect the extent of growth stress gradient. The higher the stress gradient in the original log, the greater the expected bow deformation is.

The most deformation which occurred in the sawing process was bow deformation of the lumber, it is also from the releasing of residue stress (Crompton, 2000). The results are displayed in Fig. 4.2-1 to 4.2-3 for the three different sawing strategies. The X-coordinates represent the location of lumber in the log, 0 is the core lumber and the other values represent the block number in relation to the pith of the log, Positive and minus values are used to indicate the two directions from the pith. In the live sawing and cant sawing strategies, the larger minus values represent which pieces of lumber were cut first., In the around sawing strategy the sign just represents location of the lumber (displacement from the pith).

In the sawing process, most of the lumber developed bow deformation except the core lumber. The outer the lumber position is, the bigger the bow deformation is. This is in accordance to the stress distribution inside Eucalyptus log. The stress gradient is bigger as the position is in outer place than that in the inner place. And the bow deformation has some relationship with where the lumber was located in the original log and the sequence of the cuts in the sawing process. This is apparent in Fig. 4.2-1 to 4.2-3, especially the cant sawing. The lumber sawed first had the biggest bow deformation, and the lumber sawed later had less deformation. This may result from the reason that after the former lumber sawing, the stress inside left log had been released in some extent, so the later sawed lumber had less deformation even in the similar position in the log.

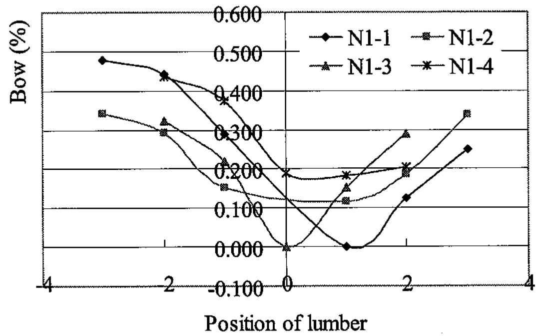

Fig. 4.2-1. The bow deformation of *E. citriodora* in live sawing

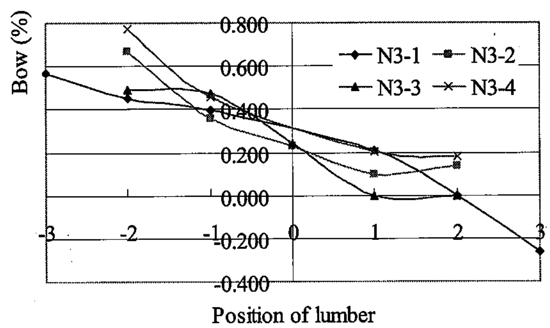

Fig. 4.2-2. The bow deformation of *E. citriodora* in cant sawing

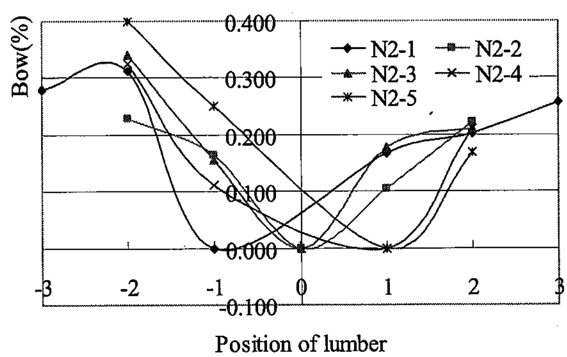

Fig. 4.2-3. The bow deformation of *E. citriodora* in around sawing

As for the deformation, the around sawing had the least value, the biggest value is just 0.4%. The biggest deformation occurred in cant sawing, after slab sawing off, the most of the wood near the heart under high compression still exists in the cant and on reaching a new equilibrium condition, will impose a higher tensile strain on the sapwood than the level which existed in the intact log (Waugh, 2000), this increased stress gradient and resulted in the bigger deformation. The deformations for 3 sawing patterns were listed in detail in Tab. 4.2-1. The deformation value range is similar with live sawing and cant sawing.

The bow deformation displayed the stress distribution and re-distribution in some extent, so the around sawing could release the residue stress more efficient than the other two sawing pattern. But the around sawing is difficult in practice for the low sawing efficiency, it is fortunate that there is the twin-saw system to take place of the around sawing with single saw system.

Tab.4.2-1 the bow deformation of *E. Citriodora* in 3 different sawing pattern

Sawing pattern		Live-sawing				Cant-sawing				Around-sawing				
Position of log		1	2	3	4	1	2	3	4	1	2	3	4	5
Location of lumber	-3	0.477	0.343			0.567				0.279				
	-2	0.442	0.291	0.324	0.434	0.452	0.669	0.491		0.311	0.228	0.341		
	-1	0.291	0.152	0.219	0.375	0.398	0.355	0.473	0.770	0.000	0.164	0.156	0.325	0.400
	0	0.000	0.117	0.000	0.190	0.208	0.230	0.241	0.455	0.166	0.000	0.000	0.112	0.251
	1	0.126	0.187	0.151	0.184	0.000	0.097	0.000	0.202	0.201	0.105	0.177	0.000	0.000
	2	0.251	0.337	0.290	0.203	-0.259	0.135	0.000	0.182	0.258	0.221	0.211	0.210	0.169

4.3 Sawing Inaccuracy

The high hardness in *E. citriodora* made the sawing route wander and resulted in considerable thickness inaccuracy during sawing. And the sawn accuracy of lumber would influence the lumber recovery. According to the national sawing standard of China, the permitted thickness deviation is ± 1mm. However, in this study, the actual sawing variation was much larger, the range being from –3 to +5 mm. This big variation not only influenced lumber recovery, but also made later processing difficult due to the uneven dimensions of the lumber. The proportion of oversize deviation in the study is displayed in tab. 4.3-1. the oversized thickness lumber proportion is bout 52%.

Tab. 4.3-1 the thickness inaccuracy influence to *E. Citriodora* lumber

Amount of slabs (Pcs)	Amount of oversize thickness deviation (Pcs)	The proportion of oversized (%)
90	47	52.22

4.4 The Influence of End-splits on Lumber Recovery

The most frequent defect is end splitting in sawing plantation Eucalyptus for the high growth stress. Heart shake appears just after tree harvested, and it will extend to some extent before sawing, most end splitting comes from heart shake in log section. Tab. 4.4-1 shows the results of end-split to lumber recovery is 8.07%, i.e. if there is no end-split, the lumber recovery will increase about 8%. So it is important to lower the end-splitting before sawing of the logs.

Tab. 4.4-1 Influence of end-split to lumber recovery in sawing experiments

log Volume (m^3)	Volume of Lumber with end-split (m^3)	Recovery rate with end-split (%)	Volume of lumber without end-split (m^3)	Recovery rate without end-split (%)
1.3936	0.8648	62.05	0.7522	53.98

4.5 Pilot Sawing

The pilot sawing was carried out in a private sawmiller in Nanning, Guangxi region.

The sawing equipment is a bandsaw with manual carriage and a resaw. The sawing strategy is displayed in Fig.4.5-1.

Logs was approximately 2.0 metre in length, and varied in small-end diameter from just under 20 cm to 41 cm. Log quality was extremely variable; some of the larger logs had surface checks, some with severe sweep and others with heavy branch stubs. The log parameters and lumber recoveries for green product is shown in Tab. 4.5-1.

The green-off-saw recovery is about 43.5%, this is similar with the result in Australia (Armstrong, 2005), their sawing results also about 40% recovery for *E. citriodora* logs with 20cm diameter.

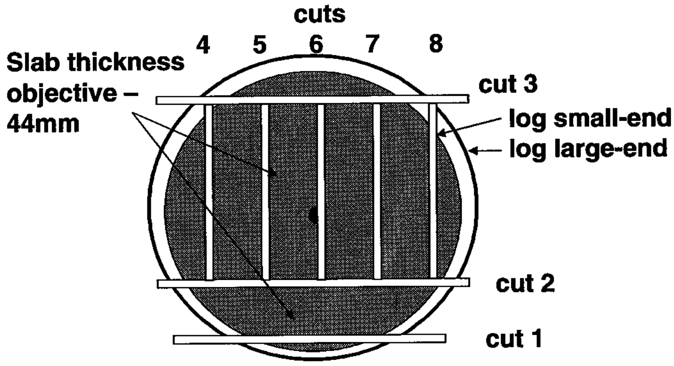

Fig. 4.5-1 Sawing strategy of log in 25 cm diameter

Tab. 4.5-1 Log and lumber parameters in pilot sawing trial

No.	Average diameter (cm)	Length (m)	Clear face	Sweep (cm)	Endsplit LE	Endsplit SE	Volume of log	Sawn lumber	Recovery (%)
1	26.8	2	4	-	-	2*1mm	0.112	0.046	40.68
2	25.4	1.99	4	2.5	-	-	0.101	0.052	51.27
3	28.2	2	4	3.5	-	-	0.127	0.040	31.14
4	22.9	2.07	3	3	-	-	0.085	0.043	50.14
5	25.1	2	4	1.5	-	-	0.099	0.048	48.78
6	27.5	2.03	4	-	4*2mm	4*2mm	0.121	0.053	43.43
total							0.646	0.281	43.5

Note: the Endsplit in LE(large end) and SE(small end) is No.* width of the split.

The lumber quality and recovery could be improved by choosing appropriate sawing strategies and sawing equipments. This would improve the potential for the use of Eucalyptus lumber for value added wood products.

5 DRYING TECHNIQUES

5.1 Air drying

Air drying is a traditional and economical drying method which mainly uses sun energy. To save kiln drying time and cost, and to improve kiln drying quality at the mean time, it is suggested to use Air drying as a pre-drying method, and then conventional kiln drying to target final MC (moisture content). Because of the uncontrolled drying conditions, the drying time, final MC and drying quality may be quite difference with the changes of season and drying arrangements. Air drying test focus on analysing wood Air drying properties and try to find its optimum Air drying technique and parameters.

5.1.1 Material and method

The size of sample for air drying is 700 mm (length) x 120-150 mm (width) x 25 mm (thickness). Two MC slices were cut in the two ends of each sample to calculate its initial MC (Fig.5.1-1).

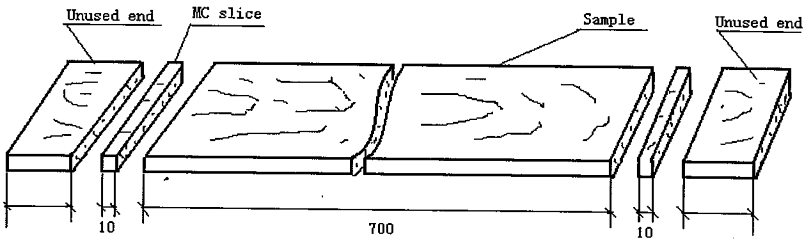

Fig.5.1-1 Drying sample making of *E. citriodora*

The samples were end-sealed with silicon, and then stacked in air-drying shed to start drying. The dry-bulb and wet-bulb temperatures in shed were recorded every day, and the weights and all visible drying defects of samples were recorded once a week at the first month, then once every two weeks till the air drying ended. When the test finished, three final MC slices and one layer MC slice for each sample were cut (Fig.5.1-2). After oven drying these slices, the final MC for each sample were be gained, and then the oven-dry weight (written as G_0) for each sample could be calculated with the equation listed below. And so, corresponding to the recorded weights of each sample in different drying times, the air-drying MC curve could be drawn.

$$G_0 = 100G_w/(100+ MC_0)$$

G_0 - oven-dry weight

G_w - initial weight

MC_0 - oven-dry MC (%)

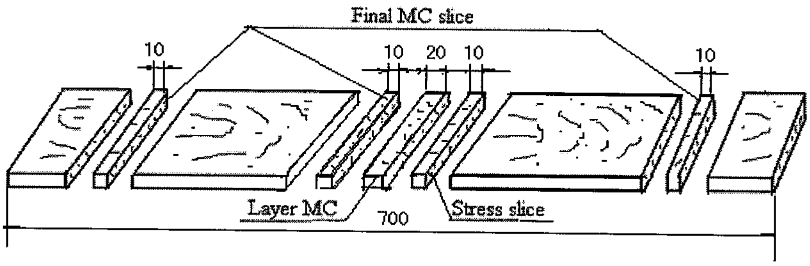

Fig.5.1-2 MC slices making of *E. citriodora*

5.1.2 Result and suggestion

The air-drying test results of *E. citriodora* are listed in Tab.5.1-1, and the air-drying MC curves in different seasons were shown in Fig.5.1-3.

Tab.5.1-1 Air-drying test results of *E. citriodora*

Season	MC_w (%)	MC_o (%)	Air-drying rate (%day)			Air-drying rate in early stage (%/day)		Defect grade ##
			60-30%	30-20%	Below 20% #	1[st] week	2[nd] week	
2002.8-11 Autumn	46.2	12.8		0.69	0.15 (15.4%)	1.9	1.1	2
	44.6	14.2		0.59	0.11 (15.3%)	1.5	1.1	3
	43.5	14.2		0.48	0.24 (16.6%)	1.9	0.6	3
2002.12-2003.3 Winter	46.5	15.9		0.25	0.20 (19.4%)	1.1	0.7	2
	47.9	12.1		0.3	0.17 (15.5%)	2.1	0.7	3
	47.4	12.6		0.33	0.14 (16.6%)	1.6	0.9	3
2003.3-2003.7 Spring	46.5	14.2		0.26	0.05 (19.4%)	0.7	0.6	3
	47.9	13.7		0.29	0.33 (15.5%)	1.2	0.4	1
	47.4	14.5		0.29	0.30 (16.6%)	1.6	0.9	3
2003.6-2003.9 Summer	31.6	14.8		0.91	0.21 (14.6%)	1.3	0.5	3
	32	15.7		0.59	0.09 (15.4%)	1.4	0.8	3
	29.1	15.8		0.45	0.09 (15.5%)	0.6	0.4	3

Note: # - The data in brackets are the final MC when test ended.

##- The standards for drying defects grade division: grade 1 – having no check, warp and cup deformations or just having end checks; grade 2 - having no more than five short end-surface checks or short-narrow surface checks, and the value of warp and cup deformations are smaller than 2mm; grade 3 - having five to ten short-narrow surface checks, and the value of warp and cup deformations are smaller than 4mm; grade 4 - having more than ten short-narrow surface checks and long-narrow or wide surface checks no more than five, or the value of warp and cup deformation are more than 4mm.

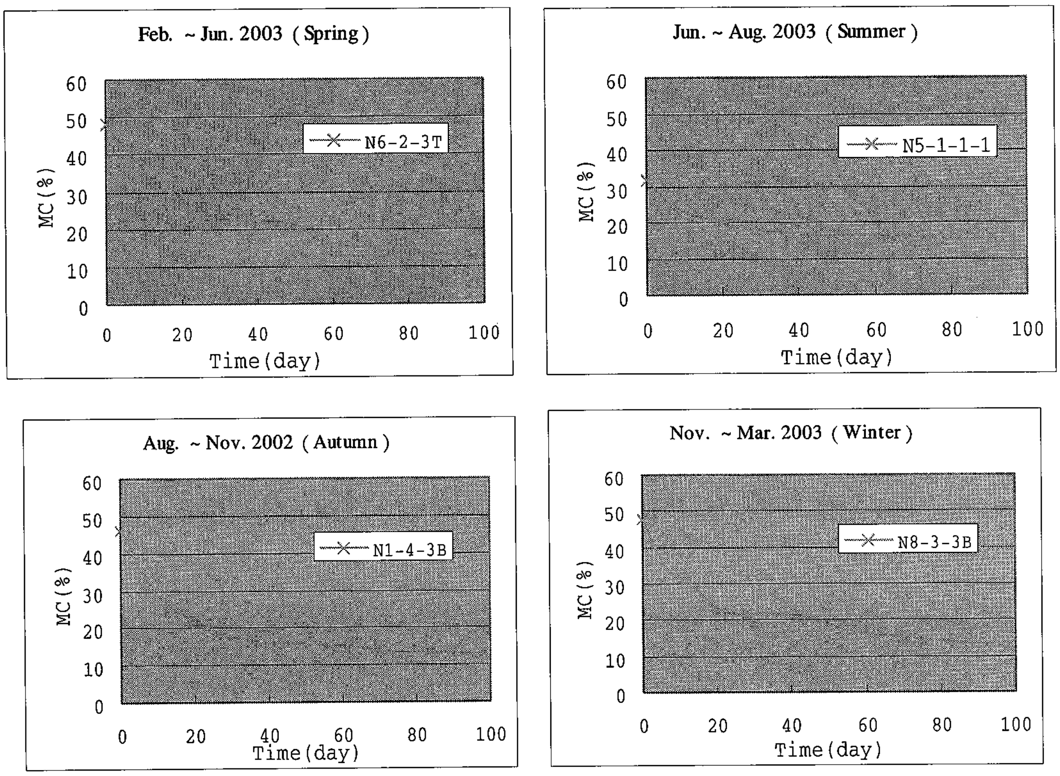

Fig.5.1-3 The air-drying MC curve of *E. citriodora*

Result showed that the air-drying rate of *E. citriodora* in summer was the fastest and that in winter in the slowest. But drying defects were very serious (grade 3 mostly), and the main drying defects were many small surface checks. So it is recommended that using controlled air-drying method to pre-dry *E. citriodora* wood before kiln drying.

5.2 Drying characteristics

5.2.1 Material and method

The sample dimension: plane-sawn lumber with 200mm x 100mm x 20mm

Other requirements of sample: planed lumber with normal colour, knot-free and straight grain, and initial moisture content is above 45%.

Equipment: Electric oven with air circulation.

100℃-test method is a fast drying test which is used to study on drying characteristics and prediction of drying schedule of plantation wood. Before test, the following data of the samples should be gained: the sample's weight, all visible surface defects, and dimension measurement data as showing in Fig.5.2-1. Then the samples were put into the electric oven with constant temperature at 100℃, and letting the samples stand erectly in the oven so that they will obtain same quantity of heat. Once the test begin, weighing the samples, observing and recording all initial defects including end checks, end-to-surface checks and surface checks at a fixed time through all the drying process. The test ended when MC was estimated below to 1%. All the samples were taken out, and then measuring cross-section deformation (Fig.5.2-2). Finally cutting moisture content slice and recording internal checks of each sample.

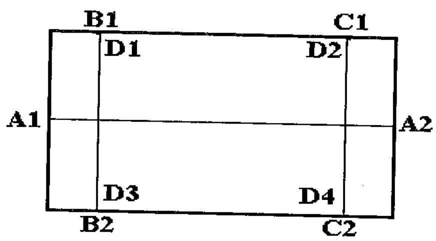

A1-A2 is length
B1-B2 and C1-C2 are width
D1,D2,D3,D4 are thickness

Fig.5.2-1 The dimension measure in 100℃-test of *E. citriodora*

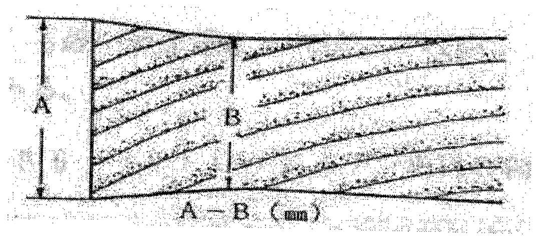

Fig.5.2-2 The cross-section measure in 100℃-tes of *E. citriodora*

To make all these defects digitalization and comparable, the grades of different drying defects are shown in Tab.5.2-1 to Tab.5.2-3.

Tab.5.2-1 The grade division of initial checks

Grade	No.1	No.2	No.3	No.4	No.5
Degree of initial check	No checks or only have end checks	Short end-to-surface checks and short-narrow surface checks	Long end-to-surface checks and long-narrow surface checks no more than two or short-narrow surface checks no more than fifteen	short-narrow surface checks more than fifteen or long-narrow and wide surface checks no more than five	short-narrow surface checks more than five or wide surface checks more than five

Note: long check -- check length ≥ 50mm; short check -- check length <50 mm; narrow check -- check width <2 mm; wide check -- check width ≥ 2mm

Tab.5.2-2 The grade division of internal checks

Grade	No.1	No.2	No.3	No.4	No.5	No.6
Degree of internal check	No :hecks	1 wide or 2 narrow checks	2-3 wide checks; 4-5 narrow checks; 1 wide and 3 narrow	4-5 wide; 7-9 narrow; 1 wide and 4-6 narrow	6-8 wide; 15 narrow; 4 wide and 6-8 narrow	15-17 wide or continuous checks

Tab.5.2-3 The grade division of cross-section deformation

Grade	No.1	No.2	No.3	No.4	No.5	No.6	No.7	No.8
A-B (mm)	0-0.3	0.3-0.5	0.5-0.8	0.8-1.2	1.2-1.8	1.8-2.5	2.5-3.5	over 3.5

Based on these drying characteristics in 100℃-test, the drying condition of this species could be gained by the relationships of drying characteristics and drying conditions showed Tab.5.2-4, which are very helpful to predict the drying schedules.

Tab.5.2-4 Drying condition based on degree of drying defects

Name	Drying condition (℃)	Grade of effects							
		No.1	No.2	No.3	No.4	No.5	No.6	No7	No8
Initial checks	Initial temperature	70	65	60	55	53	50	47	45
	Temperature depression	6.5	5.5	4.3	3.6	3.0	2.3	2.0	1.8
	Finial temperature	95	90	85	83	82	81	80	79
Cross section deformation	Initial temperature	70	66	58	54	50	49	48	47
	Temperature depression	6.5	6.0	4.7	4.0	3.6	3.3	2.8	2.5
	Finial temperature	95	88	83	80	77	75	73	70
Internal checks	Initial temperature	70	55	50	49	48	45	43	40
	Temperature depression	6.5	4.5	3.8	3.3	3.0	2.5	2.2	2.0
	Finial temperature	95	83	77	73	71	70	68	67

5.2.2 Result and suggestion

From the results of 100℃-test, the detailed data of drying defects results of *E. citriodora* were shown in Tab.5.2-5, and the consideration of all 8 test samples, the comprehensive drying defects grades of *E. citriodora* were shown in Tab.5.2-6. Corresponding to the drying condition based on degree of drying defects (Tab.5.2-4), and then the drying condition of *E. citriodora* was show in Tab.5.2-7, which would be used to determine the kiln schedule in the follow-up test. And the MC curve during 100℃-test was showed in drying Fig.5.2-3.

Tab.5.2-5 The drying defects data and grades of *E. citriodora*

No	Surface checks			End –surface checks			End checks		Grade	Internal checks			Cross section deformation	
	Long -narrow	Short -narrow	Wide	Long -narrow	Short -narrow	Wide	Wide	Short -narrow		Narrow	Wide	Grade	A-B (mm)	Grade
1	0	23	0	0	16	0	0	Many	4	5	2	3	2.10	6
2	6	22	0	1	12	0	0	Many	5	7	2	3	1.80	5
3	0	16	0	0	11	0	0	Many	4	3	0	3	0.80	4
4	0	20	0	0	17	0	0	Many	4	5	2	3	1.40	5
5	0	11	0	0	10	0	0	Many	3	1	0	2	2.17	6
6	0	16	0	0	9	0	0	Many	4	1	0	2	1.75	5
7	0	11	0	0	8	0	0	4	3	4	0	3	0.79	4
8	0	4	0	0	8	0	0	Many	3	2	0	2	1.78	5

Tab.5.2-6 The comprehensive drying defects grades of *E. citriodora*

Drying defects	Initial checks	Internal checks	Cross section deformation
Grade	No.4	No.3	No.5

Tab.5.2-7 The kiln drying condition of *E. citriodora*

Item	The initial temperature	The initial wet-bulb depression (Δt)	Final temperature)
Temperature (℃)	50	4	77

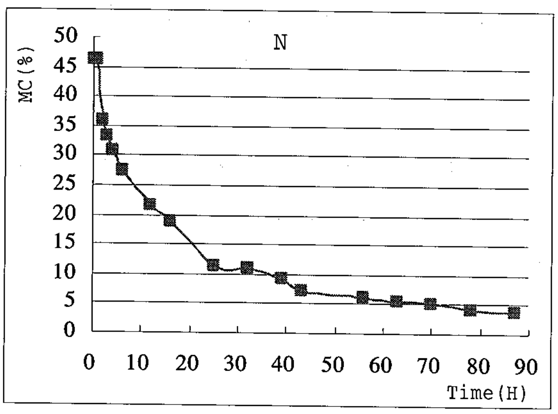

Fig.5.2-3 MC curve in 100℃-test of *E. citriodora*

5.3 Drying schedule

5.3.1 Material and method

The sample dimension was with 500mm x 110mm x 25mm, double end-sealed with silicon sealing glue. The capacity for the stack was 500x400x300 mm, so 15 pieces of samples could by dried each time. To make it easy to fetch every sample for measurement and observation, all these 15 pieces of samples were put on a special made frame, so no heavy load on top on stack during test.

The test dryer was electric heating with 3 group of heater, which could be used independently of simultaneously according to the drying test need, the maximum of 3 group of heater was 6 kW. There was an electronic heated small boiler to afford steam during conditioning. The control system of the test dryer was semi-automatic.

Other equipment: Electric oven with air circulation, electronic balance, thermo-electronic couple temperature measuring system.

Based on the results of drying characteristics test, a schedule of *E. citriodora* wood with thickness of 25 mm was drafted, seeing in Tab.5.3-1.

Tab.5.3-1 The predicted drying schedules of *E. citriodora* (25mm)

MC stage	Dry-bulb temperature (t℃)	Wet-bulb temperature depression (Δt℃)
Above 40	50	2
40-35	54	3
35-30	58	5
30-25	62	8
25-20	66	12
20-15	70	18
Below 15	77	24

Beginning with this schedule, a series of kiln drying test had been done till the optimized schedule was gained.

5.3.2 Result and suggestion

The main problem of *E. citriodora* wood drying was small surface check. To reduce this drying defect, strictly control the drying condition in drying early stage is very important. Results showed that to decrease surface check, at early drying stage, the temperature depression should not be too big, and switching from one temperature and humidity to another temperature and humidity should be very slowly.

The optimised kiln drying schedule for *E. citriodora* wood with thickness of 25 mm was listed in Tab.5.3-2.

Tab.5.3-2 Drying schedule for *E. citriodora* wood with thickness of 25 mm

MC (%)	Dry-bulb T(℃)	Wet-bulb T(℃)	Notes
Pre-heating	55	54	Pre-heating, 3 hours
Above 35	50	47	
35 ~ 30	55	50	
=30%	70	68	Conditioning, 3 hours
30 ~ 25	60	54	
25 ~ 20	65	57	
=20%	75	72	Conditioning, 3 hours
20 ~ 15	70	55	
15 ~ 10	75	55	
Below 10	80	55	
=8%	85	79	End-treatment, 3-5 hours

5.4 Pilot drying test

5.4.1 Material and method

Pilot Testing Equipments:

Pilot Plant: Beijing Youwei Wood Industry Co. Ltd., Located in Changping District, Beijing

Drying Testing Kiln: 60m^3 capacity, conventional drying kiln

Heated by hot water

Forklift stack loading

Semi-automatic controlling

Other testing facilities: Electronic heated oven, Electronic balance, Digital calipers, Portable electric-resistance MC meter and Electromagnetic MC meter, etc.

Test Material:

The detail description of testing material for pilot drying was as followings:

Species: *E. citriodora*

Sample size: 1500 x 120 x 25 mm

Initial Moisture Content: 35-40%

Target Moisture Content: 8-10%

Total number of samples: 570 pieces

Testing sample volume: 2.56 m^3

Because the total volume of *E. citriodora* plantation wood samples was not enough for the 60 m^3 capacity kiln, after consulting with the pilot plant, these *E. citriodora* plantation wood samples were finally decided to be dried mixed with the pilot plant owned wood, which drying characteristics is closed to that of *E. citriodora* plantation wood samples, so as to the total volume of wood to be dried could be match the capacity of pilot drying kiln. The detailed description of mixed drying materials was as followings:

Species: *Catalpa bungei*

End-use for: solid wood flooring

Sample size: 1000 x 100 x 30 mm

Initial Moisture Content: around 35%

Target Moisture Content: 8-10%

Total volume: around 45 m^3

Test schedule:

Based on the laboratory optimized drying test results, the pilot test drying schedule of *E. citriodora* plantation wood was selected, seeing in Tab.5.4-1.

Because the drying characteristics is closed to that of *E. citriodora* plantation wood samples, to guarantee the pilot testing result, the pilot test drying schedule of *E. citriodora* plantation wood samples was used for executive drying schedule.

Tab.5.4-1 Pilot test drying schedule

MC (%)	Dry-bulb T(℃)	Wet-bulb T(℃)	Notes
Pre-heating	55	54	Pre-heating, 3 hours
Above 35	50	47	
35 ~ 30	55	50	
=30%	70	68	Conditioning, 3 hours
30 ~ 25	60	54	
25 ~ 20	65	57	
=20%	75	72	Conditioning, 3 hours
20 ~ 15	70	55	
15 ~ 10	75	55	
Below 10	80	55	
=8%	85	79	End-treatment, 3-5 hours

Notes: Species: *E. citriodora* Sample size: 1500 x 120 x 25 mm

Initial Moisture Content: 35-40% Target Moisture Content: 8-10%

5.4.2 Result and suggestion

Visible drying defects:

During and after drying, visible drying defects including end check, end-to-surface check, surface check, and internal check. Result showed that some small end and end-to-surface checks occurred at the early drying stage. To compare the influence of end-sealing on the end checks, half of these samples were end-sealed with asphalt varnish, and the other half without end-sealing. Result showed that the end checks and end-to-surface checks of samples with end-sealing with asphalt varnish were less than those without end-sealing, but the difference was not so significant. It is suggested that in practical production, if possible, end-sealing all wood before stacking, so as to get better drying quality.

Because of the conformation of *E. citriodora* plantation wood, many very small surface checks occurred during the early drying stage, and becoming invisible with the drying process going on. After planing off about 2 mm surface layer of dried wood, all the tiny surface checks were removed. So as a result, these tiny surface checks were not taken into account as visible drying defects. For those surface checks with length more than 5 cm could have big influence on the final use of dried *E. citriodora* plantation wood, so the total length of these kinds of surface checks were calculated, being divided by the double sample length, the percentage of surface checking rate could be got. Result showed that surface checking rate for *E. citriodora* plantation wood pilot drying was 5.6%, within the National Sawn-timber Drying Quality Standard (GB/T 6491-1999) 2nd grade requirement.

No internal checks were found after cutting these *E. citriodora* plantation dried woods during follow-up finger-joint pilot testing by another project group.

Final moisture contents (W_f):

The drying curve of *E. citriodora* plantation wood pilot drying was showed in Fig.5.4-1.

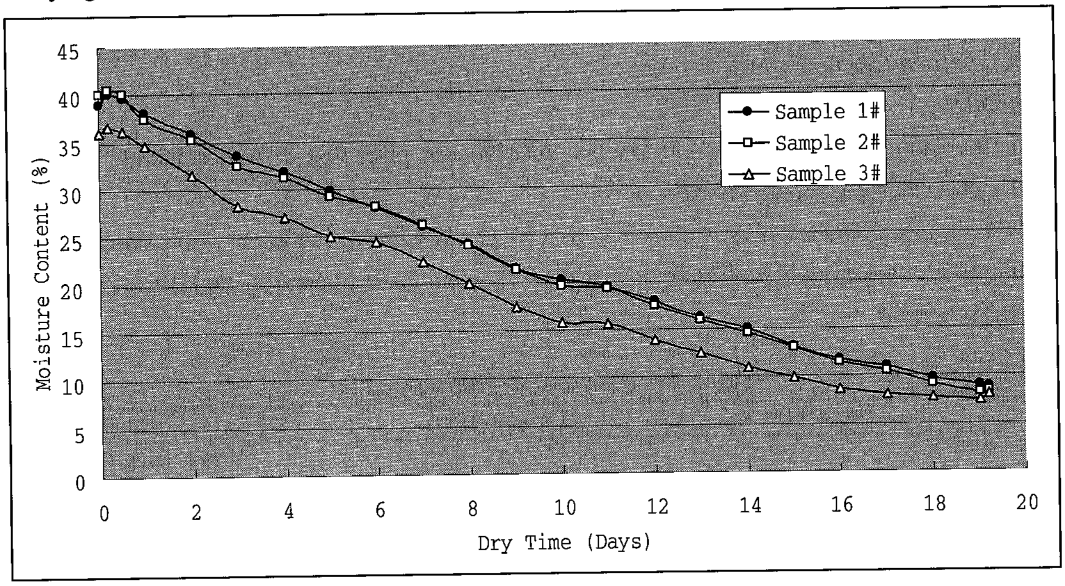

Fig.5.4-1 The drying curve of *E. citriodora* plantation wood

The moisture content after drying is one of the most factors for drying quality evaluation. In this pilot drying test, final moisture contents (W_f) and moisture content gradient along thickness direction (W_g) were measured, seeing in Tab.5.4-2.

Tab.5.4-2 Pilot test drying results on moisture content and drying stress

Index	Max.	Min.	s	V%	Average
Wi	40.5	35.2	8.21	25.2	38.5
Wf	10.9	7.2	0.61	15.8	8.5
Wg	2.2	1.1	0.16	9.8	1.9
Y	5.0	1.6	0.53	15.8	3.8

Notes: W_i—initial moisture content(%); W_f—final moisture content(%); W_g—moisture content gradient (%) along the thickness direction; Y—drying stress(%); s—variance, V%— indicates of variance(%).

Result showed that average final moisture content of *E. citriodora* plantation wood after dried was 8.5%, met the National Sawn-timber Drying Quality Standard (GB/T 6491-1999) 2nd grade requirement.

Moisture content gradient along thickness direction (W_g):

Besides the final moisture contents (W_f), another important factor of moisture content is moisture content gradient along thickness direction (W_g). If the dried wood with big moisture content gradient along thickness direction, the final wood products may not be stable in dimension. The moisture content gradient along thickness direction (W_g) of *E. citriodora* plantation wood after dried was measure and showed in Tab.5.4-2. Result showed that the average moisture content gradient along thickness direction (W_g) was 1.9%, met the National Sawn-timber Drying Quality Standard (GB/T 6491-1999) 1st grade requirement.

Drying stress index (Y):

Drying stress index (Y) is also an important factor. Similar to the influence of moisture content gradient along thickness direction, if the dried wood with big drying stress, the final wood products may not stable in dimension and in danger to occur checks.

Drying stress index (Y) of *E. citriodora* plantation wood after dried was measure and also showed in Tab.5.4-2. Result showed that the drying stress index (Y) was 3.8%, nearly met the National Sawn-timber Drying Quality Standard (GB/T 6491-1999) 2nd grade requirement (3.5%). It is suggested that in practical drying on *E. citriodora* plantation wood, longer end-treating time is needed.

Drying deformation:

The main drying deformation defects of *E. citriodora* plantation wood pilot drying was cupping, bowing and twisting. Result showed that the sample with pith or closed to pith was easy to have cupping deformation, and the drying deformations of samples on top position of stack were more serious e than those on the lower position of stack. It is suggested that in practical drying on *E. citriodora* plantation wood to reduce the drying deformations: a)Pre-sorting. The wood with pith or closed to pith can be selected out during stacking, and use special schedule for these selected woods; b) Decreasing the stickers space; c)Heavy stack top-loading.

Conclusion and suggestion:

- Through this pilot drying test, it was showed that laboratory optimized drying schedule could be use for drying of *E. citriodora* plantation wood with thickness of 25 mm.
- The drying quality based on visible defect factors met the National Sawn-timber Drying Quality Standard (GB/T 6491-1999) 2nd grade requirement.
- The final moisture content of *E. citriodora* plantation wood after dried was 8.5%, met the National Sawn-timber Drying Quality Standard 2nd grade requirement; meanwhile the average moisture content gradient along thickness direction (Wg) was 1.9%, met the 1st grade requirement.
- The drying stress index (Y) was 3.8%, nearly met the National Sawn-timber Drying Quality Standard 2nd grade requirement (3.5%). It is suggested that in practical drying on *E. citriodora* plantation wood, longer end-treating time is needed.
- The main drying deformation defects of *E. citriodora* plantation wood pilot drying was cupping, bowing and twisting. To reduce the drying deformations, It is suggested that in practical drying on *E. citriodora* plantation wood a)Pre-sorting. The wood with pith or closed to pith can be selected out during stacking, and use special schedule for these selected woods; b) Decreasing the stickers space; c)Heavy stack top-loading

6 ADHESION PROPERTIES

6.1 Finger joint

Finger-joints are commonly used to produce wood products from short pieces of lumber. Such joints must have excellent mechanical performance. To produce acceptable products, a jointer must be subjected to a proper end pressure following machining and adhesive application; also technical parameters, such as machining and gluing processes must be optimized. The condition of finger geometry and end pressure plays a major role in the gluing process and the final strength of the assemblies.

The main function of the end pressure is to bring the mating surfaces so close together that the glue forms a thin and continuous film between them. This pressure also allows a uniform distribution of the adhesive and creates an optimum glueline's thickness. So it is necessary to control the glueline's thickness to produce strong joints. Thin glueline lead to starved joints. Above the optimum glueline's thickness, stress concentration develops in the adhesive layer due to cure-shrinkage. The pressure must be applied to force fingers together to form an interlocking connection, giving a certain immediate handling strength. The increase of the end pressure up to a certain point gives a better contact of the finger to obtain strong joints. However, cell damage or splitting of the finger root can be induced by excessive pressure.

Finger-joint geometry has been proven to the most critical variable determining joint strength. Finger-tips constitute a series of butt joints and are accorded zero strength even if they are tight apparently well bonded; the tip width is the geometric parameter that most significantly influences finger-joint strength.

The objective of the study was to investigate the effect of finger profile geometry and end pressure on the performance of finger-joints in four species of Eucalyptus. The study also planned to evaluate which combination of the end pressures and finger profile geometry would result in optimum finger-joint performance in each of the four Eucalyptuses.

6.1.1 Materials

The experiments were carried-out with the samples which were planed and crosscut to dimensions of 20 by 60 by 520 mm; the total number of the samples was 90 in each kind of eucalyptus; then the 90 wood blocks were divided three groups based on the density. The result of the density condition was as Tab.6.1-1:

Tab.6.1-1. Groups divided by density

Species	Average of high density /g/cm^3	Average of medium density /g/cm^3	Average of low density /g/cm^3
E. citriodora	1.044	1.015	0.983

Two kinds of adhesive, API and PVAc, were used in the experiments. API is a kind of two-components adhesive, and is made of main reagent and cured reagent, the mixing ratio is 100:15 when the adhesive was used. The technical index of the two kinds of adhesives was Tab.6.1-2:

Tab.6.1-2. Technical indexes of two kinds of adhesive

Adhesives	Type	Colour	Solid cotent /%	pH	Viscidity /cps，25℃
PVAc	BT-09	White Emulsion	25.7	4.4	8740
API	DYNOLINK-8000G	White Emulsion	63.8	6.6	6750

6.1.2 Method of Experiments

The geometry of finger(ΔT), feed speed, the amount of adhesives spreading, end pressure, were all important factors to be investigated in the finger-joints experiments.

Three kinds of finger geometry were studies to determine finger parameter for optimum finger-joint strength, and they were selected based on specifications in standards, data from the literature. The finger-jointing machines used a carriage clamp to secure the stacks of wood samples; the samples were guided through a circular saw, a finger profile cutter, and a suction device that removed sawdust and shavings. The ends of pieces to be jointed were first trimmed and squared cleanly by the circular saw before the profile was cut. The suction completely removed all shavings from the profiled surfaces. Finger profiles were processed as vertical orientation joints subsequent test evaluation. The parameters of the three kinds of finger were as tab.6.1-3.

Tab.6.1-3. Parameters of the fingers

ΔT /mm	Length /mm	Tip width /mm	Pitch /mm	Slope
0	11	0.6	3.8	1/8
0.1	10.6	0.7	3.8	1/8
0.5	8.9	1.1	3.8	1/8

In the processing of making samples finger, the feed speed was important to affect the roughness surface of finger. In this experiment, because different Eucalyptus woods have different density, the feed speed for *E. citriodora* was chose in 5mm/min.

End pressure is needed to ensure the closest possible contact between the finger surfaces to be glued, and for the adhesive to form a thin continuous layer uniform in thickness, without damage to the strength of the wood. It is also intended to force the fingers together to the degree that a locking action is obtained, giving a certain immediate handing strength after gluing. Since the higher the pressure the more efficient the locking action, as much pressure as the wood can withstand may be used without causing damage such as splitting at the finger roots, compression failure of the wood, and squeezing out of the glue.

In the experiment, the preliminary end pressure experiment was done to get the suitable pressure. Firstly, four pieces of wood block were selected from the three groups (High, Middle, Low) and then finger were cut; ΔT of the fingers were 0mm, 0.1mm, 0.5mm; and the samples were cut to 60mm length. PVAc was used as adhesive in the experiment with the spread amount 250g/m^2. Two samples were combined and laid under the loading machine to be pressured as Fig.6.1-1. The loading speed was 2mm/min.

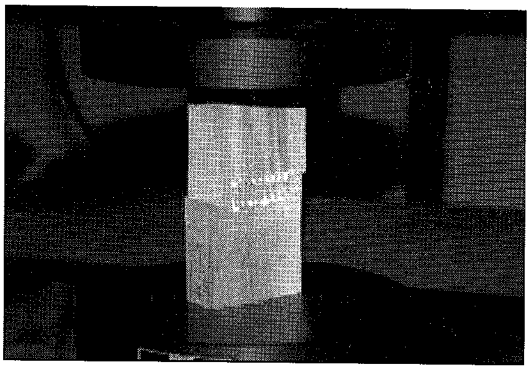

Fig.6.1-1 The method of measuring end-pressure

After the samples had been cut to finger, the samples were jointed by the finger jointer machine. 54

samples were selected from the group. The six kinds of sample were arranged as HH, HM, HL, MM, ML, LL on the basis of density. ΔT were 0, 0.1mm, 0.5mm, the end pressure was used from the result of preliminary end pressure experiments.

Because many factors affected the strength of finger-jointed lumber, for the sake of getting the better processing conditions, the end pressure and ΔT were main factors considered in the research, the design methods of full factors experiments and SAS analysis software were used to discuss the effect on the performance of finger-jointed lumber by each factor, and the interaction between the end pressure and ΔT. Finally integrative evaluation was processed by the result of SAS analysis and the appearance of finger-jointed samples to find the optimum processing condition.

After that, the finger-jointed specimens were cured over 48 hours before further processing. No pressure was applied to the specimens during curing. Both faces of a specimen were planed to a final specimen dimension of 58 by 17.5mm. The bending test was done by using the loading machine to measure MOE and MOR as Fig.6.1-2 according to JAS MAFF, Notification NO.590; support span was 420mm; loading span was 140mm and loading speed was 2mm/min.

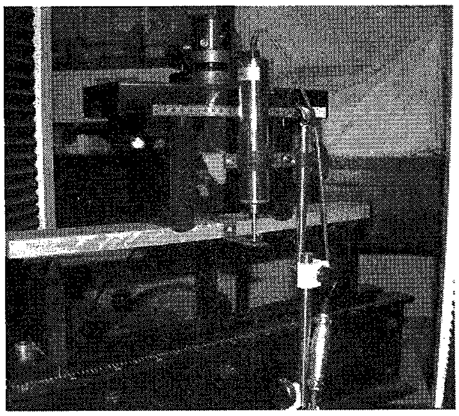

Fig.6.1-2 Four-points bending test

In the experiment, API (DYNOLNK-8000G) was used to make finger-jointed samples. Bending test were performed according to JAS MAFF, Notification NO.590; then MOE and MOR of finger-joints were compared with different kinds of adhesive

To compare the difference of MOR and MOE between V type finger(Fig.6.1-3) and H type finger(Fig.6.1-4), in the experiment, the H finger was done to make finger-jointed lumber, ΔT was 0.1mm; bending test were performed also according to JAS MAFF, Notification NO.590

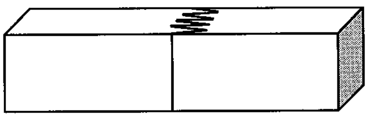

Fig.6.1-3. V-type finger-joint

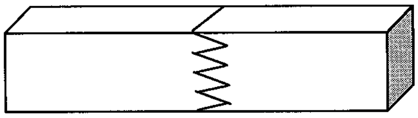

Fig.6.1-4 H-type finger-joint

6.1.3 Result and Discussion

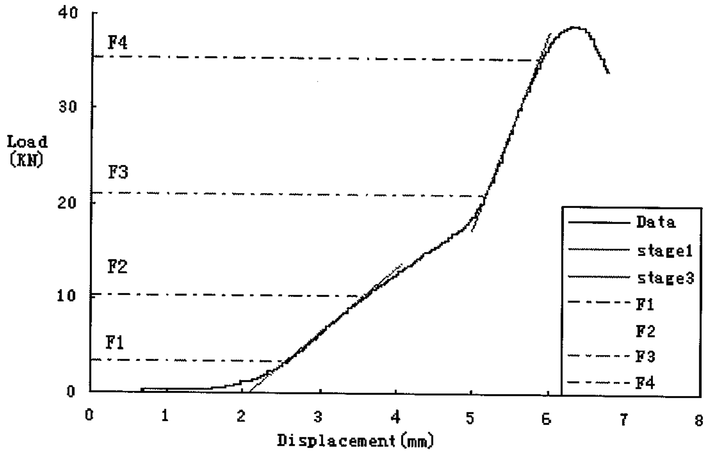

Fig.6.1-5. Load-displacement curve

Fig.6.1-5 is the typical Load-displacement curve, in this case △T is 0.5.When the cross head began to push the upper specimen, the upper specimens begin to move, the finger-tip will touch the nether specimen quickly, so when loading reached F1, it was considered the finger-tip touch the nether specimen, when the loading approached F2, it was considered the finger-tip was damaged, when the loading aroused to F3, there was splitting on the finger root, and following stage was as the same as solid wood pressured, the solid wood begin to damage when the loading increased to F4.

In the experiment, F1 was thought the suitable pressure before the finger was damage. Tab.6.1-4 was the results of end pressures in different ΔT.

Tab.6.1-4. End-pressure at different conditions

Wood species	ΔT	Average pressure /MPa
	0	11.52
E.citriodora,	0.1	13.06
	0.5	7.57

In the experiments, the four species of Eucalyptus end pressures were selected from Tab.6.1-5:

Tab.6.1-5. Different levels of the end-pressure

Wood Species	Three end pressure /KN		
	P1	P2	P3
E.citriodora	8.5	10	11.5

Tab.6.1-6 and Tab.6.1-7 were the results of the bending test analysis of *E. citriodora*

Tab.6.1-6. MOE and MOR analyzed by SAS

Index	Resource of variance	Degree of freedom	Summation of square	Average of square	F	Pr > F	Markedness
MOE	Matrix	29	245.494	8.466	1.32	0.2684	/
	Combination of density	5	90.635	18.127	2.82	0.0454	**
	End pressure	2	26.903	13.451	2.09	0.1508	/
	ΔT	2	61.756	30.878	4.81	0.0205	**
	End pressure × ΔT	4	7.207	1.802	0.28	0.8870	/
	Combination of density × pressure	8	35.947	4.493	0.70	0.6884	/
	Combination of density × ΔT	8	23.046	2.88	0.45	0.8766	/
	Error	19	122.071	6.425			
	Summation	48	367.565				
MOR	Matrix	29	1495.705	51.576	1.88	0.0777	*
	Combination of density	5	336.462	67.292	2.45	0.0713	*
	End pressure	2	275.845	137.922	5.02	0.0178	**
	ΔT	2	258.776	129.388	4.71	0.0218	**
	End pressure × ΔT	4	255.952	63.988	2.33	0.0932	*
	Combination of density × pressure	8	216.694	27.087	0.99	0.4768	/
	Combination of density × ΔT	8	151.976	18.997	0.69	0.6947	/
	Error	19	522.146	27.481			
	Summation	48	2017.851				

Mark: /means unmarkedness at 0.1; *means markedness at 0.1; **means markedness at 0.05

Tab.6.1-7 Testing for groups of each factor

Factor	Level	Number of specimen	MOE(Gpa)		MOR(Mpa)	
			Average	STDEV	Average	STDEV
End pressure	8.5	14	24.998A	3.097	33.637A	7.761
	10	17	26.255A	2.356	32.683A	4.103
	11.5	18	26.019A	2.877	38.567B	6.038
ΔT	0	14	26.230A	1.863	32.466A	5.350
	0.1	17	27.476A	2.276	38.484B	6.324
	0.5	18	23.907B	2.708	34.000A	6.381
Combination of density	HH	3	27.383A	2.425	40.651A	9.646
	HL	14	24.901AB	3.170	32.821AB	6.408
	HM	13	26.687A	2.042	37.524A	6.651
	LL	6	23.002B	1.559	31.378B	5.226
	ML	9	26.974A	2.040	35.104A	5.164
	MM	4	26.540A	3.607	36.822A	5.192

Mark: The A,B behind average in table means the checked result by T, the same word letter means there was no difference in Stat., the different letter means there was difference in Stat..

From Tab.6.1-6 it is indicated that the combination of density and ΔT had much effect on the MOR of finger-jointed lumber of *E.citirodora* wood; end pressure had much effect on MOR; the interaction of end pressure and ΔT had no effect on MOR and MOE.

From Tab.6.1-7 it is shown that the change of end pressure had no effect on MOE, but to MOR, the higher end pressure, the higher MOR of finger-jointed lumber of *E.citirodora* wood; different ΔT can lead to different MOR and MOE, the MOR was higher when ΔT was 0.1mm.

The results of finger-joints analysis of *E. citriodora* wood was as following:

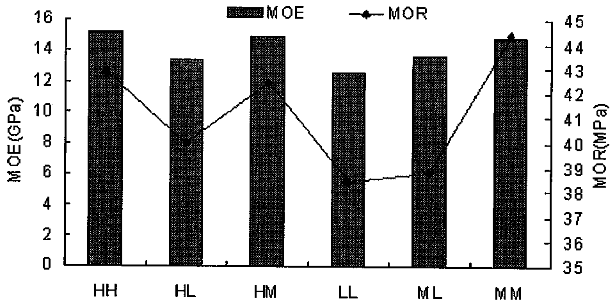

Fig.6.1-6. Combination of different density

Combination of different density has affection the MOE and MOR, especially to the MOE. From the Fig.6.1-6 it was evident that the higher density of combination, and the higher MOE and MOR of finger-joints lumber of *E. citriodora* wood; the highest density combination of MOE could reached 27.38GPa, and 40.65MPa for MOR.

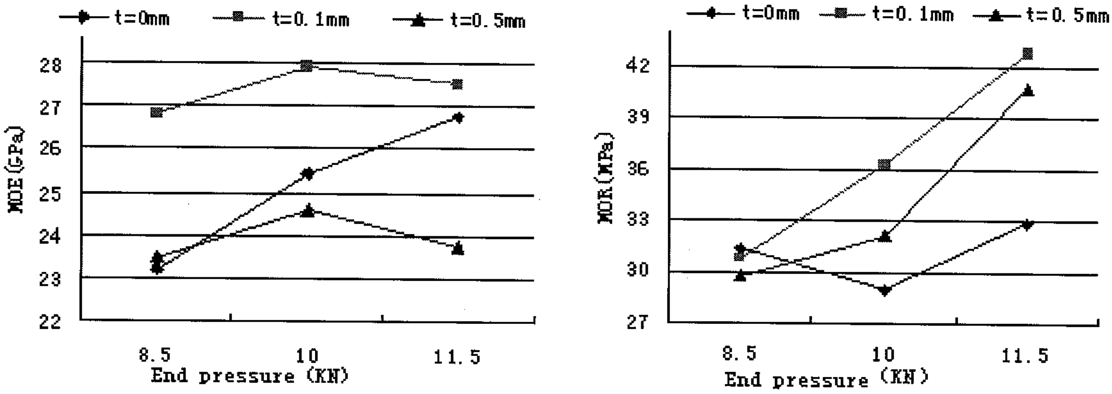

Fig.6.1-7. Effect of end-pressure on MOE and MOR

From Fig.6.1-7 it can be concluded that when the ΔT was 0mm, the MOE of finger-joints increased with the end pressure increasing from 8.5KN to 11.5KN. However, when the ΔT were 0.1mm and 0.5mm, the MOE of finger-joints increased from 8.5KN to 10KN, the MOE decreased with the increasing of end pressure when it was over 10KN. When ΔT were 0.1mm and 0.5 mm, the MOR of two type of finger-joints increased gradually as the increasing of end pressure from 8KN to 11.5KN. When ΔT was 0.1mm, the MOE and MOR of finger-jointed lumber were higher than other two kinds of finger-jointed lumber when ΔT were 0 and 0.5mm. The results shown that when the end pressure was 11.5KN, the finger-jointed lumber has the highest MOE and MOR; but there was some splitting in the root of finger. Therefore, the suitable ΔT was 0.1mm and the optimum end pressure was 10KN for finger-jointed lumber of *E. citriodora.*

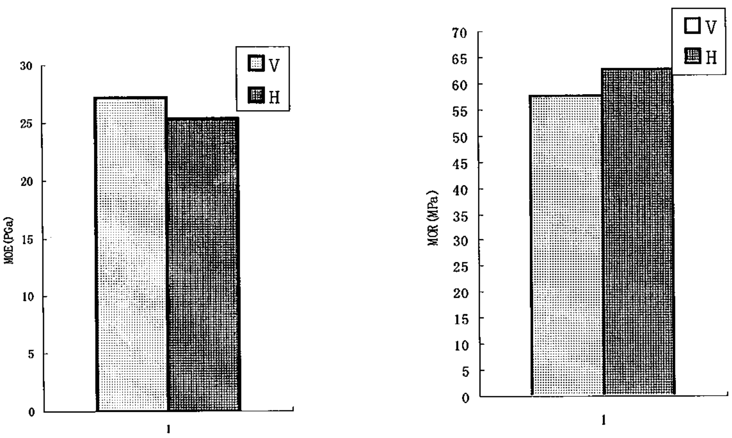

Fig.6.1-8. Comparison between V-type and H-type finger-joints on MOE and MOR

From the Fig.6.1-8 it was shown that the MOR of finger-joints with different finger type V and H were almost the same, but in the same processing condition, the MOE of finger-joints in V finger type was higher than that in H type.

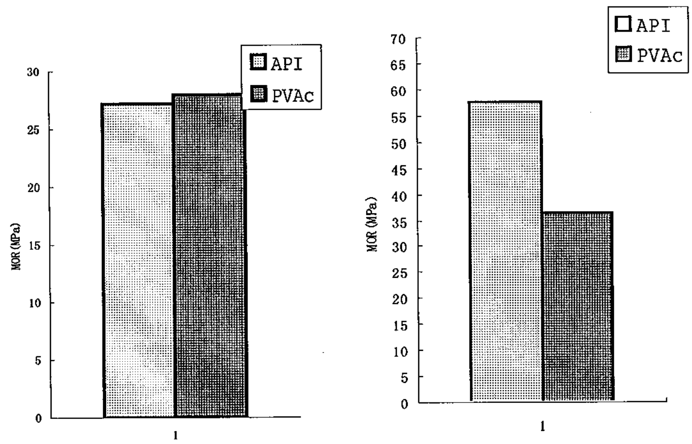

Fig.6.1-9 Comparison between API and PVAc finger-joint on MOE

From Fig.6.1-9 it was indicated that there were no much difference with API and PVAc in MOE, but for MOR, the API products was higher than PVAc remarkably, especially for *E. citriodora* wood, which was high density and had much extraction. For example, the MOR was 30.35 MPa for PVAc, but for API, the MOR increased to 57.69. Tis could be explained that for API adhesives, in the action of Vander waals force and hydrogen bond between the molecule of adhesive and molecule of wood, it forms deep-set physical bonding with wood. The gluing surface and the formed nail adhesive react with hydroxyl, carboxyl, phenolic hydroxyl and other reactive group in celluloses, hemicelluloses, lignin of wood, at the same time adhesive reacts with water in wood, then forms some chemical bond between wood and adhesive, in the end form intercross structure, thereby increases strength of gluing.

6.2 Gluing

6.2.1 Method

Based on referred data, a detailed experiment plan was set out. *E. citriodora* eucalyptus species were selected. Because of adhesion being a very important basic work on finger-joint lumber and Glulam, it is essential to make sure the adhesives selected, the suitable bonding processing. Meanwhile, gluability research was implemented combining with wood properties and wood chemical components.

Firstly, surface property of *E. citriodora* wood planed wood were measured by surface contact angle testing, and compared the results with the medium of pure water and API adhesive, furthermore, by contrast the contact angle between newly and old planed board of two eucalyptus species to search for the better gluability effect.

Shown as Tab.6.2-1 was contact angle of water and API main agent on two species planed board compared with newly planed and old planed board.

Tab.6.2-1 Contact Angle of Water and API of *E. citriodora*

Liquid	Index	Average / (°)		Radial / (°)	
		New	Old	New	Old
Water	Average	22.3	48.7	31.7	47.7
	Stedv.	2.3	5.1	3.8	4.2
API	Average	72.3	80.3	67.0	81.3
	Stedv.	0.6	3.2	5.0	2.3

Secondly, 4 kinds of adhesives UF PF API and PVAC were selected by this experiment, through comparing gluability of 4 adhesives with *E. citriodora* wood, feasible adhesive was abtained for two species. Following table 6.2-2 is comparison of shear strength of 4 kinds of adhesives.

Tab.6.2-2 The Longitudinal Shear Strength of 4 Kinds of Adhesives

Adhesives	Test number	Shear strength /MPa	Stedv. /MPa
PVAc	42	1.32	0.43
UF	42	1.41	1.05
PF	42	2.19	0.90
API	42	5.86	2.05

Thirdly, gluing process experiment arranged by Orthogonality and SAS statistical methods to gain suitable processing parameters, and these analyzed on different wood grain direct, that is, T-T (tangential to tangential bonding), T-R (tangential to radial bonding), R-R (radial to radial bonding). Finally, gluing processing microcosmic structure was observed by SEM.

Following Tab.6.2-3 shown was gluing processing that confirm suitable parameters.

Tab.6.2-3 The testing result value on each factor and level by SAS

Factor	Level	Number	Shear strength Ave. /MPa	Shear strength Stedv. /MPa	Wood failure Ave. /%	Wood failure Stedv. /%
Grain	T—T	84	5.64 A	1.81	53.93 B	30.13
	R—R	84	5.25 AB	0.94	71.77 A	19.13
	T—R	84	4.98 B	1.01	68.23 A	21.41
Pressure /MPa	1.5	126	4.97 B	1.12	65.07 A	24.46
	2.0	126	5.61 A	1.50	64.22 A	25.45
Time /Min	40	126	5.39 A	1.19	67.95 A	25.75
	60	126	5.19 A	1.43	61.34 B	24.15
Spread / g/m^2	150	84	4.90 B	1.33	56.23 B	22.68
	200	84	5.81 A	1.15	69.54 A	22.33
	250	84	5.16 B	1.31	68.18 A	23.30

According to those problems exiting in experiments, some improving methods or treatments were put forward on *E. citriodor* wood, and the better gluability was obtained by comparison experiments with different wood surface treatments.

Tab.6.2-4 Bonding strength and wood failure treated with different methods by SAS

Treatments	number	Shear strength Ave. /MPa	Shear strength Stedv. /MPa	Wood failure Ave. /%	Wood failure Stdev. /%
Untrented	42	5.29 AB	0.98	21.1 B	19.0
$FeSO_4$	42	4.80 B	0.57	56.6 A	32.9
NaOH	42	5.72 B	0.90	56.7 A	27.9
Newly planed	42	5.59 A	1.55	68.3 A	26.3

Finally, gluing durability is an essential index to gluability. With aging test in lab, different testing conditions to bonding board were adopted, which include room temp. water immersing and boiling water immersing.

Following Tab.6.2-5 was different methods to treat gluing board testing delamination.

Tab.6.2-5 The Results of Glue Line Delamination

Methods	Number	Cycle number	Delaminating number	Delaminating length /mm	Delamination /%	Delaminating rate /%
Room tep.	36	1	13	14.2	9.46	36.1
	36	2	21	26.5	17.7	58.3
	36	3	26	38.3	25.5	72.2
	36	4	30	49.6	33.1	83.3
Boiling water	36	1	31	70.2	46.8	86.1
	36	2	34	84.6	55	94.4

Through plenty of data. we referred, it is very important to find suitable adhesive, because our project mainly focus on finger-jointing, and its products are oriented at floorings, construction materials that need we select an excellent binder fitting at gluelam and lumber jointing, meanwhile it have better water resistance and weather tolerance. So 4 kinds of adhesives are picked up for our initial study used to be contrasted with each other.

4 adhesives (API, UF, PF, PVAc) have been contrasted for their Gluability with eucalyptus timber. Under the same testing conditions (i.e. spreading 250g/m^2, pressure 2.5Mpa, pressing time and temperature varying according to different adhesives), we made eucalyptus shear strength samples with 4 selected adhesives

respectively, then obtained their testing results by test machine. Comparing the shear strength results with these 4 adhesives, we found the optimal adhesive out of the 4 adhesives, which will be our foundation stone in future work.

The processing techniques of these 4 adhesives as follow Tab.6.2-6:

Tab.6.2-6 Processing technics of 4 adhesives

Parameter / Adhesive	Pressure /Mpa	Spreading / g/m^2	Temp. /℃	Pressing time
PVAc	2.5	250	Room temp.	9hrs
UF	2.5	250	100	31min
PF	2.5	250	140	42min
API	2.5	250	Room temp.	60min

The results of shear strength parallel to grain shown as follows Tab.6.2-7.

Tab.6.2-7 Shear strength on different adhesives

Adhesives	Test piece number	Ave. of shear strength /Mpa	Stedv.
PVAc	42	2.655	1.13
UF	42	1.812	1.32
PF	42	2.392	0.91
API	42	7.634	2.20

The results showed that Gluability of PVAc, UF, PF, etc. general adhesives is not so satisfied with eucalyptus timber, moreover, during sawing shear samples and checking shear strength, test samples often present a delamination or disjoining at glueline even on the condition of no strength imposed. The shear strengthes of former three adhesives are also lower than that of API adhesive drastically, and API illustrated an excellent bonding property with eucalyptus timber. So finally we adopt API as binder in finger-jointing of eucalyptus timber. Furthermore, UF and PF are hot-setting adhesives, on account of our experiment requirements (with thick plank to be glued and at the absence of high frequency equipment) and henceforth product orientation (oriented between structure and non-structure material), meanwhile, considering status quo of Glualam adhesives applied in nowadays, so API was a suitable adhesive for our demand.

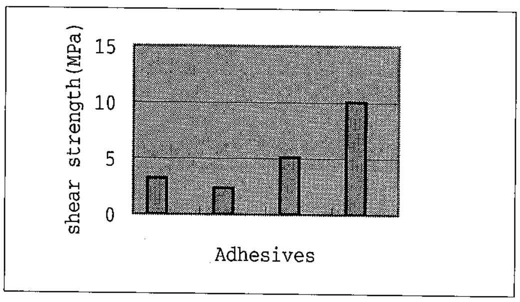

Fig.6.2-1 Shear strength comparison of 4 adhesives

Based on primary exploring experiments, we selected DYNOLINK-8000A API adhesive. Its performance indexes as shown following tab.6.2-8.

Tab.6.2-8. The indexes of DYNOLINK-8000A API adhesive

Indexes	Solid content /%	Viscosity / (cps.25℃)	Coagulation time /Min	pH	Gravity /g/cm^2
API	63.8	6750	9	6.6	1.1

At three levels of pressure, glue spreading, pressing time, shown in Tab.6.2-9, two species of eucalyptus timber were glued respectively and cut test samples from bonding blocks at parallel grain direction and three bonding forms are adopted, that is tangential to tangential (T-T), radial to radial (R-R), and tangential to radial (T-R). After 72hrs, examining shear strength of each sample.

Tab.6.2-9 Three levels of pressure, glue spreading, pressing time (room temp.)

Level	Spreading / g/m^2	Pressure /Mpa	Pressing time / Min
1	150	1.5	40
2	200	2.0	60
3	250	2.5	90

Testing results shown as follows: (shear strength: Mpa). Blank samples are wood blocks that have not glued and cut the same size as that of glued shear samples. Blank samples used to in comparison with shear strength of two eucalyptus species.

Tab.6.2-10 Shear strength of control samples (not glued test pieces) of two species

T-T			R-R		
Test number	Ave. of shear strength	Stdev.	Test number	Ave. of shear strength	Stdev.
21	24.06	2.644	21	21.37	1.33

From Tab.6.2-10 above, we can find out that the value of shear strength in T-T is more than that of R-R.

In initial experiments, $L_9(3^4)$ test is adopted and results of test are analyzed by ANOVA, then the primary conclusions can be obtained.

Tab.6.2-11 Shear strength of two species on different treat conditions

A	B	C	Pieces Num	T-T Ave	T-T Stdev.	R-R Ave	R-R Stdev	T-R Ave	T-R Stdev
1.5	40	150	36	13.81	1.37	6.853	0.337	7.67	1.66
1.5	60	200	36	12.15	1.13	11.93	1.12	13.52	1.11
1.5	90	250	36	15.12	1.52	13.70	1.57	12.88	1.36
2.0	40	200	36	8.24	1.28	10.00	0.84	13.90	1.84
2.0	60	250	36	10.30	1.49	13.75	1.27	9.55	1.25
2.0	90	150	36	13.57	1.02	8.27	1.05	13.99	1.88
2.5	40	250	36	15.67	1.81	7.98	1.39	11.44	1.38
2.5	60	150	36	14.46	1.30	11.48	1.88	9.18	0.63
2.5	90	200	36	16.82	2.0	12.37	1.08	13.42	1.52

Note:A: pressure (Mpa) B: Pressing time (min) C: Spreading (g/m^2)

Tab.6.2-11. Analysis by ANOVA on test pieces of *E. citriodora*

Source	Sum of squares	DF	Mean square	F value	Pr>F
A	27.633206	2	13.816603	16.86632	F0.1=9
B	20.005944	2	10.002972	12.210913	
C	3.701624	2	1.850812	2.2593389	
Variance	1.638366	2	0.819183		
Total	52.97914				

From the result above, A (pressure) and B (pressing time) exert certain effect on gluability of *E. citriodora* timber, but C (glue spreading) show no evident effect on bonging property of this specie.

II *Eucalyptus exserta*

The information of testing materials is as Tab.1.

Tab.1 Testing materials

Tree species	Tree age (year)	Tree number	Tree height (m) Ave.	Tree height (m) Std	Under branch height (m) Ave.	Under branch height (m) Std.	DBH (cm) Ave.	DBH (cm) Std
Eucalyptus exserta	27	10	19.96	1.6548	10.76	2.1925	26.05	1.4401

1 WOOD PROPERTIES

1.1 Anatomical characteristics

Samples (2×2×1 cm) for wood anatomical section were stored in alcohol 95% glycerine (1:1) until they sank. Transverse sections of 20μm were cut on sliding microtome, then bleached, stained with safranin, dehydrated and mounted on slides for measure anatomical properties on image analysis. Then the transverse, radial and tangential sections from each species of around 80μm were cut on the same microtome, make the samples for SEM observation and taking photos.

Prior to tracheid length measurement, the each selected growth rings were firstly separated with a chisel, then macerated in solution of acetic acid (1/3) and hydrogen peroxide 27% (2/3) for several days in 60° oven.

The measurement methods are as follows:

Measuring length and width of wood fiber and vessel element using macerated anatomical elements under fiber length measuring instrument; (2) Measuring wood fiber cell wall thickness, cell wall percentage, and tissue proportions by section method using image analysis system; (3) Measure of S_2 microfibril angle: using x-ray diffractometer.

The observation and description for macro- and micro-structure were made under the light microscope and scanning electronically microscope (SEM).

1.1.1 Tree and distribution

Evergreen a tree up to 15-25 m, 0.6 m in d.b.h., trunk straight generally in origin producing country. Bark flat split or little smooth. It naturally distributed in E Queensland in Australia. *Eucalyptus exserta* as planted species introduced into many countries in the world. In Guangdong, Guangxi, Hainan provinces large plantation was established from 50 decades in 20 century, Fujian, Jiangxi, Yunnan, Sichuan, and Zhejiang province etc. are introducing this species.

1.1.2 General characteristics

Sapwood yellow, yellowish brown, comparatively differs from heartwood, width 2~3cm. ***heartwood*** dark yellowish brown; glossy, wood without characteristic taste & odor. ***Growth rings*** indistinctly or little distinct. Wood diffuse-porous. Pores small to middle, visible to the naked eye, radial, fairly uniformly distributed throughout the ring, with tyloses. ***Longitudinal parenchyma*** vasicentric. ***Rays*** very fine to fine, visible with a hand lens; ***Ripple mark***s and ***Resin canals*** absent.

1.1.3 *Minute anatomy* (Plane I)

Vessels most solitary; radial or flexuous; cell wall thin to thick; tangential average diameter 98 μm, max 154 μm. 15 (11~19) /mm^2. Vessel element length 365 (170~570) μm, tyloses abundant, wall thin in heartwood, helical thickness absent. Simple perforation, its plate oblique. Intervessel pits ventured, alternate, round & polygonal, ventures distributed pit aperture and & chamber, most coralloid and dendritic. Vasicentrics common, located vessels intermixing parenchyma cells, with bordered pit round and ventured. Vessel- ray pits large round.

Longitudinal parenchyma vasicentric, diffuse or diffuse-aggregates. Nodular end wall of parenchyma cells inconspicuous; crystals absent.

Fiber wall thick to thick, 1233 (988~1450) μm in length, with plain simple pits.

Rays unstoried, rays 12~14/mm. Ray tissues homogeneous uniseriate and multiseriate; parenchyma cells round or oval, some with gum. Crystal and intercellular canals absent.

The data of anatomical parameter and basic density at different heights is including to the Tab.1.1-1, the vessel distribution frequencies and tangential diameters are listed in Tab.1.1-2.

Tab.1.1-1 Anatomical parameter at 1.3 m for *Eucalyptus exserta*

Fiber length (μm)		Fiber width (μm)		Fiber wall thickness (μm)		Microfibril angle (°)	
$\bar{x}$	δ_n	$\bar{x}$	δ_n	$\bar{x}$	δ_n	$\bar{x}$	δ_n
1017	74	14.3	1.11	12.58	0.798	11.42	1.511

Tab. 1.1-2 Vessel distribution frequencies and tangential diameters

Vessel distribution frequency (Number/mm^2)				Vessel tangential diameter (μm)			
Ave.	Std.	Max.	Min.	Ave.	Std.	Max.	Min.
15.16	2.4005	19.00	11.80	98.41	22.6383	154.50	36.92

1.2 Physical properties

1.2.1 *Moisture content of the green wood*

The moisture content data of the green wood at different radial sites is including Tab.1.2-1.

Tab. 1.2-1 Moisture content of green wood for *E. exserta* at different radial sites (%)

Sites(from pit to bark)	1		2		3		4		5	
	$\bar{x}$	δ_n	$\bar{x}$	δ_n	$\bar{x}$	δ_n	$\bar{x}$	δ_n	$\bar{x}$	δ_n
	85.60	12.77	66.44	11.22	50.90	8.71	58.04	11.43	55.79	9.18

1=near pith, 2=site between 1 &3, 3=center from pith to bark, 4=site between 3 &5, 5= near bark

1.2.2 *Shrinkage and Density*

Shrinkage is the contraction of wood caused by drying the material below the fiber saturation point (William T. Simpson, 1991). It can be divided into 3 types of shrinkage according to the direction of contraction: longitudinal, radial and tangential shrinkage. The longitudinal shrinkage is the shrinkage along the grain, the radial shrinkage and the tangential shrinkage is that across the grain in a radial or in a tangential direction. Wood density, the weight of wood per unit volume, is a very important index having a close relation with wood mechanical strength. In this study, wood air-dried density and basic density were used to describe the wood density.

The shrinkage is attributed to the dimension stability and checking problem, which causes a lot of problem for the wood utilization. In another word, it causes not only the contraction of wood in size, but also the checking and deformation resulted from the different contraction in tangential, radial and longitudinal direction. Understanding the characteristics of shrinkage has no doubt to be helpful for the wood utilization for the wood industry practice. Nowadays, studying on the characteristics of shrinkage during the losing of water is becoming one of the wood science discipline[Barber NF etc.1964; Barber, 1968; Chafe, 1986; 1987; Gu H et al., 2001]。This study is intended to explore the shrinkage variation of acacia in different direction (North and south), different radial position and different tree height.

The trees studied were cut from Guangxi Zhuang Autonomous Region in the South China. Each trunk has been collected above the breast height and was cut every 2 meters. Then, four discs of each tree at different heights (about 1.3m, 3.3m, 5.3m and 7.3m respectively) were taken from the logs. All the discs were marked the south-north direction. For each disc, one specimen from the sapwood near the bark, one from the heartwood near pith and one from transition zone was made at the size of 2X2X2cm (Tangential X radial X longitudinal direction) for both north side and south side.

Two diagonal lines were drawn in three sections (i.e., T×R, T×L, R×L) of each specimen to locate the central point where the size was measured. The specimens were put into water until they were totally saturated and sunk in the water. The surface water was wiped off and the sizes in three directions (L, R, T) were measured. Specimens were set in the room for air-drying. After measuring the size and weight at the air-dried stage, the specimens were oven-dried and the same measurement was carried out. The shrinkage was determined according to Chinese National Standard. The air-dried density and was also calculated of both air-dried

The shrinkage coefficient was determined by the difference between shrinkage at air-dried and at oven-dried and divided by the MC at air-dried status.

1.2.2.1 Shrinkage and density, and that of wood from south and north directions

The air-dried shrinkage in tangential direction (Ta), Radial direction (Ra) and volumetric shrinkage (Va), as well as the oven-dried shrinkage in tangential direction (To), Radial direction (Ro) and volumetric shrinkage (Vo) are listed in Table1.2-1 according to the categories of south direction, north direction and the overall. The basic density (B D) and air-dried density (A D), together with tangential shrinkage coefficient and radial shrinkage coefficient were also calculated and listed.

According to the IAWA (1989) method (the wood with an air-dried density smaller than 0.56 g/cm^3 is considered to be a small-density species, between 0.56 g/cm^3 and 0.75 g/cm^3 is considered to be a medium-density, between 0.75 g/cm^3 and 0.95 g/cm^3 is considered to be a large-density species, and bigger than 0.95 g/cm^3 is considered to be a extra-large-density species), *E. exserta* is a extra-large-density species.

According to the *CHINA WOOD* method (the wood with an air-dried tangential shrinkage smaller than 5.60%, is considered to be a small-shrinkage species, between 5.60% and 7.00% is considered with a medium-shrinkage species, and bigger than 7% is considered to be a big-shrinkage species), *E.exserta* has a medium shrinkage.

ANOVA analysis (Tab.1.2-2) showed there was no significant difference between air-dried tangential shrinkage and air-dried radial shrinkage, suggesting that the wood from north and south could be thought has the same level in shrinkage.

Tab. 1.2-2 The shrinkage and density of *E.exserta* wood from south and north side

		Ta (%)	Ra (%)	Va (%)	To (%)	Ro (%)	Vo (%)	B D (g/cm³)	A D (g/cm³)	Co-t (%)	Co-r (%)
South	Average	5.99	3.97	9.75	10.00	7.18	16.65	0.77	0.96	0.31	0.25
	Std.dev.	1.93	0.82	2.54	1.42	0.86	1.96	0.06	0.08	0.06	0.03
	CV(%)	0.32	0.21	0.26	0.14	0.12	0.12	0.08	0.09	0.19	0.12
	Number	15	15	15	15	15	15	15	15	15	15
North	Average	5.84	3.59	9.36	9.83	6.78	16.31	0.78	0.98	0.30	0.24
	Std. dev.	1.35	0.86	1.93	1.14	1.00	1.64	0.07	0.08	0.04	0.03
	CV(%)	0.23	0.24	0.21	0.12	0.15	0.10	0.08	0.09	0.14	0.14
	Number	15	15	15	15	15	15	15	15	15	15
Total	Average	5.91	3.78	9.55	9.92	6.98	16.48	0.78	0.97	0.30	0.24
	Std. dev.	1.64	0.85	2.23	1.27	0.94	1.79	0.06	0.08	0.05	0.03
	CV(%)	0.28	0.23	0.23	0.13	0.13	0.11	0.08	0.08	0.16	0.13
	Number	30	30	30	30	30	30	30	30	30	30

Tab. 1.2-3 ANOVA analysis on the shrinkage of *E. exserta* wood from north and south

	SS	df	MS	F	P-value	F crit
Ta	0.1542	1	0.1542	0.0557	0.8151	4.1960
Ra	1.0794	1	1.0794	1.5181	0.2282	4.1960

1.2.2.2 Shrinkage and density of wood from 4 different tree heights

The shrinkage, shrinkage coefficient and density from 4 different tree radial positions were listed in Tab.1.2-4. The relationship between air-dried shrinkage, basic density and tree heights were showed in Fig. 1.2-1.

ANOVA analysis (Tab.1.2-5) showed there existed significant air-dried shrinkage difference in both tangential and radial direction.

Tab.1.2-4 The shrinkage and density of *E.exserta* from different radial positions

		Ta (%)	Ra (%)	Va (%)	To (%)	Ro (%)	Vo (%)	B D (g/cm³)	A D (g/cm³)	Co-t (%)	Co-r (%)
Near bark	Average	4.84	3.34	8.07	9.00	6.75	15.33	0.74	0.91	0.33	0.27
	Std. dev.	0.42	0.60	0.72	0.72	0.84	1.15	0.06	0.07	0.03	0.03
	CV(%)	0.09	0.18	0.09	0.08	0.12	0.07	0.07	0.08	0.09	0.10
	Number	10	10	10	10	10	10	10	10	10	10
Transition	Average	5.46	3.62	9.03	9.66	6.92	16.30	0.84	1.05	0.31	0.24
	Std. dev.	1.66	0.58	1.97	0.90	0.89	1.34	0.02	0.04	0.07	0.03
	CV(%)	0.30	0.16	0.22	0.09	0.13	0.08	0.03	0.04	0.22	0.11
	Number	10	10	10	10	10	10	10	10	10	10
Near pith	Average	7.44	4.38	11.56	11.09	7.27	17.80	0.75	0.95	0.27	0.22
	Std.	1.27	1.00	2.08	1.15	1.08	1.92	0.05	0.06	0.03	0.02
	CV(%)	0.17	0.23	0.18	0.10	0.15	0.11	0.07	0.06	0.10	0.08
	Number	10	10	10	10	10	10	10	10	10	10

Tab1.2-5 ANOVA analysis on the shrinkage of *E.exserta* wood from different radial positions

	SS	df	MS	F	P-value	F crit
Ta	36.76241	2	18.3812	12.15311	0.000172	3.354131
Ra	5.779523	2	2.889761	5.13015	0.01293	3.354131

Radial shrinkage and tangential shrinkaged showed a tendency that it increased from mature wood (near bark) to juvenile wood (near pith), suggesting that the dimension stability of mature wood was better than the juvenile wood. The basic density in the transition zone also presented the maximum value.

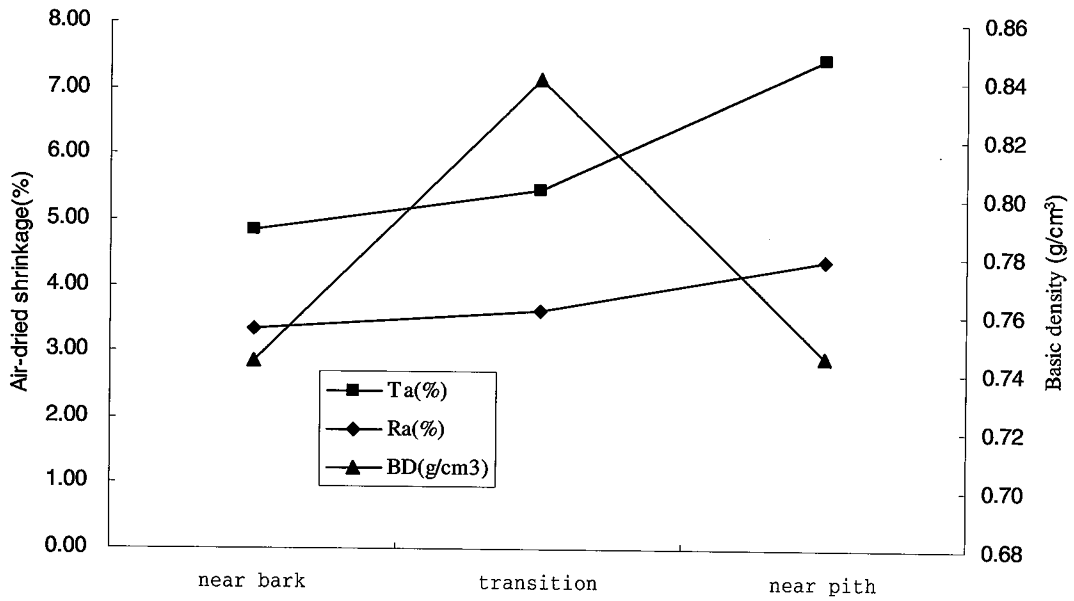

Fig.1.2-1 *E. exserta*: relationship between air-dried shrinkage (Ta&Ra), basic density (BD) and different radial positions

1.3 Mechanical properties

The small clear wood samples of moduli of elasticity (MOE), moduli of rupture (MOR) in static bending, compression strength parallel to grain and wood density were cut in accordance with Chinese National Standards (GB 1927~1943-91). The specimens were then stored in a conditioning chamber until it reached approximately 12% moisture content. Bending, compression and wood density test were carried out in accordance with Chinese National Standard. The air-dry density was calculated by air-dried weight and volume while oven-dry density was based on oven-dried weight and volume.

Generally *Eucalyptus exserta* wood interlocked-grain, texture fine and even, extremely heavyweight, very hard, shrinkage large, strength highly. The mechanical properties are including Tab.1.3-1.

Tab. 1.3-1 Mechanical properties data of *E. exserta*

Locality	Density /g/cm³		DS /%		CSPG /MPa	BS /MPa	MOE /GPa	Toughness /kJ/m²	Hardness /N		
	BD	ADD	R	T	CSPG/MPa	BS/MPa	MOE/GPa	Toughness/kJ/m²	E	R	T
Guangxi Dongmen		1.033			74.2	141	17.34	97.1			
Guangdong		0.85			69	113	11.47		7462		

BD = basic density, ADD = air-dry density, DS = dry shrinkage, CSPG = compressive strength parallel to grain, BS = bending strength, MOE = modulus of elasticity, SSPG = shear strength parallel to grain(R), E = end, R = radial, T = tangential

1.4 Chemical properties

The chemical composition was determined according to Chinese National Standards; the results at different years are listed in Tab. 1.4-1.

The chemical composition data of *Eucalyptus exserta* pH value, acid and alkaline buffering capacity are including in Tab. 1.4-2.

Tab.1.4-1 Chemical composition of *E. exserta* at different ages (%)

Tree age (years)	M	L	XY	α-C	HOC	A	CWE	HWE	1% NaOHE	BAE
4	8.2	27.35	12.54	46.26	—	0.26	2.86	4.01	12.65	1.52
4	8.67	26.52	19.14	45.63	—	0.23	2.11	3.92	13.44	0.83
7	—	28.29	18.64	—	75.44	0.24	2.80	4.45	13.86	1.81
8	11.0	31.26	16.10	44.53	—	0.21	3.90	5.93	14.00	1.71
12	—	31.74	17.07	42.81	—	0.15	4.69	7.50	15.85	3.06
12	10.95	28.44	17.47	43.98	—	0.20	3.57	5.46	14.57	1.12
13	—	28.16	16.33	—	71.36	0.18	3.40	5.81	15.69	2.46
13	9.4	27.30	18.31	44.90	—	0.43	1.35	3.72	12.53	0.90
16	10.89	35.97	9.98	42.11	—	0.25	4.78	6.50	16.10	5.42

M—Moisture, L—lignin, XY—Xylan, αC—α-Cellulose, HOC—Holocellulose, A—Ash, CWE—Cold water extractives, HWE—Hot water extractives, NaOHE—NaOH extractives, BAE—Benzene-alcohol extractives

Tab.1.4-2 Data of pH value, acid and alkaline buffering capacity of *E. exserta*

pH value		Acid buffering capacity /ml		Alkaline bufferi capacity /ml	
S	H	S	H	S	H
5.11	3.47	4.10	1.60	14.20	40.50

S- sapwood, H-heartwood

2 GROWTH STRESS

The research adopted CIRAD-Foret method to measure surface longitudinal growth strain (SLGS) of standing trees, the results at different orientations were listed in Tab.2-1.

Tab.2-1 Growth strain data for standing trees of *E. exserta*

Basic density (g/cm^3)	E		W		S		N	
	$\bar{x}$	δ_n	$\bar{x}$	δ_n	$\bar{x}$	δ_n	$\bar{x}$	δ_n
0.681	746	283.0	824	422.5	837.6	184.1	830	320.6

E=east, W=west, S=south, N=north

3 SAWING TECHNIQUES

Logs were collected from DONGMEN Forest farm in Nanning, Guangxi, and 10 stems were taken. All trees were unpruned and were planted on commercial forest land. The ends of the logs were sealed with asphalt to prevent end-drying after logging. Water spraying was applied to keep them in a green condition by preventing drying degrade.

The length of each log section was from 2.00 to 2.20 meters. The taper of this species was small, so three to four sections could be harvested from each tree. The parameters are listed in Tab. 1-1.

Tab. 4-1 The parameters of *E. exserta* trees and log sections

Height of tree (m)	Height under branch (m)	Age (years)	DBH (mm)	Diameter Range of log sections (mm)
19.96	10.76	27	261	145~194

Note: the height and DBH (diameter at breast height) are averaged.
The diameter of log sections refers to the Small End Diameter (SED), and bark is not included.

The equipment for the sawing consisted of a headrig band saw with a manually adjusted sizing carriage.

3.1 Strain in Sawing Process

The method of measuring strain is based on the method of measuring longitudinal strain (France, CIRAD-Foret Method) and instantaneous release of residue stress after drilling holes above and below gauges (M. Yoshida, T. Okuyama, 2002). The pin targets and guide for setting is displayed in Fig. 3.1-1.

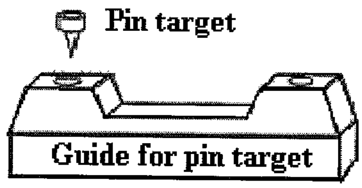

Fig. 3.1-1 Pin target and guide for measuring strain in sawing process

Height of pin target: 10mm, Internal diameter: 2.5mm, External diameter: 10mm, Distance between pin target: 45mm.

Before each sawing pass, two pin targets were placed into the existing sawn surface according to Fig.3.1-2 or in the case of the opening cut on the log side face which was to be perpendicular to the sawing surface. The distance was measured with a digital caliper with a precision of 0.001 mm. The head of each pin target was recessed to accept the pins and hold them in place. And their distance apart, measured before sawing and again just after the lumber containing the nails was sawn off. The strain changes in the longitudinal and tangential directions were then calculated using the formula:

$$strain = \frac{Da - Db}{Db} * 100\%$$

Where: Db= the dimension before the lumber is sawed off; Da= the dimension after the lumber is sawed off.

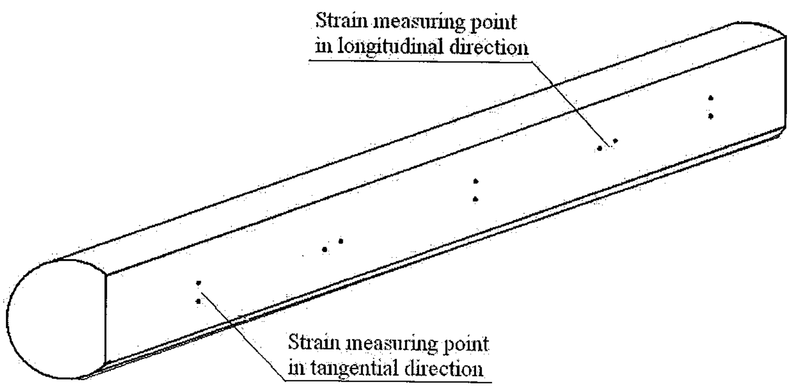

Fig. 3.1-2 Distribution of measuring point for strain change in lumber sawing

The logs were sawn using three different sawing patterns; live sawing, cant sawing and around sawing; and the strain changes were measured following the above procedure.

The strain distribution in the sawing process is analysed and displayed in Figs 3.1-3 – 3.1-4. X-coordinates show the log's position, while the number 1, 2, 3… shows the section position progressively from the bottom to the top section of the trunk. The abbreviations shown in the figures are: T—tangential, R—radial, Sap—Sapwood, Core—Core wood, Live—live sawing, Cant—cant sawing, Around—around sawing, for example, 'T_live' represents tangential direction with live sawing pattern.

The stresses are generated in newly formed wood during cell maturation in living tree. Continuous formation of growth stresses during tree growth results in an uneven distribution of residual stresses across tree stems. When logs are sawn longitudinally, the residual stresses are partially released (Crompton, 2000). And the growth stresses are presented in a random way (Tomaselli, 2000), this may resulted in the big deviation of the strain in sawing process. Fig. 3.1-3 showed the strain changes' results of *E. exserta* in sawing. The around sawing pattern showed the most even strain in tangential and radial direction, and strain difference between tangential and radial direction is small; and that of cant sawing pattern behaves the biggest fluctuation.

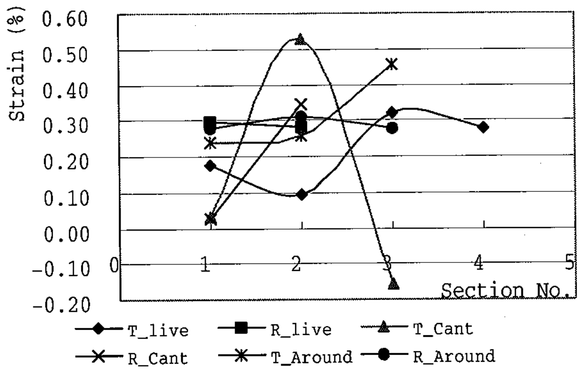

Fig. 3.1-3 Strain distribution of *E. exserta* in tangential and radial direction

As for the strain in longitudinal direction showed in Fig. 3.1-4, the biggest strain occurred in the cant sawing, and fluctuation is big. And around sawing behaved even and small either in sapwood or corewood lumber sawing. This may deduced that the residue stress of log released efficiently in around sawing than that in other sawing pattern.

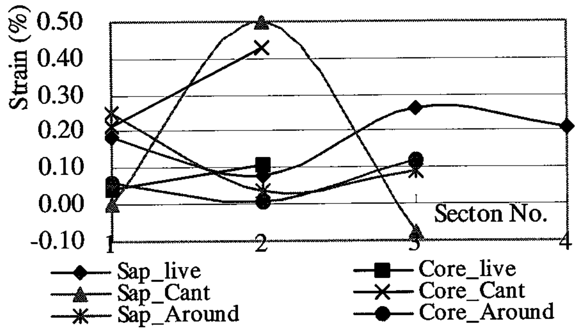

Fig. 3.1-4 Strain distribution of *E. exserta* in longitudinal direction

3.2 Bow Deformation

Bow deformation in sawn lumber (bending in the longitudinal direction) was recorded for each sawing strategy. Bow can reflect the extent of growth stress release. The higher the stress gradient in the original log, the greater the expected bow deformation is.

The most deformation which occurred in the sawing process was bow deformation of the lumber, it is also from the releasing of residue stress (Crompton, 2000). The results are displayed in Figs 3.2-1 to 3.2-3 for the three different sawing strategies. The X-coordinates represent the location of lumber in the log, 0 is the core lumber and the other values represent the block number in relation to the pith of the log, Positive and minus values are used to indicate the two directions from the pith. In the live sawing and cant sawing strategies, the larger minus values represent which pieces of lumber were cut first., In the around sawing strategy the sign just represents location of the lumber (displacement from the pith).

In the sawing process, most of the lumber developed bow deformation except the core lumber. This bow deformation has some relationship with where the lumber was located in the original log and the sequence of the cuts in the sawing process. This is apparent in Figs 3.2-1 to 3.2-3, especially the cant sawing.

The common results could be gotten from three figures, the outer the lumber position is, the bigger the bow deformation is. This is in accordance to the stress distribution inside Eucalyptus log. The stress gradient is bigger as the position is in outer place than that in the inner place.

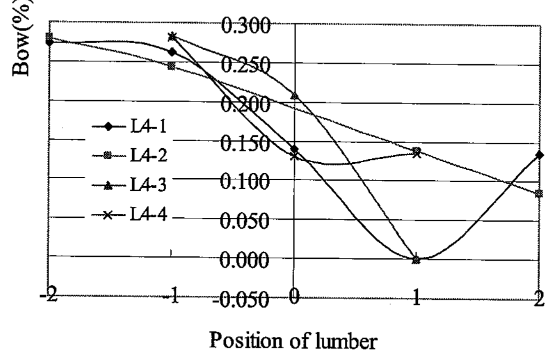

Fig. 3.2-1 The bow deformation of *E. exserta* in live sawing

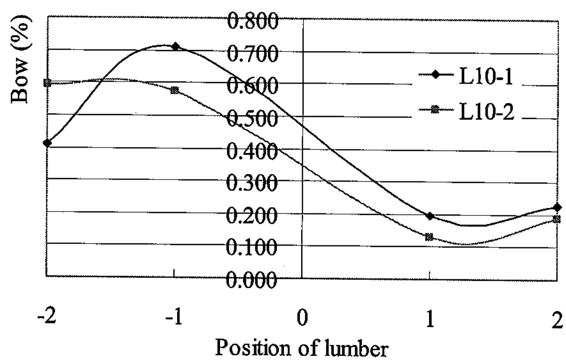

Fig. 3.2-2 The bow deformation of *E. exserta* in cant sawing

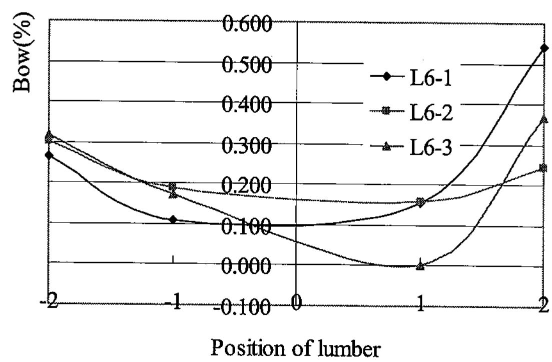

Fig. 3.2-3 The bow deformation of *E. exserta* in around sawing

The bow deformation has some relationship with the sequence in live sawing and cant sawing process. The lumber sawed first had the biggest bow deformation (left side), and the lumber sawed later had less deformation. After the former lumber sawed, the stress inside left log had been released in some extent, so the later sawed lumber had less deformation even in the similar position in the log.

Tab. 3.2-1 the bow deformation of *E. exserta* in 3 different sawing pattern

Sawing pattern		Live-sawing				Cant-sawing			Around-sawing		
Position of log		1	2	3	4	1	2	3	1	2	3
Location of lumber	-2	0.273	0.280			0.410	0.594		0.265	0.302	0.316
	-1	0.262	0.243	0.282	0.282	0.708	0.574	0.731	0.107	0.189	0.174
	0	0.140	0.138	0.209	0.131	0.194	0.128	0.449	0.154	0.157	0.000
	1	0.000	0.085	0.000	0.135	0.226	0.186	0.235	0.543	0.244	0.366
	2	0.135									

The bow deformation in around sawing and live sawing were small, the biggest value is in cant sawing with the first sawing half. After slab sawing off, the most of the wood near the heart under high compression still exists in the cant and on reaching a new equilibrium condition, will impose a higher tensile strain on the sapwood than the level which existed in the intact log (Waugh, 2000), this increased stress gradient and resulted in the bigger deformation. The detailed bow deformation was listed in Tab. 3.2-1.

The bow deformation displayed the stress distribution and re-distribution in some extent, so the around sawing could release the residue stress more efficient than the other two sawing pattern.

3.3 Sawing inaccuracy

The high growth stress in eucalypts can result in considerable distortion and sawing inaccuracy during sawing, which greatly influence the sawn accuracy of lumber as well as lumber recovery and productivity. According to the national sawing standard of China, the permitted thickness deviation is ± 1mm. However, in this study, the actual sawing variation was much larger, the range being from –4 to +4 mm. This big variation not only influenced lumber recovery, but also made later processing difficult due to the uneven dimensions of the lumber.

The data of sawing inaccuracy of lumber thickness is listed in tab. 3.3-1, the proportion of oversized deviation is about 49%, the *E. exserta* lumber is lumber is hard and it is easy for the saw to wander during sawing, resulting in thickness inaccuracy.

Tab. 3.3-1 the thickness inaccuracy influence on *E. exserta* lumber

Amount of slabs (Pcs)	Amount of oversize thickness deviation (Pcs)	The proportion of oversized (%)
65	32	49.2

3.4 The influence of end-splits on lumber recovery

The most frequent defect is end-splitting in sawing plantation Eucalyptus for the high growth stress. Heart shake appears just after tree trunk being cut down, and it will extend to some extent before sawing, most end-splitting comes from heart shake in log section. Tab. 3.4-1 shows the results of end-splits in sawing *E. exserta* timber. The end-split's influence to lumber recovery is 9%, i.e. if there is no end-split, the lumber recovery will increase about 9%. The lumber recovery of *E. exserta* is about 47%.

Tab. 3.4-1 Influence of end-split to lumber recovery in sawing experiments

log Volume (m^3)	Volume of Lumber with end-split (m^3)	Recovery rate with end-split (%)	Volume of lumber without end-split (m^3)	Recovery rate without end-split (%)
0.8326	0.4699	56.43	0.3948	47.41

The lumber quality and recovery could be improved by choosing appropriate sawing strategies and sawing equipments. This would improve the potential for the use of Eucalyptus lumber for value added wood products.

4 DRYING TECHNIQUES

4.1 Air drying

Air drying is a traditional and economical drying method which mainly uses sun energy. To save kiln drying time and cost, and to improve kiln drying quality at the mean time, it is suggested to use Air drying as a pre-drying method, and then conventional kiln drying to target final MC (moisture content). Because of the uncontrolled drying conditions, the drying time, final MC and drying quality may be quite difference with the changes of season and drying arrangements. Air drying test focus on analysing wood Air drying properties and try to find its optimum Air drying technique and parameters.

4.1.1 Material and method

The size of sample for air drying is 700 mm (length) x 120-150 mm (width) x 25 mm (thickness). Two MC slices were cut in the two ends of each sample to calculate its initial MC (Fig.4.1-1).

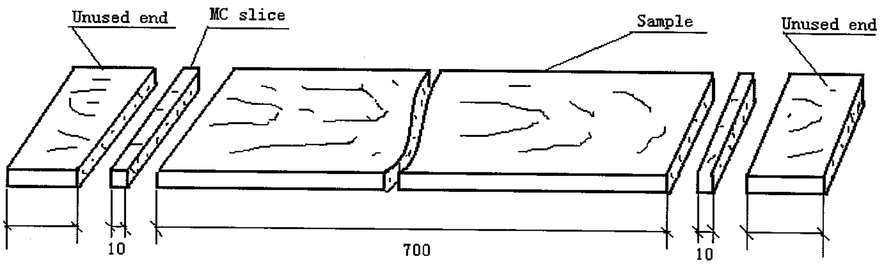

Fig.4.1-1 Drying sample making of *E. exserta*

The samples were end-sealed with silicon, and then stacked in air-drying shed to start drying. The dry-bulb and wet-bulb temperatures in shed were recorded every day, and the weights and all visible drying defects of samples were recorded once a week at the first month, then once every two weeks till the air drying ended. When the test finished, three final MC slices and one layer MC slice for each sample were cut (Fig.4.1-2). After oven drying these slices, the final MC for each sample were be gained, and then the oven-dry weight (written as G_0) for each sample could be calculated with the equation listed below. And so, corresponding to the recorded weights of each sample in different drying times, the air-drying MC curve could be drawn.

$$G_0 = 100G_w/(100+MC_0)$$

G_0 - oven-dry weight

G_w - initial weight

MC_0 - oven-dry MC (%)

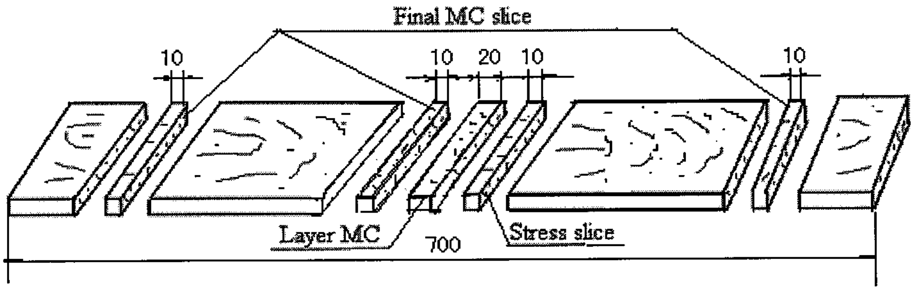

Fig.4.1-2 MC slices making of *E. exserta*

4.1.2 Result and suggestion

The air-drying test results of *E. exserta* are listed in Tab.4.1-1, and the air-drying MC curves in different seasons were shown in Fig.5.1-3.

Tab.5.1-1 Air-drying test results of *E. exserta*

Season	MCw (%)	MCo (%)	Air-drying rate (%day)			Air-drying rate in early stage (%/day)		Defect grade ##
			60-30%	30-20%	Below 20% #	1st week	2nd week	
2002.8-11 Autumn	53	15.1		0.5	0.17 (14.0%)	2.3	0.8	3
	55.3	13.5		0.98	0.34 (12.3%)	2.6	1.7	2
	30.9	14.2		0.95	0.31 (10.5%)	1.2	0.5	2
2002.12-2003.3 Winter	61.7	15.3	0.69	0.24	0.28 (17.1%)	2.3	0.5	3
	65.6	14.6	0.68	0.2	0.02 (19.6%)	2.6	1	3
	68.1	16	0.59	0.24	0.02 (19.6%)	1.9	0.7	3
2003.3-2003.7 Spring	57.9	14.9		0.47	0.27 (14.4%)	1.5	1	1
	59.2	14.7		0.71	0.24 (14.9%)	1.4	0.6	2
	54.1	15.4		0.5	0.23 (17.5%)	1.3	0.8	3
2003.6-2003.9 Summer	51.4	16.1		0.48	0.10 (15.9%)	2.2	0.9	2
	47.4	17.4		0.37	0.08 (17.5%)	1.4	0.8	3
	40	16.1		0.67	0.08 (15.7%)	1.7	0.8	3

Note: # - The data in brackets are the final MC when test ended.

##- The standards for drying defects grade division: grade 1 – having no check, warp and cup deformations or just having end checks; grade 2 - having no more than five short end-surface checks or short-narrow surface checks, and the value of warp and cup deformations are smaller than 2mm; grade 3 - having five to ten short-narrow surface checks, and the value of warp and cup deformations are smaller than 4mm; grade 4 - having more than ten short-narrow surface checks and long-narrow or wide surface checks no more than five, or the value of warp and cup deformation are more than 4mm.

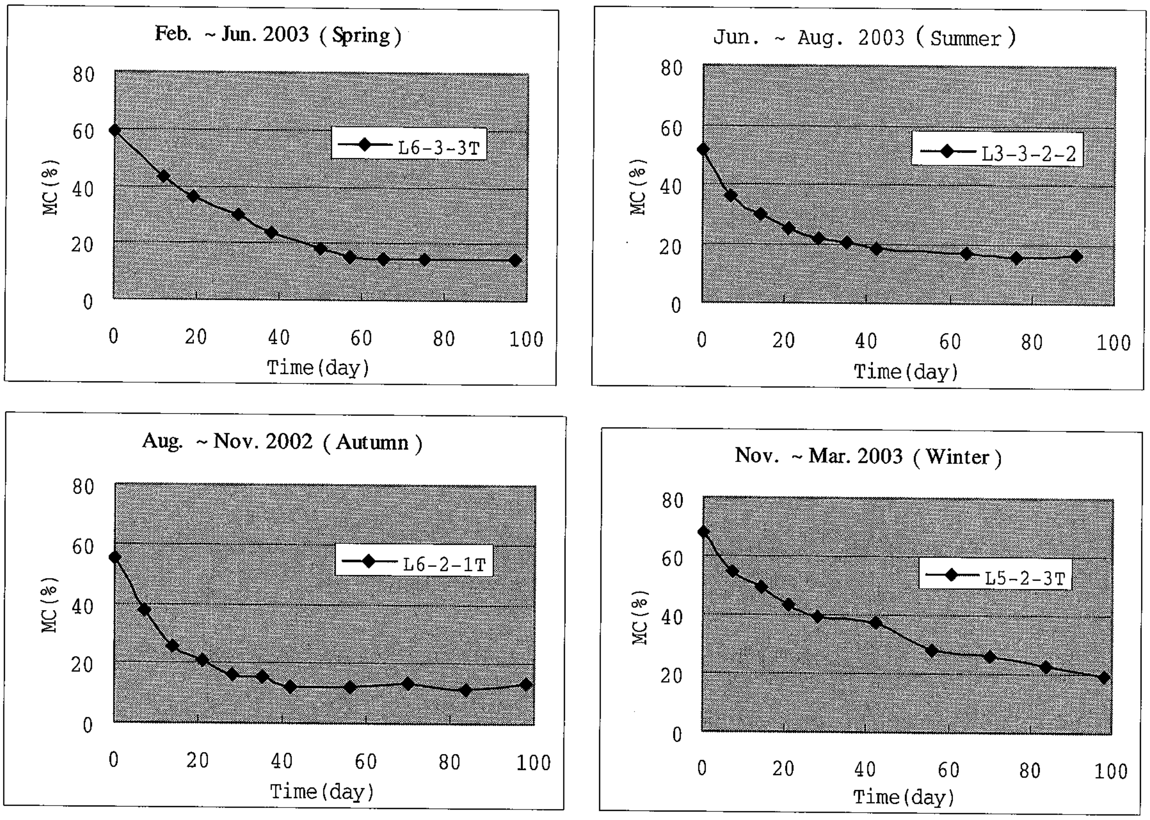

Fig.5.1-3 The air-drying MC curve of *E. exserta*

Result showed that the air-drying rate of *E. exserta* in autumn was the fastest and that in winter in the slowest. But drying defects were very serious (grade 3 mostly), and the main drying defects were deformation, but it could be decreased if put heavy load on top of the stack. So it is recommended that air-drying method could pre-dry *E. exserta* wood before kiln drying if putting heavy load on top of the stack.

4.2 Drying characteristics

4.2.1 Material and method

The sample dimension: plane-sawn lumber with 200mm x 100mm x 20mm

Other requirements of sample: planed lumber with normal colour, knot-free and straight grain, and initial moisture content is above 45%.

Equipment: Electric oven with air circulation.

100℃-test method is a fast drying test which is used to study on drying characteristics and prediction of drying schedule of plantation wood. Before test, the following data of the samples should be gained: the sample's weight, all visible surface defects, and dimension measurement data as showing in Fig.4.2-1. Then the samples were put into the electric oven with constant temperature at 100℃, and letting the samples stand erectly in the oven so that they will obtain same quantity of heat. Once the test begin, weighing the samples, observing and recording all initial defects including end checks, end-to-surface checks and surface checks at a fixed time through all the drying process. The test ended when MC was estimated below to 1%. All the samples were taken out, and then measuring cross-section deformation (Fig.4.2-2). Finally cutting moisture content slice and recording internal checks of each sample.

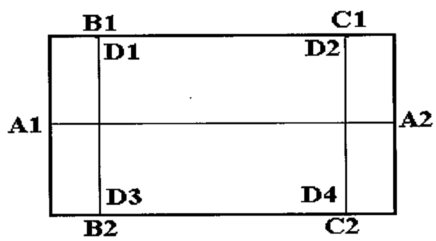

A1-A2 is length
B1-B2 and C1-C2 are width
D1,D2,D3,D4 are thickness

Fig.4.2-1 The dimension measure in 100℃-test of *E. exserta*

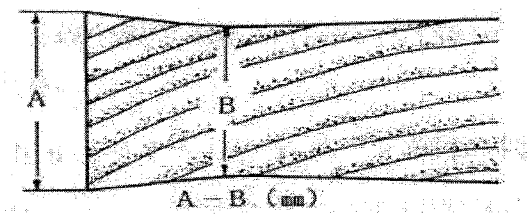

Fig.4.2-2 The cross-section measure in 100℃-tes of *E. exserta*

To make all these defects digitalization and comparable, the grades of different drying defects are shown in Tab.4.2-1 to Tab.4.2-3.

Tab.4.2-1 The grade division of initial checks

Grade	No.1	No.2	No.3	No.4	No.5
Degree of initial check	No checks or only have end checks	Short end-to-surface checks and short-narrow surface checks	Long end-to-surface checks and long-narrow surface checks no more than two or short-narrow surface checks no more than fifteen	short-narrow surface checks more than fifteen or long-narrow and wide surface checks no more than five	short-narrow surface checks more than five or wide surface checks more than five

Note: long check -- check length ≥ 50mm; short check -- check length <50 mm; narrow check -- check width <2 mm; wide check -- check width ≥ 2mm

Tab.4.2-2 The grade division of internal checks

Grade	No.1	No.2	No.3	No.4	No.5	No.6
Degree of internal check	No :hecks	1 wide or 2 narrow checks	2-3 wide checks; 4-5 narrow checks; 1 wide and 3 narrow	4-5 wide; 7-9 narrow; 1 wide and 4-6 narrow	6-8 wide; 15 narrow; 4 wide and 6-8 narrow	15-17 wide or continuous checks

Tab.4.2-3 The grade division of cross-section deformation

Grade	No.1	No.2	No.3	No.4	No.5	No.6	No.7	No.8
A-B (mm)	0-0.3	0.3-0.5	0.5-0.8	0.8-1.2	1.2-1.8	1.8-2.5	2.5-3.5	over 3.5

Based on these drying characteristics in 100℃-test, the drying condition of this species could be gained by the relationships of drying characteristics and drying conditions showed Tab.4.2-4, which are very helpful to predict the drying schedules.

Tab.4.2-4 Drying condition based on degree of drying defects

Name	Drying condition (℃)	Grade of effects							
		No.1	No.2	No.3	No.4	No.5	No.6	No7	No8
Initial checks	Initial temperature	70	65	60	55	53	50	47	45
	Temperature depression	6.5	5.5	4.3	3.6	3.0	2.3	2.0	1.8
	Finial temperature	95	90	85	83	82	81	80	79
Cross section deformation	Initial temperature	70	66	58	54	50	49	48	47
	Temperature depression	6.5	6.0	4.7	4.0	3.6	3.3	2.8	2.5
	Finial temperature	95	88	83	80	77	75	73	70
Internal checks	Initial temperature	70	55	50	49	48	45	43	40
	Temperature depression	6.5	4.5	3.8	3.3	3.0	2.5	2.2	2.0
	Finial temperature	95	83	77	73	71	70	68	67

4.2.2 Result and suggestion

From the results of 100℃-test, the detailed data of drying defects results of *E. exserta* were shown in Tab.4.2-5, and the consideration of all 8 test samples, the comprehensive drying defects grades of *E. exserta* were shown in Tab.4.2-6. Corresponding to the drying condition based on degree of drying defects (Tab.4.2-4), and then the drying condition of *E. exserta* was show in Tab.4.2-7, which would be used to determine the kiln schedule in the follow-up test. And the MC curve during 100℃-test was showed in drying Fig.4.2-3.

Tab.4.2-5 The drying defects data and grades of *E. exserta*

No	Surface checks			End –surface checks			End checks		Grade	Internal checks			Cross section deformation	
	Long -narrow	Short -narrow	Wide	Long -narrow	Short -narrow	Wide	Wide	Short -narrow		Narrow	Wide	Grade	A-B (mm)	Grade
1	3	3	0	0	10	0	0	Many	3	4	5	4	1.80	5
2	2	2	0	1	8	1	0	Many	3	11	7	5	1.61	5
3	0	3	0	0	8	2	0	Many	3	8	8	5	1.78	5
4	4	7	0	2	5	2	0	Many	4	6	8	5	1.78	5
5	0	0	0	0	3	0	0	Many	2	0	0	1	0.45	2
6	0	2	0	0	7	0	0	Many	2	3	3	3	2.25	6
7	0	2	0	0	5	2	0	8	3	2	7	5	2.20	6
8	0	2	0	0	2	2	0	6	3	1	1	2	1.44	4
9	2	9	0	0	2	4	0	Many	4	5	7	5	1.40	5
10	0	6	2	0	2	2	0	Many	3	3	7	5	0.76	5

Tab.4.2-6 The comprehensive drying defects grades of *E. exserta*

Drying defects	Initial checks	Internal checks	Cross section deformation
Grade	No.3	No.4	No.5

Tab.4.2-7 The kiln drying condition of *E. exserta*

Item	The initial temperature	The initial wet-bulb depression (Δ t)	Final temperature)
Temperature (℃)	50	3	77

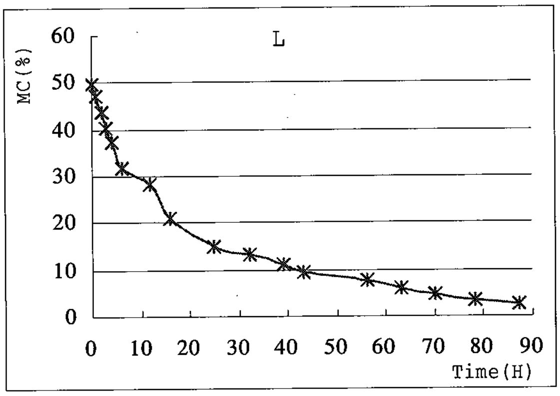

Fig.4.2-3 MC curve in 100℃-test of *E. exserta*

4.3 Drying schedule

4.3.1 Material and method

The sample dimension was with 500mm x 110mm x 25mm, double end-sealed with silicon sealing glue. The capacity for the stack was 500×400×300 mm, so 15 pieces of samples could by dried each time. To make it easy to fetch every sample for measurement and observation, all these 15 pieces of samples were put on a special made frame, so no heavy load on top on stack during test.

The test dryer was electric heating with 3 group of heater, which could be used independently of simultaneously according to the drying test need, the maximum of 3 group of heater was 6 kW. There was an electronic heated small boiler to afford steam during conditioning. The control system of the test dryer was semi-automatic.

Other equipment: Electric oven with air circulation, electronic balance, thermo-electronic couple temperature measuring system.

Based on the results of drying characteristics test, a schedule of *E. exserta* wood with thickness of 25 mm was drafted, seeing in Tab.4.3-1.

Tab.4.3-1 The predicted drying schedules of *E. exserta* (25mm)

MC stage	Dry-bulb temperature (t℃)	Wet-bulb temperature depression (Δt℃)
Above 40	50	3
40-35	54	4.5
35-30	58	7
30-25	62	10
25-20	66	14
20-15	70	20
Below 15	77	26

Beginning with this schedule, a series of kiln drying test had been done till the optimized schedule was gained.

4.3.2 Result and suggestion

The *E. exserta* plantation wood belongs to one of the difficult to dry species. Similar to *E. citriodora,* the main problem of *E. exserta* wood drying was small surface check, but not so serious. It is necessary to adopt low temperature schedule and at least two intermediate steam-conditioning needed.

The optimised kiln drying schedule for *E. exserta* wood with thickness of 25 mm was listed in Tab.4.3-2.

Tab.4.3-2 Drying schedule for *E. exserta* wood with thickness of 25 mm

MC (%)	Dry-bulb T(℃)	Wet-bulb T(℃)	Notes
Pre-heating	50	49.5-50	Pre-heating, 3 hours
Above 35	45	43	
35 ~ 30	50	46	
=30%	60	59	Conditioning, 3 hours
30 ~ 25	55	47	
25 ~ 20	60	48	
=20%	70	68	Conditioning, 3 hours
20 ~ 15	65	50	
15 ~ 10	70	50	
Below 10	75	55	
=8%	80	74	End-treatment, 3-5 hours

5 ADHESION PROPERTIES

5.1 Finger joint

Finger-joints are commonly used to produce wood products from short pieces of lumber. Such joints must have excellent mechanical performance. To produce acceptable products, a jointer must be subjected to a proper end pressure following machining and adhesive application; also technical parameters, such as machining and gluing processes must be optimized. The condition of finger geometry and end pressure plays a major role in the gluing process and the final strength of the assemblies.

The main function of the end pressure is to bring the mating surfaces so close together that the glue forms a thin and continuous film between them. This pressure also allows a uniform distribution of the adhesive and creates an optimum glueline's thickness. So it is necessary to control the glueline's thickness to produce strong joints. Thin glueline lead to starved joints. Above the optimum glueline's thickness, stress concentration develops in the adhesive layer due to cure-shrinkage. The pressure must be applied to force fingers together to form an interlocking connection, giving a certain immediate handling strength. The increase of the end pressure up to a certain point gives a better contact of the finger to obtain strong joints. However, cell damage or splitting of the finger root can be induced by excessive pressure.

Finger-joint geometry has been proven to the most critical variable determining joint strength. Finger-tips constitute a series of butt joints and are accorded zero strength even if they are tight apparently well bonded; the tip width is the geometric parameter that most significantly influences finger-joint strength.

The objective of the study was to investigate the effect of finger profile geometry and end pressure on the performance of finger-joints in four species of Eucalyptus. The study also planned to evaluate which combination of the end pressures and finger profile geometry would result in optimum finger-joint performance in each of the four Eucalyptuses.

5.1.1 Materials

The experiments were carried-out with the samples which were planed and crosscut to dimensions of 20 by 60 by 520 mm; the total number of the samples was 90 in each kind of eucalyptus; then the 90 wood blocks were divided three groups based on the density. The result of the density condition was as Tab.5.1-1:

Tab.5.1-1 Groups divided by density

Species	Average of high density /g/cm^3	Average of medium density /g/cm^3	Average of low density /g/cm^3
E. exserta	1.031	0.942	0.857

Two kinds of adhesive, API and PVAc, were used in the experiments. API is a kind of two-components adhesive, and is made of main reagent and cured reagent, the mixing ratio is 100:15 when the adhesive was used. The technical index of the two kinds of adhesives was Tab.2:

Tab.5.1-2 Technical indexes of two kinds of adhesive

Adhesives	Type	Colour	Solid content /%	pH	Viscidity /(cps, 25℃)
PVAc	BT-09	White Emulsion	25.7	4.4	8740
API	DYNOLINK-8000G	White Emulsion	63.8	6.6	6750

5.1.2 Method of Experiments

The geometry of finger(ΔT), feed speed, the amount of adhesives spreading, end pressure, were all important factors to be investigated in the finger-joints experiments.

Three kinds of finger geometry were studies to determine finger parameter for optimum finger-joint strength, and they were selected based on specifications in standards, data from the literature. The finger-jointing machines used a carriage clamp to secure the stacks of wood samples; the samples were guided through a circular saw, a finger profile cutter, and a suction device that removed sawdust and shavings. The ends of pieces to be jointed were first trimmed and squared cleanly by the circular saw before the profile was cut. The suction completely removed all shavings from the profiled surfaces. Finger profiles were processed as vertical orientation joints subsequent test evaluation. The parameters of the three kinds of finger were as Tab.5.1-3.

Tab.5.1-3 Parameters of the fingers

ΔT /mm	Length /mm	Tip width /mm	Pitch /mm	Slope
0	11	0.6	3.8	1/8
0.1	10.6	0.7	3.8	1/8
0.5	8.9	1.1	3.8	1/8

In the processing of making samples finger, the feed speed was important to affect the roughness surface of finger. In this experiment, because different Eucalyptus wood have different density, *E. exserta* wood samples was chose in 5mm/min.

End pressure is needed to ensure the closest possible contact between the finger surfaces to be glued, and for the adhesive to form a thin continuous layer uniform in thickness, without damage to the strength of the wood. It is also intended to force the fingers together to the degree that a locking action is obtained, giving a certain immediate handing strength after gluing. Since the higher the pressure the more efficient the locking action, as much pressure as the wood can withstand may be used without causing damage such as splitting at the finger roots, compression failure of the wood, and squeezing out of the glue.

In the experiment, the preliminary end pressure experiment was done to get the suitable pressure. Firstly, four pieces of wood block were selected from the three groups(High, Middle, Low) and then finger were cut; ΔT of the fingers were 0mm, 0.1mm, 0.5mm; and the samples were cut to 60mm length. PVAc was used as adhesive in the experiment with the spread amount 250g/m^2. Two samples were combined and laid under the loading machine to be pressured as Fig.5.1-1. The loading speed was 2mm/min.

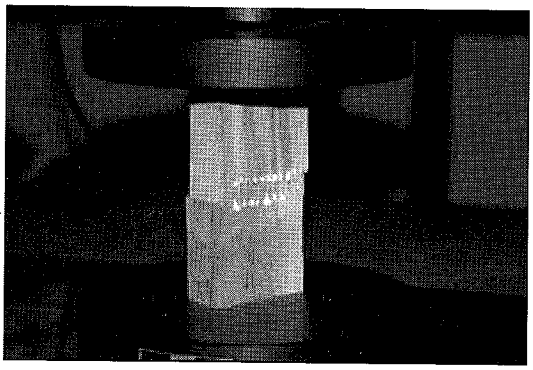

Fig.5.1-1. The method of measuring end-pressure

After the samples had been cut to finger, the samples were jointed by the finger jointer machine. 54 samples were selected from the group. The six kinds of sample were arranged as HH, HM, HL, MM, ML, LL on the basis of density. ΔT were 0, 0.1mm, 0.5mm, the end pressure was used from the result of preliminary end pressure experiments.

Because many factors affected the strength of finger-jointed lumber, for the sake of getting the better processing conditions, the end pressure and ΔT were main factors considered in the research, the design methods of full factors experiments and SAS analysis software were used to discuss the effect on the performance of finger-jointed lumber by each factor, and the interaction between the end pressure and ΔT. Finally integrative evaluation was processed by the result of SAS analysis and the appearance of finger-jointed samples to find the optimum processing condition.

After that, the finger-jointed specimens were cured over 48 hours before further processing. No pressure was applied to the specimens during curing. Both faces of a specimen were planed to a final specimen dimension of 58 by 17.5mm. The bending test was done by using the loading machine to measure MOE and MOR as Fig.5.1-2 according to JAS MAFF, Notification NO.590; support span was 420mm; loading span was 140mm and loading speed was 2mm/min

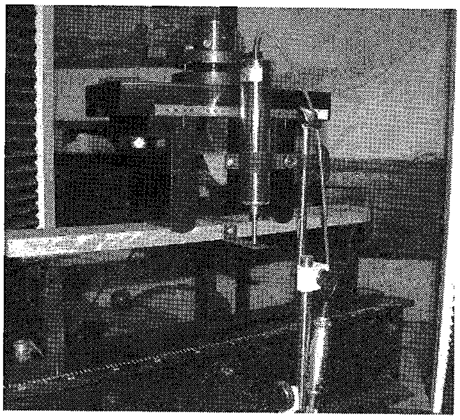

Fig.5.1-2 Four-points bending test

In the experiment, API (DYNOLNK-8000G) was used to make finger-jointed samples. Bending test were performed according to JAS MAFF, Notification NO.590; then MOE and MOR of finger-joints were compared with different kinds of adhesive

To compare the difference of MOR and MOE between V type finger(Fig.5.1-3) and H type finger(Fig.5.1-4), in the experiment, the H finger was done to make finger-jointed lumber, ΔT was 0.1mm; bending test were performed also according to JAS MAFF, Notification NO.590

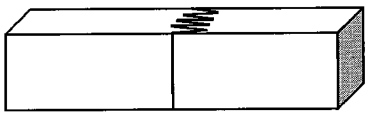

Fig.5.1-3. V-type finger-joint

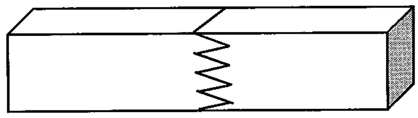

Fig.5.1-4. H-type finger-joint

5.1.3 Result and Discussion

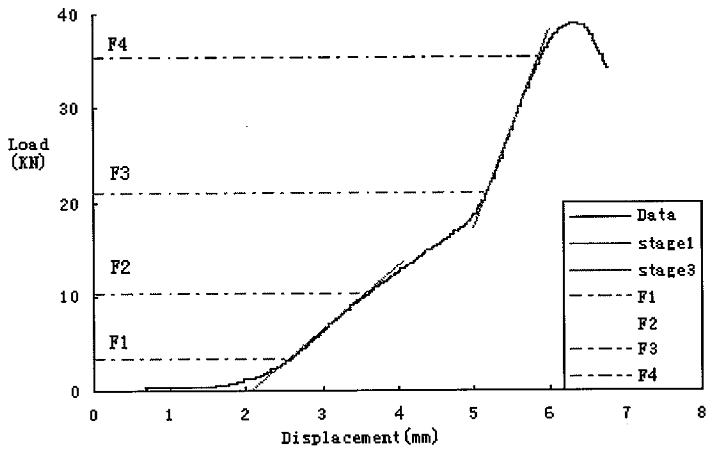

Fig.5.1-5. Load-displacement curve

Fig.5.1-5 is the typical Load-displacement curve, in this case ΔT is 0.5. When the cross head began to push the upper specimen, the upper specimens begin to move, the finger-tip will touch the nether specimen quickly, so when loading reached F1, it was considered the finger-tip touch the nether specimen, when the loading approached F2, it was considered the finger-tip was damaged, when the loading aroused to F3, there was splitting on the finger root, and following stage was as the same as solid wood pressured, the solid wood begin to damage when the loading increased to F4.

In the experiment, F1 was thought the suitable pressure before the finger was damage. Tab.5.1-4 was the results of end pressures in different ΔT.

Tab.5.1-4. End-pressure at different conditions

Wood species	ΔT	Average pressure /MPa
	0	10.38
E. exserta	0.1	13.20
	0.5	8.60

In the experiments, the four species of Eucalyptus end pressures were selected from Tab.5.1-5.

Tab.5.1-5. Different levels of the end-pressure

Wood species	Three end pressure /KN		
	P1	P2	P3
E. exserta	8	10	12

Tab.5.1-6 and Tab.5.1-7 were the results of the bending test analysis of *E. exserta.*

Tab.5.1-6. MOE and MOR analyzed by SAS

Index	Resource of variance	Degree of freedom	Summation of square	Average of square	F	Pr > F	Markedness
MOE	Matrix	32	391.869	12.246	4.07	0.0017	***
	Combination of density	5	187.226	37.445	12.45	0.0001	***
	End pressure	2	6.765	3.382	1.12	0.3479	/
	ΔT	2	4.180	2.090	0.69	0.5128	/
	End pressure × ΔT	4	25.790	6.447	2.14	0.1197	/
	Combination of density × pressure	10	85.351	8.535	2.84	0.0282	**
	Combination of density × ΔT	9	82.558	9.173	3.05	0.0229	**
	Error	17	51.142	3.008			
	Summation	49	443.011				
MOR	Matrix	32	1756.847	54.901	1.22	0.3363	/
	Combination of density	5	265.259	53.052	1.18	0.3582	/
	End pressure	2	182.033	91.017	2.03	0.1621	/
	ΔT	2	445.593	222.796	4.97	0.0200	**
	End pressure × ΔT	4	215.320	53.830	1.20	0.3467	/
	Combination of density × pressure	10	449.757	44.976	1.00	0.4785	/
	Combination of density × ΔT	9	198.885	22.098	0.49	0.8597	/
	Error	17	762.478	44.852			
	Summation	49	2519.324				

Mark: /means unmarkedness at 0.1; *means markedness at 0.1; **means markedness at 0.05

Tab.5.1-7 Testing for groups of each factor

Factor	Level	Number of specimen	MOE(Gpa)		MOR(Mpa)	
			Average	STDEV	Average	STDEV
End pressure	8	18	15.814A	3.220	37.794A	3.958
	10	17	16.294A	3.397	39.426A	8.891
	12	15	15.547A	2.352	42.721A	7.491
ΔT	0	15	17.312A	3.221	35.501A	6.903
	0.1	18	15.024B	2.789	42.403B	6.078
	0.5	17	15.573B	2.738	40.917B	7.089
Combination of density	HH	7	19.271A	3.420	36.795A	7.703
	HL	11	16.720B	1.541	43.274A	8.822
	HM	9	17.131B	2.906	39.243A	8.019
	LL	7	14.183C	2.403	39.918A	2.798
	LM	9	13.549C	1.865	37.394A	5.665
	MM	7	14.377C	2.305	41.230A	7.089

Mark: The A,B behind average in table means the checked result by T, the same word letter means there was no difference in Stat., the different letter means there was difference in Stat..

From Tab.5.1-6 it is indicated that the combination of density and ΔT had much effect on the MOR of finger-jointed lumber of *E. exserta* wood; end pressure had much effect on MOR; the interaction of end pressure and ΔT had no effect on MOR and MOE.

From Tab.5.1-7 it is shown that the change of end pressure had no effect on MOE, but to MOR, the higher end pressure, the higher MOR of finger-jointed lumber of *E. exserta* wood; different ΔT can lead to different MOR and MOE, the MOR was higher when ΔT was 0.1mm.

The results of finger-joints analysis of *E. exserta* wood was as following:

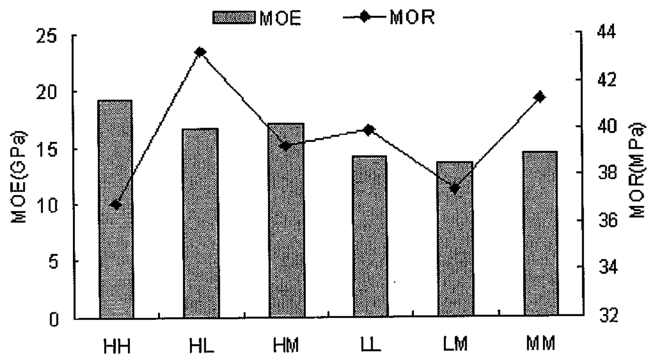

Fig.5.1-6 Combination of different density

Combination of different density has affection the MOE and MOR, especially to the MOE. From the Fig.5.1-6 it is evident that the higher density of combination, and the higher MOE and MOR of finger-joints lumber of *E. exserta* wood; the highest density combination of MOE could reach 78.756Gpa and15.450GPa.

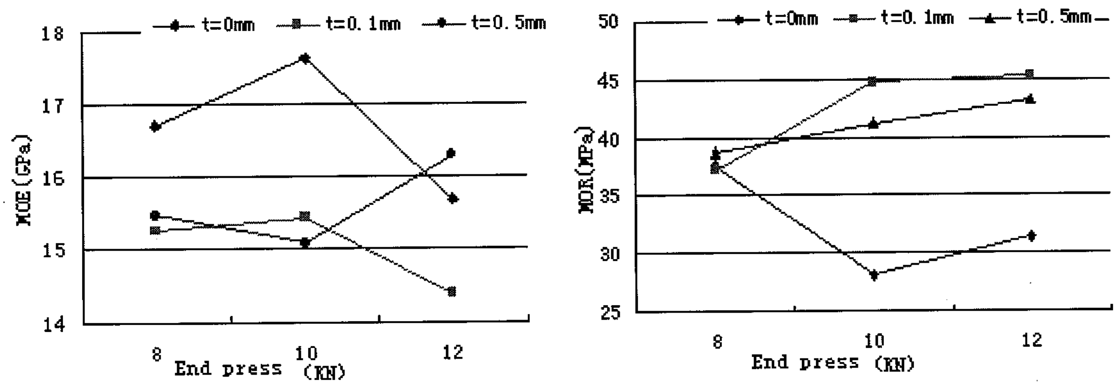

Fig.5.1-7 Effect of end-pressure on MOE and MOR

From Fig.5.1-7 it can be concluded that when the ΔT was 0mm and 0.1mm, the MOE of finger-joints increased with the end pressure increasing from 8.5KN to 11.5KN, when the end pressure was over 10KN, the MOE decreased from 78.756Gpa and 15.456Gpa to 16406 and 14.365 seperately. When ΔT were 0.1mm and 0.5 mm, the MOR of two type of finger-joints increased gradually as the increasing of end pressure as the increaing of end pressure. Therefore, the suitable ΔT was 0.1mm and the optimum end pressure was 10KN for finger-jointed lumber of *E. exserta*.

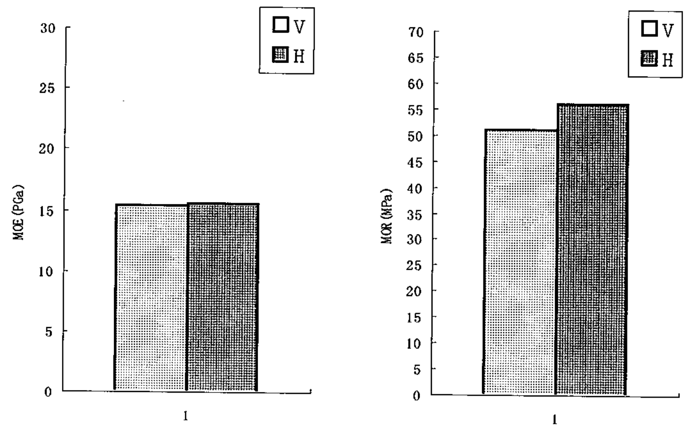

Fig.5.1-8 Comparison between V-type and H-type finger-joints on MOE and MOR

From the Fig.5.1-8 it was shown that the MOR of finger-joints with different finger type V and H were almost the same, but in the same processing condition, the MOE of finger-joints in V finger type was higher than that in H type.

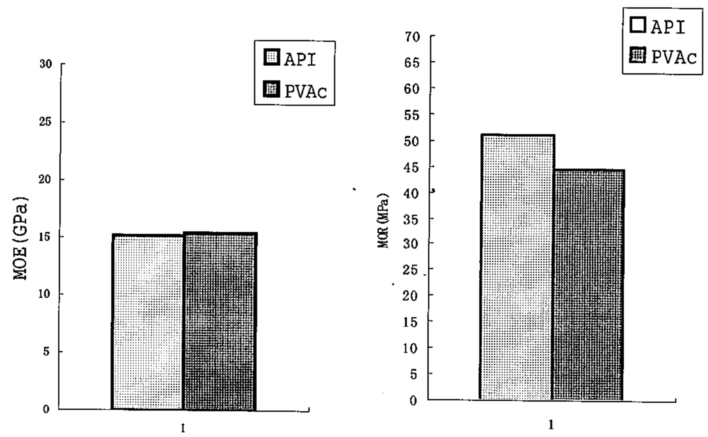

Fig.5.1-9 Comparison between API and PVAc finger-joint on MOE

From Fig.5.1-9 it was indicated that there were no much difference with API and PVAc in MOE, but for MOR, the API products was higher than PVAc remarkably, especially for E. citriodora wood, which was high density and had much extraction. For example, the MOR was 30.35 MPa for PVAc, but for API, the MOR increased to 57.69MPa. Tis could be explained that for API adhesives, in the action of Vander waals force and hydrogen bond between the molecule of adhesive and molecule of wood, it forms deep-set physical bonding with wood. The gluing surface and the formed nail adhesive react with hydroxyl, carboxyl, phenolic hydroxyl and other reactive group in celluloses, hemicelluloses, lignin of wood, at the same time adhesive reacts with water in wood, then forms some chemical bond between wood and adhesive, in the end form intercross structure, thereby increases strength of gluing.

5.2 Gluing

Based on referred data, a detailed experiment plan was set out. *E. exserta* eucalyptus species were selected. Because of adhesion being a very important basic work on finger-joint lumber and Glulam, it is essential to make sure the adhesives selected, the suitable bonding processing. Meanwhile, gluability research was implemented combining with wood properties and wood chemical components.

Firstly, surface property of *E. exserta* wood planed wood were measured by surface contact angle testing, and compared the results with the medium of pure water and API adhesive, furthermore, by contrast the contact angle between newly and old planed board of two eucalyptus species to search for the better gluability effect.

Shown as Tab.5.2-1 are contact angle of water and API main agent on two species planed board compared with newly planed and old planed board.

Tab.5.2-1 Contact Angle of Water and API of *E. exserta*

Liquid	Index	Average / (°)		Radial / (°)	
		New	Old	New	Old
Water	Average	32.3	46.0	21.0	37.7
	Stedv.	2.5	5.2	3.6	4.9
API	Average	71.7	79.7	61.3	76.2
	Stedv.	2.1	5.7	2.7	1.5

Secondly, 4 kinds of adhesives UF PF API and PVAC were selected by this experiment, through comparing gluability of 4 adhesives with *E. citriodora* wood, feasible adhesive was abtained for two species. Following table9 is comparison of shear strength of 4 kinds of adhesives.

Tab.5.2-2 The Longitudinal Shear Strength of 4 Kinds of adhesives

Adhesives	Test number	Shear strength /MPa	Stedv. /MPa
PVAc	42	1.63	0.42
UF	42	1.34	0.19
PF	42	2.08	0.38
API	42	5.83	1.66

Thirdly, gluing process experiment arranged by Orthogonality and SAS statistical methods to gain suitable processing parameters, and these analyzed on different wood grain direct, that is, T-T (tangential to tangential bonding), T-R (tangential to radial bonding), R-R (radial to radial bonding). Finally, gluing processing microcosmic structure were observed by SEM.

Following shown are gluing processing that confirm suitable parameters.

Tab5.2-3 The Testing Result Value on Each Factor and Level by SAS

Factor	Level	Number	Shear strength		Wood failure	
			Ave. /MPa	Stedv. /MPa	Ave. /%	Stedv. /%
Grain	T—T	84	5.77 A	1.37	54.1 B	33.0
	R—R	84	4.72 B	1.21	59.9 AB	34.0
	T—R	84	5.09 B	1.06	67.4 A	24.9
Pressure /MPa	1.5	126	4.96 B	1.27	60.7 A	28.9
	2.0	126	5.43 A	1.33	60.2 A	34.0
Time /min	40	126	4.87 B	1.17	63.7 A	21.3
	60	126	5.51 A	1.38	57.3 A	31.0
Spread /g/m^2	150	84	5.24 A	1.39	43.9 B	29.6
	200	84	4.99 A	0.98	65.8 A	27.1
	250	84	5.35 A	1.12	71.7 A	28.2

According to those problems exiting in experiments, some improving methods or treatments were put forward on *E. citriodor* wood, and the better gluability was obtained by comparison experiments with different wood surface treatments.

Tab.5.2-4 Bonding Strength and Wood Failure Treated with Different Methods by SAS

Treatments	Numb er	Shear strength		Wood failure	
		Ave. /MPa	Stedv. /MPa	Ave. /%	Stedv. /%
Nntrented	42	4.51 C	0.46	4.95 BC	6.58
FeSO4	42	3.04 D	0.44	0.00 C	0.00
NaOH	42	5.29 B	0.75	12.5 B	9.56
Newly planed	42	6.18 A	1.07	65.6 A	15.5

Finally, gluing durability is an essential index to gluability. With aging test in lab., different testing conditions to bonding board were adopted, which include room temp. water immersing and boiling water immersing.

Following Tab.5.2-5 were different methods to treat gluing board testing delamination.

Tab.5.2-5 The Results of Glue Line Delamination

Methods	Number	Cycle number	Delaminating Number	Delaminating length /mm	Delamination /%	Delaminating rate /%
Room tep.	36	1	7	10.4	6.91	16.7
	36	2	12	19.1	12.7	33.3
	36	3	16	26.7	17.8	44.4
	36	4	19	32.2	21.5	52.8
Boiling water	36	1	26	60.0	40	72.2
	36	2	29	74.5	43	80.5

Through plenty of data. we referred, it is very important to find suitable adhesive, because our project mainly focus on finger-jointing, and its products are oriented at floorings, construction materials that need we select an excellent binder fitting at glualam and lumber jointing, meanwhile it have better water resistance and weather tolerance. So 4 kinds of adhesives are picked up for our intial study used to be contrasted with each other.

4 adhesives (API, UF, PF, PVAc) have been contrasted for their Gluability with eucalyptus timber. Under the same testing conditions (i.e. spreading 250g/m^2, pressure 2.5Mpa, pressing time and temperature varying according to different adhesives), we made eucalyptus shear strength samples with 4 selected adhesives respectively, then obtained their testing results by test machine. Comparing the shear strength results with these 4 adhesives, we found the optimal adhesive out of the 4 adhesives, which will be our foundation stone in future work.

The processing technics of these 4 adhesives as follow Tab.5.2-6:

Tab.5.2-6 Processing technics of 4 adhesives

Parameter / Adhesive	Pressure /Mpa	Spreading /g/m^2	Temp. /℃	Pressing time
PVAc	2.5	250	Room temp.	9hrs
UF	2.5	250	100	31min
PF	2.5	250	140	42min
API	2.5	250	room temp.	60min

The results of shear strength parallel to grain shown as follow Tab.5.2-7.

Tab.5.2-7 Shear strength on different adhesives.

Adhesives	Test piece number	Ave. of shear strength /Mpa	Stedv.
PVAc	42	3.218	2.19
UF	42	2.338	1.68
PF	42	5.078	2.19
API	42	10.044	2.34

The results showed that Gluability of PVAc, UF, PF, etc. general adhesives is not so satisfied with eucalyptus timber, moreover, during sawing shear samples and checking shear strength, test samples often present a delamination or disjoining at glueline even on the condition of no strength imposed. The shear strengths of former three adhesives are also lower than that of API adhesive drastically, and API illustrated an excellent bonding property with eucalyptus timber. So finally we adopt API as binder in finger-jointing of eucalyptus timber. Furthermore, UF and PF are hot-setting adhesives, on account of our experiment requirements (with thick plank to be glued and at the absence of high frequeecy equipment) and henceforth product orientation (oriented between structure and non-structure material), meanwhile, considering status quo of Glualam adhesives applied in nowadays, so API is a suitable adhesive for our demand.

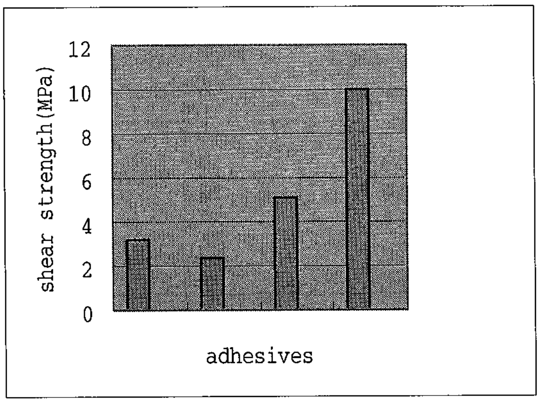

Fig.5.2-1 Shear strength comparisons of 4 adhesives

Based on primary exploring experiments, we selected DYNOLINK-8000A API adhesive. Its performance indexes as shown following:

Tab.5.2-8 The indexes of DYNOLINK-8000A API adhesive

Indexes	Solid content /%	Viscosity /cps.25℃	Coagulation time /(min, 25℃)	pH	Gravity / (g/cm^2)
API	63.8	6750	9	6.6	1.1

At three levels of pressure, glue spreading, pressing time, shown in Tab.5.2-8, two species of eucalyptus timber were glued respectively and cut test samples from bonding blocks at parallel grain direct, and three bonding forms are adopted, that is tangential to tangential (T-T), radial to radial (R-R), and tangential to radial (T-R). After 72hrs, examining shear strength of each sample.

Tab.5.2-9 Three levels of pressure, glue spreading, pressing time (Room temp.)

Level	Spreading $/g/m^2$	Pressure /Mpa	Pressing time /min
1	150	1.5	40
2	200	2.0	60
3	250	2.5	90

Testing results shown as follows: (shear strength: Mpa). Blank samples are wood blocks that have not glued and cut the same size as that of glued shear samples. Blank samples used to in comparison with shear strength of two eucalyptus species.

Tab.5.2-10. Shear strength of control samples

T-T			R-R		
Test number	Ave. of shear strength	Stdev.	Test number	Ave. of shear strength	Stdev.
21	23.37	0.60	21	19.7	1.82

From the Tab.5.2-10 we can find out that the value of shear strength in T-T is more than that of R-R..

In initial experiments, $L_9(3^4)$ test is adopted and results of test are analyzed by ANOVA, then the primary conclusions can be obtained.

Tab.5.2-11 Shear strength of two species on different treat conditions

A	B	C	Pieces Num	T-T		R-R		T-R	
				Ave	Stdev	Ave	Stdev	Ave	Stdev
1.5	40	150	36	13.81	1.37	6.853	0.337	7.67	1.66
1.5	60	200	36	12.15	1.13	11.93	1.12	13.52	1.11
1.5	90	250	36	15.12	1.52	13.70	1.57	12.88	1.36
2.0	40	200	36	8.24	1.28	10.00	0.84	13.90	1.84
2.0	60	250	36	10.30	1.49	13.75	1.27	9.55	1.25
2.0	90	150	36	13.57	1.02	8.27	1.05	13.99	1.88
2.5	40	250	36	15.67	1.81	7.98	1.39	11.44	1.38
2.5	60	150	36	14.46	1.30	11.48	1.88	9.18	0.63
2.5	90	200	36	16.82	2.0	12.37	1.08	13.42	1.52

Note:A: pressure (Mpa) B: Pressing time (min) C: Spreading (g/m^2)

Tab.5.2-12 Analysis by ANOVA on test pieces of *E. exserta*

Source	Sum of squares	DF	Mean square	F value	Pr>F
A	11.43677489	2	5.7183874	12.503851	F0.1=9
B	10.48925422	2	5.2446271	11.467924	
C	8.299916222	2	4.1499581	9.0743164	
Variance	0.914660222	2	0.4573301		
Total	31.14060556				

From the result above, A (pressure) and B (pressing time) exert certain effect on gluability of *E. exserta* timber, but C (glue spreading) show no evident effect on bonging property of this specie.

III *Eucalyptus urophylla×grandis*

The information of testing materials is as Tab.1.

Tab.1 Testing materials

Tree species	Tree age (year)	Tree number	Tree height (m)		Under branch height (m)		DBH (cm)	
			Ave.	Std	Ave.	Std.	Ave.	Std
E. urophylla x *grandis*	14	10	31.08	0.8929	20.26	3.9376	24.77	2.0122

1 WOOD PROPERTIES

1.1 Anatomical characteristics

Samples (2x2x1 cm) for wood anatomical section were stored in alcohol 95% : glycerine (1:1) until they sank. Transverse sections of 20μm were cut on sliding microtome, then bleached, stained with safranin, dehydrated and mounted on slides for measure anatomical properties on image analysis. Then the transverse, radial and tangential sections from each species of around 80μm were cut on the same microtome, make the samples for SEM observation and taking photos.

Prior to tracheid length measurement, the each selected growth rings were firstly separated with a chisel, then macerated in solution of acetic acid (1/3) and hydrogen peroxide 27% (2/3) for several days in 60° oven.

The measurement methods are as follows:

Measuring length and width of wood fiber and vessel element using macerated anatomical elements under fiber length measuring instrument; (2) Measuring wood fiber cell wall thickness, cell wall percentage, and tissue proportions by section method using image analysis system; (3) Measure of S2 microfibril angle: using x-ray diffractometer.

The observation and description for macro- and micro-structure were made under the light microscope and scanning electronically microscope (SEM).

1.1.1 Tree and distribution

Eucalyptus urophylla×grandis is a hybrid species breeding by Brazil. A tree up to 18 m, 20.3 cm in DBH, is comparing with *Eucalyptus urophylla*, higher 60% and 27% in tree height and d.b.h respectively; higher 66% and 22% than *E. grandis* respectively. There is has successful an integrated technology for tissue culture on the factory-scale.

The Dongmen farm in Guangxi is introducing *E. urophylla* x *grandis* in 1984 from Brazil. The trees grow very well. Guangdong, Guangxi, Hainan and Fujian province etc. are introducing this species and wide plant.

1.1.2 General characteristics

Sapwood yellow, yellowish brown, comparatively differs from heartwood, width 2~3 cm. *heartwood* dark yellowish brown; glossy, wood without characteristic taste & odor. *Growth rings* indistinct. Wood diffuse-porous. Pores small to middle, visible to the naked eye, fairly uniformly distributed throughout the ring, radial, tyloses visible. *Longitudinal parenchyma* vasicentric. *Rays* very fine to fine, visible with a hand lens;

Ripple marks and *Resin canals* absent.

1.1.3 Minute anatomy (Plane II)

Vessels most solitary; radial or flexuous; cell wall thin to thick; tangential average diameter 125 μm, max 219 μm. 11 (8~15) /mm^2 . Vessel element length 378 (180~590) μm, tyloses visible and wall thin, helical thickness absent. Simple perforation, its plate oblique. Intervessel pits ventured, alternate, round & polygonal, ventures distributed pit aperture and & chamber, most coralloid and lumpish. Vasicentrics common, located vessels intermixing parenchyma cells, with bordered pit round and ventured. Vessel- ray pits large round.

Longitudinal parenchyma vasicentric, diffuse or diffuse-aggregates. Nodular end wall of parenchyma cells inconspicuous; crystals absent.

Fiber wall thick to thick, 1233 (960~1396) μm in length, with plain simple pits.

Rays unstoried, rays 12~14/mm, mostly uniseriate rays 2~14 cells, multiseriate rays width 2 cells, height 6~12 cells. Ray tissues homogeneous uniseriate and multiseriate; parenchyma cells round or oval, some with gum. Crystal and intercellular canals absent. The proportion of wood tissue: Fiber: 71.8%, vessel: 13.2%, Rays: 13.6%, parenchyma: 1.5%.Cell wall: 70.45%.

The data of anatomical parameter and basic density at different heights is including to the Tab. 1.1-1, the tissue proportion at different heights and the vessel distribution frequencies and tangential diameters are listed in Tab. 1.1-2 and 1.1-3 respectively.

Tab.1.1-1 Anatomical parameter and basic density at different heightsfor *E. urophylla* × *grandis*

Item	1.3m		3.3m		5.3m		7.3m	
	$\bar{x}$	δ_n	$\bar{x}$	δ_n	$\bar{x}$	δ_n	$\bar{x}$	δ_n
Fiber length (μm)	1273	26	1270	51	1251	40	1249	70
Fiber width (μm)	18.3	1.1	18.5	0.8	18.3	1.1	17.6	0.8
Fiber wall thickness	10.84	0.823	11.24	0.827	10.83	0.732	10.88	1.365
Microfibril angle (°)	10.61	1.706	9.29	1.024	8.82	0.529	8.70	0.625
Basic density (g/cm^3)	0.552	0.018	0.561	0.040	0.563	0.041	0.561	0.038

Tab.1.1-2 Tissue proportion of *E. urophylla* × *grandis* at different heights for (%)

Item	1.3m		3.3m		5.3m		7.3m	
	$\bar{x}$	δ_n	$\bar{x}$	δ_n	$\bar{x}$	δ_n	$\bar{x}$	δ_n
Fiber	71.8	2.113	72.48	2.782	73.54	1.707	72.21	3.069
Vessels	13.17	1.259	13.80	2.189	13.34	1.783	13.76	2.308
Rays	13.56	2.098	12.25	1.875	11.82	2.179	12.81	1.979
Longitudinal parenchyma	1.47	1.367	1.48	0.385	1.27	0.267	1.22	0.306
Cell wall	70.45	2.63	68.71	2.149	70.15	2.876	69.54	3.616

Tab.1.1-3 Vessel distribution frequencies and tangential diameters

Vessel distribution frequency (Number/mm^2)				Vessel tangential diameter (μm)			
Ave.	Std.	Max.	Min.	Ave.	Std.	Max.	Min.
11.40	2.2215	14.63	8.10	125.48	37.0975	219.74	36.99

1.2 Physical properties

1.2.1 Moisture content of the green wood

The moisture content data of the green wood at different tree heights and radial sites is including Tab. 1.2-1 and Fig. 1.2-1 respectively.

Tab.1.2-1 MC of E. urophylla×grandis green wood at different tree heights and radial sites (%)

Side	1.3m		3.3m		5.3m		7.3m	
	$\overline{x}$	δ_n	$\overline{x}$	δ_n	$\overline{x}$	δ_n	$\overline{x}$	δ_n
1	127.54	16.80	113.15	20.02	113.92	11.68	110.01	14.86
2	124.99	21.64	104.01	22.82	106.28	13.77	103.80	13.74
3	99.33	17.47	98.35	14.81	91.75	11.12	93.27	22.34
4	99.76	10.01	103.49	13.16	101.26	9.79	97.78	13.20
5	87.01	7.04	95.38	7.32	94.47	9.45	92.05	10.16

1=near pith, 2=site between 1 &3, 3=center from pith to bark, 4=site between 3 &5, 5= near bark

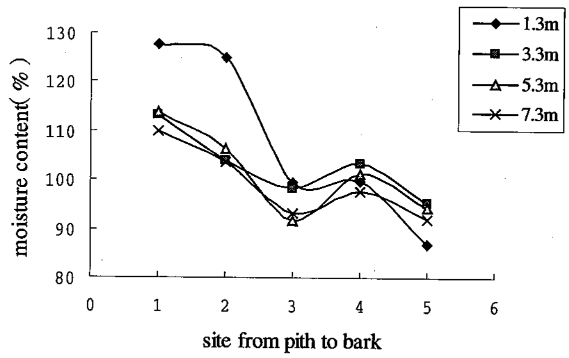

Fig.1.2-1 Moisture content of green wood for *E. urophylla* × *grandis* at different heights

1.2.2 Shrinkage and Density

Shrinkage is the contraction of wood caused by drying the material below the fiber saturation point (William T. Simpson, 1991). It can be divided into 3 types of shrinkage according to the direction of contraction: longitudinal, radial and tangential shrinkage. The longitudinal shrinkage is the shrinkage along the grain, the radial shrinkage and the tangential shrinkage is that across the grain in a radial or in a tangential direction. Wood density, the weight of wood per unit volume, is a very important index having a close relation with wood mechanical strength. In this study, wood air-dried density and basic density were used to describe the wood density.

The shrinkage is attributed to the dimension stability and checking problem, which causes a lot of problem for the wood utilization. In another word, it causes not only the contraction of wood in size, but also the checking and deformation resulted from the different contraction in tangential, radial and longitudinal direction. Understanding the characteristics of shrinkage has no doubt to be helpful for the wood utilization for the wood industry practice. Nowadays, studying on the characteristics of shrinkage during the losing of water is becoming one of the wood science discipline[Barber NF etc.1964; Barber, 1968; Chafe, 1986; 1987; Gu H et al., 2001]。 This study is intended to explore the shrinkage variation of acacia in different direction (North and south), different radial position and different tree height.

The trees studied were cut from Guangxi Zhuang Autonomous Region in the South China. Each trunk has been collected above the breast height and was cut every 2 meters. Then, four discs of each tree at different heights (about 1.3m, 3.3m, 5.3m and 7.3m respectively) were taken from the logs. All the discs were marked the south-north direction. For each disc, one specimen from the sapwood near the bark, one from the heartwood near pith and one from transition zone was made at the size of 2X2X2cm (Tangential X radial X longitudinal direction) for both north side and south side.

Two diagonal lines were drawn in three sections (i.e., T×R, T×L, R×L) of each specimen to locate the central point where the size was measured. The specimens were put into water until they were totally saturated and sunk in the water. The surface water was wiped off and the sizes in three directions (L, R, T) were measured. Specimens were set in the room for air-drying. After measuring the size and weight at the air-dried stage, the specimens were oven-dried and the same measurement was carried out. The shrinkage was determined according to Chinese National Standard. The air-dried density and was also calculated of both air-dried
The shrinkage coefficient was determined by the difference between shrinkage at air-dried and at oven-dried and divided by the MC at air-dried.

1.2.2.1 Shrinkage and density, and that of wood from south and north directions

The air-dried shrinkage in tangential direction (Ta), Radial direction (Ra) and volumetric shrinkage (Va), as well as the oven-dried shrinkage in tangential direction (To), Radial direction (Ro) and volumetric shrinkage (Vo) are listed in Tab.1.2-2 according to the categories of south direction, north direction and the overall. The basic density (B D) and air-dried density (A D), together with tangential shrinkage coefficient and radial shrinkage coefficient were also calculated and listed.

According to the IAWA (1989) method (the wood with an air-dried density smaller than 0.56 g/cm^3 is considered to be a small-density species, between 0.56 g/cm^3 and 0.75 g/cm^3 is considered to be a medium-density, between 0.75 g/cm^3 and 0.95 g/cm^3 is considered to be a large-density species, and bigger than 0.95 g/cm^3 is considered to be a extra-large-density species), *E.urophylla×grandis* wood has a medium density.

According to the *CHINA WOOD* method (the wood with an air-dried tangential shrinkage smaller than 5.60% is considered to be a small-shrinkage species, between 5.60% and 7.00% is considered with a medium-shrinkage species, and bigger than 7% is considered to be a big-shrinkage species), *E .urophylla* × *grandis* has a big shrinkage, suggesting more attention should be paid when sawing and drying.

ANOVA analysis (Tab.1.2-3) showed there was no significant difference between air-dried tangential shrinkage and air-dried radial shrinkage, suggesting that the wood from north and south could be thought has the same level in shrinkage.

Tab.1.2-2 The shrinkage and density of *E. urophylla* × *grandis* wood from south and north side

		Ta (%)	Ra (%)	Va (%)	To (%)	Ro (%)	Vo (%)	B D (g/cm^3)	A D (g/cm^3)	Co-t (%)	Co-r (%)
South	Average	7.36	4.34	11.48	10.46	6.89	16.90	0.50	0.63	0.29	0.24
	Std.dev.	1.15	0.68	1.45	1.16	0.99	1.58	0.04	0.05	0.25	0.21
	CV(%)	0.16	0.16	0.13	0.11	0.14	0.09	0.08	0.08	0.86	0.90
	Number	114	114	114	114	114	114	114	114	114	114
North	Average	7.43	4.14	11.36	10.63	6.86	17.07	0.50	0.64	0.26	0.22
	Std. dev.	1.27	0.78	1.73	1.32	1.17	1.97	0.05	0.06	0.03	0.06
	CV(%)	0.17	0.19	0.15	0.12	0.17	0.12	0.09	0.10	0.13	0.28
	Number	116	116	116	116	116	116	116	116	116	116
Total	Average	7.40	4.24	11.42	10.54	6.88	16.99	0.50	0.64	0.27	0.23
	Std. dev.	1.21	0.74	1.60	1.24	1.08	1.79	0.04	0.06	0.17	0.16
	CV(%)	0.16	0.17	0.14	0.12	0.16	0.11	0.08	0.09	0.64	0.68
	Number	230	230	230	230	230	230	230	230	230	230

Tab.1.2-3 ANOVA analysis on the shrinkage of *E.urophylla* x *grandis* wood from north and south

	SS	df	MS	F	P-value	F crit
Ta	0.2381	1	0.2381	0.1619	0.6878	3.8826
Ra	2.2193	1	2.2193	4.1288	0.0433	3.8826

1.2.2.2 Shrinkage and density of wood from 4 different tree heights

The shrinkage, shrinkage coefficient and density from 4 different tree heights were listed in Tab.1.2-4. The relationship between air-dried shrinkage, basic density and tree heights were showed in Fig. 1.2- .

ANOVA analysis (Tab.1.2-5) showed there existed significant air-dried shrinkage difference both in tangential and radial directions among 4 different tree heights.

Tab. 1.2-4The shrinkage and density of *E.urophylla* × *grandis* wood from different heights

		Ta (%)	Ra (%)	Va (%)	To (%)	Ro (%)	Vo (%	BD (g/cm³)	AD (g/cm³)	Co-t (%)	Co-r (%)
1.3m	Average	7.83	4.04	11.66	10.87	6.43	16.94	0.50	0.63	0.25	0.20
	Std. dev.	1.29	0.81	1.77	1.31	1.00	1.88	0.04	0.06	0.02	0.02
	CV(%)	0.17	0.20	0.15	0.12	0.16	0.11	0.09	0.10	0.09	0.11
	Number	59	59	59	59	59	59	59	59	59	59
3.3m	Average	7.40	4.19	11.34	10.53	6.85	16.91	0.49	0.62	0.26	0.22
	Std. dev.	1.17	0.74	1.59	1.23	1.08	1.79	0.04	0.05	0.03	0.06
	CV(%)	0.16	0.18	0.14	0.12	0.16	0.11	0.08	0.08	0.14	0.29
	Number	58	58	58	58	58	58	58	58	58	58
5.3m	Average	7.23	4.36	11.36	10.54	7.03	17.12	0.51	0.65	0.28	0.22
	Std. dev.	1.25	0.74	1.62	1.15	1.02	1.81	0.04	0.06	0.06	0.03
	CV(%)	0.17	0.17	0.14	0.11	0.15	0.11	0.08	0.09	0.23	0.12
	Number	56	56	56	56	56	56	56	56	56	56
7.3m	Average	7.11	4.38	11.32	10.22	7.21	16.99	0.51	0.64	0.31	0.28
	Std. dev.	1.01	0.61	1.39	1.23	1.10	1.71	0.04	0.06	0.34	0.30
	CV(%)	0.14	0.14	0.12	0.12	0.15	0.10	0.08	0.09	1.10	1.08
	Number	57	57	57	57	57	57	57	57	57	57

Tab.1.2-5 ANOVA analysis on the shrinkage of *E.urophylla* × *grandis* wood from different heights

	SS	df	MS	F	P-value	F crit
Ta	17.2180	3	5.7393	4.0757	0.0076	2.6445
Ra	4.4730	3	1.4910	2.8011	0.0408	2.6445

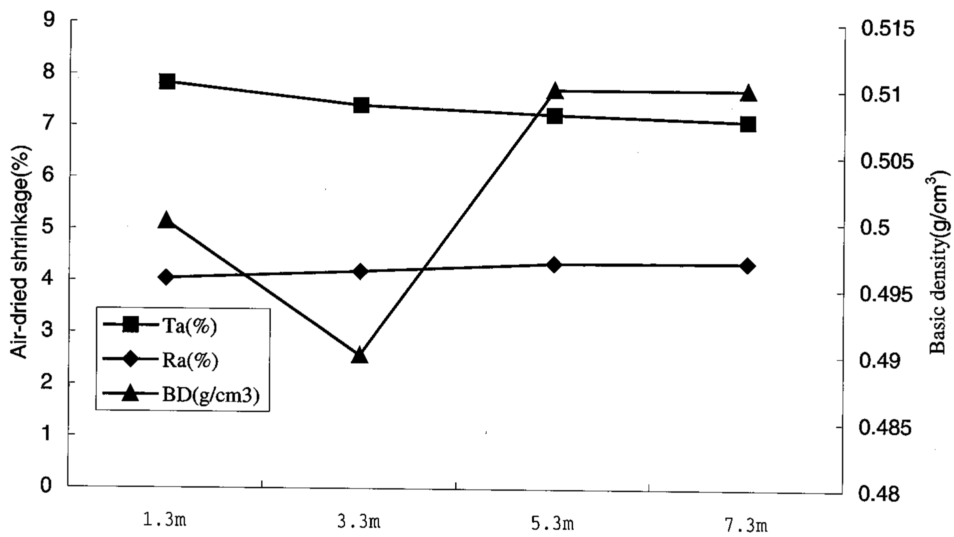

Fig.1.2-2*E.urophyllaxgrandis*: relationship between air-dried shrinkage (Ta&Ra), basic density (BD) and tree heights

1.2.2.3 Shrinkage and density of wood at different radial positions

The shrinkage, shrinkage coefficient and density from 4 different tree radial positions were listed in Tab.1.2-6. The relationship between air-dried shrinkage, basic density and tree heights were showed in Fig. 1.2-6.

ANOVA analysis (Tab.1.2-7) showed there existed significant air-dried shrinkage difference in both tangential and radial direction.

Both the radial and tangential shrinkage in the transition zone presented the maximum value. The basic density in the juvenile presented the minimum value.

Tab. 1.2-6 The shrinkage and density of *E. urophylla* × *grandis* from different radial positions

		Ta (%)	Ra (%)	Va (%)	To (%)	Ro (%)	Vo (%)	B D (g/cm^3)	A D (g/cm^3)	Co-t (%)	Co-r (%)
Near bark	Average	6.78	4.34	10.97	10.07	6.99	16.69	0.52	0.65	0.31	0.26
	Std. dev.	1.04	0.59	1.33	0.98	0.80	1.42	0.03	0.04	0.29	0.26
	CV(%)	0.15	0.14	0.12	0.10	0.11	0.09	0.06	0.06	0.93	1.00
	Number	78	78	78	78	78	78	78	78	78	78
Transition	Average	7.92	4.53	12.18	11.10	7.34	17.92	0.52	0.66	0.26	0.23
	Std. dev.	0.98	0.67	1.42	1.16	1.03	1.60	0.03	0.05	0.04	0.06
	CV(%)	0.12	0.15	0.12	0.10	0.14	0.09	0.06	0.07	0.14	0.26
	Number	80	80	80	80	80	80	80	80	80	80
Near pith	Average	7.49	3.81	11.06	10.44	6.24	16.27	0.46	0.59	0.24	0.20
	Std. dev.	1.33	0.77	1.74	1.36	1.12	1.92	0.04	0.05	0.04	0.06
	CV(%)	0.18	0.20	0.16	0.13	0.18	0.12	0.08	0.09	0.15	0.31
	Number	72	72	72	72	72	72	72	72	72	72

Tab.1.2-7 ANOVA analysis on the shrinkage of *E.urophylla* × *grandis* wood from different radial positions

	SS	df	MS	F	P-value	F crit	SS
Ta	52.31559	2	26.1578	20.97054	4.39E-09	3.035623	52.31559
Ra	21.07731	2	10.53865	23.07065	7.57E-10	3.035623	21.07731

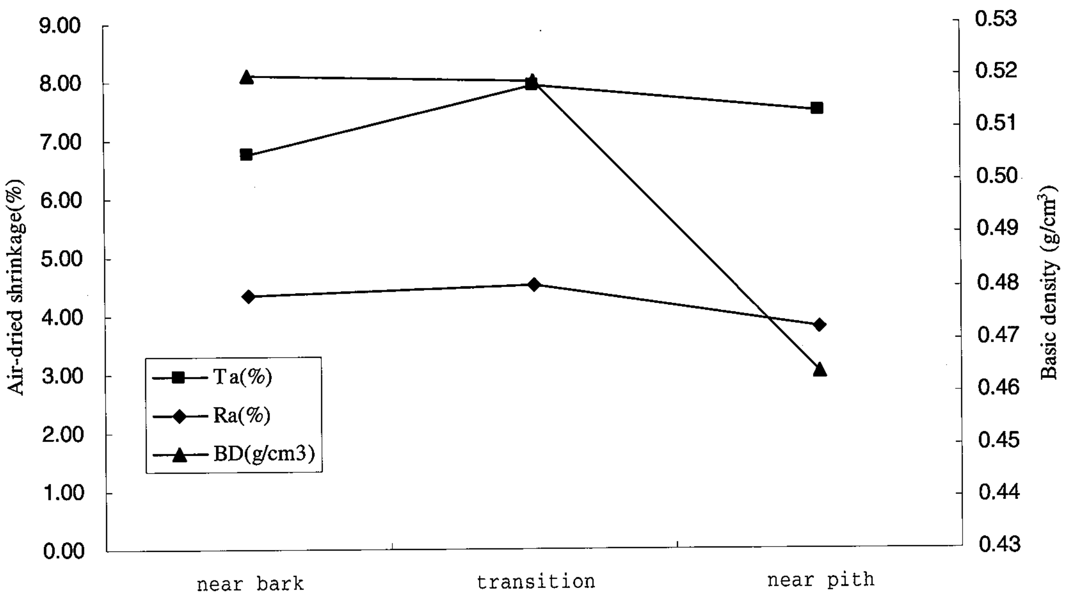

Fig.1.2-3*E.urophylla* × *grandis*: relationship between air-dried shrinkage (Ta&Ra), basic density (BD) and different radial positions

1.3 Mechanical properties

The small clear wood samples of moduli of elasticity (MOE), moduli of rupture (MOR) in static bending, compression strength parallel to grain and wood density were cut in accordance with Chinese National Standards (GB 1927~1943-91). The specimens were then stored in a conditioning chamber until it reached approximately 12% moisture content. Bending, compression and wood density test were carried out in accordance with Chinese National Standard. The air-dry density was calculated by air-dried weight and volume while oven-dry density was based on oven-dried weight and volume.

Generally *E. urophylla×grandis* wood grain strait or oblique, texture fine to middle and even, weight middle, little hard, shrinkage large, strength middle or highly. Nail holding power (N/mm): Radial: 49.9 Tangential: 48.8 Parallel to grain: 34.5. The mechanical properties are including tab.1.3-1.

Tab.1.3-1 Mechanical properties data of *E. urophylla×grandis*

Locality	Density /g/cm³		DS /%		CSPG /MPa	BS /MPa	MOE /GPa	Toughness /kJ/m²	Hardness /N		
	BD	ADD	R	T	CSPG/MPa	BS/MPa	MOE/GPa	Toughness/kJ/m²	E	R	T
Guangxi Dongmen		1.033			74.2	141	17.34	79.8			

BD = basic density, ADD = air-dry density, DS = dry shrinkage, CSPG = compressive strength parallel to grain, BS = bending strength, MOE = modulus of elasticity, SSPG = shear strength parallel to grain(R), E = end, R = radial, T = tangential.

1.4 Chemical properties

The chemical composition was determined according to Chinese National Standards, the results are listed in Tab. 1.4-1, pH values, acid and alkaline buffering capacities and hydroxybenzene and acid of fragrance in acid soluble lignin are listed in tab.1.4-2 and 1.4-3 respectively.

Tab.1.4-1 Chemical composition of *E. urophylla×grandis* (%)

lignin	Holocellulose	α-Cellulose	Hemicellulose	1% NaOH extractives	Benzene-alcohol extractives	Hot water extractives
25.26	75.75	45.31	30.44	16.19	1.65	4.15

Tab.1.4-2 Data of pH value, acid and alkaline buffering capacity of *E. urophylla×grandis*

S	H	S	H	S	H
4.83	3.71	4.30	2.48	17.10	34.20

S- sapwood, H-heartwood

Tab.1.4-3 Hydroxybenzene and acid of fragrance in acid soluble lignin of *E.urophylla×grandis*

Gallic acid	Catechin	Prycatechol	p-hydroxyl benzoic acid	Ferulic acid	All hydroxybenzene
32.65	7.51	2.81	——	——	42.97

2 GROWTH STRESS

The research adopted CIRAD-Foret method to measure surface longitudinal growth strain (SLGS) of standing trees, the results at different orientations were listed in Tab.2-1. The research adopted CIRAD-Foret method to measure surface longitudinal growth strain (SLGS) of standing trees, the results at different orientations were listed in tab.2-1. And the growth strain data for 3 clones at different orientations is including in Tab.2-2.

Tab.2-1Growth strain data for standing trees of *E. urophylla×grandis*

Basic density	E		W		S		N	
(g/cm^3)	$\bar{x}$	δ_n	$\bar{x}$	δ_n	$\bar{x}$	δ_n	$\bar{x}$	δ_n
0.561	1050	148.8	971	249.3	1196	428.2	1139	180.3

E=east, W=west, S=south, N=north

Tab. 2-2 Growth strain data for standing trees of 3 clones for *E. urophylla* x *grandis*

No.	Clone			W		S		N	
		$\bar{x}$	δ_n	$\bar{x}$	δ_n	$\bar{x}$	δ_n	$\bar{x}$	δ_n
1	DH33	992	36.66	1220	182.1	1112	4 98.3	1248	181.2
2	DH32	1071	209.5	819	99.13	1425	461.2	1152	216.7
3	DH30	1080	158.7	924	298.6	976	263.5	1012	24.97

E=east, W=west, S=south, N=north

3 MACHINING PROPERTIES

The logs of *E. urophylla×grandis* plantation with the age of 8 to10 years old were supplied by Guangxi Chengda Wood Products Company. And its diameter was about 20~30cm. The moisture contents after kiln drying were 8 to12%. The test specimens were made based on the ASTM standard, whose dimension was 20 mm ×127 mm ×1200 mm (thickness×width×length). According to ASTM standards the test lumber should be clear and sound, which means free from all defects, including knots, stain, incipient decay, surface checks, end splits, and reaction wood. However, for *E. urophylla×grandis* plantation wood, to thoroughly avoid all these defects is considerable difficult. The method of drawn at random was taken in order to show the real characteristics of this wood. The size for smaller samples is showed in Tab.3-1.

Tab.3-1 Smaller samples size for individual test

Individual test	Size: Thickness x Width x Length(mm)	Number
Planning	19 x 102 x 910	30
Sanding	19 x 102 x 400	30
Shaping	19 x 76 x 305	30
Boring	19 x 76 x 305	30
Mortising	19 x 76 x 305	30
Turing	19 x 19 x 305	30

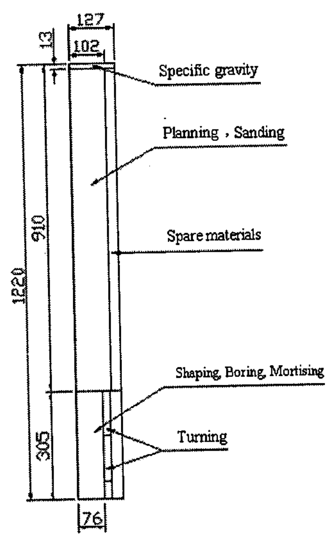

Fig.3-1 Diagram for sawing lumber into smaller samples for individual tests

3.1 Methods

3.1.1 Planning

The planning test was conducted on KUW-500F1 planer. Some adjustments of the bottom spindle allowed its cutting circle beneath the bench. The knife parameters should be stabilized. The wedge angle was 30° .The material of knife is the industry standard high-speed steel (HSS). Five treatments based on two control factors (planning thickness and feed rate) have been conducted.

Tab.3.1-1 Five treatments of planning

Treatment	Cutting thickness（mm）	KMPI	Feed velocity（m/min）
1	1.6	20	8
2	2.5	40	8
3	1.6	48	9.5
4	1.6	20	19
5	2.5	48	19

3.1.2 Sanding

WS-65 wide belt-sanding machine made by Japanese AMITE Company was used to test sanding properties. This sander has only one head and is automatic feed. The scope of feed rate is from 4.3 to 20.3m/min. 5.8m/min feed rate was used in the sanding test, while the feed rate recommend by ASTM is 6.1m/min. ASTM standard did not prescribe concrete sanding thickness. Based on China's practical production and the testing of EDVARD KARDELJ University, in this study the cutting thickness was 0.6mm. The grit of sand paper was 120.

3.1.3 Shaping

A single spindle shaper was used to test shaping properties, which was equipped with a moulding milling cutter. This hand feed shaper was made by Mudanjiang Wood Machining Factory in China and has 4 spindle rotations, of which 6 000 r/min was used in this testing. The milling cutter was produced by Chaoyang Tool Factory in Beijing.

Before shaping the specimens need to be sawn. Then make a preliminary roughing cut along the grain as soon as possible and make a 2mm deep finishing cut. However the cutting thickness recommended by ASTM was 1.6 mm.

3.1.4 Boring

Two types of bits (namely center bit and solid nose bit) were used in the boring tests. The center bit was equipped into a B13S bench borer produced by Japan. Its maximum spindle rotations was 3 000 r/min and the minimum spindle rotations was 500 r/min. The solid nose bit was equipped into a ZQ3025×5 hand feed borer, whose maximum boring diameter was 25mm.Its maximum and minimum of spindle rotation were 2 800 and 320r/min respectively.

Diameter for two types of bits was also 25 mm. The spindle rotation for B13S borer was 2 000 r/min, for ZQ3025×5 borer was 500 r/min. Although the solid nose bit is not commonly used in wood industry, it is necessary to compare different manufacturing methods for an exploring test. The bit needs to sharpen before every test. According to ASTM the rate of boring should be enough low to insure normally cut.

3.1.5 Mortising

MK312 foot feed moister produced in China was used in this test, whose maximum machining width was 20 mm. 13 mm hollow chisel recommended by ASTM was equipped on the mortising machine. According to ASTM run-thorough mortise should be processed, while the run-not thorough mortise is more commonly used in China's furniture industry. In this test two run-thorough mortises were manufactured in each specimen. The mortises should be two sides parallel to the grain and two sides perpendicular to it.

3.1.6 Turning

Turning test was conducted in Italy TS-120 wood working lathe, which is automatic feed knife. The feeding velocity for cutter block was 0-10 m/min, and returning velocity was 0-12 m/min. three spindle rotations, 2120, 3110, and 4210 r/min, could be chosen. The maximum length for work piece was 1200 mm; the maximum diameter was 200 mm.

In this test the spindle rotation speed was 3110 r/min; the feeding velocity for cutter block was 6 m/min. The material for knife was carbide. The pattern panel was equipped with the machine. The size for the pieces was 20 mm × 20 mm × 305 mm (width×thickness×length). According to ASTM, it needs to adjust the position of the knife to make turning 7.5mm thickness at the thinnest point of piece. All the pieces were processed four times. The cutting thickness for the first 3 times was 1 mm, for the last was 0.7 mm. After turning the pieces were sanding by 150-grit sandpaper.

3.2 Results and discussions

3.2.1 Planning

The grade for planning quality is based on the form and quantity of defects. Based on ASTM standard, the planning qualities are divided into 5 grades (Excellent, Good, Fair, Poor and Very poor) and the number of samples for excellent grade should be statistic. The severity and main form of planning defect for *E. urophally×grandis* plantation wood is showed as the following Fig.3.2-1, 2, 3.

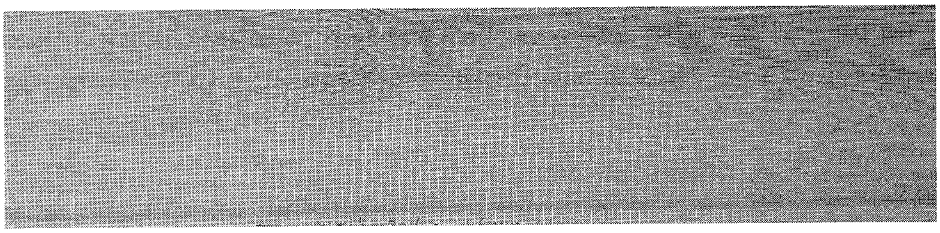

Fig.3.2-1 Clean sample

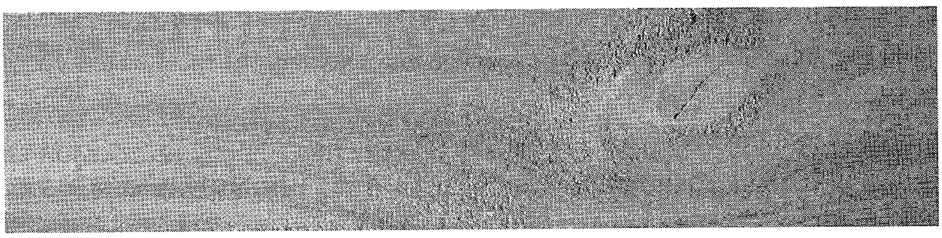

Fig.3.2-2 Torn grain in sample

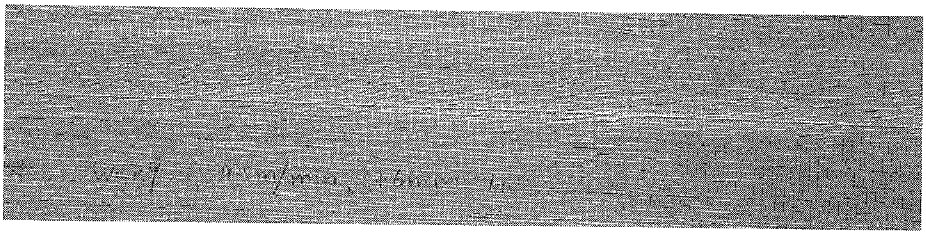

Fig. 3.2-3 "Qiqian" on sample

The study indicates that torn grain and "qiqian" are the two main planning defects. With the feed rate increasing, the planning defects will be more serious. When the feed rate is 19m/min, the planning defect is extremely serious, the total proportion of "Fair, and Poor and Very poor" pieces for two cutting thicknesses (1.6 and 2.5mm) is 70.0%. However, when the feed rate is 8m/min and the cutting thickness is 1.6mm, the proportion is only 24.1%. Obviously, the cutting thickness has a greater influence on the planning quality at high feed rate than low feed rate. The proportions for different treatments are in Fig.3.2-4, 5.

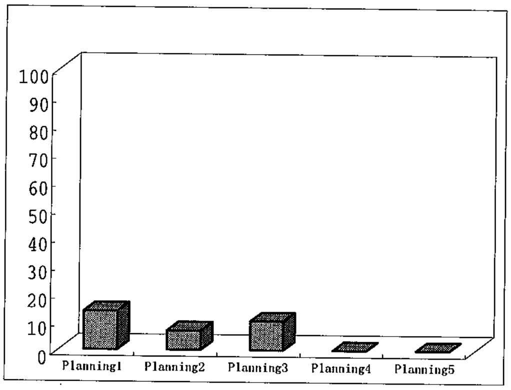

Fig.3.2-4 Proportion for excellent samples

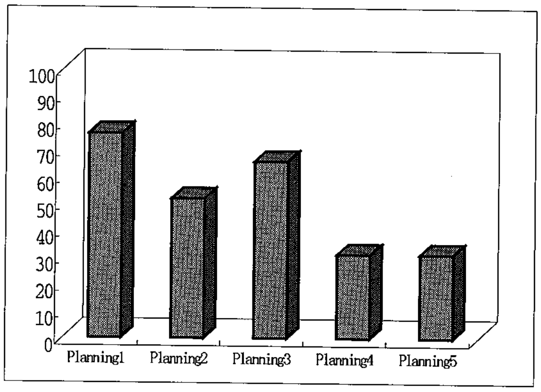

Fig.3.2-5 Proportion for excellent and good samples

On the observation of the torn grain under stereoscope, it could be found that fiber bundles were torn out. There is an angle between the direction of fiber and longitude of the piece in the position of torn grain occurrence. Most of torn grains occurred around the knots. The statistics shows the percents of torn grain nearby knots are about 43.0% for treatment 1, 74.1% for treatment 2, 47.2% for treatment 3, 75% for treatment 4, and 85.1% for treatment 5 separately. Obviously, knots have a great passive influence on planning quality. What's more torn grain also occurred frequently at the position of twist grain. This maybe due to the texture around knots and twisted grain, which are not even. "Qiqian" is also a frequent planning defect. Both its quantity and severity are lighter than those of torn grain. This kind of defect often takes place in the cross part between heartwood and sapwood. Observed "Qiqian" under stereoscope, it can be found that the fiber was torn out, but its form is different from that of torn grain. Namely, the fomer's severity is less than the later. What's more the grains in the position of "Qiqian" usually are diagonal grain, interlocked grain and twisted grain. In order to control the influences of knives on planning quality, the knives need to be sharpened prior to planning. And the cutter head is adjusted to make every knife located in the same cutting circle.

3.2.2 Sanding

The experiment result shows the planning defects can be well removed by wood-sanding. For example, when the feed rate is 19m/min, the extreme planning defects could be produced and thoroughly gotten rid of through followed sanding (Fig.3.2-6). The defects occurred nearby the knots and out of straight were also lightened after sanding. Sanding quality for nearby knots is good. Although the planning defects have been got rid of, a new kind of defect occurred that is surface fuzzy (Fig.3.2-7). Its percent is 75.9%, while the proportion for excellent samples is only 31.0%. This new kind of defect will not occur if the samples surface only sanding and not be scratched yet. Even if scratching the samples surface lengthways the defect also not appeared. But when scratching the transverse surface, a lot of fuzzy occurred. Under stereoscope a number of fibers distributed randomly, which may caused by small abrasives cutting the fibers. However this defect can be improved by hand sanding of using 150-grit sand paper. So the piece quality with surface fuzzy is degraded. The statistics shows the proportional for excellent and good pieces still reach to 100%.

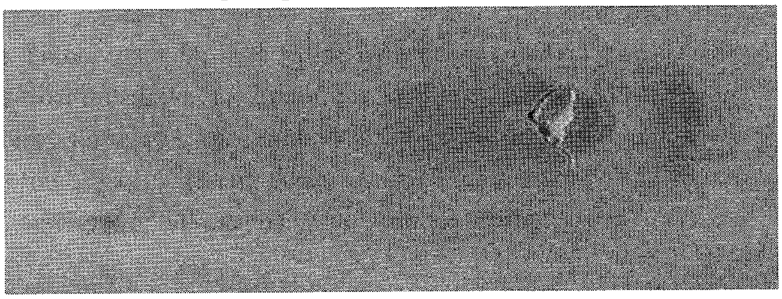

Fig. 3.2-6 Surface quality nearby knot after sanding

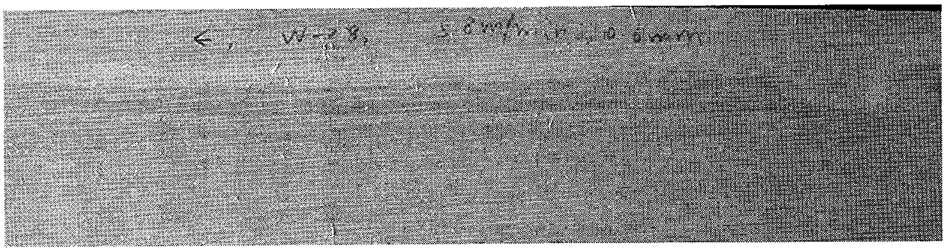

Fig. 3.2-7 Sanding defect: surface fuzzy

3.2.3 Shaping

The test shows that shaping properties of *E. urophally*×*grandis* plantation wood is considerably good (Fig.3.2-8). The proportion of excellent samples is 89.7%. Only 2 samples have occurred torn-grain and 1sample has occurred coarse end grain. But its severity is very light. Some common defects of wood products, such as raised grain, fuzzy grain and chipped grain, did not occur in this test. The profile along the straight grain is smooth and clear, while the profile along end grain is not smooth and clear. Observing the profile nearby end grain under stereoscope, it can be found cutting fibers distributed evenly on the surface. No defects such as fuzzy and tearing happened on this surface. Although the surface roughness along the end grain is less than that along the straight grain, its severity has not reached to the degree regarded as defects.

However there are 4 samples whose profile contained knots and checks. The checks, possibly produced by drying, increase the possibility that the samples were discarded. For example the maximum length of check is up to 13.5 cm. So when shaping, the knots need escape as soon as possible. What's more some measures should be taken to control the check.

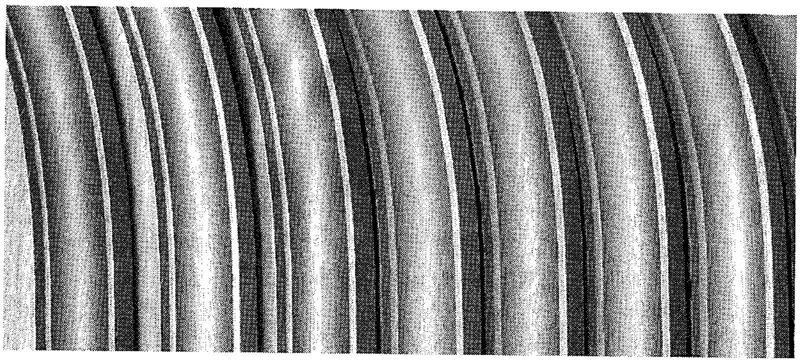

Fig.3.2-8 Excellent samples for shaping

3.2.4 Boring

When boring with center bit, the hole processing quality is considerably good, and the proportion for excellent samples being 100%. The wall of hole is neat and smooth. No defects occurred in the top round edge of the hole, while some defects appeared in the bottom round edge such as fuzzy and tear out which severity was very light and almost can be neglected. But these defects cannot be avoided for boring of solid wood. The reason for fuzzy and tear-out possibly was brought by the hardboard backing. If the hardboard backing is moved after every boring to ensure the specimen and the hardboard backing touched closely, these light defects can be further eased. Observing the wall of the hole under the stereoscope, no torn grain and wood fuzzy occurred.

The hole boring quality of the solid nose bit is worse than that of the brad bit, the proportion for excellent sample being only 37.9%. Even in the same grade, the quality still has some difference between two manufacturing methods. The quality of wall and round edge of the hole manufactured by single twist bit is worse than that produced by the brad point bit. Slight fuzzy have already occurred on the top round edge; medium fuzzy and sever tear out, even extreme tear out which made the samples discarded have occurred on the bottom round edge. There are 3 specimens with extreme defects in total 29 specimens, whose proportion is 10.3%. However the proportion for good and excellent specimens can still account for 75.9%.

When using these two different bits, the boring properties have a great difference (Fig. 3.2-9 to 10). The difference is made by different cutting theory.

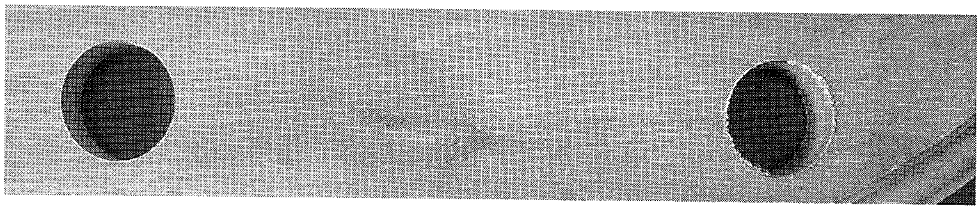

Fig.3.2-9 Front face of sample for boring (no defects)

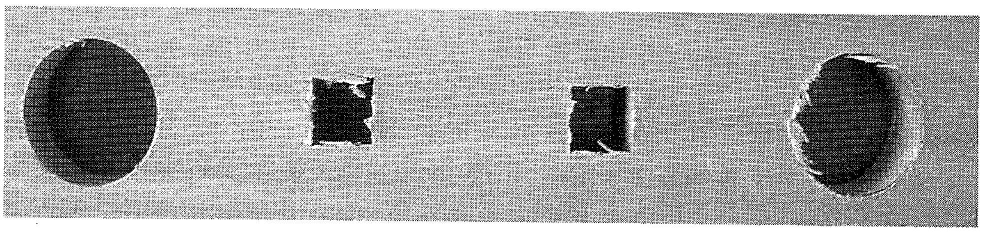

Left hole — no defects manufactured by brad point bit
Right hole — fuzzy manufactured by single twist bit

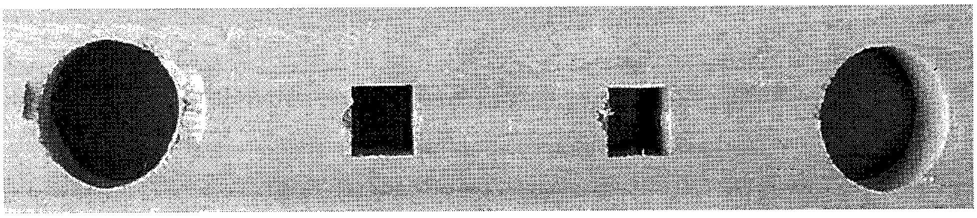

Left hole — tear out manufactured by single twist bit
Right hole — no defects manufactured by brad point bit

Fig.3.2-10 Back face of sample for boring

3.2.5 Mortisng

The study reveals that mortising property is not as good as its boring property (Fig. 1.3.2.5-1 to 2). Among total 56 mortises manufactured, only two however are excellent samples, the proportion being only 3.45%. Others have defects with different degrees. The most frequent defect for mortising is fuzzy grain on mortising wall whose proportion is 96.6%. Fuzz is another common defect whose proportion is 46.6%. Although the number of tear-out samples is less than that of fuzzy grain and fuzzy specimens, its severity is far more than the two kinds of defects. The proportion of fair, poor, very poor pieces of tear-out samples is 17.3%. The quality of top edge of slot mortise is better than that of bottom edge, which is the same as boring property. The fuzz and tear-out often occurred on the bottom edge, which are caused possibly by two sides: (1) the hardboard backing can't be used properly; (2) the processing method should be responsible for these defects. The machine is foot feed, which produced a considerable impact on the specimen. This impact is far more than that of produced by boring machines. Fuzzy grain is the most serious machining defect for the wall of mortises. When observing fuzz grain under the stereoscope, it can be found lots of fibers are torn out that distributed randomly. The roughness of the wall of mortise is worse than that of boring hole. There are four specimens discarded during mortising, whose proportion is 13.8%. Obviously the high density, great variation of density for *E. urophally* × *grandis* plantation wood and feed method of this machine should be responsible for these. However, the quality for top edge can be accepted. Its severity for fuzz and tear-out is very light. If making the run-not-thorough mortise, the mortising quality will be improved and the proportion for excellent samples will also increase. In this testing, the proportion of excellent and good samples is 70.0%.

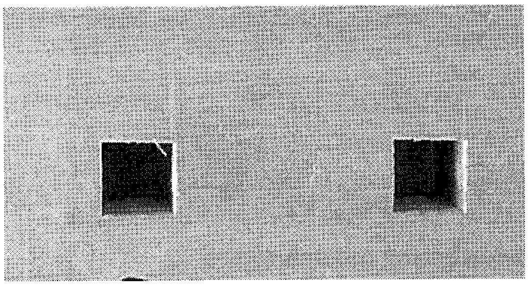

Fig.3.2-11 Top edge of mortise

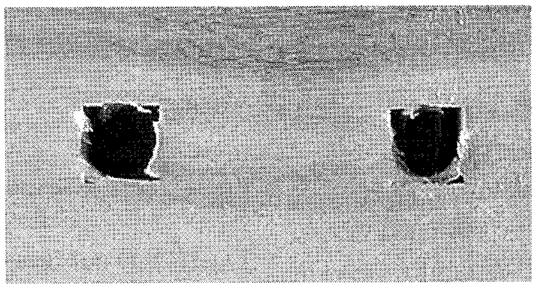

Fig.3.2-12 Bottom edge of mortise

3.2.6 Turning

Before testing, there were four pieces, among which three with inner check and one with big knot were discarded. So 25 pieces were manufactured, of which three pieces were discarded because of occurrence of cracking during processing. Only 1 piece is without defects in totally 29 pieces after turning, whose proportion is 3.45%. The study reveals that fuzz, torn grain and raised grain are main defects for turning. When observing these defects under stereoscope, it could be found that fiber bundles in the position of torn grain were torn-out thoroughly. Although this also occurred in the position of fuzz grain, its tear-out was not so thorough, whose fiber bundles were not off from the wood surface so that the coarse fuzz grain was produced. The raised grain was produced possibly by two reasons that specimen size and knives are improper. The size for specimens is 20 mm × 20 mm × 305 mm (thickness × width × length), and obviously its cross section is too small. The rigidity of pieces is not enough for manufacturing. If the knives cut the pieces under a high rotation speed, the curving distortion will be produced along the axis of pieces because of the low rigidity and the sharpness less of the knife. In practical production , the minimum cross section of work pieces for TS-120 wood- working machine is 26 mm × 26 mm, and the maximum cutting thickness in the thinnest position is 8 mm. Twenty-five test pieces were manufactured in this test, of which 3 pieces were discarded during turning. The proportion for good to excellent samples based on 25 pieces is 76.0%, if based on 29 (adding the four discarded pieces before testing) the proportion is 65.5%. So it is necessary to study the drying characteristics to decrease the inner check and the means to avoid the influence by knots as soon as possible. ASTM did not prescribe sanding after turning; however sanding is commonly used in China's wood plants. In this study a 150-grit sandpaper was used for sanding treatments. The surface roughness after sanding was improved obviously (Fig.3.2-13 to 14).

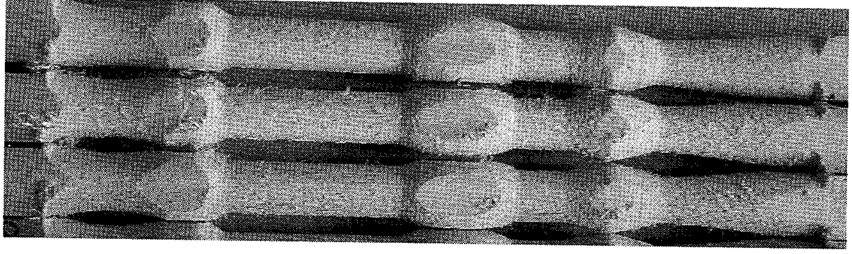

Fig.3.2-13 Turning samples before sanding

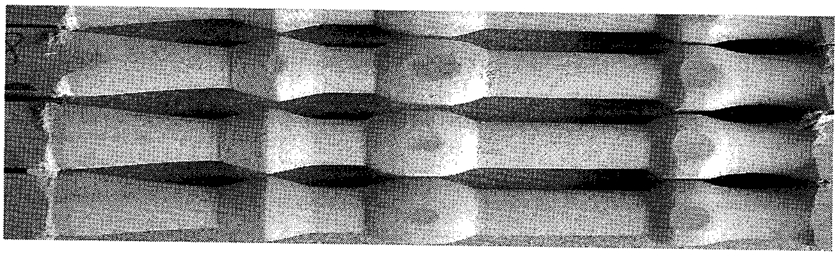

Fig.3.2-14 Turning samples after sanding

3.3 General conclusion

3.3.1 The frequent planning defects for *E. urophally×grandis* plantation wood are torn grain and "Qiqian". Knots have a great influence on planning. Out of straight grain (diagonal grain, interlocked grain and twisted grain) also has some influence on planning properties. The feed rate has a big influence on wood-planning properties. As a result of the decreasing of the feed rate, the defects will be fewer and less severe. Cutting thickness also has an obvious influence on planning quality. The study reveals the 1st treatment (8m/min feed rate and 1.6mm cutting thickness) is the optimal processing for planning of *E. urophally×grandis* plantation wood. So, in order to obtain high planning quality, the small cutting thickness and slower feed rate should be used.

3.3.2 Sanding is a necessary process before painting. The planning defect can be removed though sanding. The product quality nearby knots and out of straight grain is also improved greatly by sanding. For the new sanding defect-surface fuzzy, hand sanding is a good method to resolve. It is obvious that the high surface quality can be obtained through sanding.

3.3.3 E. urophally×grandis plantation wood has a considerably good shaping property. But the knot and check bring some negative influences on shaping properties. Besides, spindle rotation, which is 6 000 r/min in this test, should be increased.

3.3.4 The center bit should be the first choice for boring, while the quality of top round edge is better than that of bottom round edge under two types of bits, which produced by the hardboard backing. So the specimens should be touched the hardboard backing closely as soon as possible. It is necessary to move the hardboard backing after every boring.

3.3.5 The mortising property for *E. urophally×grandis* plantation wood is not good. The frequency of defects is high. The study reveals that the hardboard backing has an important influence on mortising. So the board should be properly used. Because the quality of the bottom edge is worse than that of top edge, the run-not-through mortise should be processed as soon as possible.

3.3.6 The frequent turning defects for *E. urophally×grandis* plantation wood are fuzzy grain, torn grain and raised grain. The reasons for pieces discarded are knots, inner check and twist grain. The cross section of pieces recommend by ASTM is too small, it is necessary for China's industry to increase it.

4 SAWING TECHNIQUES

Logs were collected from DONGMEN Forest farm in Nanning, Guangxi, and 10 stems were taken. All trees were unpruned and were planted on commercial forest land. The ends of the logs were sealed with asphalt to prevent end-drying after logging. Water spraying was applied to keep them in a green condition by preventing drying degrade.

The length of each log section was from 2.00 to 2.20 meters. The taper of this species was small, so three to four sections could be harvested from each tree. The parameters are listed in Tab. 4-1.

Tab. 4-1. The parameters of *E. urophylla×grandis* trees and log sections

Height of tree (m)	Height under branch (m)	Age (years)	DBH (mm)	Diameter Range of log sections (mm)
31.08	20.26	14	248	175~220

Note: the height and DBH (diameter at breast height) are averaged.

The diameter of log sections refers to the Small End Diameter (SED), and bark is not included.

The equipment for the sawing consisted of a headrig band saw with a manually adjusted sizing carriage.

4.1 Strain in Sawing Process

The method of measuring strain is based on the method of measuring longitudinal strain (France, CIRAD-Foret Method) and instantaneous release of residue stress after drilling holes above and below gauges (M. Yoshida, T. Okuyama, 2002). The pin targets and guide for setting is displayed in Fig. 4.1-1.

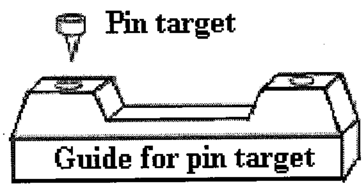

Fig. 4.1-1 Pin target and guide for measuring strain in sawing process

Height of pin target: 10mm, Internal diameter: 2.5mm, External diameter: 10mm, Distance between pin target: 45mm.

Before each sawing pass, two pin targets were placed into the existing sawn surface according to Fig. 4.1-2 or in the case of the opening cut on the log side face which was to be perpendicular to the sawing surface. The distance was measured with a digital caliper with a precision of 0.001 mm. The head of each pin target was recessed to accept the pins and hold them in place. And their distance apart, measured before sawing and again just after the lumber containing the nails was sawn off. The strain changes in the longitudinal and tangential directions were then calculated using the formula:

$$strain = \frac{Da - Db}{Db} * 100\%$$

Where: Db= the dimension before the lumber is sawed off; Da= the dimension after the lumber is sawed off.

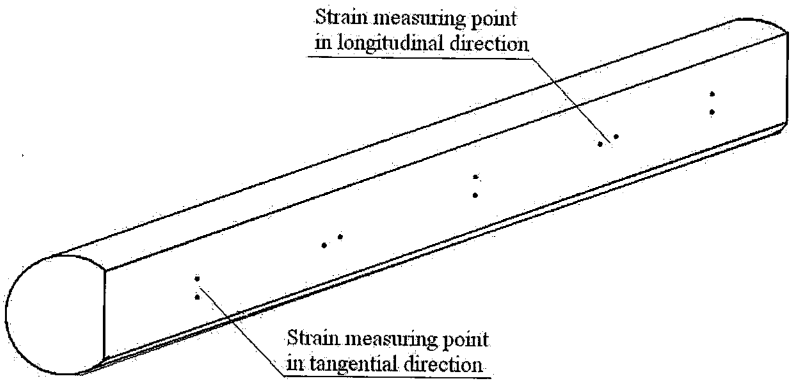

Fig. 4.1-2 Distribution of measuring point for strain change in lumber sawing

The logs were sawn using three different sawing patterns: live sawing, cant sawing and around sawing; and the strain changes were measured following the above procedure.

The strain distribution in the sawing process is analysed and displayed in Figs 4.1-3 – 4.1-4. X-coordinates show the log's position, while the number 1, 2, 3… shows the section position progressively from the bottom to the top section of the trunk. The abbreviations shown in the figures are: T—tangential, R—radial, Sap—Sapwood, Core—Core wood, Live—live sawing, Cant—cant sawing, Around—around sawing, for example, 'T_live' represents tangential direction with live sawing pattern.

The stresses are generated in newly formed wood during cell maturation in living tree. Continuous formation of growth stresses during tree growth results in an uneven distribution of residual stresses across tree stems. When logs are sawn longitudinally, the residual stresses are partially released (Crompton, 2000). And the growth stresses are presented in a random way (Tomaselli, 2000), this may resulted in the big deviation of the strain in sawing process. Fig. 4.1-3 showed that the strain in *E. urophylla* ×*grandis* lumber was minus value except of around sawing pattern. The strain with live sawing and cant sawing pattern is tension strain, and the strain value with cant sawing is the smallest among the 3 kinds of sawing pattern.

The strain curves in Fig. 4.1-4 also displayed that the strain in longitudinal direction with around sawing pattern was compression strain, the others are tension strain. The strain difference between sap and core in longitudinal direction with live sawing pattern is small.

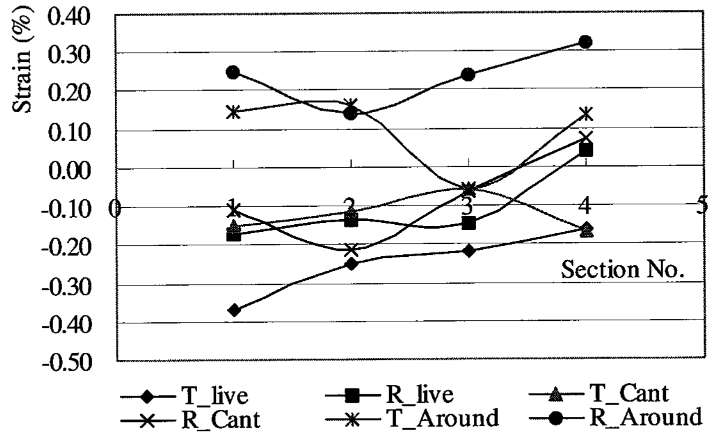

Fig. 4.1-3 Strain distribution of *E. urophylla×grandis* in Tangential and Radial direction

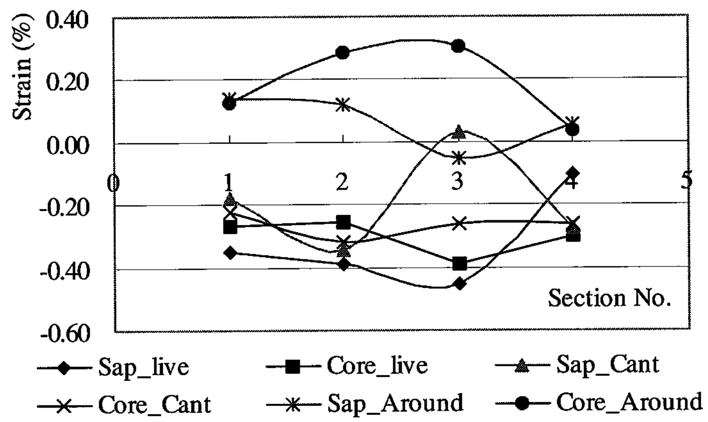

Fig. 4.1-4 Strain distribution of *E. urophylla× grandis* in longitudinal direction

4.2 Bow Deformation

Bow deformation in sawn lumber (bending in the longitudinal direction) was recorded for each sawing strategy. Bow can reflect the extent of growth stress release. The higher the stress gradient in the original log, the greater the expected bow deformation is.

The most deformation which occurred in the sawing process was bow deformation of the lumber, it is also from the releasing of residue stress (Crompton, 2000). The results are displayed in Figs 4.2-1 to 4.2-3 for the three different sawing strategies. The X-coordinates represent the location of lumber in the log, 0 is the core lumber and the other values represent the block number in relation to the pith of the log, Positive and minus values are used to indicate the two directions from the pith. In the live sawing and cant sawing strategies, the larger minus values represent which pieces of lumber were cut first., In the around sawing strategy the sign just represents location of the lumber (displacement from pith).

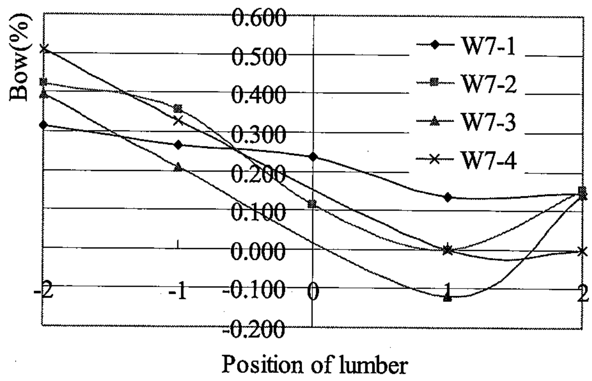

Fig. 4.2-1 The bow deformation of *E. urophylla× grandis* in live sawing

In the sawing process, most of the lumber developed bow deformation except the core lumber. This bow deformation has some relationship with where the lumber was located in the original log and the sequence of cuts in sawing process. This is apparent in Figs 4.2-1 to 4.2-3, especially the cant sawing.

The common results could be gotten from the figures, the outer the lumber position is, the bigger the bow deformation is. The bow deformation has evident relationship with the sequence in live sawing and cant sawing process. The lumber sawed first had the biggest bow deformation (left side), and the lumber sawed later had least deformation. After the former lumber sawed, the stress inside left log had been released in some extent, so the later sawed lumber had less deformation even in the similar position in the log.

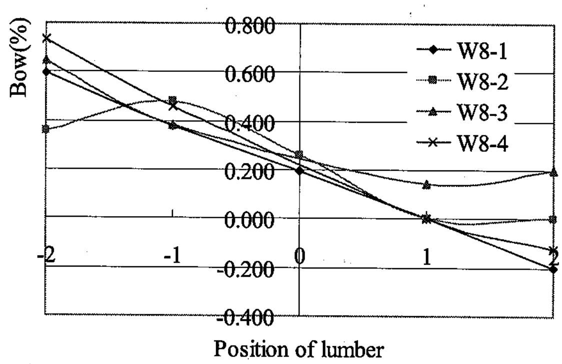

Fig. 4.2-2 The bow deformation of *E. urophylla× grandis* in cant sawing

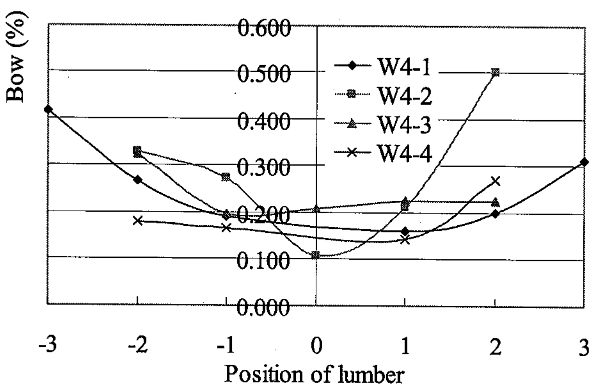

Fig. 4.2-3 The bow deformation of *E. urophylla× grandis* in around sawing

The bow deformation in around sawing and live sawing were small, the biggest value is in cant sawing with the first sawing half. The biggest deformation occurred in cant sawing, after slab sawing off, the most of the wood near the heart under high compression still exists in the cant and on reaching a new equilibrium condition, will impose a higher tensile strain on the sapwood than the level which existed in the intact log (Waugh, 2000), this increased stress gradient and resulted in the bigger deformation.

Tab. 4.2-1 the bow deformation of *E. urophylla*× *grandis* in 3 different sawing pattern

Sawing pattern		Live-sawing				Cant-sawing				Around-sawing			
Position of log		1	2	3	4	1	2	3	4	1	2	3	4
Location of lumber	-3	0.313	0.422			0.596	0.360			0.417			
	-2	0.265	0.356	0.395	0.510	0.379	0.482	0.646	0.736	0.266	0.328	0.325	
	-1	0.238	0.114	0.210	0.328	0.196	0.259	0.384	0.459	0.193	0.272	0.197	0.181
	0	0.136	0.000	-0.120	0.000	0.000	0.000	0.143	0.000	0.160	0.108	0.207	0.165
	1	0.144	0.154	0.141	0.000	-0.202	0.000	0.201	-0.127	0.200	0.212	0.227	0.145
	2									0.313	0.501	0.226	0.270

The bow deformations for 3 sawing patterns were listed in detail in Tab. 4.2-1. The bow deformation displayed the stress distribution and re-distribution in some extent, so the around sawing could release the residue stress more efficient than the other two sawing pattern, and the bow deformation is similar with both side lumber.

4.3 Sawing Inaccuracy

The high growth stress in eucalypts can result in considerable distortion and sawing inaccuracy during sawing (Waugh, 2000), which greatly influence the sawn accuracy of lumber as well as lumber recovery and productivity. According to the national sawing standard of China, the permitted thickness deviation is ± 1mm. However, in this study, the actual sawing variation was much larger, the range being from –3 to +3 mm. This big variation not only influenced lumber recovery, but also made later processing difficult due to the uneven dimensions of the lumber.

The data of sawing inaccuracy of lumber thickness is listed in tab. 4.3-1, the proportion of oversized deviation is about 57%, the residue stress of *E. urophylla*×*grandis* is very big, so it is easy for the lumber to depart from normal position in sawing process, and then result in the thickness inaccuracy.

Tab. 4.3-1 the thickness inaccuracy influence to *E. urophylla*×*grandis* lumber

Amount of slabs (Pcs)	Amount of oversize thickness deviation (Pcs)	The proportion of oversized (%)
82	47	57.3

4.4 The Influence of End-splits on Lumber Recovery

The most frequent defect is end splitting in sawing plantation Eucalyptus for the high growth stress. Heart shake appears just after tree trunk being cut down, and it will extend to some extent before sawing, most end-splitting comes from heart shake in log section. Tab. 4.4-1 shows the results of end-split to lumber recovery. It is about 16%, i.e. if there is no end-split, the lumber recovery will increase about 16%. So it is very important to decrease the growth stress before sawing. The lumber recovery is about 47%.

The dimension accuracy could be improved by choosing appropriate sawing strategies and sawing equipments. The balanced tangential sawing strategy could be utilized, for the deformation of lumber could be minimized (Pandey, 2000). And the lumber recovery could be higher if suitable measure be taken in controlling the end-splitting in tree harvesting. This would improve the potential for the use of Eucalyptus lumber for value added wood products.

Tab. 4.4-1 Influence of end-split to lumber recovery in sawing experiments

log Volume (m^3)	Volume of Lumber with end-split (m^3)	Recovery rate with end-split (%)	Volume of lumber without end-split (m^3)	Recovery rate without end-split (%)
1.1075	0.7003	63.24	1.5219	47.13

5 DRYING TECHNIQUES

5.1 Air drying

Air drying is a traditional and economical drying method which mainly uses sun energy. To save kiln drying time and cost, and to improve kiln drying quality at the mean time, it is suggested to use Air drying as a pre-drying method, and then conventional kiln drying to target final MC (moisture content). Because of the uncontrolled drying conditions, the drying time, final MC and drying quality may be quite difference with the changes of season and drying arrangements. Air drying test focus on analysing wood Air drying properties and try to find its optimum Air drying technique and parameters.

5.1.1 Material and method

The size of sample for air drying is 700 mm (length) x 120-150 mm (width) x 25 mm (thickness). Two MC slices were cut in the two ends of each sample to calculate its initial MC (Fig.5.1-1).

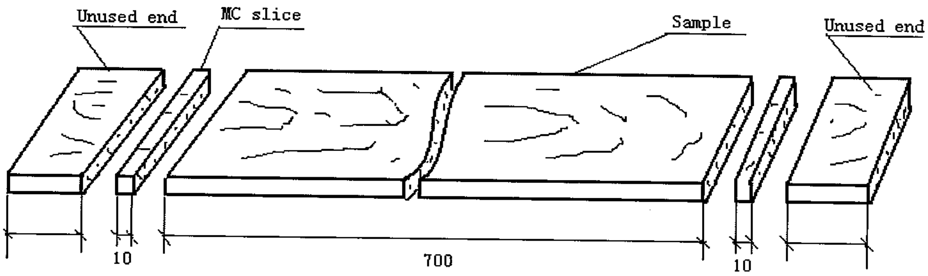

Fig.5.1-1 Drying sample making of *E. urophylla×grandis*

The samples were end-sealed with silicon, and then stacked in air-drying shed to start drying. The dry-bulb and wet-bulb temperatures in shed were recorded every day, and the weights and all visible drying defects of samples were recorded once a week at the first month, then once every two weeks till the air drying ended. When the test finished, three final MC slices and one layer MC slice for each sample were cut (Fig.5.1-2). After oven drying these slices, the final MC for each sample were be gained, and then the oven-dry weight (written as G_0) for each sample could be calculated with the equation listed below. And so, corresponding to the recorded weights of each sample in different drying times, the air-drying MC curve could be drawn.

$$G_0 = 100G_w/(100+ MC_0)$$

G_0 - oven-dry weight

G_w - initial weight

MC_0 - oven-dry MC (%)

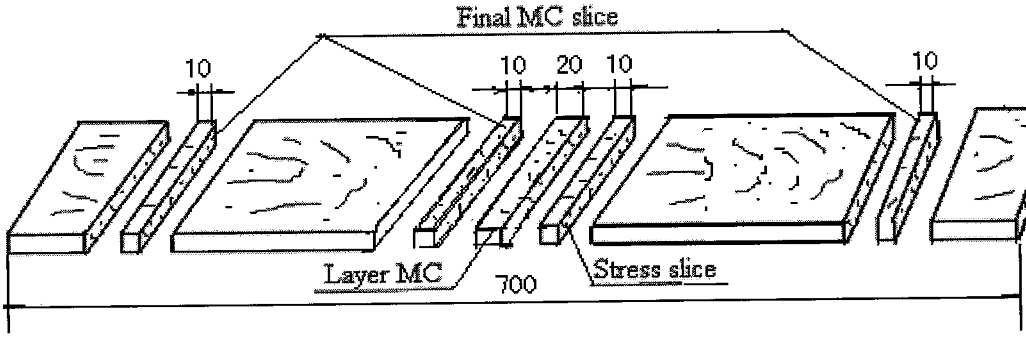

Fig.5.1-2 MC slices making of *E. urophylla×grandis*

5.1.2 Result and suggestion

The air-drying test results of *E. urophylla×grandis* are listed in Tab.5.1-1, and the air-drying MC curves in different seasons were shown in Fig.5.1-3.

Tab.5.1-1 Air-drying test results of *E. urophylla×grandis*

Season	MCw (%)	MCo (%)	Air-drying rate (%day)			Air-drying rate in early stage (%/day)		Defect grade ##
			60-30%	30-20%	Below 20% #	1st week	2nd week	
2002.8-11 Autumn	79.8	12.9	2.14	1.43	0.44 (12.9%)	4.1	1.9	3
	106.1	12.2	2.73	2.5	0.44 (13.9%)	4.2	4	3
	77.1	12.9	2.13	2	0.95 (6.7%)	3.3	2.9	3
2002.12-2003.3 Winter	98.4	12.2	0.94	0.83	0.21 (14.1%)	3.9	2.1	2
	88.2	13.5	0.5	0.43	0.11 (17.9%)	3	0.9	2
	93.6	11.6	0.95	0.71	0.25 (13.1%)	3.9	1.7	2
2003.3-2003.7 Spring	99.6	13.7	1.58	1.05	0.55 (12.8%)	2.7	1.4	1
	97	13.8	1.36	0.83	0.77 (14.6%)	2.5	1	2
	74.2	13.6	2.93	1.11	0.68 (13.5%)	4.2	2	2
2003.6-2003.9 Summer	72.4	14.2	2.93	0.8	0.40 (14.4%)	4	1.9	2
	57.6	14.6	2.88	0.77	0.38 (14.7%)	2.8	1.3	1
	79.8	12.9	2.14	1.43	0.44 (12.9%)	4.1	1.9	3

Note: # - The data in brackets are the final MC when test ended.

##- The standards for drying defects grade division: grade 1 – having no check, warp and cup deformations or just having end checks; grade 2 - having no more than five short end-surface checks or short-narrow surface checks, and the value of warp and cup deformations are smaller than 2mm; grade 3 - having five to ten short-narrow surface checks, and the value of warp and cup deformations are smaller than 4mm; grade 4 - having more than ten short-narrow surface checks and long-narrow or wide surface checks no more than five, or the value of warp and cup deformation are more than 4mm.

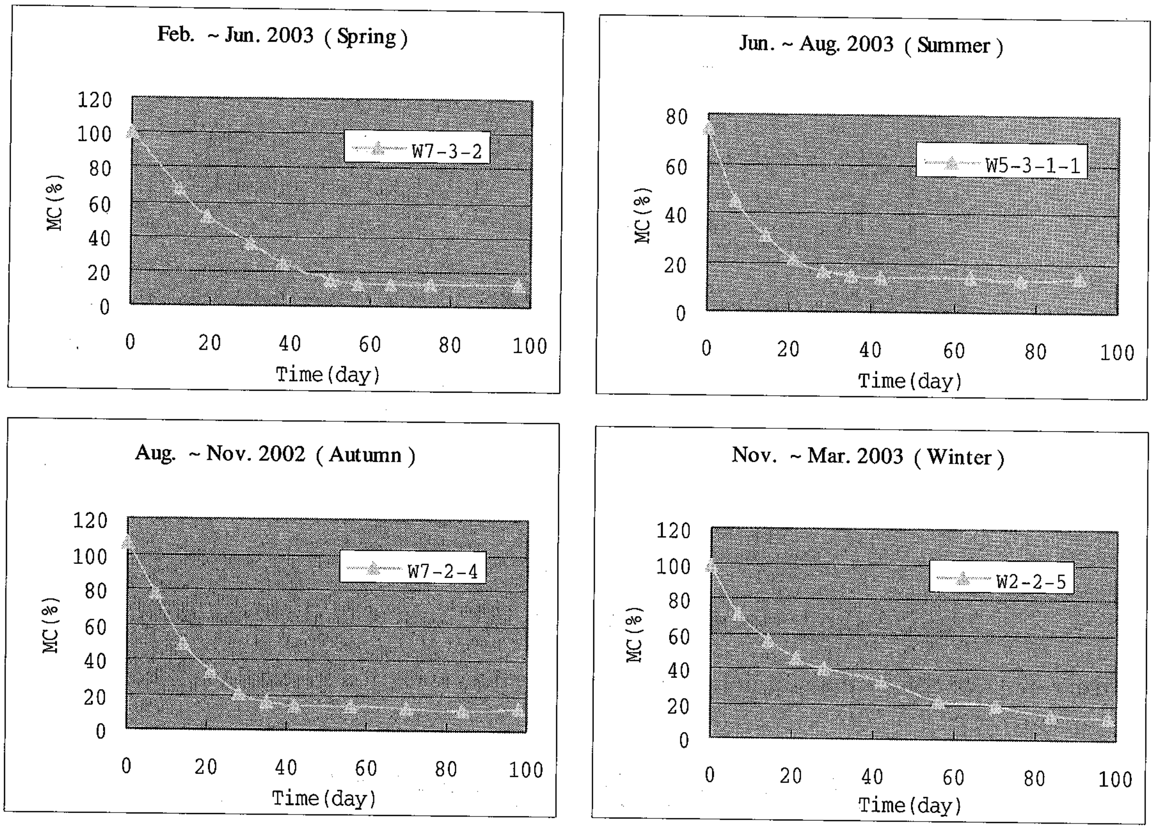

Fig.5.1-3 The air-drying MC curve of *E. urophylla×grandis*

Result showed that the air-drying rate of *E. urophylla×grandis* in summer was the fastest and that in winter in the slowest. But drying defects were very serious (grade 3 mostly), and the main drying defects were many small surface checks. So it is recommended that using controlled air-drying method to pre-dry *E. urophylla×grandis* wood before kiln drying.

5.2 Drying characteristics

5.2.1 Material and method

The sample dimension: plane-sawn lumber with 200mm x 100mm x 20mm

Other requirements of sample: planed lumber with normal colour, knot-free and straight grain, and initial moisture content is above 45%.

Equipment: Electric oven with air circulation.

100℃-test method is a fast drying test which is used to study on drying characteristics and prediction of drying schedule of plantation wood. Before test, the following data of the samples should be gained: the sample's weight, all visible surface defects, and dimension measurement data as showing in Fig.5.2-1. Then the samples were put into the electric oven with constant temperature at 100℃, and letting the samples stand erectly in the oven so that they will obtain same quantity of heat. Once the test begin, weighing the samples, observing and recording all initial defects including end checks, end-to-surface checks and surface checks at a fixed time through all the drying process. The test ended when MC was estimated below to 1%. All the samples were taken out, and then measuring cross-section deformation (Fig.5.2-2). Finally cutting moisture content slice and recording internal checks of each sample.

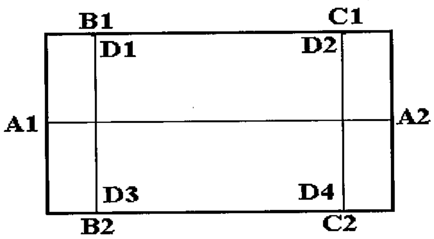

A1-A2 is length
B1-B2 and C1-C2 are width
D1,D2,D3,D4 are thickness

Fig.5.2-1 The dimension measure in 100℃-test of *E. urophylla×grandis*

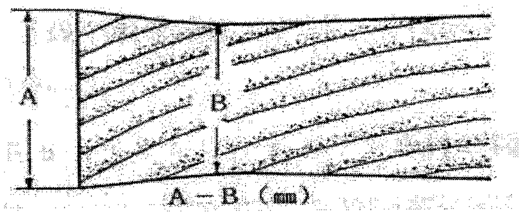

Fig.5.2-2 The cross-section measure in 100℃-test of *E. urophylla×grandis*

To make all these defects digitalization and comparable, the grades of different drying defects are shown in Tab.5.2-1 to Tab.5.2-3.

Tab.5.2-1 The grade division of initial checks

Grade	No.1	No.2	No.3	No.4	No.5
Degree of initial check	No checks or only have end checks	Short end-to-surface checks and short-narrow surface checks	Long end-to-surface checks and long-narrow surface checks no more than two or short-narrow surface checks no more than fifteen	short-narrow surface checks more than fifteen or long-narrow and wide surface checks no more than five	short-narrow surface checks more than five or wide surface checks more than five

Note: long check -- check length ≥ 50mm; short check -- check length <50 mm; narrow check -- check width <2 mm; wide check -- check width ≥ 2mm

Tab.5.2-2 The grade division of internal checks

Grade	No.1	No.2	No.3	No.4	No.5	No.6
Degree of internal check	No :hecks	1 wide or 2 narrow checks	2-3 wide checks; 4-5 narrow checks; 1 wide and 3 narrow	4-5 wide; 7-9 narrow; 1 wide and 4-6 narrow	6-8 wide; 15 narrow; 4 wide and 6-8 narrow	15-17 wide or continuous checks

Tab.5.2-3 The grade division of cross-section deformation

Grade	No.1	No.2	No.3	No.4	No.5	No.6	No.7	No.8
A-B (mm)	0-0.3	0.3-0.5	0.5-0.8	0.8-1.2	1.2-1.8	1.8-2.5	2.5-3.5	over 3.5

Based on these drying characteristics in 100℃-test, the drying condition of this species could be gained by the relationships of drying characteristics and drying conditions showed Tab.5.2-4, which are very helpful to predict the drying schedules.

Tab.5.2-4 Drying condition based on degree of drying defects

Name	Drying condition (℃)	Grade of effects							
		No.1	No.2	No.3	No.4	No.5	No.6	No7	No8
Initial checks	Initial temperature	70	65	60	55	53	50	47	45
	Temperature depression	6.5	5.5	4.3	3.6	3.0	2.3	2.0	1.8
	Finial temperature	95	90	85	83	82	81	80	79
Cross section deformation	Initial temperature	70	66	58	54	50	49	48	47
	Temperature depression	6.5	6.0	4.7	4.0	3.6	3.3	2.8	2.5
	Finial temperature	95	88	83	80	77	75	73	70
Internal checks	Initial temperature	70	55	50	49	48	45	43	40
	Temperature depression	6.5	4.5	3.8	3.3	3.0	2.5	2.2	2.0
	Finial temperature	95	83	77	73	71	70	68	67

5.2.2 Result and suggestion

From the results of 100℃-test, the detailed data of drying defects results of *E. urophylla×grandis* were shown in Tab.5.2-5, and the consideration of all 8 test samples, the comprehensive drying defects grades of *E. urophylla×grandis* were shown in Tab.5.2-6. Corresponding to the drying condition based on degree of drying defects (Tab.5.2-4), and then the drying condition of *E. urophylla×grandis* was show in Tab.5.2-7, which would be used to determine the kiln schedule in the follow-up test. And the MC curve during 100℃-test was showed in drying Fig.5.2-3.

Tab.5.2-5 The drying defects data and grades of *E. urophylla×grandis*

No	Surface checks			End –surface checks			End checks		Grade	Internal checks			Cross section deformation	
	Long -narrow	Short -narrow	Wide	Long -narrow	Short -narrow	Wide	Wide	Short -narrow		Narrow	Wide	Grade	A-B (mm)	Grade
1	0	1	0	0	1	0	0	1	2	continuous	6	5	4.82	8
2	0	3	0	0	2	1	0	3	2	6	14	6	5.05	8
3	0	1	0	0	2	0	0	2	2	3	10	6	4.73	8
4	0	2	0	0	4	0	0	3	2	4	17	6	5.88	8
5	0	0	0	0	3	0	0	2	2	12	15	6	5.35	8
6	0	0	0	0	1	0	0	6	2	continuous	6	5	4.66	8
7	0	0	0	0	0	0	0	0	1	4	7	5	5.85	8
8	0	2	0	0	2	0	0	2	2	4	7	5	6.02	8

Tab.5.2-6 The comprehensive drying defects grades of *E. urophylla×grandis*

Drying defects	Initial checks	Internal checks	Cross section deformation
Grade	No.2	No.6	No.8

Tab.5.2-7 The kiln drying condition of *E. urophylla×grandis*

Item	The initial temperature	The initial wet-bulb depression (Δt)	Final temperature)
Temperature (℃)	40	2	67

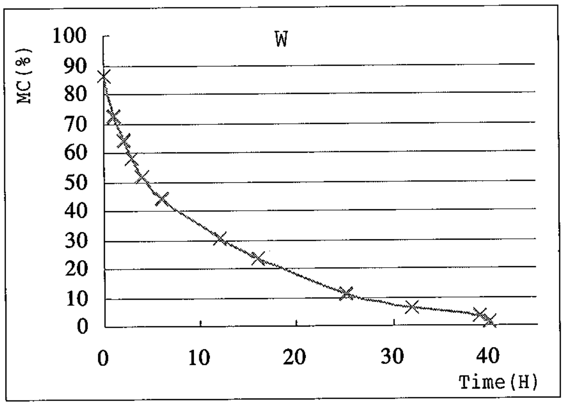

Fig.5.2-3 MC curve in 100℃-test of *E. urophylla*×*grandis*

5.3 Drying schedule

5.3.1 Material and method

The sample dimension was with 500mm x 110mm x 25mm, double end-sealed with silicon sealing glue. The capacity for the stack was 500x400x300 mm, so 15 pieces of samples could by dried each time. To make it easy to fetch every sample for measurement and observation, all these 15 pieces of samples were put on a special made frame, so no heavy load on top on stack during test.

The test dryer was electric heating with 3 group of heater, which could be used independently of simultaneously according to the drying test need, the maximum of 3 group of heater was 6 kW. There was an electronic heated small boiler to afford steam during conditioning. The control system of the test dryer was semi-automatic.

Other equipment: Electric oven with air circulation, electronic balance, thermo-electronic couple temperature measuring system.

Based on the results of drying characteristics test, a schedule of *E. urophylla*×*grandis* wood with thickness of 25 mm was drafted, seeing in Tab.5.3-1.

Tab.5.3-1 The predicted drying schedules of *E. urophylla*×*grandis* (25mm)

MC stage	Dry-bulb temperature (t℃)	Wet-bulb temperature depression (Δt℃)
Above 40	40	2
40-35	44	3
35-30	48	5
30-25	52	9
25-20	56	12
20-15	60	16
Below 15	67	22

Beginning with this schedule, a series of kiln drying test had been done till the optimized schedule was gained.

5.3.2 Result and suggestion

The main drying defects of *E. urophylla*×*grandis* plantation wood drying were check and deformation. Using air-drying to pre-dry *E. urophylla*×*grandis* plantation wood to MC around 30% and then kiln drying could effectively reduce these drying defects.

The optimised kiln drying schedule for *E. urophylla*×*grandis* wood with thickness of 25 mm was listed in

Tab.5.3-2.

Tab.5.3-2 Drying schedule for *E. urophylla×grandis* wood with thickness of 25 mm

MC (%)	Dry-bulb T(℃)	Wet-bulb T(℃)	Notes
Pre-heating	50	49-50	Pre-heating, 3 hours
Above 35	40	37	
35 ~ 30	45	42	
=30%	55	54	Conditioning, 3 hours
30 ~ 25	50	46	
25 ~ 20	55	49	
=20%	65	63	Conditioning, 3 hours
20 ~ 15	60	50	
15 ~ 10	65	50	
Below 10	70	50	
=8%	75	69	End-treatment, 3-5 hours

The lab test results showed that using this schedule to dry *E. urophylla×grandis* plantation wood with thickness of 25mm, the drying quality could meet the National Sawn-timber Drying Quality Standard (GB/T 6491-1999) 2^{nd} grade requirement.

6 ADHESION PROPERTIES

6.1 Finger joint

Finger-joints are commonly used to produce wood products from short pieces of lumber. Such joints must have excellent mechanical performance. To produce acceptable products, a jointer must be subjected to a proper end pressure following machining and adhesive application; also technical parameters, such as machining and gluing processes must be optimized. The condition of finger geometry and end pressure plays a major role in the gluing process and the final strength of the assemblies.

The main function of the end pressure is to bring the mating surfaces so close together that the glue forms a thin and continuous film between them. This pressure also allows a uniform distribution of the adhesive and creates an optimum glueline's thickness. So it is necessary to control the glueline's thickness to produce strong joints. Thin glueline lead to starved joints. Above the optimum glueline's thickness, stress concentration develops in the adhesive layer due to cure-shrinkage. The pressure must be applied to force fingers together to form an interlocking connection, giving a certain immediate handling strength. The increase of the end pressure up to a certain point gives a better contact of the finger to obtain strong joints. However, cell damage or splitting of the finger root can be induced by excessive pressure.

Finger-joint geometry has been proven to the most critical variable determining joint strength. Finger-tips constitute a series of butt joints and are accorded zero strength even if they are tight apparently well bonded; the tip width is the geometric parameter that most significantly influences finger-joint strength.

The objective of the study was to investigate the effect of finger profile geometry and end pressure on the performance of finger-joints in four species of Eucalyptus. The study also planned to evaluate which combination of the end pressures and finger profile geometry would result in optimum finger-joint performance in each of the four Eucalyptuses.

6.1. Materials

The experiments were carried-out with the samples which were planed and crosscut to dimensions of 20 by

60 by 520 mm; the total number of the samples was 90 in the kind of Eucalyptus; then the 90 wood blocks were divided three groups based on the density. The result of the density condition was as Tab.6.1-1:

Tab.6.1-1. Groups divided by density

Species	Average of high density /g/cm^3	Average of medium density /g/cm^3	Average of low density /g/cm^3
E. grandis x E.urophylla	0.713	0.670	0.641

Two kinds of adhesive, API and PVAc, were used in the experiments. API is a kind of two-components adhesive, and is made of main reagent and cured reagent, the mixing ratio is 100:15 when the adhesive was used. The technical index of the two kinds of adhesives was Tab.6.1-2:

Tab.6.1-2. Technical indexes of two kinds of adhesive

Adhesives	Type	Colour	Solid content /%	pH	Viscidity /(cps, 25℃)
PVAc	BT-09	White Emulsion	25.7	4.4	8740
API	DYNOLINK-8000G	White Emulsion	63.8	6.6	6750

6.1.2 Method of Experiments

The geometry of finger(ΔT), feed speed, the amount of adhesives spreading, end pressure, were all important factors to be investigated in the finger-joints experiments.

Three kinds of finger geometry were studies to determine finger parameter for optimum finger-joint strength, and they were selected based on specifications in standards, data from the literature. The finger-jointing machines used a carriage clamp to secure the stacks of wood samples; the samples were guided through a circular saw, a finger profile cutter, and a suction device that removed sawdust and shavings. The ends of pieces to be jointed were first trimmed and squared cleanly by the circular saw before the profile was cut. The suction completely removed all shavings from the profiled surfaces. Finger profiles were processed as vertical orientation joints subsequent test evaluation. The parameters of the three kinds of finger were as Tab.6.1-3.

Tab.6.1-3 Parameters of the fingers

ΔT /mm	Length /mm	Tip width /mm	Pitch /mm	Slope
0	11	0.6	3.8	1/8
0.1	10.6	0.7	3.8	1/8
0.5	8.9	1.1	3.8	1/8

In the processing of making samples finger, the feed speed was important to affect the roughness surface of finger. In this experiment, because different Eucalyptus wood have different density, *E. grandis×urophylla* wood samples was chose in 10mm/min.

End pressure is needed to ensure the closest possible contact between the finger surfaces to be glued, and for the adhesive to form a thin continuous layer uniform in thickness, without damage to the strength of the wood. It is also intended to force the fingers together to the degree that a locking action is obtained, giving a certain immediate handing strength after gluing. Since the higher the pressure the more efficient the locking action, as much pressure as the wood can withstand may be used without causing damage such as splitting at the finger roots, compression failure of the wood, and squeezing out of the glue.

In the experiment, the preliminary end pressure experiment was done to get the suitable pressure. Firstly, four pieces of wood block were selected from the three groups(High, Middle, Low) and then finger were cut; ΔT of the fingers were 0mm, 0.1mm, 0.5mm; and the samples were cut to 60mm length. PVAc was used as adhesive in the experiment with the spread amount $250g/m^2$. Two samples were combined and laid under the loading machine to be pressured as Fig.6.1-1. The loading speed was 2mm/min.

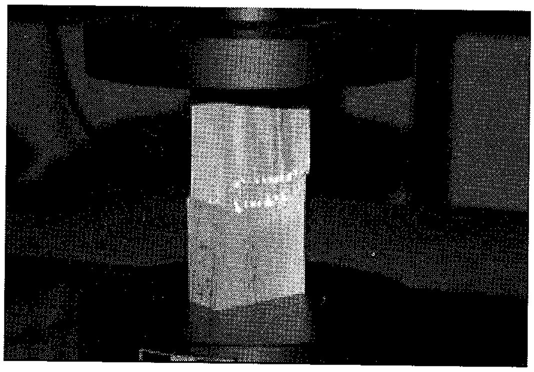

Fig.6.1-1. The method of measuring end-pressure

After the samples had been cut to finger, the samples were jointed by the finger jointer machine. 54 samples were selected from the group. The six kinds of sample were arranged as HH, HM, HL, MM, ML, LL on the basis of density. ΔT were 0, 0.1mm, 0.5mm, the end pressure was used from the result of preliminary end pressure experiments.

Because many factors affected the strength of finger-jointed lumber, for the sake of getting the better processing conditions, the end pressure and ΔT were main factors considered in the research, the design methods of full factors experiments and SAS analysis software were used to discuss the effect on the performance of finger-jointed lumber by each factor, and the interaction between the end pressure and ΔT. Finally integrative evaluation was processed by the result of SAS analysis and the appearance of finger-jointed samples to find the optimum processing condition.

After that, the finger-jointed specimens were cured over 48 hours before further processing. No pressure was applied to the specimens during curing. Both faces of a specimen were planed to a final specimen dimension of 58 by 17.5mm. The bending test was done by using the loading machine to measure MOE and MOR as Fig.6.1-2 according to JAS MAFF, Notification NO.590; support span was 420mm; loading span was 140mm and loading speed was 2mm/min.

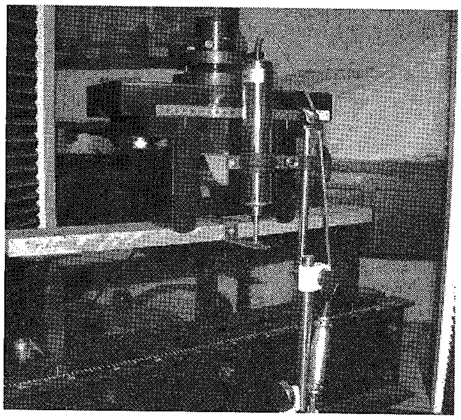

Fig.6.1-2. Four-point bending test

In the experiment, API (DYNOLNK-8000G) was used to make finger-jointed samples. Bending test were performed according to JAS MAFF, Notification NO.590; then MOE and MOR of finger-joints were compared with different kinds of adhesive

To compare the difference of MOR and MOE between V type finger(Fig.6.1-3) and H type finger(Fig.6.1-4), in the experiment, the H finger was done to make finger-jointed lumber, ΔT was 0.1mm; bending test were performed also according to JAS MAFF, Notification NO.590

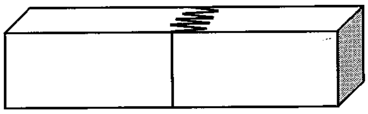

Fig.6.1-3. V-type finger-joint

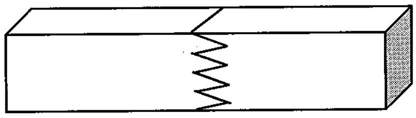

Fig.6.1-4. H-type finger-joint

6.1.3 Result and Discussion

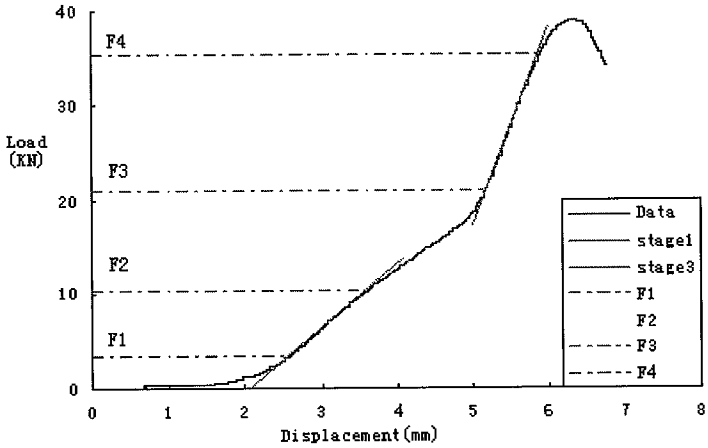

Fig.6.1-5. Load-displacement curve

Fig.6.1-5 is the typical Load-displacement curve, in this case ΔT is 0.5. When the cross head began to push the upper specimen, the upper specimens begin to move, the finger-tip will touch the nether specimen quickly, so when loading reached F1, it was considered the finger-tip touch the nether specimen, when the loading approached F2, it was considered the finger-tip was damaged, when the loading aroused to F3, there was splitting on the finger root, and following stage was as the same as solid wood pressured, the solid wood begin to damage when the loading increased to F4.

In the experiment, F1 was thought the suitable pressure before the finger was damage. Tab.6.1-4 was the results of end pressures in different ΔT.

Tab.6.1-4. End-pressure at different conditions

Wood species	ΔT	Average pressure /MPa
E.grandis×* *urophylla	0	9.82
	0.1	13.72
	0.5	5.74

In the experiments, the four species of Eucalyptus end pressures were selected from Tab.6.1-5.

Tab.6.1-5. Different levels of the end-pressure

Wood Species	Three end pressure /kN		
	P1	P2	P3
E.grandis×Urophylla	7.5	10	12.5

Tab.6.1-6 and Tab.6.1-7 were the results of the bending test analysis of *E. grandis × uraphylla*

Tab.6.1-6. MOE and MOR analyzed by SAS

Index	Resource of variance	Degree of freedom	Summation of square	Average of square	F	Pr > F	Markedness
MOE	Matrix	32	120.446	3.764	1.12	0.3986	/
	Combination of density	5	26.971	5.394	1.61	0.2017	/
	End pressure	2	2.397	1.198	0.36	0.7039	/
	ΔT	2	35.020	17.510	5.22	0.0145	**
	End pressure × ΔT	4	11.883	2.971	0.89	0.4898	/
	Combination of density × pressure	10	34.495	3.833	1.14	0.3786	/
	Combination of density × ΔT	9	9.681	0.968	0.29	0.9766	/
	Error	17	70.484	3.356			
	Summation	49	190.930				
MOR	Matrix	32	765.617	23.926	1.64	0.1198	/
	Combination of density	5	170.100	34.020	2.33	0.0787	*
	End pressure	2	225.705	112.852	7.72	0.0031	***
	ΔT	2	60.138	30.069	2.06	0.1527	/
	End pressure × ΔT	4	92.854	23.214	1.59	0.2143	/
	Combination of density × pressure	10	110.971	12.330	0.84	0.5858	/
	Combination of density × ΔT	9	105.849	10.585	0.72	0.6938	/
	Error	17	306.886	14.614			
	Summation	49	1072.503				

Mark: /means unmarkedness at 0.1; *means markedness at 0.1; **means markedness at 0.05

Tab6.1-7 Testing for groups of each factor

Factor	Level	Number of specimen	MOE(Gpa)		MOR(Mpa)	
			Average	STDEV	Average	STDEV
End pressure	8.5	14	24.998A	3.097	33.637A	7.761
	10	17	26.255A	2.356	32.683A	4.103
	11.5	18	26.019A	2.877	38.567B	6.038
ΔT	0	14	26.230A	1.863	32.466A	5.350
	0.1	17	27.476A	2.276	38.484B	6.324
	0.5	18	23.907B	2.708	34.000A	6.381
Combination Of density	HH	3	27.383A	2.425	40.651A	9.646
	HL	14	24.901AB	3.170	32.821AB	6.408
	HM	13	26.687A	2.042	37.524A	6.651
	LL	6	23.002B	1.559	31.378B	5.226
	ML	9	26.974A	2.040	35.104A	5.164
	MM	4	26.540A	3.607	36.822A	5.192

Mark: The A,B behind average in table means the checked result by T, the same word letter means there was no difference in Stat., the different letter means there was difference in Stat..

From Tab.6.1-6 it is indicated that the combination of density and ΔT had much effect on the MOR of finger-jointed lumber of the wood; end pressure had much effect on MOR; the interaction of end pressure and ΔT had no effect on MOR and MOE.

From Tab.6.1-7 it is shown that the change of end pressure had no effect on MOE, but to MOR, the higher end pressure, the higher MOR of finger-jointed lumber of the wood; different ΔT can lead to different MOR and MOE, the MOR was higher when ΔT was 0.1mm.

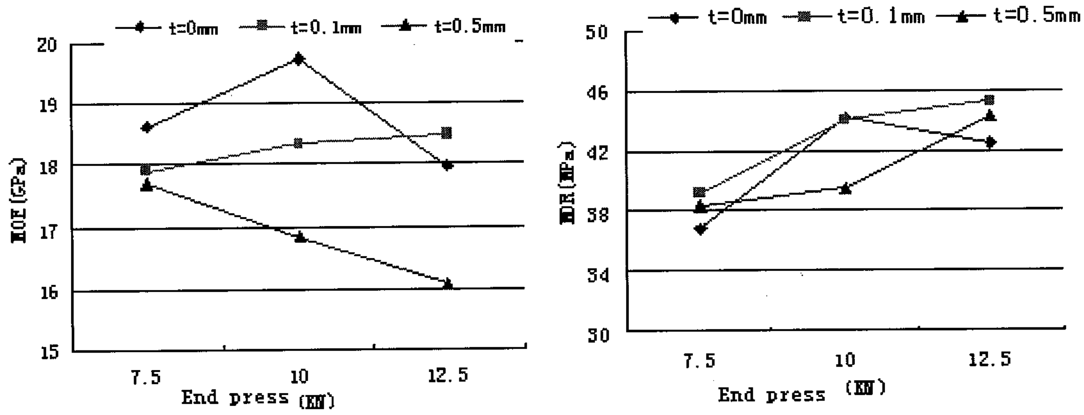

Fig.6.1-6. Effect of end-pressure on MOE and MOR

From Fig.6.1-6 it can be concluded that when the ΔT was 0mm, the MOE and MOR increased as the increasing of end press from 7.5KN to 10KN, the end press was over 10KN, the MOE decreased from 19.727 to 17.993Gpa, and MOR decreased from 44.128 to 42.431MPa. When ΔT was 0.1mm, the MOE and MOR increased to the maxmium 18.492Gpa and 45.287MPa as the end press increase from 7.5KN to 12.5KN.The failture of wood was get when the end press was 12.5KN. So the suitable end press was 10KN.

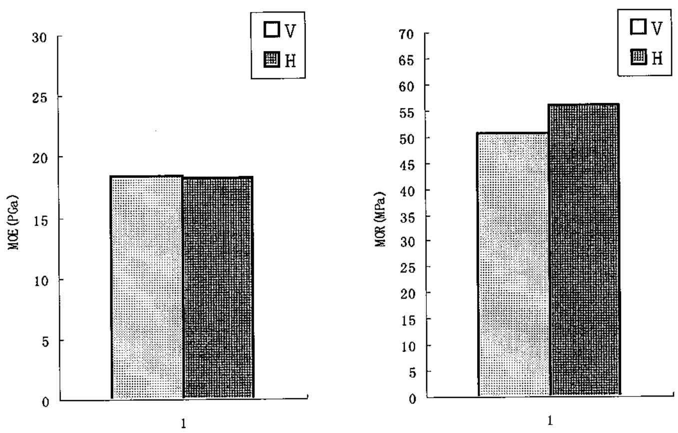

Fig.6.1-7 Comparison between V-type and H-type finger-joints on MOE and MOR

From the Fig.6.1-7 it was shown that the MOR of finger-joints with different finger type V and H were almost the same, but in the same processing condition, the MOE of finger-joints in V finger type was higher than that in H type.

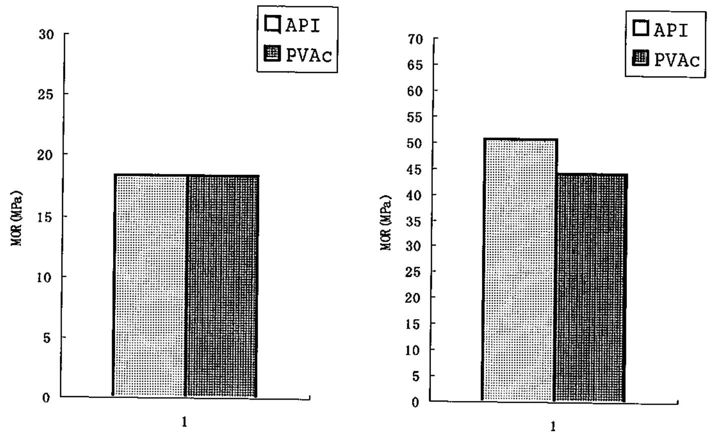

Fig.6.1-8 Comparison between API and PVAc finger-joint on MOE

From Fig.6.1-8 it was indicated that there were no much difference with API and PVAc in MOE, but for MOR, the API products was higher than PVAc remarkably, especially for *E. citriodora* wood, which was high density and had much extraction. For example, the MOR was 30.35 MPa for PVAc, but for API, the MOR increased to 57.69MPa. Tis could be explained that for API adhesives, in the action of Vander waals force and hydrogen bond between the molecule of adhesive and molecule of wood, it forms deep-set physical bonding with wood. The gluing surface and the formed nail adhesive react with hydroxyl, carboxyl, phenolic hydroxyl and other reactive group in celluloses, hemicelluloses, lignin of wood, at the same time adhesive reacts with water in wood, then forms some chemical bond between wood and adhesive, in the end form intercross structure, thereby increases strength of gluing.

IV *Eucalyptus grandis*

The information of testing materials is as Tab.1.

Tab.1 Testing materials

Tree species	Tree age (year)	Tree number	Tree height (m)		Under branch height (m)		DBH (cm)	
			Ave.	Std	Ave.	Std.	Ave.	Std
Eucalyptus grandis	13	10	27.49	2.5049	12.04	4.6198	24.6	5.5987

1 WOOD PROPERTIES

1.1 Anatomical characteristics

Samples (2×2×1 cm) for wood anatomical section were stored in alcohol 95% : glycerine (1:1) until they sank. Transverse sections of 20μm were cut on sliding microtome, then bleached, stained with safranin, dehydrated and mounted on slides for measure anatomical properties on image analysis. Then the transverse, radial and tangential sections from each species of around 80μm were cut on the same microtome, make the samples for SEM observation and taking photos.

Prior to tracheid length measurement, the each selected growth rings were firstly separated with a chisel, then macerated in solution of acetic acid (1/3) and hydrogen peroxide 27% (2/3) for several days in 60° oven.

The measurement methods are as follows:

Measuring length and width of wood fiber and vessel element using macerated anatomical elements under fiber length measuring instrument; (2) Measuring wood fiber cell wall thickness, cell wall percentage, and tissue proportions by section method using image analysis system; (3) Measure of S_2 microfibril angle: using x-ray diffractometer.

The observation and description for macro- and micro-structure were made under the light microscope and scanning electronically microscope (SEM).

1.1.1 Tree and distribution

A tree up to 45-55 m, 1.2-2.0 m in d.b.h., trunk straight generally in origin producing country. Bark peeling off in long strips on old tree. Bark smooth and silvery white, with whiting after peeling off. There is has successful an integrated technology for tissue culture on the factory-scale.

The farms in tropical and subtropical reigns planted *E. grandis* plantations on large scales. Our country is introduced this species in resent years; Zhejiang, Fujian, Guangdong, Guangxi, Hainan and Yunnan province etc. made the systemic provenance experiments.

1.1.2 General characteristics

Sapwood yellowish brown, comparatively differs from heartwood, width 3~4 cm. ***heartwood*** dark yellowish brown to reddish brown; glossy, wood without characteristic taste & odor. ***Growth rings*** indistinct. Wood diffuse-porous. Pores small to middle, visible to the naked eye, fairly uniformly distributed throughout the ring, radial, tyloses visible. ***Longitudinal parenchyma*** vasicentric. ***Rays*** very fine to fine, visible with a hand lens; ***Ripple mark***s and ***Resin canals*** absent.

1.1.3 Minute anatomy (Plane II)

Vessels most solitary; radial or flexuous; cell wall thin to thick; tangential average diameter 125 μm, max 219 μm. 11 (7~14) /mm^2 . Vessel element length 366 (198~566) μm, tyloses visible and wall thin, helical thickness absent. Simple perforation, its plate oblique. Intervessel pits ventured, alternate, round & polygonal, ventures distributed pit aperture and & chamber. Vasicentrics common, located vessels intermixing parenchyma cells, with bordered pit round and ventured. Vessel- ray pits large round.

Longitudinal parenchyma vasicentric, diffuse or diffuse-aggregates. Nodular end wall of parenchyma cells inconspicuous, some cells contain round inclusion; crystals absent.

Fiber wall thick to thick, 1097 (945~1420) μm in length, with plain simple pits.

Rays unstoried, rays 9~12/mm, mostly uniseriate rays 1~11 cells, multiseriate rays width 2 cells, height ~13 cells seldom. Ray tissues homogeneous uniseriate and multiseriate; parenchyma cells round or oval, most with inclusion. Crystal and intercellular canals absent.

The data of anatomical parameter and vessel distribution frequencies and tangential diameters at 1.3 m is including to the tab.1.1-1 and 1.1-2 respectively.

Tab. 1.1-1 Anatomical parameter at 1.3 m for *Eucalyptus grandis*

Fiber length (μm)		Fiber width (μm)		Fiber wall thickness (μm)		Microfibril angle (°)	
$\bar{x}$	δ_n	$\bar{x}$	δ_n	$\bar{x}$	δ_n	$\bar{x}$	δ_n
1097	81	16.4	0.7	9.01	0.801	13.88	2.630

Tab. 1.1-2 Vessel distribution frequencies and tangential diameters

Vessel distribution frequency (Number/mm^2)				Vessel tangential diameter (μm)			
Ave.	Std.	Max.	Min.	Ave.	Std.	Max.	Min.
11.00	2.1417	13.80	7.40	107.78	34.5639	217.54	33.51

1.2 Physical properties

1.2.1 Moisture content of the green wood

The moisture content data of the green wood at different radial sites is including Tab.1.2-1.

Tab. 1.2-1 Moisture content of green wood for *E. grandis* at different radial sites (%)

1		2		3		4		5	
$\bar{x}$	δ_n	$\bar{x}$	δ_n	$\bar{x}$	δ_n	$\bar{x}$	δ_n	$\bar{x}$	δ_n
100.9	20.13	100.1	20.74	94.6	23.86	96.4	10.27	81.1	18.05

1=near pith, 2=site between 1 &3, 3=center from pith to bark, 4=site between 3 &5, 5= near bark

1.2.2 Shrinkage and Density

Shrinkage is the contraction of wood caused by drying the material below the fiber saturation point (William T. Simpson, 1991). It can be divided into 3 types of shrinkage according to the direction of contraction: longitudinal, radial and tangential shrinkage. The longitudinal shrinkage is the shrinkage along the grain, the radial shrinkage and the tangential shrinkage is that across the grain in a radial or in a tangential direction. Wood density, the weight of wood per unit volume, is a very important index having a close relation with wood mechanical strength. In this study, wood air-dried density and basic density were used to describe the wood density.

The shrinkage is attributed to the dimension stability and checking problem, which causes a lot of problem for the wood utilization. In another word, it causes not only the contraction of wood in size, but also the checking and deformation resulted from the different contraction in tangential, radial and longitudinal direction. Understanding the characteristics of shrinkage has no doubt to be helpful for the wood utilization for the wood industry practice. Nowadays, studying on the characteristics of shrinkage during the losing of water is becoming one of the wood science discipline[Barber NF etc.1964; Barber, 1968; Chafe, 1986; 1987; Gu H et al., 2001]。 This study is intended to explore the shrinkage variation of acacia in different direction (North and south), different radial position and different tree height.

The trees studied were cut from Guangxi Zhuang Autonomous Region in the South China. Each trunk has been collected above the breast height and was cut every 2 meters. Then, four discs of each tree at different heights (about 1.3m, 3.3m, 5.3m and 7.3m respectively) were taken from the logs. All the discs were marked the south-north direction. For each disc, one specimen from the sapwood near the bark, one from the heartwood near pith and one from transition zone was made at the size of 2X2X2cm (Tangential X radial X longitudinal direction) for both north side and south side.

Two diagonal lines were drawn in three sections (i.e., T×R, T×L, R×L) of each specimen to locate the central point where the size was measured. The specimens were put into water until they were totally saturated and sunk in the water. The surface water was wiped off and the sizes in three directions (L, R, T) were measured. Specimens were set in the room for air-drying. After measuring the size and weight at the air-dried stage, the specimens were oven-dried and the same measurement was carried out. The shrinkage was determined according to Chinese National Standard. The air-dried density and was also calculated of both air-dried

The shrinkage coefficient was determined by the difference between shrinkage at air-dried and at oven-dried and divided by the MC at air-dried.

1.2.2.1 Shrinkage and density, and that of wood from south and north directions

The air-dried shrinkage in tangential direction (Ta), Radial direction (Ra) and volumetric shrinkage (Va), as well as the oven-dried shrinkage in tangential direction (To), Radial direction (Ro) and volumetric shrinkage (Vo) are listed in Tab.1.2-2 according to the categories of south direction, north direction and the overall. The basic density (B D) and air-dried density (A D), together with tangential shrinkage coefficient and radial shrinkage coefficient were also calculated and listed.

According to the IAWA (1989) method (the wood with an air-dried density smaller than 0.56 g/cm^3 is considered to be a small-density species, between 0.56 g/cm^3 and 0.75 g/cm^3 is considered to be a medium-density, between 0.75 g/cm^3 and 0.95 g/cm^3 is considered to be a large-density species, and bigger than 0.95 g/cm^3 is considered to be a extra-large-density species),*E.grandis* wood has a medium density.

According to the *CHINA WOOD* method (the wood with an air-dried tangential shrinkage smaller than 5.60% is considered to be a small-shrinkage species, between 5.60% and 7.00% is considered with a medium-shrinkage species, and bigger than 7% is considered to be a big-shrinkage species), *E grandis* has a big shrinkage, suggesting more attention should be paid when sawing and drying.

ANOVA analysis (Tab.1.2-3) showed there was no significant difference between air-dried tangential shrinkage and air-dried radial shrinkage, suggesting that the wood from north and south could be thought has the same level in shrinkage.

Tab. 1.2-2 The shrinkage and density of *E.grandis* wood from south and north side

		Ta (%)	Ra (%)	Va (%)	To (%)	Ro (%)	Vo (%)	B D (g/cm3)	A D (g/cm3)	Co-t (%)	Co-r (%)
South	Average	8.01	3.41	11.22	11.38	5.79	16.79	0.53	0.67	0.26	0.18
	Std.dev.	1.82	0.72	2.26	1.88	0.92	2.43	0.06	0.09	0.03	0.03
	CV(%)	0.23	0.21	0.20	0.17	0.16	0.14	0.12	0.13	0.13	0.14
	Number	15	15	15	15	15	15	15	15	15	15
North	Average	8.70	3.47	11.97	12.10	5.97	17.65	0.53	0.69	0.26	0.19
	Std. dev.	1.69	0.84	2.06	1.66	0.97	2.11	0.06	0.09	0.02	0.02
	CV(%)	0.19	0.24	0.17	0.14	0.16	0.12	0.11	0.12	0.07	0.09
	Number	15	15	15	15	15	15	15	15	15	15
Total	Average	8.36	3.44	11.60	11.74	5.88	17.22	0.53	0.68	0.26	0.19
	Std. dev.	1.76	0.77	2.16	1.78	0.94	2.28	0.06	0.09	0.03	0.02
	CV(%)	0.21	0.22	0.19	0.15	0.16	0.13	0.11	0.13	0.10	0.12
	Number	30	30	30	30	30	30	30	30	30	30

Tab1.2-3 ANOVA analysis on the shrinkage of *E. grandis* wood from north and south

	SS	df	MS	F	P-value	F crit
Ta	3.5392	1	3.5392	1.1519	0.2923	4.1960
Ra	0.0259	1	0.0259	0.0423	0.8385	4.1960

1.2.2.2 Shrinkage and density of wood at different radial positions

The shrinkage, shrinkage coefficient and density from 4 different tree radial positions were listed in Tab.12-4. The relationship between air-dried shrinkage, basic density and tree heights were showed in Fig. 1.2- .

ANOVA analysis (Tab.1.2-5 showed there existed significant air-dried radial shrinkage difference among different radial position, while the tangential shrinkage did not exist significant difference. This coincide with the affect of different radial position on shrinkage of *E. citriodora*.

Both the radial and tangential shrinkage in the transition zone presented the maximum value. The basic density in the juvenile presented the minimum value.

Fig.1.2-1showed the tangential and radial shrinkage increased gradually from juvenile wood (near pith) to mature wood (near bark), this coincide the change of basic density, meaning that the shrinkage has the positive correlation with basic density. Newlin and Wilson (1919) reported that the volumetric shrinkage had the positive correlation with basic density. The relations between shrinkage and different radial position of *E. grandis* showed in Fig.1.2- also agreed with Lu Jianxiong's (2005) report on I-72 poplar and Chinese fir.

Tab. 1.2-4 The shrinkage and density of *E.grandis* from different radial positions

		Ta (%)	Ra (%)	Va (%)	To (%)	Ro (%)	Vo (%)	B D (g/cm^3)	A D (g/cm^3)	Co-t (%)	Co-r (%)
near bark	Average	8.68	3.92	12.35	12.23	6.60	18.30	0.57	0.74	0.28	0.21
	Std. dev.	2.28	0.67	2.69	2.25	0.77	2.65	0.03	0.06	0.03	0.01
	CV(%)	0.26	0.17	0.22	0.18	0.12	0.14	0.06	0.08	0.12	0.07
	Number	10	10	10	10	10	10	10	10	10	10
transition	Average	8.56	3.50	11.86	11.95	5.90	17.47	0.54	0.70	0.25	0.18
	Std. dev.	0.79	0.48	1.11	0.76	0.60	1.17	0.05	0.06	0.02	0.01
	CV(%)	0.09	0.14	0.09	0.06	0.10	0.07	0.08	0.08	0.07	0.07
	Number	10	10	10	10	10	10	10	10	10	10
near pith	Average	7.83	2.91	10.59	11.04	5.15	15.90	0.47	0.60	0.24	0.17
	Std.	1.91	0.80	2.16	1.93	0.84	2.25	0.05	0.07	0.01	0.01
	CV(%)	0.24	0.28	0.20	0.17	0.16	0.14	0.10	0.12	0.06	0.08
	Number	10	10	10	10	10	10	10	10	10	10

Tab.1.2-5 ANOVA analysis on the shrinkage of *E.grandis* wood from different radial positions

	SS	df	MS	F	P-value	F crit
Ta	4.259582	2	2.129791	0.674059	0.518004	3.354131
Ra	5.152816	2	2.576408	5.806533	0.007989	3.354131

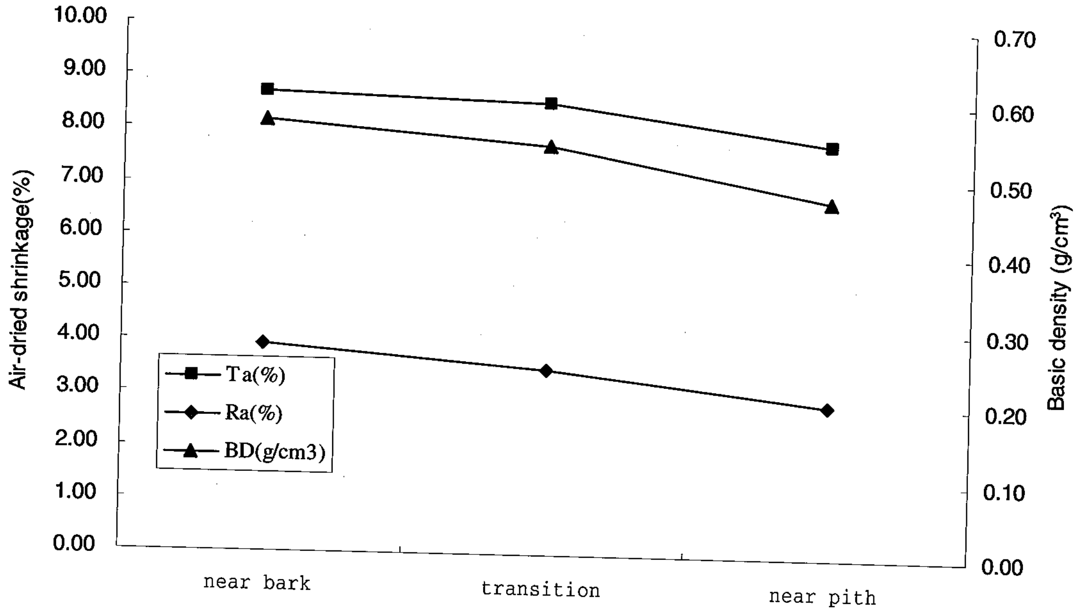

Fig.1.2-1 *E. grandis*: relationship between air-dried shrinkage (Ta&Ra), basic density (BD) and different radial positions

1.3 Mechanical properties

The small clear wood samples of moduli of elasticity (MOE), moduli of rupture (MOR) in static bending, compression strength parallel to grain and wood density were cut in accordance with Chinese National Standards (GB 1927~1943-91). The specimens were then stored in a conditioning chamber until it reached approximately 12% moisture content. Bending, compression and wood density test were carried out in accordance with Chinese National Standard. The air-dry density was calculated by air-dried weight and volume while oven-dry density was based on oven-dried weight and volume.

Generally *E. grandis* wood grain straight or oblique, texture fine to middle and even, weight middle, hard, shrinkage large, strength highly. Nail holding power (N/mm): Radial: 50.1 Tangential: 53.4 Parallel to grain: 36.3. The mechanical properties are including tab.1.3-1.

Tab.1.3-1 Mechanical properties data of *E. Grandis*

Locality	Density /g/cm³		DS /%		CSPG /MPa	BS /MPa	MOE /GPa	Toughness /kJ/m²	Hardness /N		
	BD	ADD	R	T	CSPG/MPa	BS/MPa	MOE/GPa	Toughness/kJ/m²	E	R	T
Guangxi Dongmen		0.713			57	123	12.68	74.4			

BD = basic density, ADD = air-dry density, DS = dry shrinkage, CSPG = compressive strength parallel to grain, BS = bending strength, MOE = modulus of elasticity, SSPG = shear strength parallel to grain(R), E = end, R = radial, T = tangential

1.4 Chemical properties

The chemical composition was determined according to Chinese National Standards, the chemical composition results and pH values, acid and alkaline buffering capacities are listed in Tab. 1.4-1 and 1.4-2 respectively.

Tab.1.4-1 Chemical composition of *E. grandis* (%)

α-Cellulose	lignin	Xylan	1% NaOH extractives	Benzene-alcohol extractives	Cold water extractives	Hot water extractives	Ash
46.17	21.44	21.20	15.61	2.90	1.64	3.63	0.42

Tab.1.4-2 Data of pH value, acid and alkaline buffering capacity of *E. grandis*

S	H	S	H	S	H
4.56	3.66	4.64	2.52	29.70	43.80

S- sapwood, H-heartwood

2 GROWTH STRESS

The research adopted CIRAD-Foret method to measure surface longitudinal growth strain (SLGS) of standing trees, the results at different orientations were listed in Tab.2-1.

Tab. 2-1 Growth strain data for standing trees of *E. grandis*

Basic density (g/cm^3)	E		W		S		N	
	$\bar{x}$	δ_n	$\bar{x}$	δ_n	$\bar{x}$	δ_n	$\bar{x}$	δ_n
0.587	887	245.6	852	328.2	743	234.7	1043	344.1

E=east, W=west, S=south, N=north

3 SAWING TECHNIQUES

Logs were collected from DONGMEN Forest farm in Nanning, Guangxi, and 10 stems were taken. All trees were unpruned and were planted on commercial forest land. The ends of the logs were sealed with asphalt to prevent end-drying after logging. Water spraying was applied to keep them in a green condition by preventing drying degrade.

The length of each log section was from 2.00 to 2.20 meters. The taper of this species was small, three to four sections could be harvested from each tree. The tree and log parameters are listed in Tab. 4-1.

Tab. 4-1 The parameters of *E. grandis* trees and log sections

Height of tree (m)	Height under branch (m)	Age (years)	DBH (mm)	Diameter Range of log sections (mm)
27.49	12.02	13	282	175~249

Note: the height and DBH (diameter at breast height) in Table are averaged.

The diameter of log sections refers to the Small End Diameter (SED), and bark is not included.

The equipment for the sawing consisted of a headrig band saw with a manually adjusted sizing carriage.

3.1 Strain in Sawing Process

The method of measuring strain is based on the method of measuring longitudinal strain (France, CIRAD-Foret Method) and instantaneous release of residue stress after drilling holes above and below gauges

(M. Yoshida, T. Okuyama, 2002). The pin targets and guide for setting is displayed in Fig. 3.1-1.

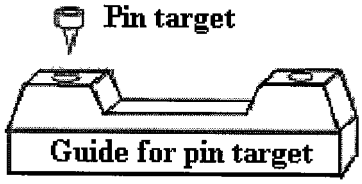

Fig. 3.1-1 Pin target and guide for measuring strain in sawing process

Height of pin target: 10mm, Internal diameter: 2.5mm, External diameter: 10mm, Distance between pin target: 45mm.

Before each sawing pass, two pin targets were placed into the existing sawn surface according to Fig.3.1-2, or in the case of the opening cut on the log side face which was to be perpendicular to the sawing surface. The distance was measured with a digital caliper with a precision of 0.001 mm. The head of each pin target was recessed to accept the pins and hold them in place. And their distance apart, measured before sawing and again just after the lumber containing the nails was sawn off. The strain changes in the longitudinal and tangential directions were then calculated using the formula:

$$strain = \frac{Da - Db}{Db} * 100\%$$

Where: Db= the dimension before the lumber is sawed off; Da= the dimension after the lumber is sawed off.

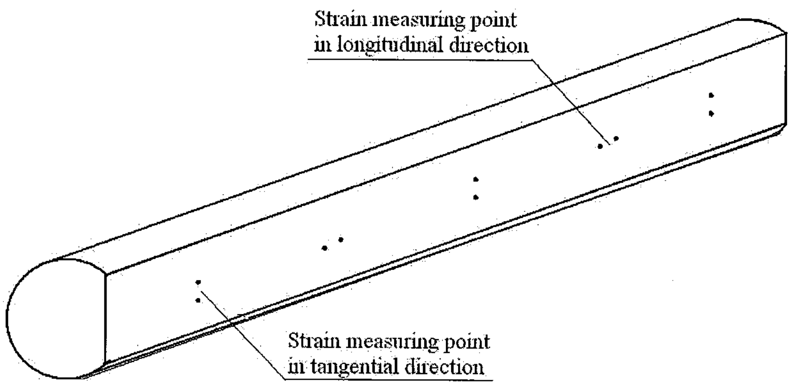

Fig. 3.1-2 Distribution of measuring point for strain change in lumber sawing

The logs were sawn using three different sawing patterns; live sawing, cant sawing and around sawing; and the strain changes were measured following the above procedure.

The strain distribution in the sawing process is analysed and displayed in Figs 3.1-3 – 3.1-4. X-coordinates show the log's position, while the number 1, 2, 3… shows the section position progressively from the bottom to the top section of the trunk. The abbreviations shown in the figures are: T—tangential, R—radial, Sap—Sapwood, Core—Core wood, Live—live sawing, Cant—cant sawing, Around—around sawing, for example, 'T_live' represents tangential direction with live sawing pattern.

The stresses are generated in newly formed wood during cell maturation in living tree. Continuous formation of growth stresses during tree growth results in an uneven distribution of residual stresses across tree stems. When logs are sawn longitudinally, the residual stresses are partially released (Crompton, 2000). And the growth stresses are presented in a random way (Tomaselli, 2000), this may resulted in the big deviation of the strain in sawing process. Fig. 3.1-3 showed that the strain in *E. grandis* in live sawing, cant sawing and around sawing pattern. The strain changes is even in live sawing and cant sawing process, the strain changes fluctuated the biggest in around sawing. Fig. 3.1-4 displayed the strain changes in longitudinal direction. The result showed the sapwood in cant sawing and corewood in around sawing had even strain, others all behave big fluctuation.

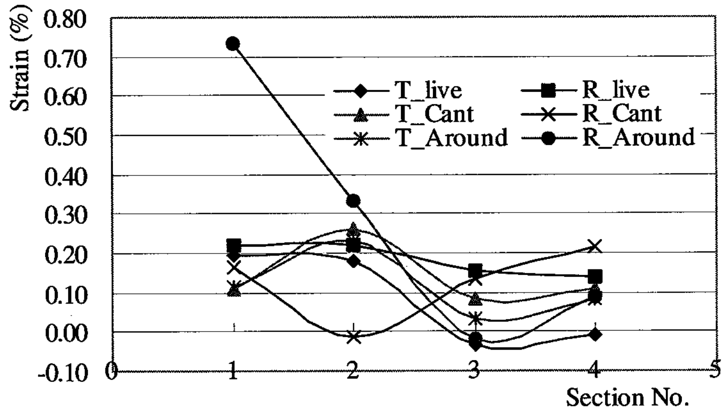

Fig. 3.1-3 Strain distribution of *E. grandis* in tangential and radial direction

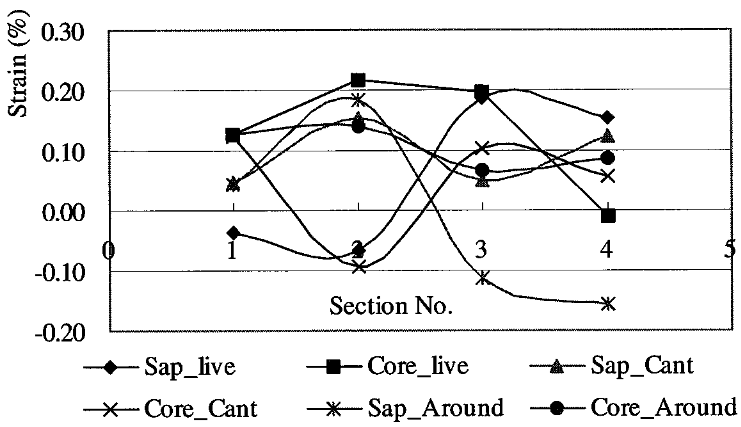

Fig. 3.1-4 Strain distribution of *E. grandis* in longitudinal direction

3.2 Bow Deformation

Bow deformation in sawn lumber (bending in the longitudinal direction) was recorded for each sawing strategy. Bow can reflect the extent of growth stress release. The higher the stress gradient in the original log, the greater the expected bow deformation is.

The most deformation which occurred in the sawing process was bow deformation of the lumber, it is also from the releasing of residue stress (Crompton, 2000). The results are displayed in Fig. 3.2-1 to 3.2-3 for the three different sawing strategies. The X-coordinates represent the location of lumber in the log, 0 is the core lumber and the other values represent the block number in relation to the pith of the log, Positive and minus values are used to indicate the two directions from the pith. In the live sawing and cant sawing strategies, the larger minus values represent which pieces of lumber were cut first., In the around sawing strategy the sign just represents location of the lumber (displacement from the pith).

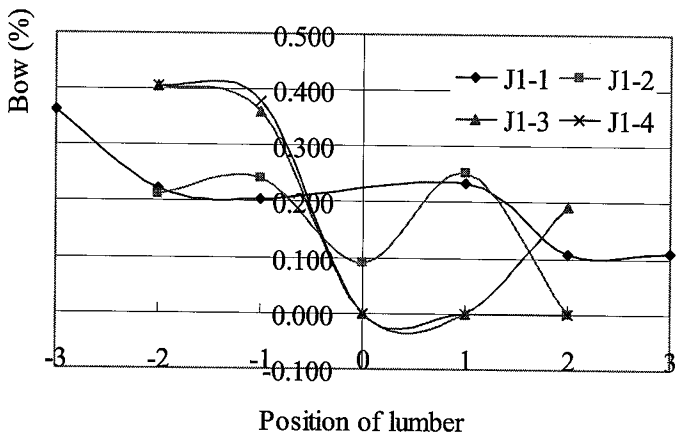

Fig.3.2-1 The bow deformation of *E. grandis* in live sawing

In the sawing process, most of the lumber developed bow deformation except the core lumber. This bow deformation has some relationship with where the lumber was located in the original log and the sequence of the cuts in the sawing process. This is apparent in Figs 3.2-1 to 3.2-3, especially the cant sawing.

The results showed that the outer the lumber position is, the bigger the bow deformation is. There is evident relationship of bow with the sequence in live sawing and cant sawing process. The lumber sawed first had the biggest bow deformation (left side), and the lumber sawed later had least deformation. This is from the reason, after the former lumber sawed, the stress inside left log had been released and re-balanced in some extent, so the later sawed lumber had less deformation even in the similar position in the log.

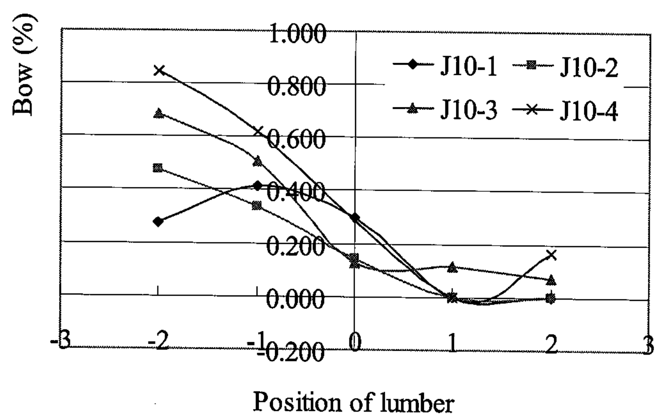

Fig. 3.2-2 The bow deformation of *E. grandis* in cant sawing

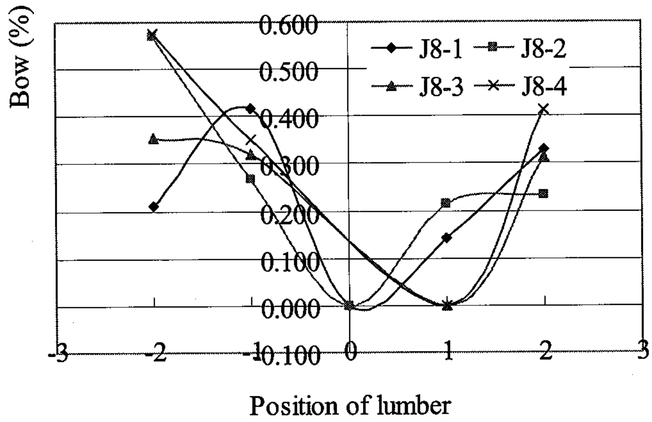

Fig. 3.2-3 The bow deformation of *E. grandis* in around sawing

The bow deformation in live sawing was small, the biggest value is in cant sawing with the first sawing half. After slab sawing off, the most of the wood near the heart under high compression still exists in the cant and on reaching a new equilibrium condition, will impose a higher tensile strain on the sapwood than the level which existed in the intact log (Waugh, 2000), this increased stress gradient and resulted in the bigger deformation. The detailed bow deformation value for 3 sawing patterns was listed in Tab. 3.2-1.

Tab. 3.2-1 the bow deformation of *E. grandis* in 3 different sawing pattern

Sawing pattern		Live-sawing				Cant-sawing				Around-sawing			
Position of log		1	2	3	4	1	2	3	4	1	2	3	4
Location of lumber	-3	0.361											
	-2	0.223	0.213	0.405	0.405	0.275	0.473	0.687	0.846	0.211	0.570	0.355	0.574
	-1	0.204	0.242	0.359	0.379	0.412	0.337	0.508	0.618	0.415	0.268	0.322	0.350
	0	0.233	0.091	0.000	0.000	0.299	0.144	0.124	0.000	0.000	0.000	0.000	0.000
	1	0.107	0.254	0.000	0.000	0.000	0.000	0.114	0.165	0.142	0.215	0.315	0.414
	2	0.109	0.000	0.194	0.000	0.000	0.000	0.072		0.329	0.232		

The bow deformation displayed the stress distribution and re-distribution in some extent, so the live sawing could release the residue stress more efficient than the other two sawing pattern.

3.3 Sawing Inaccuracy

The high growth stress in eucalypts can result in considerable distortion and sawing inaccuracy during sawing, as well as lumber recovery and productivity. According to the national sawing standard of China, the permitted thickness deviation is ±1mm. However, in this study, the actual sawing variation was much larger, the range being from –4 to +4 mm. This big variation not only influenced lumber recovery, but also made later processing difficult due to the uneven dimensions of the lumber.

The data of sawing inaccuracy of lumber thickness is listed in tab. 3.3-1, the proportion of oversized deviation is about 39.8%, the residue stress of *E. grandis* is big, so it is easy for the lumber to depart from normal position in sawing process, and then result in the thickness inaccuracy.

Tab. 3.3-1 the thickness inaccuracy influence to *E. grandis* lumber

Amount of slabs (Pcs)	Amount of oversize thickness deviation (Pcs)	The proportion of oversized (%)
98	39	39.80

3.4 The Influence of End-splits on Lumber Recovery

The most frequent defect is end splitting in sawing plantation Eucalyptus for the high growth stress. Heart shake appears just after tree trunk being cut down, and it will extend to some extent before sawing, most end-splitting comes from heart shake in log section. Tab. 3.4-1 shows the results of end-split to lumber recovery in *E. grandis* sawing. The end-split's influence to lumber recovery is about 15%, i.e. if there is no end-split, the lumber recovery will increase about 15%. And this is similar with the result of sawing *E. grandis* in South African, the splitting related losses in sawmills exceeds 10% (Botha Margee, 2000).

Tab. 3.4-1 Influence of end-split to lumber recovery in sawing experiments

log Volume (m^3)	Volume of Lumber with end-split (m^3)	Recovery rate with end-split (%)	Volume of lumber without end-split (m^3)	Recovery rate without end-split (%)
1.7259	1.0972	63.57	0.8336	48.30

The lumber recovery is about 48%, it is reasonable comparison with the *E. grandis* sawing in Australia. The green-off-recovery is 51% for 40cm logs sawing experiments (Northway R., 1997).

The dimension accuracy could be improved if suitable equipments can be used, and the lumber recovery could be higher if suitable measure can be taken in controlling the end-splitting in tree harvesting and storing.

4 DRYING TECHNIQUES

4.1 Air drying

Air drying is a traditional and economical drying method which mainly uses sun energy. To save kiln drying time and cost, and to improve kiln drying quality at the mean time, it is suggested to use Air drying as a pre-drying method, and then conventional kiln drying to target final MC (moisture content). Because of the uncontrolled drying conditions, the drying time, final MC and drying quality may be quite difference with the changes of season and drying arrangements. Air drying test focus on analysing wood Air drying properties and try to find its optimum Air drying technique and parameters.

4.1.1 Material and method

The size of sample for air drying is 700 mm (length) x 120-150 mm (width) x 25 mm (thickness). Two MC slices were cut in the two ends of each sample to calculate its initial MC (Fig.4.1-1).

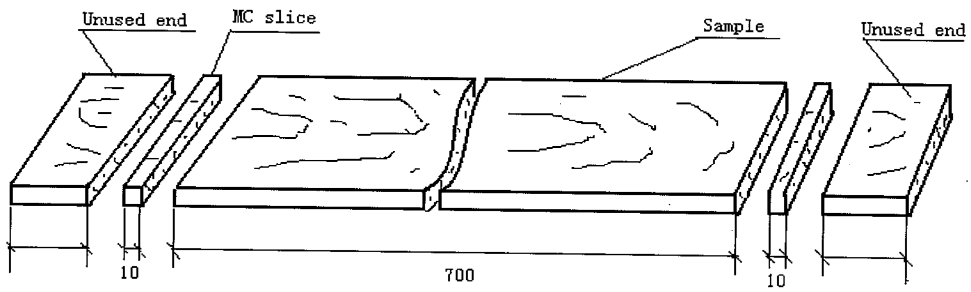

Fig.4.1-1 Drying sample making of *E. grandis*

The samples were end-sealed with silicon, and then stacked in air-drying shed to start drying. The dry-bulb and wet-bulb temperatures in shed were recorded every day, and the weights and all visible drying defects of samples were recorded once a week at the first month, then once every two weeks till the air drying ended.

When the test finished, three final MC slices and one layer MC slice for each sample were cut (Fig.4.1-2). After oven drying these slices, the final MC for each sample were be gained, and then the oven-dry weight (written as G_0) for each sample could be calculated with the equation listed below. And so, corresponding to the recorded weights of each sample in different drying times, the air-drying MC curve could be drawn.

$$G_0 = 100G_w/(100+ MC_0)$$

G_0 - oven-dry weight

G_w - initial weight

MC_0 - oven-dry MC (%)

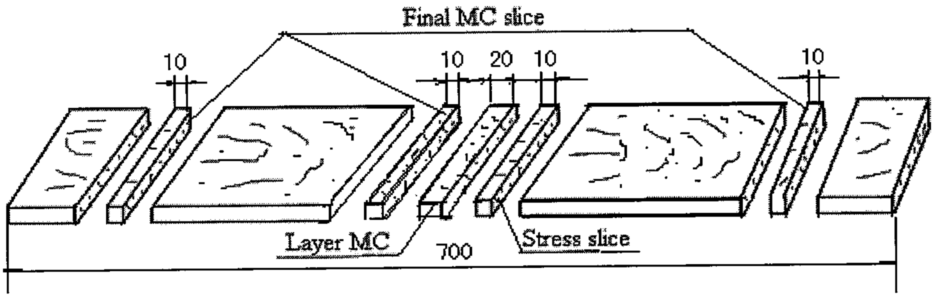

Fig.4.1-2 MC slices making of *E. grandis*

4.1.2 Result and suggestion

The air-drying test results of *E. grandis* are listed in Tab.4.1-1, and the air-drying MC curves in different seasons were shown in Fig.4.1-3.

Tab.4.1-1 Air-drying test results of *E. grandis*

Season	MCw (%)	MCo (%)	Air-drying rate (%day)			Air-drying rate in early stage (%/day)		Defect grade ##
			60-30%	30-20%	Below 20% #	1st week	2nd week	
2002.8-11 Autumn	108.5	13.3	2.5	1.33	0.55 (14.2%)	4.8	3.3	2
	92.4	12	2.22	1.43	0.89 (12.9%)	4.8	2.5	3
	76.7	13.1	2.14	1.43	0.46 (16.3%)	2.9	2.3	2
2002.12-2003.3 Winter	77.4	8.1	0.64	0.33	0.40 (14.4%)	2.5	1.5	2
	85.2	12.5	0.82	0.38	0.21 (14%)	3.7	1.1	2
	90.1	12.6	0.85	0.38	0.25 (13.4%)	3.7	1.5	2
2003.3-2003.7 Spring	88.7	14	1.36	1	0.52 (13.3%)	2.4	1.1	1
	65.5	14.2	1.25	0.83	0.38 (12.8%)	1.7	0.8	2
	68.9	13.5	1.2	1	0.41 (12.2%)	1.6	0.9	2
2003.6-2003.9 Summer	86.9	14	2.7	1.11	0.18 (13.4%)	4.6	2.5	3
	79.5	14.8	2.7	1.18	0.31 (14.5%)	4.5	2.3	3
	65.5	15.7	2.4	0.77	0.30 (15.5%)	3.5	1.6	2

Note: # - The data in brackets are the final MC when test ended.

##- The standards for drying defects grade division: grade 1 – having no check, warp and cup deformations or just having end checks; grade 2 - having no more than five short end-surface checks or short-narrow surface checks, and the value of warp and cup deformations are smaller than 2mm; grade 3 - having five to ten short-narrow surface checks, and the value of warp and cup deformations are smaller than 4mm; grade 4 - having more than ten short-narrow surface checks and long-narrow or wide surface checks no more than five, or the value of warp and cup deformation are more than 4mm.

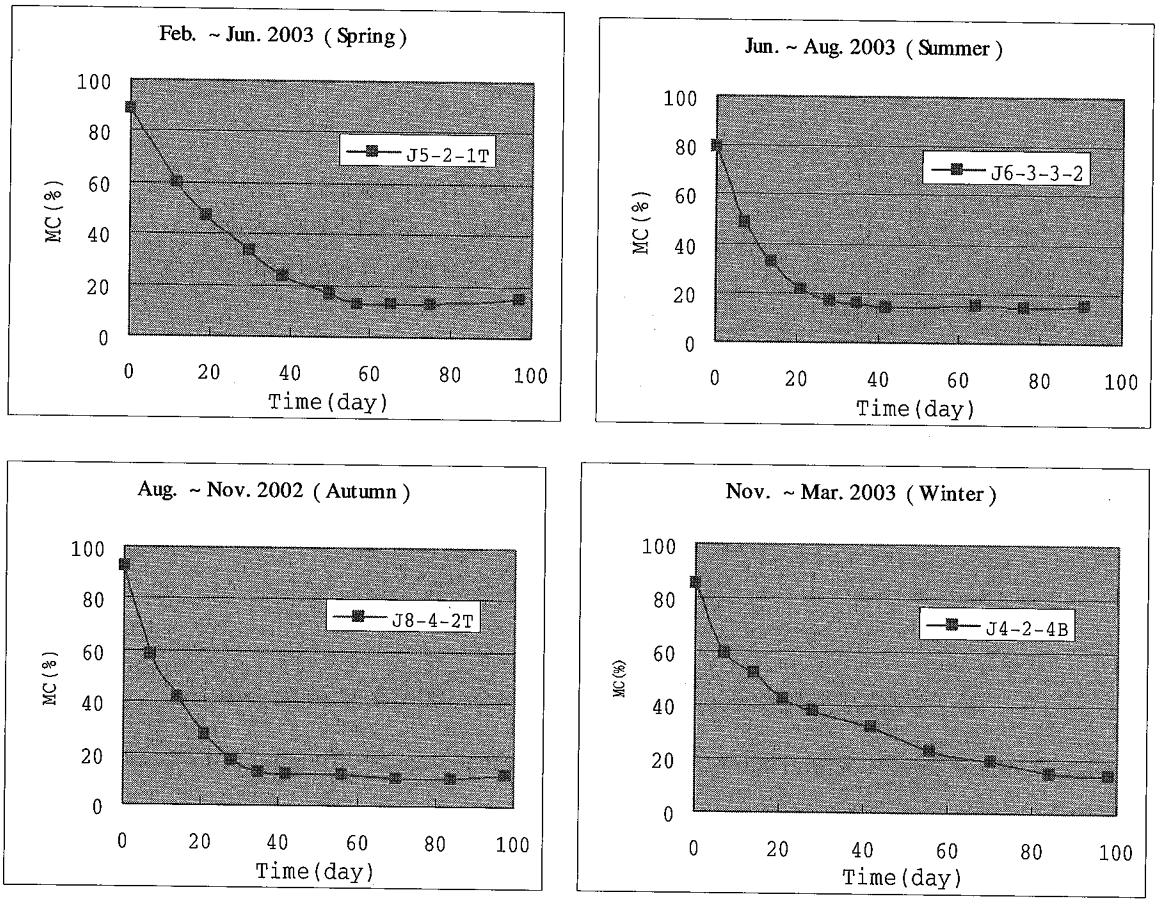

Fig.4.1-3 The air-drying MC curve of *E. grandis*

Result showed that the air-drying rate of *E. grandis* in summer was the fastest and that in winter in the slowest. But drying defects were very serious (grade 3 mostly), and the main drying defects were many small surface checks. So it is recommended that using controlled air-drying method to pre-dry *E. grandis* wood before kiln drying.

4.2 Drying characteristics

4.2.1 Material and method

The sample dimension: plane-sawn lumber with 200mm x 100mm x 20mm

Other requirements of sample: planed lumber with normal colour, knot-free and straight grain, and initial moisture content is above 45%.

Equipment: Electric oven with air circulation.

100℃-test method is a fast drying test which is used to study on drying characteristics and prediction of drying schedule of plantation wood. Before test, the following data of the samples should be gained: the sample's weight, all visible surface defects, and dimension measurement data as showing in Fig.4.2-1. Then the samples were put into the electric oven with constant temperature at 100℃, and letting the samples stand erectly in the oven so that they will obtain same quantity of heat. Once the test begin, weighing the samples, observing and recording all initial defects including end checks, end-to-surface checks and surface checks at a fixed time through all the drying process. The test ended when MC was estimated below to 1%. All the samples were taken out, and then measuring cross-section deformation (Fig.4.2-2). Finally cutting moisture content slice and recording internal checks of each sample.

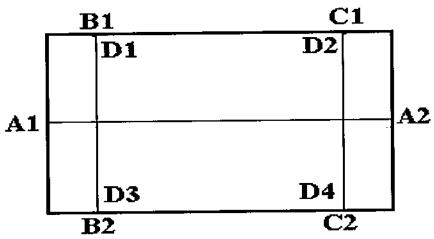

A1-A2 is length
B1-B2 and C1-C2 are width
D1,D2,D3,D4 are thickness

Fig.4.2-1 The dimension measure in 100℃-test of *E. grandis*

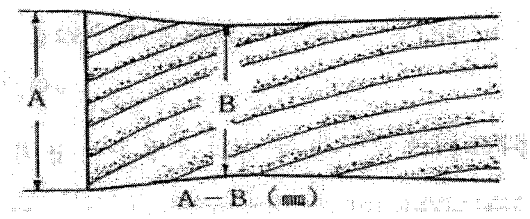

Fig.4.2-2 The cross-section measure in 100℃-test of *E. grandis*

To make all these defects digitalization and comparable, the grades of different drying defects are shown in Tab.4.2-1 to Tab.4.2-3.

Tab.4.2-1 The grade division of initial checks

Grade	No.1	No.2	No.3	No.4	No.5
Degree of initial check	No checks or only have end checks	Short end-to-surface checks and short-narrow surface checks	Long end-to-surface checks and long-narrow surface checks no more than two or short-narrow surface checks no more than fifteen	short-narrow surface checks more than fifteen or long-narrow and wide surface checks no more than five	short-narrow surface checks more than five or wide surface checks more than five

Note: long check -- check length ≥ 50mm; short check -- check length <50 mm; narrow check -- check width <2 mm; wide check -- check width ≥ 2mm

Tab.4.2-2 The grade division of internal checks

Grade	No.1	No.2	No.3	No.4	No.5	No.6
Degree of internal check	No checks	1 wide or 2 narrow checks	2-3 wide checks; 4-5 narrow checks; 1 wide and 3 narrow	4-5 wide; 7-9 narrow; 1 wide and 4-6 narrow	6-8 wide; 15 narrow; 4 wide and 6-8 narrow	15-17 wide or continuous checks

Tab.4.2-3 The grade division of cross-section deformation

Grade	No.1	No.2	No.3	No.4	No.5	No.6	No.7	No.8
A-B (mm)	0-0.3	0.3-0.5	0.5-0.8	0.8-1.2	1.2-1.8	1.8-2.5	2.5-3.5	over 3.5

Based on these drying characteristics in 100℃-test, the drying condition of this species could be gained by the relationships of drying characteristics and drying conditions showed Tab.4.2-4, which are very helpful to predict the drying schedules.

Tab.4.2-4 Drying condition based on degree of drying defects

Name	Drying condition (℃)	Grade of effects							
		No.1	No.2	No.3	No.4	No.5	No.6	No7	No8
Initial checks	Initial temperature	70	65	60	55	53	50	47	45
	Temperature depression	6.5	5.5	4.3	3.6	3.0	2.3	2.0	1.8
	Finial temperature	95	90	85	83	82	81	80	79
Cross section deformation	Initial temperature	70	66	58	54	50	49	48	47
	Temperature depression	6.5	6.0	4.7	4.0	3.6	3.3	2.8	2.5
	Finial temperature	95	88	83	80	77	75	73	70
Internal checks	Initial temperature	70	55	50	49	48	45	43	40
	Temperature depression	6.5	4.5	3.8	3.3	3.0	2.5	2.2	2.0
	Finial temperature	95	83	77	73	71	70	68	67

4.2.2 Result and suggestion

From the results of 100℃-test, the detailed data of drying defects results of *E. grandis* were shown in Tab.4.2-5, and the consideration of all 8 test samples, the comprehensive drying defects grades of *E. grandis* were shown in Tab.4.2-6. Corresponding to the drying condition based on degree of drying defects (Tab.4.2-4), and then the drying condition of *E. grandis* was show in Tab.4.2-7, which would be used to determine the kiln schedule in the follow-up test. And the MC curve during 100℃-test was showed in drying Fig.4.2-3.

Tab.4.2-5 The drying defects data and grades of *E. grandis*

No	Surface checks			End –surface checks			End checks		Grade	Internal checks			Cross section deformation	
	Long -narrow	Short -narrow	Wide	Long -narrow	Short -narrow	Wide	Wide	Short -narrow		Narrow	Wide	Grade	A-B (mm)	Grade
1	0	0	0	0	2	0	0	15	2	1	2	2	4.22	8
2	6	0	0	0	1	0	0	0	2	1	2	3	5.48	8
3	0	0	0	0	0	0	0	0	1	3	0	5	4.33	8
4	0	0	0	0	1	0	0	0	2	1	2	5	5.15	8
5	0	0	0	0	0	0	0	2	1	4	0	7	4.99	8

Tab.4.2-6 The comprehensive drying defects grades of *E. grandis*

Drying defects	Initial checks	Internal checks	Cross section deformation
Grade	No.2	No.4	No.8

Tab.4.2-7 The kiln drying condition of *E. grandis*

Item	The initial temperature	The initial wet-bulb depression (Δ t)	Final temperature)
Temperature (℃)	47	2.5	70

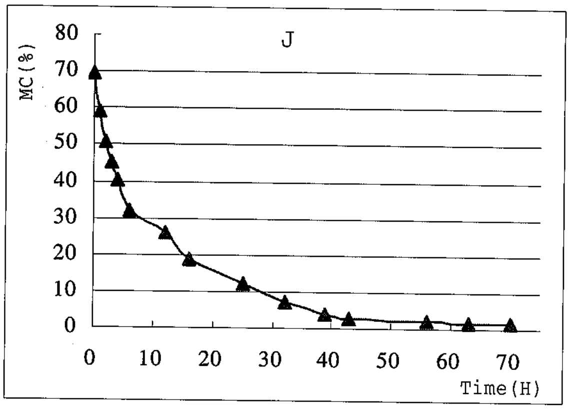

Fig.4.2-3 MC curve in 100℃-test of *E. grandis*

4.3 Drying schedule

4.3.1 *Material and method*

The sample dimension was with 500mm x 110mm x 25mm, double end-sealed with silicon sealing glue. The capacity for the stack was 500x400x300 mm, so 15 pieces of samples could by dried each time. To make it easy to fetch every sample for measurement and observation, all these 15 pieces of samples were put on a special made frame, so no heavy load on top on stack during test.

The test dryer was electric heating with 3 group of heater, which could be used independently of simultaneously according to the drying test need, the maximum of 3 group of heater was 6 kW. There was an electronic heated small boiler to afford steam during conditioning. The control system of the test dryer was semi-automatic.

Other equipment: Electric oven with air circulation, electronic balance, thermo-electronic couple temperature measuring system.

Based on the results of drying characteristics test, a schedule of *E. grandis* wood with thickness of 25 mm was drafted, seeing in Tab.4.3-1.

Tab.4.3-1 The predicted drying schedules of *E. grandis* (25mm)

MC stage	Dry-bulb temperature (t℃)	Wet-bulb temperature depression (Δt℃)
Above 40	47	2.5
40-35	50	4
35-30	53	6
30-25	56	9
25-20	60	12
20-15	65	18
Below 15	70	24

Beginning with this schedule, a series of kiln drying test had been done till the optimised schedule was gained.

4.3.2 *Result and suggestion*

The drying characteristics of *E. grandis* is similar to *E. urophylla×grandis* but with less defects than the latter. Using air-drying to pre-dry *E. grandis* plantation wood to MC around 30% was also a good way not only to save drying time, but also drying cost, to upgrade the drying quality and the mean time.

The optimised kiln drying schedule for *E. grandis* wood with thickness of 25 mm was listed in Tab.4.3-2.

Tab.4.3-2 Drying schedule for *E. grandis* wood with thickness of 25 mm

MC (%)	Dry-bulb T(℃)	Wet-bulb T(℃)	Notes
Pre-heating	55	54-55	Pre-heating, 3 hours
Above 35	47	44	
35 ~ 30	50	47	
=30%	68	67	Conditioning, 3 hours
30 ~ 25	53	48	
25 ~ 20	56	48	
=20%	65	63	Conditioning, 3 hours
20 ~ 15	60	45	
15 ~ 10	65	45	
Below 10	70	45	
=8%	75	69	End-treatment, 3-5 hours

The lab test results showed that using this schedule to dry *E. grandis* plantation wood with thickness of

25mm, the drying quality could meet the National Sawn-timber Drying Quality Standard (GB/T 6491-1999) 2nd grade requirement.

5 ADHESIVE PROPERTIES: FINGER JOINT

Finger-joints are commonly used to produce wood products from short pieces of lumber. Such joints must have excellent mechanical performance. To produce acceptable products, a jointer must be subjected to a proper end pressure following machining and adhesive application; also technical parameters, such as machining and gluing processes must be optimized. The condition of finger geometry and end pressure plays a major role in the gluing process and the final strength of the assemblies.

The main function of the end pressure is to bring the mating surfaces so close together that the glue forms a thin and continuous film between them. This pressure also allows a uniform distribution of the adhesive and creates an optimum glueline's thickness. So it is necessary to control the glueline's thickness to produce strong joints. Thin glueline lead to starved joints. Above the optimum glueline's thickness, stress concentration develops in the adhesive layer due to cure-shrinkage. The pressure must be applied to force fingers together to form an interlocking connection, giving a certain immediate handling strength. The increase of the end pressure up to a certain point gives a better contact of the finger to obtain strong joints. However, cell damage or splitting of the finger root can be induced by excessive pressure.

Finger-joint geometry has been proven to the most critical variable determining joint strength. Finger-tips constitute a series of butt joints and are accorded zero strength even if they are tight apparently well bonded; the tip width is the geometric parameter that most significantly influences finger-joint strength.

The objective of the study was to investigate the effect of finger profile geometry and end pressure on the performance of finger-joints in four species of Eucalyptus. The study also planned to evaluate which combination of the end pressures and finger profile geometry would result in optimum finger-joint performance in each of the four Eucalyptuses.

5.1 Materials

The experiments were carried-out with the samples which were planed and crosscut to dimensions of 20 by 60 by 520 mm; the total number of the samples was 90 in the kind of Eucalyptus; then the 90 wood blocks were divided three groups based on the density. The result of the density condition was as Tab.5.1-1:

Tab.5.1-1. Groups divided by density

Species	Average of high density /g/cm^3	Average of medium density /g/cm^3	Average of low density /g/cm^3
E. grandis	0.672	0.599	0.557

Two kinds of adhesive, API and PVAc, were used in the experiments. API is a kind of two-components adhesive, and is made of main reagent and cured reagent, the mixing ratio is 100:15 when the adhesive was used. The technical index of the two kinds of adhesives was Tab.5.1-2:

Tab.5.1-2. Technical indexes of two kinds of adhesive

Adhesives	Type	Colour	Solid cotent /%	pH	Viscidity(cps, 25℃)
PVAc	BT-09	White Emulsion	25.7	4.4	8740
API	DYNOLINK-8000G	White Emulsion	63.8	6.6	6750

5.2 Methods of experiments

The geometry of finger(ΔT), feed speed, the amount of adhesives spreading, end pressure, were all important factors to be investigated in the finger-joints experiments.

Three kinds of finger geometry were studies to determine finger parameter for optimum finger-joint strength, and they were selected based on specifications in standards, data from the literature. The finger-jointing machines used a carriage clamp to secure the stacks of wood samples; the samples were guided through a circular saw, a finger profile cutter, and a suction device that removed sawdust and shavings. The ends of pieces to be jointed were first trimmed and squared cleanly by the circular saw before the profile was cut. The suction completely removed all shavings from the profiled surfaces. Finger profiles were processed as vertical orientation joints subsequent test evaluation. The parameters of the three kinds of finger were as Tab.5.1-3.

Tab.5.1-3. Parameters of the fingers

ΔT /mm	Length /mm	Tip width /mm	Pitch /mm	Slope
0	11	0.6	3.8	1/8
0.1	10.6	0.7	3.8	1/8
0.5	8.9	1.1	3.8	1/8

In the processing of making samples finger, the feed speed was important to affect the roughness surface of finger. In this experiment, because different Eucalyptus wood have different density, *E. grandis* wood samples was chose in 10mm/min.

End pressure is needed to ensure the closest possible contact between the finger surfaces to be glued, and for the adhesive to form a thin continuous layer uniform in thickness, without damage to the strength of the wood. It is also intended to force the fingers together to the degree that a locking action is obtained, giving a certain immediate handing strength after gluing. Since the higher the pressure the more efficient the locking action, as much pressure as the wood can withstand may be used without causing damage such as splitting at the finger roots, compression failure of the wood, and squeezing out of the glue.

In the experiment, the preliminary end pressure experiment was done to get the suitable pressure. Firstly, four pieces of wood block were selected from the three groups(High, Middle, Low) and then finger were cut; ΔT of the fingers were 0mm, 0.1mm, 0.5mm; and the samples were cut to 60mm length. PVAc was used as adhesive in the experiment with the spread amount 250g/m^2. Two samples were combined and laid under the loading machine to be pressured as Fig.5.1-1. The loading speed was 2mm/min.

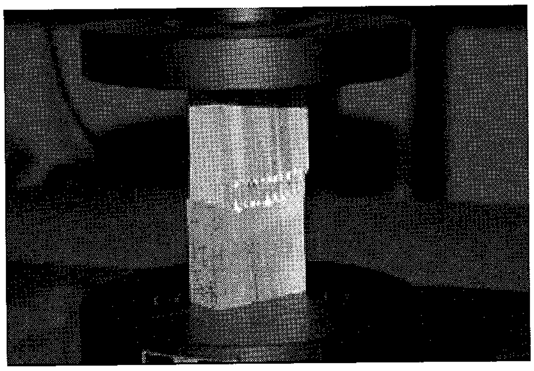

Fig.5.1-1. The method of measuring end-pressure

After the samples had been cut to finger, the samples were jointed by the finger jointer machine. 54

samples were selected from the group. The six kinds of sample were arranged as HH, HM, HL, MM, ML, LL on the basis of density. ΔT were 0, 0.1mm, 0.5mm, the end pressure was used from the result of preliminary end pressure experiments.

Because many factors affected the strength of finger-jointed lumber, for the sake of getting the better processing conditions, the end pressure and ΔT were main factors considered in the research, the design methods of full factors experiments and SAS analysis software were used to discuss the effect on the performance of finger-jointed lumber by each factor, and the interaction between the end pressure and ΔT. Finally integrative evaluation was processed by the result of SAS analysis and the appearance of finger-jointed samples to find the optimum processing condition.

After that, the finger-jointed specimens were cured over 48 hours before further processing. No pressure was applied to the specimens during curing. Both faces of a specimen were planed to a final specimen dimension of 58 by 17.5mm. The bending test was done by using the loading machine to measure MOE and MOR as Fig.5.1-2 according to JAS MAFF, Notification NO.590; support span was 420mm; loading span was 140mm and loading speed was 2mm/min

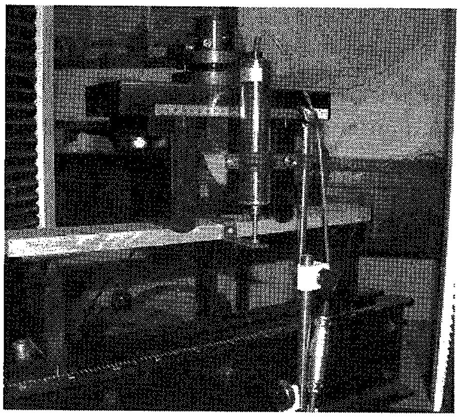

Fig.5.1-2. Four-point bending test

In the experiment, API (DYNOLNK-8000G) was used to make finger-jointed samples. Bending test were performed according to JAS MAFF, Notification NO.590; then MOE and MOR of finger-joints were compared with different kinds of adhesive

To compare the difference of MOR and MOE between V type finger(Fig.5.1-3) and H type finger(Fig.5.1-4), in the experiment, the H finger was done to make finger-jointed lumber, ΔT was 0.1mm; bending test were performed also according to JAS MAFF, Notification NO.590

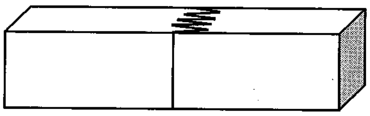

Fig.5.1-3. V-type finger-joint

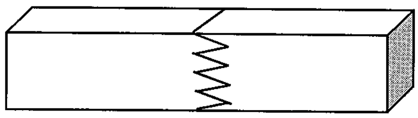

Fig.5.1-4. H-type finger-joint

5 3 Result and Discussion

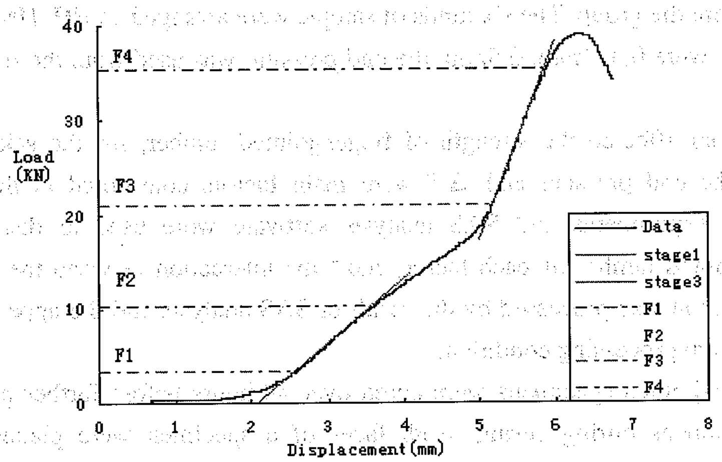

Fig.5.1-5. Load-displacement curve

Fig.5.1-5 is the typical Load-displacement curve, in this case ΔT is 0.5. When the cross head began to push the upper specimen, the upper specimens begin to move, the finger-tip will touch the nether specimen quickly, so when loading reached F1, it was considered the finger-tip touch the nether specimen, when the loading approached F2, it was considered the finger-tip was damaged, when the loading aroused to F3, there was splitting on the finger root, and following stage was as the same as solid wood pressured, the solid wood begin to damage when the loading increased to F4.

In the experiment, F1 was thought the suitable pressure before the finger was damage. Tab.5.1-4 was the results of end pressures in different ΔT.

Tab.5.1-4. End-pressure at different conditions

Wood species	ΔT	Average pressure /MPa
	0	11.46
E.grandis	0.1	14.63
	0.5	5.35

In the experiments, the four species of Eucalyptus end pressures were selected from Tab.5.1-5.

Tab.5.1-5. Different levels of the end-pressure

Wood species	Three end pressure /kN		
	P1	P2	P3
E. grandis	9	11.5	13.5

Tab.5.1-6 and Tab.5.1-7 were the results of the bending test analysis of *E. grandis.*

Tab.5.1-6. MOE and MOR analyzed by SAS

Index	Resource of variance	Degree of freedom	Summation of square	Average of square	F	Pr > F	Markedness
MOE	Matrix	66.637	2.468	2.53	0.0122	**	66.637
	Combination of density	37.868	7.574	7.76	0.0002	***	37.868
	End pressure	2.289	1.144	1.17	0.3266	/	2.289
	ΔT	7.454	3.727	3.82	0.0363	**	7.454
	End pressure×ΔT	10.194	2.549	2.61	0.0607	*	10.194
	Combination of density×pressure	4.881	0.610	0.63	0.7484	/	4.881
	Combination of density×ΔT	3.952	0.659	0.68	0.6709	/	3.952
	Error	23.418	0.976				23.418
	Summation	90.055					90.055
MOR	Matrix	948.967	35.147	3.71	0.0009	***	948.967
	Combination of density	224.474	44.895	4.73	0.0038	***	224.474
	End pressure	116.126	58.063	6.12	0.0071	***	116.126
	ΔT	228.716	114.358	12.06	0.0002	***	228.716
	End pressure×ΔT	108.193	27.048	2.85	0.0457	**	108.193
	Combination of density×pressure	103.979	12.997	1.37	0.2588	/	103.979
	Combination of density×ΔT	167.478	27.913	2.94	0.0268	**	167.478
	Error	227.572	9.482				227.572
	Summation	1176.539					1176.539

Mark: /means unmarkedness at 0.1; *means markedness at 0.1; **means markedness at 0.05

Tab.5.1-7 Testing for groups of each factor

Factor	Level	Number of specimen	MOE(Gpa) Average	MOE(Gpa) STDEV	MOR(Mpa) Average	MOR(Mpa) STDEV
End pressure	9	18	13.776A	1.342	39.768A	4.400
	11.5	18	13.753A	1.442	39.795A	5.291
	13.5	16	14.635B	1.022	43.885B	3.512
ΔT	0	17	14.494A	1.099	42.954A	3.531
	0.1	17	14.017AB	1.608	42.297A	5.159
	0.5	18	13.611B	1.151	38.057B	4.214
Combination of density	HH	5	15.122A	0.846	42.870A	3.806
	HL	14	13.436BC	1.213	40.024AB	5.523
	HM	10	14.905A	0.961	42.423A	5.236
	LL	6	12.533B	1.538	38.457B	5.018
	ML	9	13.694B	0.851	38.830B	3.365
	MM	8	14.809A	0.782	44.397A	2.217

Mark: The A,B behind average in table means the checked result by T, the same word letter means there was no difference in Stat., the different letter means there was difference in Stat..

From Tab.5.1-6 it is indicated that the combination of density and ΔT had much effect on the MOR of finger-jointed lumber of the wood; end pressure had much effect on MOR; the interaction of end pressure and ΔT had no effect on MOR and MOE.

From Tab.5.1-7 it is shown that the change of end pressure had no effect on MOE, but to MOR, the higher end pressure, the higher MOR of finger-jointed lumber of *E.grandis* wood; different ΔT can lead to different MOR and MOE, the MOR was higher when ΔT was 0.1mm.

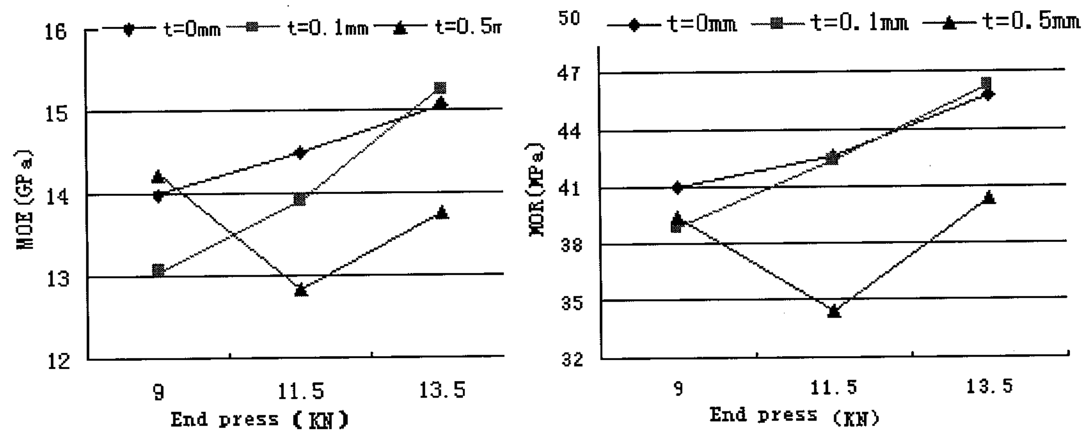

Fig.5.1-6 Effect of end-pressure on MOE and MOR

From Fig.5.1-6 it can be concluded that when the ΔT was 0mm and 0.1mm, the MOE and MOR increased as the increasing of end press from 9KN to 13.5KN, the MOE increased from 13.998GPa and 13.081GPa to 15.074GPa and 15.252GPa separately, the MOR increased from 41.023MPa and 38.871MPa to 45.751MPa.

From the result of T, MOR and MOE had no much difference when ΔT were 0mm and 0.1mm.Buth there were some gap and failure in the surface of finger-jointed lumber. There were much difference of MOR and MOE when the end press were 11.5KN and 13.5KN, when MOR and MOE were higher when the end press was 13.5KN, but there were failure. So the suitable ΔT was 0.1mm, and end pressure was 11.5KN

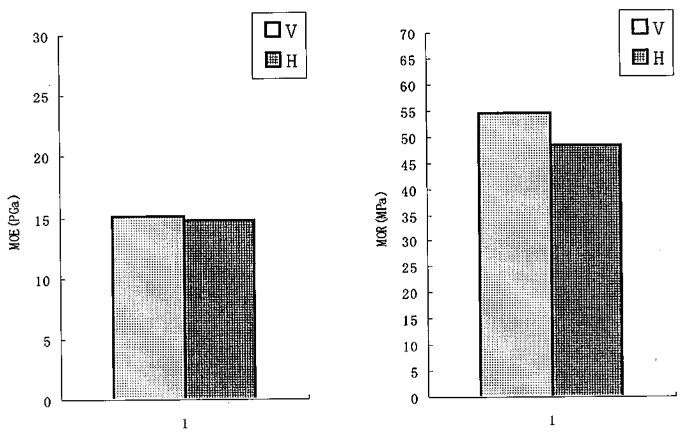

Fig.5.1-7 Comparison between V-type and H-type finger-joints on MOE and MOR

From the Fig.5.1-7 it was shown that the MOR of finger-joints with different finger type V and H were almost the same, but in the same processing condition, the MOE of finger-joints in V finger type was higher than that in H type.

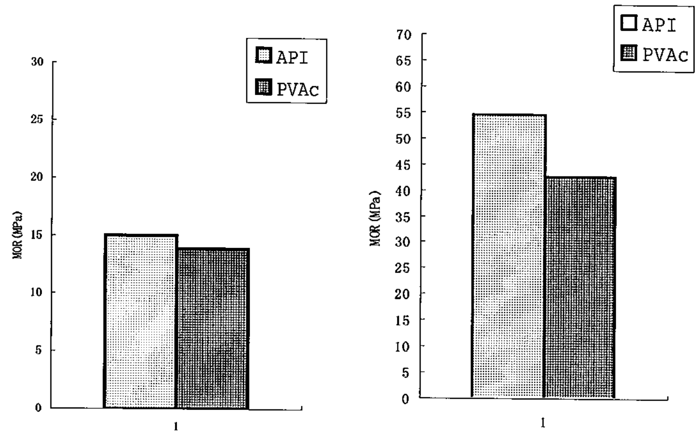

Fig.5.1-8 Comparison between API and PVAc finger-joint on MOE

From Fig.5.1-8 it was indicated that there were no much difference with API and PVAc in MOE, but for MOR, the API products was higher than PVAc remarkably, especially for *E. grandis* wood, which was high density and had much extraction. For example, the MOR was 30.35 MPa for PVAc, but for API, the MOR increased to 57.69MPa. This could be explained that for API adhesives, in the action of Vander waals force and hydrogen bond between the molecule of adhesive and molecule of wood, it forms deep-set physical bonding with wood. The gluing surface and the formed nail adhesive react with hydroxyl, carboxyl, phenolic hydroxyl and other reactive group in celluloses, hemicelluloses, lignin of wood, at the same time adhesive reacts with water in wood, then forms some chemical bond between wood and adhesive, in the end form intercross structure, thereby increases strength of gluing.

V *Eucalyptus urophylla*

The information of testing materials is as Tab.1.

Tab.1 Testing materials

Tree species	Tree age (year)	Tree number	Tree height (m)		Under branch height (m)		DBH (cm)	
			Ave.	Std	Ave.	Std.	Ave.	Std
Eucalyptus urophylla	13	5	28.3	1.5443	15.1	3.6654	25.4	1.2410

1 WOOD PROPERTIES

1.1 Anatomical characteristics

Samples (2x2x1 cm) for wood anatomical section were stored in alcohol 95% : glycerine (1:1) until they sank. Transverse sections of 20μm were cut on sliding microtome, then bleached, stained with safranin, dehydrated and mounted on slides for measure anatomical properties on image analysis. Then the transverse, radial and tangential sections from each species of around 80μm were cut on the same microtome, make the samples for SEM observation and taking photos.

Prior to tracheid length measurement, the each selected growth rings were firstly separated with a chisel, then macerated in solution of acetic acid (1/3) and hydrogen peroxide 27% (2/3) for several days in 60° oven.

The measurement methods are as follows:

Measuring length and width of wood fiber and vessel element using macerated anatomical elements under fiber length measuring instrument; (2) Measuring wood fiber cell wall thickness, cell wall percentage, and tissue proportions by section method using image analysis system; (3) Measure of S_2 microfibril angle: using x-ray diffractometer.

The observation and description for macro- and micro-structure were made under the light microscope and scanning electronically microscope (SEM).

1.1.1 Tree and distribution

Evergreen a tree up to 55 m, 2.0 m in d.b.h., trunk straight generally in origin producing country, Indonesia. Bark reddish brown, coarse for lower; bark gay white, smooth, peeling off in long strips on top tree. *Eucalyptus urophylla* was introduced to Brazil and Bali Island in 1919 & 1935 respectively. Our country is introduced this species in 80 of century; made the systemic provenance experiments. In Guangdong, Hainan and Guangxi there are large scales plantations.

1.1.2 General characteristics

Sapwood yellow, yellowish brown, comparatively differs from heartwood, width 3~4 cm. ***heartwood*** dark yellowish brown or pinkish brown; glossy, wood without characteristic taste & odor. ***Growth rings*** slightly distinct. Wood diffuse-porous, with semi-ring-porous wood trend. Pores small to middle, visible to the naked eye, fairly uniformly distributed throughout the ring, radial, tyloses visible. ***Longitudinal parenchyma*** vasicentric. ***Rays*** very fine to fine, visible with a hand lens. ***Ripple mark***s and ***Resin canals*** absent.

1.1.3 *Minute anatomy* (Plane III)

Vessels most solitary; in radial multiples of 2 few, radial or flexuous; cell wall thin to thick; tangential average diameter 124 μm, max 194 μm. 11 (8~15) /mm^2 . Vessel element length 365 (160~520) μm, tyloses visible and wall thin, helical thickness absent. Simple perforation, its plate oblique. Intervessel pits ventured, alternate, round & polygonal, ventures distributed pit aperture and & chamber, and full of the chamber. Vasicentrics common, located vessels intermixing parenchyma cells, with bordered pit round and ventured. Vessel- ray pits large round.

Longitudinal parenchyma vasicentric, diffuse or diffuse-aggregates. Nodular end wall of parenchyma cells inconspicuous, some cells contain round inclusion; crystals absent.

Fiber wall thicker to thick, 1158 (940~1350) μm in length, with plain simple pits.

Rays unstoried, rays 10~12/mm, mostly uniseriate rays 2~25 cells, multiseriate rays width 2 cells, height 2~18 cells seldom. Ray tissues homogeneous uniseriate and multiseriate; parenchyma cells round or oval, most with gum. Crystal and intercellular canals absent.

The data of anatomical parameter at different heights and vessel distribution frequencies and tangential diameters is including to the Tab. 1.1-1 and 1.1-2 respectively.

Tab.1.1-1 Anatomical parameter and basic density at different heights for *E. urophylla*

Item	1.3m		3.3m		5.3m		7.3m	
	$\bar{x}$	δ_n	$\bar{x}$	δ_n	$\bar{x}$	δ_n	$\bar{x}$	δ_n
Fiber length (μm)	1158	27	1176	83	1081	58	1176	54
Fiber width (μm)	17.6	0.7	17.5	0.5	16.9	0.8	17.6	0.5
Fiber wall thickness	10.40	1.1785	12.1	0.8520	10.40	1.007	10.15	0.9419
Microfibril angle (°)	9.80	0.702	9.02	0.881	10.98	2.096	10.51	0.987
Basic density (g/cm^3)	0.602	0.030	0.590	0.048	0.561	0.082	0.590	0.036

Tab.1.1-2 Vessel distribution frequencies and tangential diameters

Vessel distribution frequency (Number/mm^2)				Vessel tangential diameter (μm)			
Ave.	Std.	Max.	Min.	Ave.	Std.	Max.	Min.
11.18	2.4516	15.22	7.78	123.64	33.4686	194.07	37.55

1.2 Physical properties

1.2.1 *Moisture content of the green wood*

The moisture content data of the green wood at different heights is including Tab.1.2-1 and Fig.1.2-1.

Tab.1.2-1 Moisture content of green wood at different heights from *E. urophylla* (%)

Sites (from pith to bark)	1.3m		3.3m		5.3m		7.3m	
	$\bar{x}$	δ_n	$\bar{x}$	δ_n	$\bar{x}$	δ_n	$\bar{x}$	δ_n
1	143.84	17.34	127.59	10.98	113.09	16.26	124.98	9.26
2	134.34	23.67	116.99	7.49	114.73	17.45	107.38	9.64
3	122.25	14.46	113.98	19.09	105.57	11.74	100.33	13.05
4	110.30	14.64	100.91	21.10	98.44	17.82	84.51	6.52
5	79.36	6.25	85.43	33.65	90.99	18.79	83.66	5.61

1=near pith, 2=site between 1 &3, 3=center from pith to bark, 4=site between 3 &5, 5= near bark

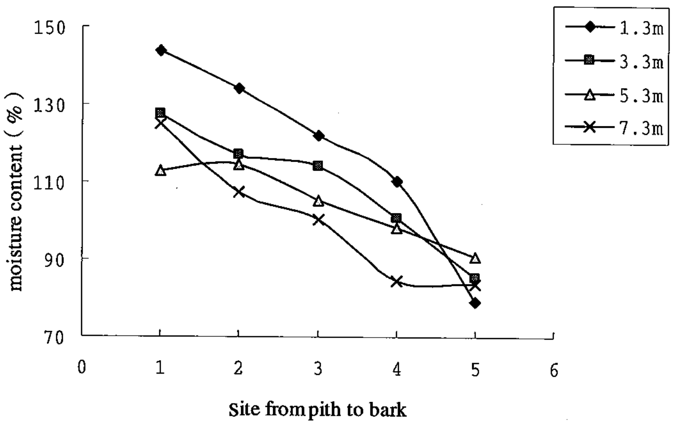

Fig. 1.2-1 Variation in moisture content of *E. urophylla* green wood at different tree heights and radial sites

1.2.2 Shrinkage and Density

Shrinkage is the contraction of wood caused by drying the material below the fibre saturation point (William T. Simpson, 1991). It can be divided into 3 types of shrinkage according to the direction of contraction: longitudinal, radial and tangential shrinkage. The longitudinal shrinkage is the shrinkage along the grain, the radial shrinkage and the tangential shrinkage is that across the grain in a radial or in a tangential direction. Wood density, the weight of wood per unit volume, is a very important index having a close relation with wood mechanical strength. In this study, wood air-dried density and basic density were used to describe the wood density.

The shrinkage is attributed to the dimension stability and checking problem, which causes a lot of problem for the wood utilization. In another word, it causes not only the contraction of wood in size, but also the checking and deformation resulted from the different contraction in tangential, radial and longitudinal direction. Understanding the characteristics of shrinkage has no doubt to be helpful for the wood utilization for the wood industry practice. Nowadays, studying on the characteristics of shrinkage during the losing of water is becoming one of the wood science discipline[Barber NF etc.1964; Barber, 1968; Chafe, 1986; 1987; Gu H et al., 2001]。 This study is intended to explore the shrinkage variation of acacia in different direction (North and south), different radial position and different tree height.

The trees studied were cut from Guangxi Zhuang Autonomous Region in the South China. Each trunk has been collected above the breast height and was cut every 2 meters. Then, four discs of each tree at different heights (about 1.3m, 3.3m, 5.3m and 7.3m respectively) were taken from the logs. All the discs were marked the south-north direction. For each disc, one specimen from the sapwood near the bark, one from the heartwood near pith and one from transition zone was made at the size of 2X2X2cm (Tangential X radial X longitudinal direction) for both north side and south side.

Two diagonal lines were drawn in three sections (i.e., T×R, T×L, R×L) of each specimen to locate the central point where the size was measured. The specimens were put into water until they were totally saturated and sunk in the water. The surface water was wiped off and the sizes in three directions (L, R, T) were measured. Specimens were set in the room for air-drying. After measuring the size and weight at the air-dried stage, the specimens were oven-dried and the same measurement was carried out. The shrinkage was determined according to Chinese National Standard. The air-dried density and was also calculated of both air-dried

The shrinkage coefficient was determined by the difference between shrinkage at air-dried and at oven-dried and divided by the MC at air-dried.

1.2.2.1 Shrinkage and density, and that of wood from south and north directions

The air-dried shrinkage in tangential direction (Ta), Radial direction (Ra) and volumetric shrinkage (Va), as well as the oven-dried shrinkage in tangential direction (To), Radial direction (Ro) and volumetric shrinkage (Vo) are listed in Tab.1.2-2 according to the categories of south direction, north direction and the overall. The basic density (B D) and air-dried density (A D), together with tangential shrinkage coefficient and radial shrinkage coefficient were also calculated and listed.

According to the IAWA (1989) method (the wood with an air-dried density smaller than 0.56 g/cm^3 is considered to be a small-density species, between 0.56 g/cm^3 and 0.75 g/cm^3 is considered to be a medium-density, between 0.75 g/cm^3 and 0.95 g/cm^3 is considered to be a large-density species, and bigger than 0.95 g/cm^3 is considered to be a extra-large-density species), *E.urophylla* wood has a medium density.

According to the *CHINA WOOD* method (the wood with an air-dried tangential shrinkage smaller than 5.60% is considered to be a small-shrinkage species, between 5.60% and 7.00% is considered with a medium-shrinkage species, and bigger than 7% is considered to be a big-shrinkage species), *E .urophylla×grandis* has a big shrinkage, suggesting more attention should be paid on checking or splitting when sawing and drying.

ANOVA analysis (Tab.1.2-3) showed there was no significant difference between air-dried tangential shrinkage and air-dried radial shrinkage, suggesting that the wood from north and south could be thought has the same level in shrinkage.

Tab. 1.2-2 The shrinkage and density of *E.urophylla* wood from south and north side

		Ta (%)	Ra (%)	Va (%)	To (%)	Ro (%)	Vo (%)	B D (g/cm^3)	A D (g/cm^3)	Co-t (%)	Co-r (%)
South	Average	7.88	4.26	11.89	11.08	6.67	17.31	0.53	0.67	0.27	0.20
	Std.dev.	1.26	0.75	1.61	1.32	1.03	1.88	0.06	0.08	0.05	0.03
	CV(%)	0.16	0.18	0.14	0.12	0.15	0.11	0.12	0.13	0.18	0.14
	Number	53	53	53	53	53	53	53	53	53	53
North	Average	8.19	4.46	12.35	11.28	7.01	17.76	0.53	0.68	0.26	0.22
	Std. dev.	1.02	0.91	1.60	1.14	1.38	2.01	0.06	0.09	0.03	0.06
	CV(%)	0.12	0.20	0.13	0.10	0.20	0.11	0.11	0.13	0.11	0.30
	Number	54	54	54	54	54	54	54	54	54	54
Total	Average	8.03	4.36	12.12	11.19	6.84	17.54	0.53	0.68	0.27	0.21
	Std. dev.	1.15	0.84	1.62	1.23	1.23	1.95	0.06	0.08	0.04	0.05
	CV(%)	0.14	0.19	0.13	0.11	0.18	0.11	0.12	0.13	0.15	0.24
	Number	107	107	107	107	107	107	107	107	107	107

Tab.1.2-3 ANOVA analysis on the shrinkage of *E. urophylla* wood from north and south

	SS	df	MS	F	P-value	F crit
Ta	2.6272	1	2.6272	1.9991	0.1603	3.9315
Ra	1.1283	1	1.1283	1.6159	0.2065	3.9315

1.2.2.2 Shrinkage and density of wood from 4 different tree heights

The shrinkage, shrinkage coefficient and density from 4 different tree heights were listed in Tab.1.2-4. The relationship between air-dried shrinkage, basic density and tree heights were showed in Fig. 1.2- 2

ANOVA analysis (Tab.1.2-5) showed there existed significant air-dried shrinkage difference both in tangential and radial directions among 4 different tree heights.

Tab. 1.2-4 The shrinkage and density of *E.urophylla s* wood from different heights

		Ta (%)	Ra (%)	Va (%)	To (%)	Ro (%)	Vo (%)	BD (g/cm^3)	AD (g/cm^3)	Co-t (%)	Co-r (%)
1.3m	Average	8.41	4.19	12.34	11.53	6.70	17.77	0.52	0.67	0.26	0.21
	Std. dev.	1.25	0.83	1.70	1.26	1.59	2.12	0.06	0.09	0.03	0.09
	CV(%)	0.15	0.20	0.14	0.11	0.24	0.12	0.12	0.13	0.11	0.45
	Number	24	24	24	24	24	24	24	24	24	24
3.3m	Average	7.91	4.20	11.88	11.27	6.65	17.44	0.52	0.67	0.28	0.20
	Std. dev.	1.28	0.97	1.89	1.31	1.32	2.25	0.07	0.09	0.07	0.03
	CV(%)	0.16	0.23	0.16	0.12	0.20	0.13	0.13	0.14	0.24	0.15
	Number	21	21	21	21	21	21	21	21	21	21
5.3m	Average	8.00	4.53	12.28	11.08	7.00	17.62	0.53	0.67	0.26	0.21
	Std. dev.	1.11	0.69	1.45	1.31	0.96	1.83	0.06	0.08	0.03	0.03
	CV(%)	0.14	0.15	0.12	0.12	0.14	0.10	0.12	0.13	0.13	0.14
	Number	30	30	30	30	30	30	30	30	30	30
7.3m	Average	7.79	4.48	11.94	10.92	6.98	17.36	0.55	0.70	0.27	0.21
	Std.	0.99	0.84	1.56	1.08	1.08	1.80	0.06	0.08	0.03	0.03
	CV(%)	0.13	0.19	0.13	0.10	0.15	0.10	0.10	0.11	0.10	0.12
	Number	30	30	30	30	30	30	30	30	30	30

Tab.1.2-5 ANOVA analysis on the shrinkage of *E.urophylla* wood from different heights

	SS	df	MS	F	P-value	F crit
Ta	5.5640	3	1.8547	1.4069	0.2452	2.6946
Ra	2.4754	3	0.8251	1.2140	0.3086	2.6946

Tangential shrinkage showed a tendency that it decreased with the incease of tree height, radial shrinkage showed a tendency that it increased with the increase of tree height, and the basic density has a tendency that it increased with the increase of tree height.

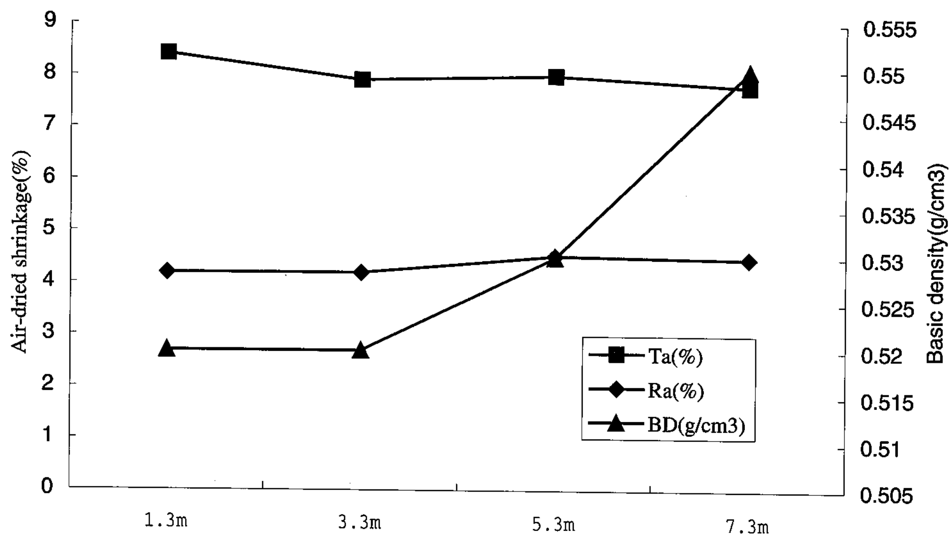

Fig.1.2-2 *E.urophylla*: relationship between air-dried shrinkage (Ta&Ra), basic density (BD) and tree heights

1.2.2.3 Shrinkage and density of wood at different radial positions

The shrinkage, shrinkage coefficient and density from 4 different tree radial positions were listed in Tab.1.2-6 The relationship between air-dried shrinkage, basic density and tree heights were showed in Fig. 1.2-3.

ANOVA analysis (Tab.1.2-7) showed there existed significant air-dried radial shrinkage difference both in tangential and radial directions among different radial position.

Tab. 1.2-6 The shrinkage and density of *E.urophylla* from different radial positions

		Ta (%)	Ra (%)	Va (%)	To (%)	Ro (%)	Vo (%)	B D (g/cm^3)	A D (g/cm^3)	Co-t (%)	Co-r (%)
近树皮 near bark	Average	7.64	4.71	12.10	11.02	7.52	18.01	0.57	0.73	0.29	0.24
	Std. dev.	0.97	0.62	1.44	1.05	1.08	1.70	0.04	0.06	0.02	0.07
	CV(%)	0.13	0.13	0.12	0.10	0.14	0.09	0.07	0.08	0.08	0.29
	Number	36	36	36	36	36	36	36	36	36	36
过渡区 transitio n	Average	8.92	4.77	13.28	12.17	7.29	18.78	0.55	0.71	0.27	0.21
	Std. dev.	0.93	0.57	1.24	0.77	0.74	1.26	0.04	0.05	0.05	0.02
	CV(%)	0.10	0.12	0.09	0.06	0.10	0.07	0.07	0.07	0.19	0.08
	Number	35	35	35	35	35	35	35	35	35	35
近髓心 near pith	Average	7.57	3.61	11.01	10.40	5.73	15.86	0.47	0.59	0.24	0.18
	Std.	1.04	0.74	1.31	1.14	0.95	1.54	0.05	0.06	0.02	0.02
	CV(%)	0.14	0.20	0.12	0.11	0.17	0.10	0.10	0.11	0.10	0.14
	Number	36	36	36	36	36	36	36	36	36	36

Tab.1.2-7 ANOVA analysis on the shrinkage of *E.urophylla* wood from different radial positions

	SS	Df	MS	F	P-value	F crit
Ta	40.55325	2	20.27663	21.07446	2.07E-08	3.083706
Ra	30.70709	2	15.35355	36.50746	9.75E-13	3.083706

Fig.1.2-3 showed the radial shrinkage increased gradually from juvenile wood (near pith) to mature wood (near bark), this coincide the change of basic density, meaning that the radial shrinkage has the positive correlation with basic density. However, the tangential shrinkage did not showed a positive correlation with the basic density, presenting a maximum basic density at the transition zone.

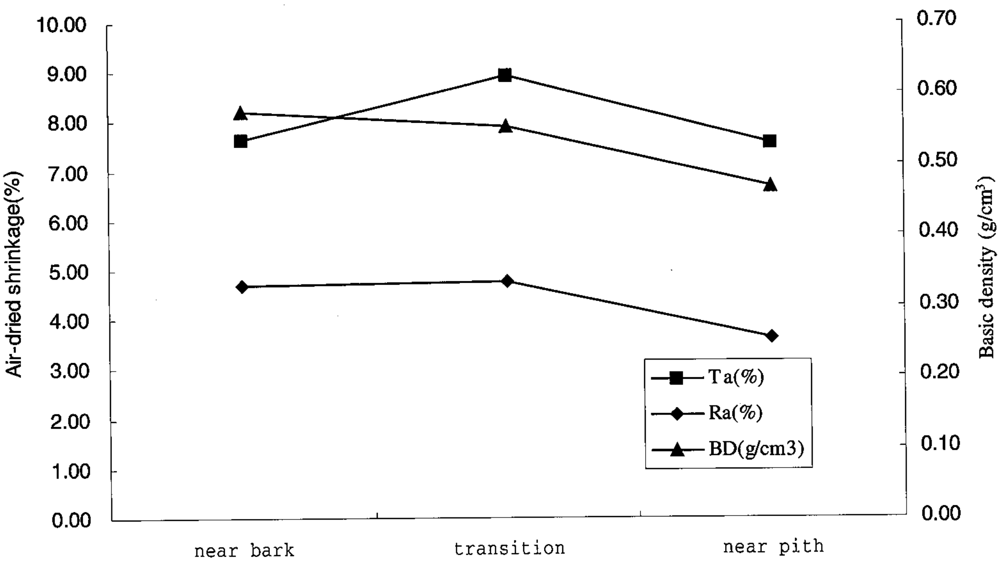

Fig.1.2-3 *E.urophylla*: relationship between air-dried shrinkage (Ta&Ra), basic density (BD) and different radial positions

1.3 Mechanical properties

The small clear wood samples of moduli of elasticity (MOE), moduli of rupture (MOR) in static bending, compression strength parallel to grain and wood density were cut in accordance with Chinese National Standards (GB 1927~1943-91). The specimens were then stored in a conditioning chamber until it reached approximately 12% moisture content. Bending, compression and wood density test were carried out in accordance with Chinese National Standard. The air-dry density was calculated by air-dried weight and volume while oven-dry density was based on oven-dried weight and volume.

Generally *E. urophylla* wood grain straight or little oblique, texture fine and even, wood weight middle to height, relatively hard, shrinkage large, strength highly. Nail holding power (N/mm): Radial: 41.7 Tangential: 38.8 Parallel to grain: 27.1. The mechanical properties are including tab.1.3-1.

Tab.1.3-1 Mechanical properties data of *E. urophylla*

Locality	Density /g/cm^3		DS /%		CSPG /MPa	BS /MPa	MOE /GPa	Toughness /kJ/m^2	Hardness /N		
	BD	ADD	R	T	CSPG/MPa	BS/MPa	MOE/GPa	Toughness/kJ/m^2	E	R	T
Guangxi Dongmen		0.783			62	173	25.47	45.4			

BD = basic density, ADD = air-dry density, DS = dry shrinkage, CSPG = compressive strength parallel to grain, BS = bending strength, MOE = modulus of elasticity, SSPG = shear strength parallel to grain(R), E = end, R = radial, T = tangential

1.4 Chemical properties

The chemical composition was determined according to Chinese National Standards, the chemical composition results and pH values, acid and alkaline buffering capacities are listed in Tab. 1.4-1, and 1.4-2 respectively.

Tab.1.4-1 Chemical composition of *E. urophylla* (%)

Lignin	Holocellulose	α-Cellulose	Hemicellulose	1%NaOH extractives	Benzene-alcohol extractives	Hot water extractives
24.68	72.77	44.39	28.38	18.10	1.80	7.97

Tab.1.4-2 Data of pH value, acid and alkaline buffering capacity of *E. urophylla*

S	H	S	H	S	H
4.61	3.62	3.38	1.62	19.60	81.00

S=sapwood, H=heartwood

2 GROWTH STRESS

The research adopted CIRAD-Foret method to measure surface longitudinal growth strain (SLGS) of standing trees, the results at different orientations were listed in Tab.2-1.

Tab. 2-1 Growth strain data for standing trees of *E. urophylla*

Basic density (g/cm^3)	E		W		S		N	
	$\bar{x}$	δ_n	$\bar{x}$	δ_n	$\bar{x}$	δ_n	$\bar{x}$	δ_n
0.590	1610	384.4	1512	490.4	1260	432.0	1795	949.6

E=east, W=west, S=south, N=north

VI *Eucalyptus cloeziane*

The information of testing materials is as Tab.1.

Tab.1 Testing materials

Tree species	Tree age (year)	Tree number	Tree height (m)		Under branch height (m)		DBH (cm)	
			Ave.	Std	Ave.	Std.	Ave.	Std
Ecalyptus. cloeziane	16	5	30.9	1.8493	16.8	4.0577	25.9	1.8748

1 WOOD PROPERTIES

1.1 Anatomical characteristics

Samples (2x2x1 cm) for wood anatomical section were stored in alcohol 95% : glycerine (1:1) until they sank. Transverse sections of 20μm were cut on sliding microtome, then bleached, stained with safranin, dehydrated and mounted on slides for measure anatomical properties on image analysis. Then the transverse, radial and tangential sections from each species of around 80μm were cut on the same microtome, make the samples for SEM observation and taking photos.

Prior to tracheid length measurement, the each selected growth rings were firstly separated with a chisel, then macerated in solution of acetic acid (1/3) and hydrogen peroxide 27% (2/3) for several days in 60° oven.

The measurement methods are as follows:

Measuring length and width of wood fiber and vessel element using macerated anatomical elements under fiber length measuring instrument; (2) Measuring wood fiber cell wall thickness, cell wall percentage, and tissue proportions by section method using image analysis system; (3) Measure of S_2 microfibril angle: using x-ray diffractometer.

The observation and description for macro- and micro-structure were made under the light microscope and scanning electronically microscope (SEM).

1.1.1 Tree and distribution

A tree up to 35~45 m, 0.4~0.6 m in d.b.h., trunk straight generally in origin producing country. Bark dark brown, squama & fibrous, softer. *Eucalyptus cloeziane* was introduced to South Africa, Kenya, Zambia, Brazil, Congo, Madagascar, Nigeria and Sri Lanka in last 30 years respectively. Our country is introduced this species as solid wood products in Guangdong and Guangxi.

1.1.2 General characteristics

Sapwood yellowish brown, comparatively differs from heartwood, width 3~4 cm. ***heartwood*** yellowish brown to light reddish brown; glossy, wood without characteristic taste & odor. ***Growth rings*** indistinct. Wood diffuse-porous. Pores small to middle, visible to the naked eye, fairly uniformly distributed throughout the ring, radial, tyloses visible. ***Longitudinal parenchyma*** vasicentric. ***Rays*** very fine to fine, visible with a hand lens. ***Ripple mark***s and ***Resin canals*** absent.

1.1.3 Minute anatomy (Plane III)

Vessels most solitary; in radial multiples of 2 few, radial or flexuous; cell wall thin to thick; tangential average diameter 97 μm, max 163 μm. 19 (13~25) /mm^2 . Vessel element length 357 (158~526) μm, tyloses visible and wall thicker or thick, helical thickness absent. Simple perforation, its plate oblique. Intervessel pits ventured, alternate, round & polygonal, ventures distributed pit aperture and & chamber, and full of the chamber. Vasicentrics common, located vessels intermixing parenchyma cells, with bordered pit round and ventured. Vessel- ray pits large round.

Longitudinal parenchyma vasicentric, diffuse or diffuse-aggregates. Nodular end wall of parenchyma cells inconspicuous, some cells contain round inclusion; crystals absent.

Fiber wall thicker to thick, 1272 (980~1380) μm in length, with plain simple pits.

Rays unstoried, rays 10~12/mm, mostly uniseriate rays 2~25 cells, multiseriate rays width 2 cells, height 2~18 cells seldom. Ray tissues homogeneous uniseriate and multiseriate; parenchyma cells round or oval, most with gum. Crystal and intercellular canals absent.

The data of anatomical parameter at different heights and vessel distribution frequencies and tangential diameters is including to the Tab. 1.1-1 and 1.1-2 respectively.

Tab.1.1-1 Anatomical parameter and basic density at different heights for *E. cloeziane*

Item	1.3m		3.3m		5.3m		7.3m	
	$\bar{x}$	δ_n	$\bar{x}$	δ_n	$\bar{x}$	δ_n	$\bar{x}$	δ_n
Fiber length (μm)	1272	70	1312	109	1327	12	1311	90
Fiber width (μm)	18.9	1.3	20.0	2.1	19.4	1.8	19.2	1.0
Fiber wall thickness	10.83	1.035	10.60	0.943	10.77	0.308	10.38	0.627
Microfibril angle (°)	10.43	1.193	9.90	0.767	9.52	0.826	9.64	0.655
Basic density (g/cm^3)	0.688	0.051	0.702	0.056	0.719	0.051	0.717	0.056

Tab.1.1-2 Vessel distribution frequencies and tangential diameters

Vessel distribution frequency (Number/mm^2)				Vessel tangential diameter (μm)			
Ave.	Std.	Max.	Min.	Ave.	Std.	Max.	Min.
18.96	4.0921	24.70	12.80	96.92	27.6268	163.02	33.09

1.2 Physical properties

1.2.1 Moisture content of the green wood

The moisture content data of the green wood at different heights is including Tab.1.2-1 and Fig.1.2-1.

Tab.1.2-1 Green wood moisture content of *E. cloeziane* at different tree heights and radial sites

Side	1.3m		3.3m		5.3m		7.3m	
	$\bar{x}$	δ_n	$\bar{x}$	δ_n	$\bar{x}$	δ_n	$\bar{x}$	δ_n
1	112.63	9.16	109.29	18.48	84.25	13.67	99.60	34.25
2	90.55	16.04	104.75	10.48	95.30	28.26	87.48	36.45
3	85.41	43.60	85.06	5.30	78.93	19.62	78.27	8.28
4	76.00	27.15	79.08	27.03	77.58	16.86	73.09	13.43
5	66.25	19.31	71.14	5.90	70.91	6.77	71.29	11.92

1=near pith, 2=site between 1 &3, 3=center from pith to bark, 4=site between 3 &5, 5= near bark

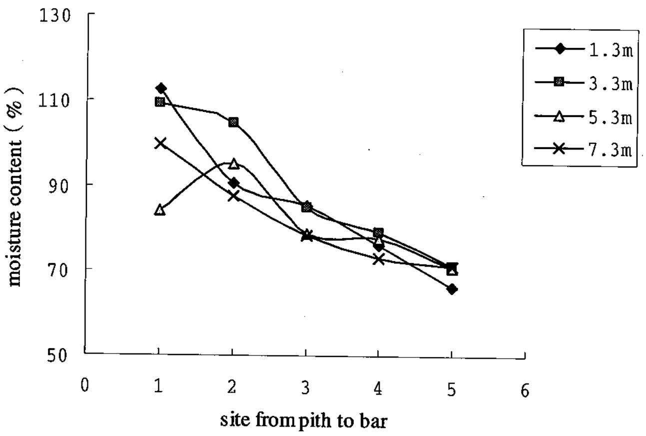

Fig.1.2-1 Moisture content of green wood for *E. cloeziane* at different heights and sites

1.2.2 Shrinkage and Density

Shrinkage is the contraction of wood caused by drying the material below the fiber saturation point (William T. Simpson, 1991). It can be divided into 3 types of shrinkage according to the direction of contraction: longitudinal, radial and tangential shrinkage. The longitudinal shrinkage is the shrinkage along the grain, the radial shrinkage and the tangential shrinkage is that across the grain in a radial or in a tangential direction. Wood density, the weight of wood per unit volume, is a very important index having a close relation with wood mechanical strength. In this study, wood air-dried density and basic density were used to describe the wood density.

The shrinkage is attributed to the dimension stability and checking problem, which causes a lot of problem for the wood utilization. In another word, it causes not only the contraction of wood in size, but also the checking and deformation resulted from the different contraction in tangential, radial and longitudinal direction. Understanding the characteristics of shrinkage has no doubt to be helpful for the wood utilization for the wood industry practice. Nowadays, studying on the characteristics of shrinkage during the losing of water is becoming one of the wood science discipline [Barber NF etc.1964; Barber, 1968; Chafe, 1986; 1987; Gu H et al., 2001]。This study is intended to explore the shrinkage variation of acacia in different direction (North and south), different radial position and different tree height.

The trees studied were cut from Guangxi Zhuang Autonomous Region in the South China. Each trunk has been collected above the breast height and was cut every 2 meters. Then, four discs of each tree at different heights (about 1.3m, 3.3m, 5.3m and 7.3m respectively) were taken from the logs. All the discs were marked the south-north direction. For each disc, one specimen from the sapwood near the bark, one from the heartwood near pith and one from transition zone was made at the size of 2X2X2cm (Tangential X radial X longitudinal direction) for both north side and south side.

Two diagonal lines were drawn in three sections (i.e., T×R, T×L, R×L) of each specimen to locate the central point where the size was measured. The specimens were put into water until they were totally saturated and sunk in the water. The surface water was wiped off and the sizes in three directions (L, R, T) were measured. Specimens were set in the room for air-drying. After measuring the size and weight at the air-dried stage, the specimens were oven-dried and the same measurement was carried out. The shrinkage was determined according to Chinese National Standard. The air-dried density and was also calculated of both air-dried

The shrinkage coefficient was determined by the difference between shrinkage at air-dried and at oven-dried and divided by the MC at air-dried.

1.2.2.1 Shrinkage and density, and that of wood from south and north directions

The air-dried shrinkage in tangential direction (Ta), Radial direction (Ra) and volumetric shrinkage (Va), as well as the oven-dried shrinkage in tangential direction (To), Radial direction (Ro) and volumetric shrinkage (Vo) are listed in Tab.1.2-2 according to the categories of south direction, north direction and the overall. The basic density (B D) and air-dried density (A D), together with tangential shrinkage coefficient and radial shrinkage coefficient were also calculated and listed.

According to the IAWA (1989) method (the wood with an air-dried density smaller than 0.56 g/cm^3 is considered to be a small-density species, between 0.56 g/cm^3 and 0.75 g/cm^3 is considered to be a medium-density, between 0.75 g/cm^3 and 0.95 g/cm^3 is considered to be a large-density species, and bigger than 0.95 g/cm^3 is considered to be a extra-large-density species), *E.cloesiane* wood has a large density.

According to the *CHINA WOOD* method (the wood with an air-dried tangential shrinkage smaller than 5.60% is considered to be a small-shrinkage species, between 5.60% and 7.00% is considered with a medium-shrinkage species, and bigger than 7% is considered to be a big-shrinkage species), *E.urophylla×grandis* has a big shrinkage, suggesting more attention should be paid on checking or splitting when sawing and drying.

ANOVA analysis (Tab.1.2-3) showed there was no significant difference between air-dried tangential shrinkage and air-dried radial shrinkage, suggesting that the wood from north and south could be thought has the same level in shrinkage.

Tab. 1.2-2 The shrinkage and density of *E.cloesiane* wood from south and north side

		Ta (%)	Ra (%)	Va (%)	To (%)	Ro (%)	Vo (%)	B D (g/cm^3)	A D (g/cm^3)	Co-t (%)	Co-r (%)
South	Average	7.51	4.42	11.69	11.00	7.09	17.65	0.68	0.86	0.29	0.23
	Std.dev.	1.44	0.59	1.61	1.19	0.84	1.56	0.07	0.09	0.06	0.03
	CV(%)	0.19	0.13	0.14	0.11	0.12	0.09	0.10	0.10	0.21	0.13
	Number	55	55	55	55	55	55	55	55	55	55
North	Average	7.29	4.41	11.47	10.84	7.15	17.51	0.68	0.86	0.30	0.23
	Std. dev.	1.56	0.58	1.72	1.33	0.87	1.46	0.07	0.09	0.09	0.04
	CV(%)	0.21	0.13	0.15	0.12	0.12	0.08	0.11	0.11	0.30	0.19
	Number	58	58	58	58	58	58	58	58	58	58
Total	Average	7.40	4.41	11.58	10.92	7.12	17.58	0.68	0.86	0.30	0.23
	Std. dev.	1.50	0.58	1.66	1.26	0.85	1.51	0.07	0.09	0.08	0.04
	CV(%)	0.20	0.13	0.14	0.12	0.12	0.09	0.10	0.10	0.26	0.17
	Number	113	113	113	113	113	113	113	113	113	113

Tab.1.2-3 ANOVA analysis on the shrinkage of *E. cloeziane* wood from north and south

	SS	df	MS	F	P-value	F crit
Ta	1.4083	1	1.4083	0.6239	0.4313	3.9266
Ra	0.0002	1	0.0002	0.0007	0.9793	3.9266

1.2.2.2 Shrinkage and density of wood from 4 different tree heights

The shrinkage, shrinkage coefficient and density from 4 different tree heights were listed in Tab.1.2-4. The relationship between air-dried shrinkage, basic density and tree heights were showed in Fig. 1.2-2.

ANOVA analysis (Tab.1.2-5) showed there existed significant air-dried shrinkage difference both in tangential and radial directions among 4 different tree heights.

Tangential shrinkage showed a tendency that it decreased with the incease of tree height, radial shrinkage showed a tendency that it increased with the increase of tree height, and the basic density in 3.3m height had a minimal value and afterwards, it increased with the increase of tree height.

Tab. 1.2-4 The shrinkage and density of *E. cloeziane s* wood from different heights

		Ta (%)	Ra (%)	Va (%)	To (%)	Ro (%)	Vo (%)	B D (g/cm³)	A D (g/cm³)	Co-t (%)	Co-r (%)
1.3m	Average	7.68	4.18	11.71	11.05	6.81	17.50	0.68	0.87	0.28	0.22
	Std. dev.	1.57	0.53	1.65	1.50	0.87	1.56	0.08	0.09	0.03	0.04
	CV(%)	0.20	0.13	0.14	0.14	0.13	0.09	0.11	0.11	0.11	0.18
	Number	29	29	29	29	29	29	29	29	29	29
3.3m	Average	7.79	4.45	11.95	11.19	7.06	17.71	0.67	0.86	0.29	0.22
	Std. dev.	1.08	0.55	1.27	0.99	0.74	1.29	0.07	0.09	0.03	0.03
	CV(%)	0.14	0.12	0.11	0.09	0.10	0.07	0.10	0.10	0.10	0.12
	Number	29	29	29	29	29	29	29	29	29	29
5.3m	Average	7.14	4.48	11.38	10.65	7.29	17.54	0.68	0.86	0.30	0.24
	Std. dev.	1.30	0.56	1.48	1.27	0.90	1.62	0.08	0.10	0.10	0.05
	CV(%)	0.18	0.12	0.13	0.12	0.12	0.09	0.11	0.12	0.34	0.21
	Number	27	27	27	27	27	27	27	27	27	27
7.3m	Average	6.93	4.56	11.24	10.76	7.35	17.57	0.69	0.87	0.32	0.24
	Std.	1.85	0.64	2.13	1.21	0.83	1.61	0.06	0.08	0.11	0.03
	CV(%)	0.27	0.14	0.19	0.11	0.11	0.09	0.08	0.09	0.33	0.12
	Number	28	28	28	28	28	28	28	28	28	28

Tab.1.2-5 ANOVA analysis on the shrinkage of *E. cloeziane* wood from different heights

	SS	df	MS	F	P-value	F crit
Ta	14.6230	3	4.8743	2.2384	0.0879	2.6879
Ra	2.3737	3	0.7912	2.4173	0.0702	2.6879

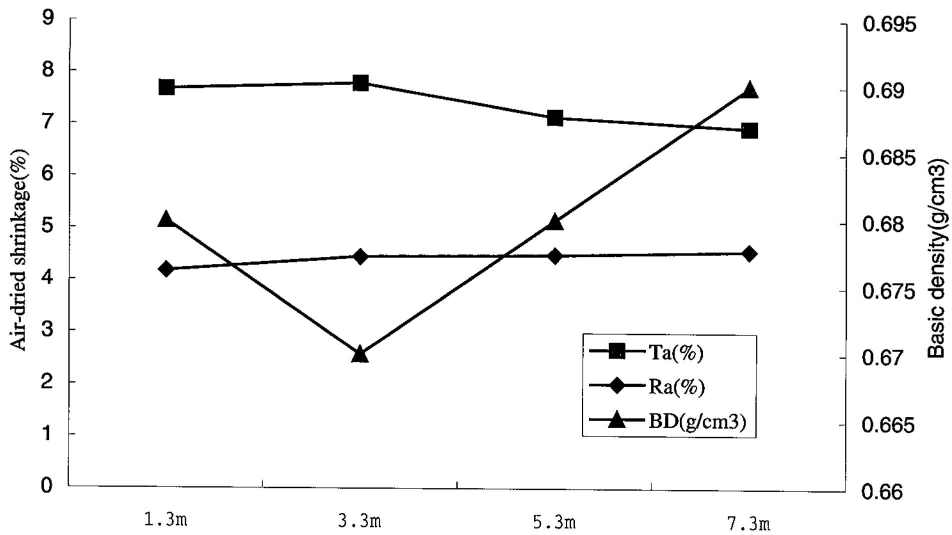

Fig.1.2-2 *E.cloeziane*: relations between air-dried shrinkage (Ta&Ra), basic density (BD) and tree heights

1.2.2.3 Shrinkage and density of wood at different radial positions

The shrinkage, shrinkage coefficient and density from 4 different tree radial positions were listed in Tab.1.2-6. The relationship between air-dried shrinkage, basic density and tree heights were showed in Fig.

1.2-3.

ANOVA analysis (Tab. 1.2-7) showed there existed significant air-dried radial shrinkage difference in tangential directions among different radial position, while no significant difference in radial shrinkage.

Fig.1.2-3 showed the tangential shrinkage decreased gradually from juvenile wood (near pith) to mature wood (near bark), suggesting that the mature wood has a better dimension stabaility than the juvenile wood. No obvious change was found in radial shrinkage amond different radial positions . This agrees the ANOVA test result that there did not exist significant radial shrinkage difference among different radial positions.

Tab.1.2-6 The shrinkage and density of *E.cloeziane* from different radial positions

		Ta (%)	Ra (%)	Va (%)	To (%)	Ro (%)	Vo (%)	BD (g/cm^3)	AD (g/cm^3)	Co-t (%)	Co-r (%)
Near bark	Average	6.64	4.37	10.82	10.14	7.28	16.98	0.71	0.89	0.30	0.25
	Std. dev.	0.79	0.59	1.22	1.07	0.85	1.42	0.05	0.07	0.04	0.04
	CV(%)	0.12	0.14	0.11	0.11	0.12	0.08	0.07	0.08	0.13	0.15
	Number	40	40	40	40	40	40	40	40	40	40
Transition	Average	7.43	4.50	11.70	11.04	7.30	17.90	0.70	0.89	0.30	0.23
	Std. dev.	1.23	0.50	1.33	0.97	0.71	1.32	0.05	0.07	0.07	0.03
	CV(%)	0.17	0.11	0.11	0.09	0.10	0.07	0.08	0.08	0.24	0.12
	Number	40	40	40	40	40	40	40	40	40	40
Near pith	Average	8.27	4.36	12.34	11.72	6.72	17.91	0.62	0.79	0.28	0.19
	Std.	1.94	0.66	2.09	1.25	0.90	1.63	0.07	0.09	0.11	0.03
	CV(%)	0.23	0.15	0.17	0.11	0.13	0.09	0.11	0.12	0.38	0.13
	Number	33	33	33	33	33	33	33	33	33	33

Tab.1.2-7 ANOVA analysis on the shrinkage of *E.cloeziane* wood from different radial positions

	SS	df	MS	F	P-value	F crit
Ta	48.36851	2	24.18426	13.06547	8.11E-06	3.078824
Ra	0.434095	2	0.217048	0.634693	0.532028	3.078824

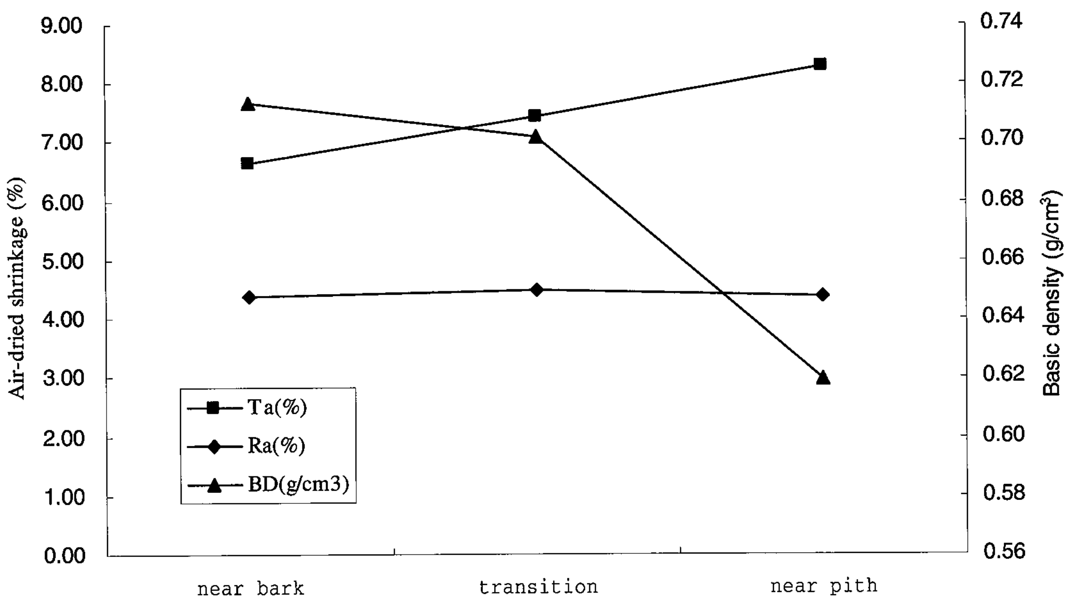

Fig.1.2-3 *E.cloeziane*: relationship between air-dried shrinkage (Ta&Ra), basic density (BD) and different radial positions

1.3 Mechanical properties

The small clear wood samples of moduli of elasticity (MOE), moduli of rupture (MOR) in static bending, compression strength parallel to grain and wood density were cut in accordance with Chinese National Standards (GB 1927~1943-91). The specimens were then stored in a conditioning chamber until it reached approximately 12% moisture content. Bending, compression and wood density test were carried out in accordance with Chinese National Standard. The air-dry density was calculated by air-dried weight and volume while oven-dry density was based on oven-dried weight and volume.

Generally *E. cloeziane* wood grain strait, texture fine to middle and even, weight middle to high, hard, shrinkage middle, strength highly. Nail holding power (N/mm): Radial: 41.7 Tangential: 38.8 Parallel to grain: 27.1. The mechanical properties are including tab.1.3-1.

Tab.1.3-1 Mechanical properties data of *E. Cloezian*

Locality	Density /g/cm^3		DS /%		CSPG /MPa	BS /MPa	MOE /GPa	Toughness /kJ/m^2	Hardness /N		
	BD	ADD	R	T	CSPG/MPa	BS/MPa	MOE/GPa	Toughness/kJ/m^2	E	R	T
Guangxi Dongmen		0.783			62	173	25.47	98.3			

BD = basic density, ADD = air-dry density, DS = dry shrinkage, CSPG = compressive strength parallel to grain, BS = bending strength, MOE = modulus of elasticity, SSPG = shear strength parallel to grain(R), E = end, R = radial, T = tangential.

1.4 Chemical properties

The chemical composition was determined according to Chinese National Standards, the chemical composition results and pH values, acid and alkaline buffering capacities are listed in Tab. 1.4-1, and 1.4-2 respectively.

Tab.1.4-1 Chemical composition of *E. cloeziane* (%)

Lignin	Holocellulose	α-Cellulose	Hemicellulose	1%NaOH extractives	Benzene-alcohol extractives	Hot water extractives
28.11	75.20	48.56	26.65	10.89	0.80	3.61

Tab.1.4-2 Data of pH value, acid and alkaline buffering capacity of *E. cloeziane*

S	H	S	H	S	H
4.45	3.45	3.80	2.10	35.30	90.40

S- sapwood, H-heartwood

2 GROWTH STRESS

The research adopted CIRAD-Foret method to measure surface longitudinal growth strain (SLGS) of standing trees, the results at different orientations were listed in Tab.2-1.

Tab. 2-1 Growth strain data for standing trees of *E. cloeziane*

Basic density (g/cm^3)	E		W		S		N	
	$\bar{x}$	δ_n	$\bar{x}$	δ_n	$\bar{x}$	δ_n	$\bar{x}$	δ_n
0.590	1610	384.4	1512	490.4	1260	432.0	1795	949.6

E=east, W=west, S=south, N=north

VII *Eucalyptus pellita*

The information of testing materials is as Tab.1.

Tab.1 Testing materials

Tree species	Tree age (year)	Tree number	Tree height (m)		Under branch height (m)		DBH (cm)	
			Ave.	Std	Ave.	Std.	Ave.	Std
E. pellita	13	9	22.03	2.4090	9.27	1.9732	19.93	2.6949

1 WOOD PROPERTIES

1.1 Anatomical characteristics

Samples (2×2×1 cm) for wood anatomical section were stored in alcohol 95% : glycerine (1:1) until they sank. Transverse sections of 20μm were cut on sliding microtome, then bleached, stained with afranine, dehydrated and mounted on slides for measure anatomical properties on image analysis. Then the transverse, radial and tangential sections from each species of around 80μm were cut on the same microtome, make the samples for SEM observation and taking photos.

Prior to tracheid length measurement, the each selected growth rings were firstly separated with a chisel, then macerated in solution of acetic acid (1/3) and hydrogen peroxide 27% (2/3) for several days in 60° oven.

The measurement methods are as follows:

Measuring length and width of wood fiber and vessel element using macerated anatomical elements under fiber length measuring instrument; (2) Measuring wood fiber cell wall thickness, cell wall percentage, and tissue proportions by section method using image analysis system; (3) Measure of S_2 microfibril angle: using x-ray diffractometer.

The observation and description for macro- and micro-structure were made under the light microscope and scanning electronically microscope (SEM).

1.1.1 Tree and distribution

A tree up to 47 m, trunk straight generally in origin producing country, Australia. Bark coarse, fiber shorter. *Eucalyptus pellita* was introduced to Brazil in last years respectively, it is grows very well as important plantation species. Our country is introducing this species as solid wood products in Guangdong, Guangxi and Hainan.

1.1.2 General characteristics

Sapwood yellowish brown, differs from heartwood, width 2~3 cm. ***heartwood*** dark red to reddish brown; glossy, wood without characteristic taste & odor. ***Growth rings*** indistinct to little distinct. Wood diffuse-porous. Pores small to middle, visible to the naked eye, fairly uniformly distributed throughout the ring, radial, tyloses visible. ***Longitudinal parenchyma*** vasicentric. ***Rays*** very fine to fine, visible with a hand lens. ***Ripple mark***s and ***Resin canals*** absent.

1.1.3 *Minute anatomy* (Plane IV)

Vessels most solitary; in radial multiples of 2 few, radial or flexuous; cell wall thin to thick; tangential average diameter 124 μm, max 204 μm. 11 (8~15) /mm^2 . Vessel element length 336 (128~515) μm, tyloses visible and wall thicker or thick, helical thickness absent. Simple perforation, its plate oblique. Intervessel pits ventured, alternate, round & polygonal, ventures distributed pit aperture and & chamber, and full of the chamber. Vasicentrics common, located vessels intermixing parenchyma cells, with bordered pit round and ventured. Vessel- ray pits large round.

Longitudinal parenchyma vasicentric, diffuse or diffuse-aggregates. Nodular end wall of parenchyma cells inconspicuous, some cells contain round inclusion; crystals absent.

Fiber wall thicker to thick, 1272 (980~1380) μm in length, with plain simple pits.

Rays unstoried, rays 10~12/mm, mostly uniseriate rays 2~25 cells, multiseriate rays width 2 cells, height 2~18 cells seldom. Ray tissues homogeneous uniseriate and multiseriate; parenchyma cells round or oval, most with gum. Crystal and intercellular canals absent.

The data of anatomical parameter at different heights and vessel distribution frequencies and tangential diameters is including to the Tab. 1.1-1 and 1.1-2 respectively.

Tab.1.1-1 Anatomical parameter and basic density at different heights for *Eucalyptus pellita*

Item	1.3m		3.3m		5.3m		7.3m	
	$\bar{x}$	δ_n	$\bar{x}$	δ_n	$\bar{x}$	δ_n	$\bar{x}$	δ_n
Fiber length (μm)	1109	34	1116	62	1108	22	1126	41
Fiber width (μm)	15.2	0.1	15.5	1.3	14.7	1.5	14.7	0.5
Fiber wall thickness	7.49	0.879	7.81	0.336	7.34	1.155	7.50	0.094
Microfibril angle (°)	10.19	1.554	9.52	1.086	9.77	0.595	8.71	0.564
Basic density (g/cm^3)	0.630	0.041	0.630	0.030	0.651	0.025	0.665	0.040

Tab.1.1-2 Vessel distribution frequencies and tangential diameters

Vessel distribution frequency (Number/mm^2)				Vessel tangential diameter (μm)			
Ave.	Std.	Max.	Min.	Ave.	Std.	Max.	Min.
11.00	2.6363	14.73	7.64	123.51	36.1728	206.29	38.47

1.2 Physical properties

1.2.1 *Moisture content of the green wood*

The moisture content data of the green wood at different heights is including Tab.1.2-1 and Fig.1.2-1.

Tab.1.2-1 Moisture content of green wood in *E. pellita* (%)

Item	1.3m		3.3m		5.3m		7.3m	
	$\bar{x}$	δ_n	$\bar{x}$	δ_n	$\bar{x}$	δ_n	$\bar{x}$	δ_n
Fiber	90.8	35.16	89.4	18.98	92.9	17.99	87.6	21.66
Vessels	84.5	17.40	74.6	10.46	72.5	11.64	76.1	8.03
Rays	76.4	14.43	67.0	12.27	65.2	8.84	65.9	10.20
Longitudinal parenchyma	72.8	8.42	67.0	4.98	66.5	8.02	63.5	5.26
Cell wall	72.2	5.55	72.4	6.52	55.8	21.76	68.8	8.70

1=near pith, 2=site between 1 &3, 3=center from pith to bark, 4=site between 3 &5, 5= near bark

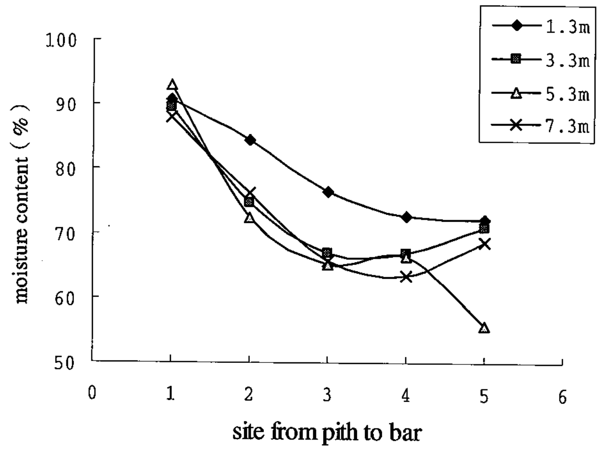

Fig.1.2-1 Moisture content of green wood for *E. pellita* at different heights and sites

1.2.2 Shrinkage and Density

Shrinkage is the contraction of wood caused by drying the material below the fiber saturation point (William T. Simpson, 1991). It can be divided into 3 types of shrinkage according to the direction of contraction: longitudinal, radial and tangential shrinkage. The longitudinal shrinkage is the shrinkage along the grain, the radial shrinkage and the tangential shrinkage is that across the grain in a radial or in a tangential direction. Wood density, the weight of wood per unit volume, is a very important index having a close relation with wood mechanical strength. In this study, wood air-dried density and basic density were used to describe the wood density.

The shrinkage is attributed to the dimension stability and checking problem, which causes a lot of problem for the wood utilization. In another word, it causes not only the contraction of wood in size, but also the checking and deformation resulted from the different contraction in tangential, radial and longitudinal direction. Understanding the characteristics of shrinkage has no doubt to be helpful for the wood utilization for the wood industry practice. Nowadays, studying on the characteristics of shrinkage during the losing of water is becoming one of the wood science discipline[Barber NF etc.1964; Barber, 1968; Chafe, 1986; 1987; Gu H et al., 2001]。 This study is intended to explore the shrinkage variation of acacia in different direction (North and south), different radial position and different tree height.

The trees studied were cut from Guangxi Zhuang Autonomous Region in the South China. Each trunk has been collected above the breast height and was cut every 2 meters. Then, four discs of each tree at different heights (about 1.3m, 3.3m, 5.3m and 7.3m respectively) were taken from the logs. All the discs were marked the south-north direction. For each disc, one specimen from the sapwood near the bark, one from the heartwood near pith and one from transition zone was made at the size of 2X2X2cm (Tangential X radial X longitudinal direction) for both north side and south side.

Two diagonal lines were drawn in three sections (i.e., T×R, T×L, R×L) of each specimen to locate the central point where the size was measured. The specimens were put into water until they were totally saturated and sunk in the water. The surface water was wiped off and the sizes in three directions (L, R, T) were measured. Specimens were set in the room for air-drying. After measuring the size and weight at the air-dried stage, the specimens were oven-dried and the same measurement was carried out. The shrinkage was determined according to Chinese National Standard. The air-dried density and was also calculated of both air-dried

The shrinkage coefficient was determined by the difference between shrinkage at air-dried and at oven-dried and divided by the MC at air-dried.

1.2.2.1 Shrinkage and density, and that of wood from south and north directions

The air-dried shrinkage in tangential direction (Ta), Radial direction (Ra) and volumetric shrinkage (Va), as well as the oven-dried shrinkage in tangential direction (To), Radial direction (Ro) and volumetric shrinkage (Vo) are listed in Tab.1.2-2 according to the categories of south direction, north direction and the overall. The basic density (B D) and air-dried density (A D), together with tangential shrinkage coefficient and radial shrinkage coefficient were also calculated and listed.

According to the IAWA (1989) method (the wood with an air-dried density smaller than 0.56 g/cm^3 is considered to be a small-density species, between 0.56 g/cm^3 and 0.75 g/cm^3 is considered to be a medium-density, between 0.75 g/cm^3 and 0.95 g/cm^3 is considered to be a large-density species, and bigger than 0.95 g/cm^3 is considered to be a extra-large-density species), *E.pellita* wood has a large density.

According to the *CHINA WOOD* method (the wood with an air-dried tangential shrinkage smaller than 5.60% is considered to be a small-shrinkage species, between 5.60% and 7.00% is considered with a medium-shrinkage species, and bigger than 7% is considered to be a big-shrinkage species), *E.pellita* is a medium-shrinkage species, suggesting that it has the potential for solid wood utilization comparing with some other eucalyptus species.

ANOVA analysis (Tab.1.2-3) showed there was no significant difference between air-dried tangential shrinkage and air-dried radial shrinkage, suggesting that the wood from north and south could be thought has the same level in shrinkage.

Tab. 1.2-2 The shrinkage and density of *E.pellita* wood from south and north side

		Ta (%)	Ra (%)	Va (%)	To (%)	Ro (%)	Vo (%)	B D (g/cm^3)	A D (g/cm^3)	Co-t (%)	Co-r (%)
South	Average	6.80	3.75	10.41	10.44	6.78	16.80	0.60	0.77	0.27	0.22
	Std.dev.	1.78	0.72	2.17	1.85	0.93	2.25	0.08	0.10	0.06	0.04
	CV(%)	0.26	0.19	0.21	0.18	0.14	0.13	0.13	0.13	0.23	0.18
	Number	32	32	32	32	32	32	32	32	32	32
North	Average	7.07	3.84	10.76	10.96	7.07	17.58	0.62	0.79	0.28	0.23
	Std. dev.	1.89	0.84	2.47	1.72	0.99	2.30	0.08	0.10	0.04	0.04
	CV(%)	0.27	0.22	0.23	0.16	0.14	0.13	0.12	0.13	0.16	0.19
	Number	31	31	31	31	31	31	31	31	31	31
Total	Average	6.93	3.80	10.58	10.69	6.92	17.19	0.61	0.78	0.27	0.23
	Std. dev.	1.82	0.77	2.31	1.79	0.97	2.29	0.08	0.10	0.05	0.04
	CV(%)	0.26	0.20	0.22	0.17	0.14	0.13	0.13	0.13	0.19	0.18
	Number	63	63	63	63	63	63	63	63	63	63

Tab.1.2-3 ANOVA analysis on the shrinkage of *E. pellita* wood from north and south

	SS	df	MS	F	P-value	F crit
Ta	1.1524	1	1.1524	0.3433	0.5601	3.9985
Ra	0.1238	1	0.1238	0.2035	0.6535	3.9985

1.2.2.2 Shrinkage and density of wood from 4 different tree heights

The shrinkage, shrinkage coefficient and density from 4 different tree heights were listed in Tab.1.2-4. The relationship between air-dried shrinkage, basic density and tree heights were showed in Fig. 1.2-2.

ANOVA analysis (Tab.1.2-5) showed there did not exist significant air-dried shrinkage difference both in tangential and radial directions among 4 different tree heights.

Tangential shrinkage showed a tendency that it decreased with the incease of tree height, while that in 7.3 m was an exception. The radial shrinkage showed a tendency that it increased with the increase of tree height, and the basic density showed no regular pattern.

Tab. 1.2-4 The shrinkage and density of *E.pellita* wood from different heights

		Ta (%)	Ra (%)	Va (%)	To (%)	Ro (%)	Vo (%)	B D (g/cm^3)	A D (g/cm^3)	Co-t (%)	Co-r (%)
1.3m	Average	7.10	3.55	10.51	10.85	6.57	17.04	0.59	0.77	0.25	0.20
	Std. dev.	2.22	0.47	2.43	2.13	0.60	2.24	0.08	0.11	0.06	0.05
	CV(%)	0.31	0.13	0.23	0.20	0.09	0.13	0.14	0.15	0.23	0.23
	Number	17	17	17	17	17	17	17	17	17	17
3.3m	Average	6.67	3.84	10.40	10.35	6.98	16.96	0.62	0.79	0.27	0.23
	Std. dev.	1.42	0.80	2.04	1.77	0.95	2.34	0.08	0.10	0.06	0.03
	CV(%)	0.21	0.21	0.20	0.17	0.14	0.14	0.13	0.13	0.24	0.14
	Number	18	18	18	18	18	18	18	18	18	18
5.3m	Average	6.62	3.78	10.25	10.57	7.04	17.10	0.64	0.80	0.29	0.24
	Std. dev.	1.42	0.82	2.05	1.23	0.97	1.93	0.07	0.08	0.04	0.04
	CV(%)	0.21	0.22	0.20	0.12	0.14	0.11	0.11	0.10	0.13	0.15
	Number	17	17	17	17	17	17	17	17	17	17
7.3m	Average	7.59	4.14	11.52	11.21	7.17	17.90	0.59	0.75	0.28	0.23
	Std. dev.	2.29	0.98	2.96	2.07	1.37	2.90	0.07	0.11	0.04	0.05
	CV(%)	0.30	0.24	0.26	0.18	0.19	0.16	0.12	0.14	0.13	0.19
	Number	11	11	11	11	11	11	11	11	11	11

Tab.1.2-5ANOVA analysis on the shrinkage of *E.pellita* wood from different heights

	SS	df	MS	F	P-value	F crit
Ta	8.1948	3	2.7316	0.8151	0.4906	2.7608
Ra	2.3523	3	0.7841	1.3269	0.2742	2.7608

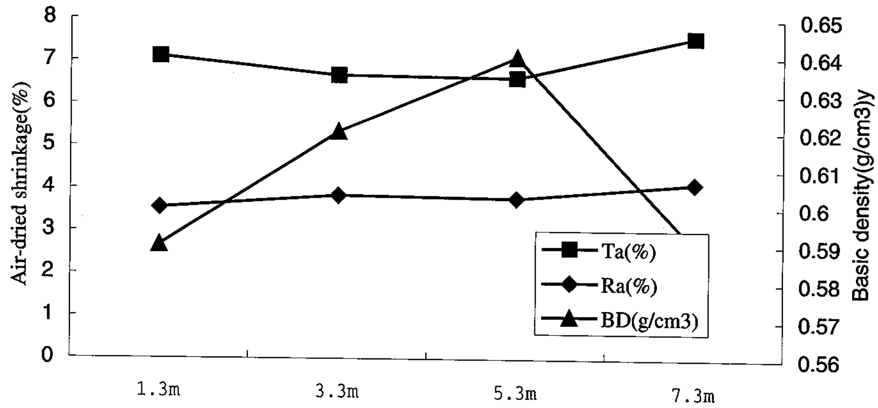

Fig.1.2-2 *E.pellita*: relationship between air-dried shrinkage (Ta&Ra), basic density (BD) and tree heights

1.2.2.3 Shrinkage and density of wood at different radial positions

The shrinkage, shrinkage coefficient and density from 4 different tree radial positions were listed in Tab.1.2-6. The relationship between air-dried shrinkage, basic density and tree heights were showed in Fig.

1.2-3.

ANOVA analysis (Tab. 1.2-7) showed there did not exist significant air-dried shrinkage difference both in tangential and radial directions among different radial position.

Fig.1.2-3 showed the tangential shrinkage decreased gradually from juvenile wood (near pith) to mature wood (near bark), suggesting that the mature wood has a better dimension stability than the juvenile wood. No obvious change was found in radial shrinkage among different radial positions, agreeing with the ANOVA test result that there did not exist significant radial shrinkage difference among different radial positions. The basis density presented a maximum value in transition zone.

Tab. 1.2-6 The shrinkage and density of *E.pellita* from different radial positions

		Ta (%)	Ra (%)	Va (%)	To (%)	Ro (%)	Vo (%)	B D (g/cm^3)	A D (g/cm^3)	Co-t (%)	Co-r (%)
Near bark	Average	6.40	3.88	10.14	10.20	7.21	17.01	0.62	0.79	0.27	0.24
	Std. dev.	1.21	0.51	1.56	1.49	0.74	1.93	0.05	0.07	0.08	0.05
	CV(%)	0.19	0.13	0.15	0.15	0.10	0.11	0.09	0.09	0.29	0.22
	Number	22	22	22	22	22	22	22	22	22	22
Transition	Average	7.13	3.88	10.86	11.04	7.17	17.69	0.65	0.82	0.29	0.24
	Std. dev.	1.82	0.73	2.33	1.67	0.77	2.14	0.08	0.10	0.03	0.02
	CV(%)	0.25	0.19	0.21	0.15	0.11	0.12	0.12	0.13	0.09	0.08
	Number	21	21	21	21	21	21	21	21	21	21
Near pith	Average	7.32	3.62	10.79	10.87	6.34	16.85	0.57	0.73	0.26	0.20
	Std. dev,	2.28	1.03	2.95	2.15	1.14	2.77	0.08	0.10	0.03	0.03
	CV(%)	0.31	0.28	0.27	0.20	0.18	0.16	0.14	0.14	0.11	0.13
	Number	20	20	20	20	20	20	20	20	20	20

Tab1.2-7ANOVA analysis on the shrinkage of *E.pellita* wood from different radial positions

	SS	df	MS	F	P-value	F crit
Ta	10.09433	2	5.047163	1.546507	0.22136	3.150411
Ra	0.933393	2	0.466697	0.771757	0.466733	3.150411

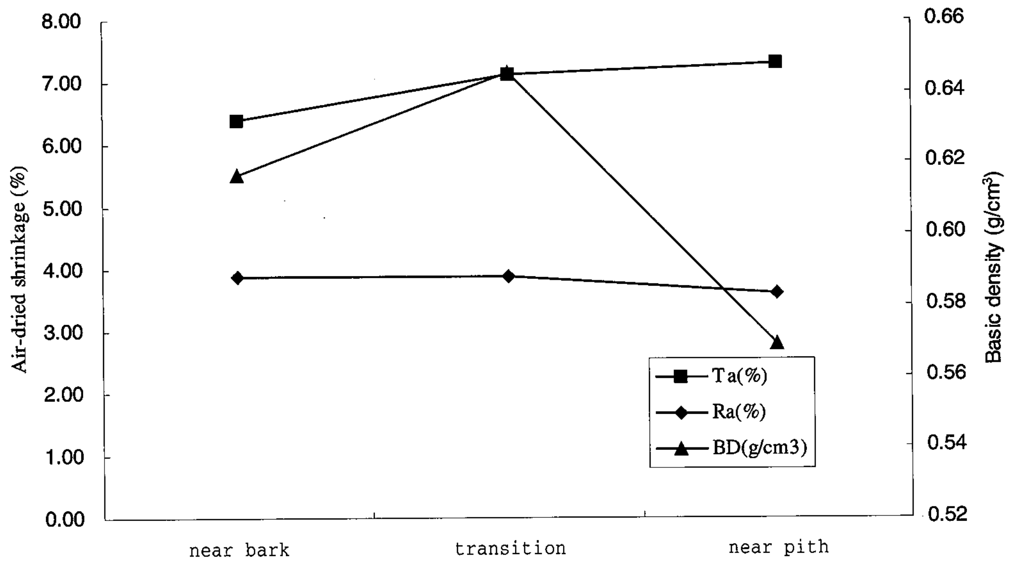

Fig.3-2-16 *E.pellita*: relationship between air-dried shrinkage (Ta&Ra), basic density (BD) and different radial positions

1.3 Mechanical properties

The small clear wood samples of moduli of elasticity (MOE), moduli of rupture (MOR) in static bending, compression strength parallel to grain and wood density were cut in accordance with Chinese National Standards (GB 1927~1943-91). The specimens were then stored in a conditioning chamber until it reached approximately 12% moisture content. Bending, compression and wood density test were carried out in accordance with Chinese National Standard. The air-dry density was calculated by air-dried weight and volume while oven-dry density was based on oven-dried weight and volume.

Generally *E. pellitta* wood. grain strait, texture fine to middle and even, weight middle to high, hard, shrinkage middle, strength highly. Nail holding power (N/mm): Radial: 58.6 Tangential: 64.4 Parallel to grain: 42.3. The mechanical properties are including tab.1.3-1.

Tab.1.3-1 Mechanical properties data of *E. pellitta*

Locality	Density $/g/cm^3$		DS /%		CSPG /MPa	BS /MPa	MOE /GPa	Toughness $/kJ/m^2$	Hardness /N		
	BD	ADD	R	T	CSPG/MPa	BS/MPa	MOE/GPa	Toughness/kJ/m^2	E	R	T
Guangxi Dongmen		0.872			77	146	17.39	84.8			

BD = basic density, ADD = air-dry density, DS = dry shrinkage, CSPG = compressive strength parallel to grain, BS = bending strength, MOE = modulus of elasticity, SSPG = shear strength parallel to grain(R), E = end, R = radial, T = tangential.

1.4 Chemical properties

The chemical composition was determined according to Chinese National Standards, pH values, acid and alkaline buffering capacities are listed in Tab. 1.4-1.

Tab.1.4-1 Data of pH value, acid and alkaline buffering capacity of *E. pellita*

S	H	S	H	S	H
4.76	3.57	5.20	1.90	35.40	111.20

S- sapwood, H-heartwood

2 GROWTH STRESS

The research adopted CIRAD-Foret method to measure surface longitudinal growth strain (SLGS) of standing trees, the results at different orientations were listed in Tab.2-1.

Tab.2-1 Growth strain data for standing trees of *E. pellita*

Basic density (g/cm^3)	E		W		S		N	
	$\bar{x}$	δ_n	$\bar{x}$	δ_n	$\bar{x}$	δ_n	$\bar{x}$	δ_n
0.665	1512	129.8	1232	69.3	900	391.1	1116	292.4

E=east, W=west, S=south, N=north

VIII *Eucalyptus tereticornis*

The information of testing materials is as Tab.1.

Tab.1 Testing materials

Tree species	Tree age (year)	Tree number	Tree height (m)		Under branch height (m)		DBH (cm)	
			Ave.	Std	Ave.	Std.	Ave.	Std
Eucalyptus tereticornis	15	9	26.53	0.2887	11.77	0.2887	21.34	4.8583

1 WOOD PROPERTIES

1.1 Anatomical characteristics

Samples (2x2x1 cm) for wood anatomical section were stored in alcohol 95% : glycerine (1:1) until they sank. Transverse sections of 20μm were cut on sliding microtome, then bleached, stained with safranin, dehydrated and mounted on slides for measure anatomical properties on image analysis. Then the transverse, radial and tangential sections from each species of around 80μm were cut on the same microtome, make the samples for SEM observation and taking photos.

Prior to tracheid length measurement, the each selected growth rings were firstly separated with a chisel, then macerated in solution of acetic acid (1/3) and hydrogen peroxide 27% (2/3) for several days in 60° oven.

The measurement methods are as follows:

Measuring length and width of wood fiber and vessel element using macerated anatomical elements under fiber length measuring instrument; (2) Measuring wood fiber cell wall thickness, cell wall percentage, and tissue proportions by section method using image analysis system; (3) Measure of S_2 microfibril angle: using x-ray diffractometer.

The observation and description for macro- and micro-structure were made under the light microscope and scanning electronically microscope (SEM).

1.1.1 Tree and distribution

A tree up to 25~50 m, 2 m in d.b.h trunk straight generally in origin producing country, Australia. Bark smooth, reddish brown, the old bark on the basic trunk. *Eucalyptus tereticornis* was introduced to tropical and sub-tropical countries, such as India, Congou, Argentina, Columbia, Ghana and Uruguay in last years respectively. It is grows very well as important plantation species. Our country is introducing this species as solid wood products in Guangxi, Hainan, Fujian, and Guangdong.

1.1.2 General characteristics

Sapwood yellowish brown, comparatively differs from heartwood, width 2~3 cm. ***heartwood*** dark yellowish brown; glossy, wood without characteristic taste & odor. ***Growth rings*** indistinct. Wood diffuse-porous. Pores small to middle, visible to the naked eye, fairly uniformly distributed throughout the ring, radial, tyloses visible. ***Longitudinal parenchyma*** vasicentric. ***Rays*** very fine to fine, visible with a hand lens.

Ripple marks and ***Resin canals*** absent.

1.1.3 Minute anatomy (Plane IV)

Vessels most solitary; in radial multiples of 2 few, radial or flexuous; cell wall thin to thick; tangential average diameter 127 μm, max 205 μm. 10 (6~15) /mm^2 . Vessel element length 379 (166~572) μm, tyloses visible and wall thicker or thick, helical thickness absent. Simple perforation, its plate oblique. Intervessel pits ventured, alternate, round & polygonal, ventures distributed pit aperture and & chamber, and full of the chamber. Vasicentrics common, located vessels intermixing parenchyma cells, with bordered pit round and ventured. Vessel- ray pits large round.

Longitudinal parenchyma vasicentric, diffuse or diffuse-aggregates. Nodular end wall of parenchyma cells inconspicuous; prismatic crystals commonly in parenchyma cells.

Fiber wall thicker to thick, 1272 (980~1380) μm in length, with plain simple pits.

Rays unstoried, rays 10~14/mm, mostly uniseriate rays 2~18 cells, multiseriate rays width 2 cells, height 7~18 cells seldom. Ray tissues homogeneous uniseriate and multiseriate; parenchyma cells round or oval, most with gum. Crystal and intercellular canals absent. Nodular end wall of parenchyma cells inconspicuous to conspicuous.

The data of anatomical parameter at different heights and vessel distribution frequencies and tangential diameters is including to the Tab. 1.1-1 and 1.1-2 respectively.

Tab.1.1-1 Anatomical parameter and basic density at different heights for *E. tereticornis*

Item	1.3m		3.3m		5.3m		7.3m	
	$\bar{x}$	δ_n	$\bar{x}$	δ_n	$\bar{x}$	δ_n	$\bar{x}$	δ_n
Fiber length (μm)	1084	13	1129	42	1148	69	1133	18
Fiber width (μm)	14.1	0.3	14.3	0.3	13.8	0.5	14.2	1.4
Fiber wall thickness	7.42	0.859	6.63	0.445	6.49	0.392	6.67	0.221
Microfibril angle (°)	13.57	3.864	9.45	1.054	9.55	0.621	9.38	0.266
Basic density (g/cm^3)	0.618	0.008	0.661	0.026	0.662	0.030	0.651	0.043

Tab.1.1-2 Vessel distribution frequencies and tangential diameters

Vessel distribution frequency (Number/mm^2)				Vessel tangential diameter (μm)			
Ave.	Std.	Max.	Min.	Ave.	Std.	Max.	Min.
10.20	3.0025	14.50	6.08	127.09	37.0855	205.43	37.63

1.2 Physical properties

1.2.1 Moisture content of the green wood

The moisture content data of the green wood at different heights is including Tab.1.2-1 and Fig.1.2-1.

Tab.1.2-1 Moisture content of green wood in *E. tereticornis* (%)

Item	1.3m		3.3m		5.3m		7.3m	
	$\bar{x}$	δ_n	$\bar{x}$	δ_n	$\bar{x}$	δ_n	$\bar{x}$	δ_n
Fiber	79.82	4.60	84.24	20.42	68.85	7.81	65.50	0.82
Vessels	66.94	2.50	65.98	4.00	56.69	9.26	56.26	2.92
Rays	62.66	2.11	61.44	3.68	55.20	5.53	55.66	1.67
Longitudinal parenchyma	73.60	6.31	72.49	6.56	67.96	13.13	72.30	2.56
Cell wall	68.19	2.03	69.33	3.31	68.80	0.55	73.73	4.69

1=near pith, 2=site between 1 &3, 3=center from pith to bark, 4=site between 3 &5, 5= near bark

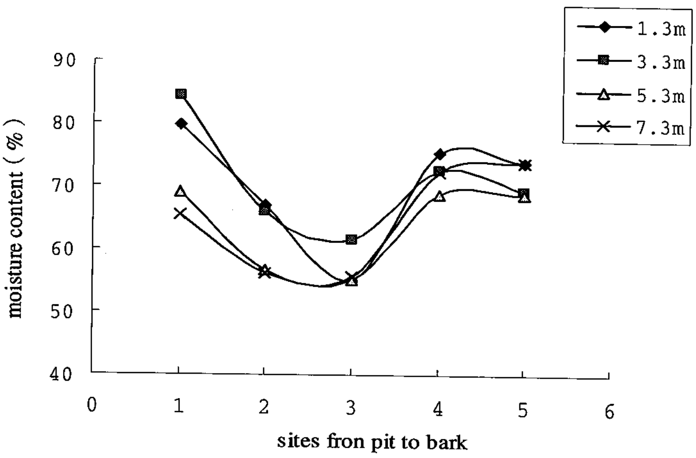

Fig.1.2-1 Moisture content of green wood for *E. tereticornis* at different heights and sites

1.2.2 Shrinkage and Density

Shrinkage is the contraction of wood caused by drying the material below the fiber saturation point (William T. Simpson, 1991). It can be divided into 3 types of shrinkage according to the direction of contraction: longitudinal, radial and tangential shrinkage. The longitudinal shrinkage is the shrinkage along the grain, the radial shrinkage and the tangential shrinkage is that across the grain in a radial or in a tangential direction. Wood density, the weight of wood per unit volume, is a very important index having a close relation with wood mechanical strength. In this study, wood air-dried density and basic density were used to describe the wood density.

The shrinkage is attributed to the dimension stability and checking problem, which causes a lot of problem for the wood utilization. In another word, it causes not only the contraction of wood in size, but also the checking and deformation resulted from the different contraction in tangential, radial and longitudinal direction. Understanding the characteristics of shrinkage has no doubt to be helpful for the wood utilization for the wood industry practice. Nowadays, studying on the characteristics of shrinkage during the losing of water is becoming one of the wood science discipline[Barber NF etc.1964; Barber, 1968; Chafe, 1986; 1987; Gu H et al., 2001]。 This study is intended to explore the shrinkage variation of acacia in different direction (North and south), different radial position and different tree height.

The trees studied were cut from Guangxi Zhuang Autonomous Region in the South China. Each trunk has been collected above the breast height and was cut every 2 meters. Then, four discs of each tree at different heights (about 1.3m, 3.3m, 5.3m and 7.3m respectively) were taken from the logs. All the discs were marked the south-north direction. For each disc, one specimen from the sapwood near the bark, one from the heartwood near pith and one from transition zone was made at the size of 2X2X2cm (Tangential X radial X longitudinal direction) for both north side and south side.

Two diagonal lines were drawn in three sections (i.e., T×R, T×L, R×L) of each specimen to locate the central point where the size was measured. The specimens were put into water until they were totally saturated and sunk in the water. The surface water was wiped off and the sizes in three directions (L, R, T) were measured. Specimens were set in the room for air-drying. After measuring the size and weight at the air-dried stage, the specimens were oven-dried and the same measurement was carried out. The shrinkage was determined according to Chinese National Standard. The air-dried density and was also calculated of both air-dried

The shrinkage coefficient was determined by the difference between shrinkage at air-dried and at oven-dried and divided by the MC at air-dried.

1.2.2.1 Shrinkage and density, and that of wood from south and north directions

The air-dried shrinkage in tangential direction (Ta), Radial direction (Ra) and volumetric shrinkage (Va), as well as the oven-dried shrinkage in tangential direction (To), Radial direction (Ro) and volumetric shrinkage (Vo) are listed in Tab.1.2-2 according to the categories of south direction, north direction and the overall. The basic density (B D) and air-dried density (A D), together with tangential shrinkage coefficient and radial shrinkage coefficient were also calculated and listed.

According to the IAWA (1989) method (the wood with an air-dried density smaller than 0.56 g/cm^3 is considered to be a small-density species, between 0.56 g/cm^3 and 0.75 g/cm^3 is considered to be a medium-density, between 0.75 g/cm^3 and 0.95 g/cm^3 is considered to be a large-density species, and bigger than 0.95 g/cm^3 is considered to be a extra-large-density species), *E. tereticornis* wood has a large density.

According to the *CHINA WOOD* method (the wood with an air-dried tangential shrinkage smaller than 5.60% is considered to be a small-shrinkage species, between 5.60% and 7.00% is considered with a medium-shrinkage species, and bigger than 7% is considered to be a big-shrinkage species), *E. tereticornis* is a medium-shrinkage species.

ANOVA analysis (Tab.1.2-3) showed there was no significant difference between air-dried tangential shrinkage and air-dried radial shrinkage, suggesting that the wood from north and south could be thought has the same level in shrinkage.

Tab. 1.2-2 The shrinkage and density of *E.tereticornis* wood from south and north side

		Ta (%)	Ra (%)	Va (%)	To (%)	Ro (%)	Vo (%)	B D (g/cm^3)	A D (g/cm^3)	Co-t (%)	Co-r (%)
South	Average	6.40	4.40	10.64	10.23	7.56	17.35	0.66	0.84	0.30	0.24
	Std.dev.	1.94	1.26	2.72	1.61	1.42	2.34	0.04	0.06	0.07	0.06
	CV(%)	0.30	0.29	0.26	0.16	0.19	0.13	0.06	0.08	0.25	0.25
	Number	30	30	30	30	30	30	30	30	30	30
North	Average	6.85	4.39	11.08	10.61	7.46	17.61	0.66	0.84	0.28	0.23
	Std. dev.	2.36	1.74	3.30	2.23	1.73	2.96	0.04	0.06	0.06	0.04
	CV(%)	0.34	0.40	0.30	0.21	0.23	0.17	0.06	0.07	0.20	0.18
	Number	33	33	33	33	33	33	33	33	33	33
Total	Average	6.64	4.40	10.87	10.43	7.51	17.49	0.66	0.84	0.29	0.24
	Std. dev.	2.16	1.52	3.02	1.96	1.58	2.66	0.04	0.06	0.07	0.05
	CV(%)	0.33	0.35	0.28	0.19	0.21	0.15	0.06	0.07	0.23	0.22
	Number	63	63	63	63	63	63	63	63	63	63

Tab.1.2-3 ANOVA analysis on the shrinkage of *E. tereticornis* wood from north and south

	SS	df	MS	F	P-value	F crit
Ta	3.1570	1	3.1570	0.6708	0.4160	3.9985
Ra	0.0001	1	0.0001	0.0000	0.9953	3.9985

1.2.2.2 Shrinkage and density of wood from 4 different tree heights

The shrinkage, shrinkage coefficient and density from 4 different tree heights were listed in Tab.1.2-4. The relationship between air-dried shrinkage, basic density and tree heights were showed in Fig. 1.2-2.

ANOVA analysis (Tab.1.2-4) showed there did not exist significant air-dried shrinkage difference both in tangential and radial directions among 4 different tree heights.

Tab.1.2-4 The shrinkage and density of *Etereticornis s* wood from different heights

		Ta (%)	Ra (%)	Va (%)	To (%)	Ro (%)	Vo (%)	B D (g/cm³)	A D (g/cm³)	Co-t (%)	Co-r (%)
1.3m	Average	7.42	4.25	11.47	11.33	6.98	17.87	0.66	0.84	0.30	0.21
	Std. dev.	2.98	1.26	3.79	2.60	1.26	3.35	0.05	0.07	0.10	0.03
	CV(%)	0.40	0.30	0.33	0.23	0.18	0.19	0.07	0.09	0.33	0.14
	Number	17	17	17	17	17	17	17	17	17	17
3.3m	Average	7.06	4.62	11.46	10.69	7.65	17.84	0.66	0.85	0.28	0.24
	Std. dev.	1.85	1.37	2.87	1.82	1.24	2.59	0.04	0.06	0.03	0.02
	CV(%)	0.26	0.30	0.25	0.17	0.16	0.15	0.06	0.07	0.09	0.10
	Number	16	16	16	16	16	16	16	16	16	16
5.3m	Average	6.10	4.27	10.28	9.71	7.51	16.89	0.66	0.84	0.27	0.24
	Std. dev.	1.39	2.30	2.79	1.41	2.36	2.58	0.04	0.06	0.05	0.05
	CV(%)	0.23	0.54	0.27	0.15	0.31	0.15	0.06	0.07	0.19	0.21
	Number	14	14	14	14	14	14	14	14	14	14
7.3m	Average	5.84	4.44	10.16	9.84	7.92	17.26	0.66	0.84	0.31	0.27
	Std.	1.71	1.15	2.39	1.32	1.32	2.04	0.04	0.06	0.07	0.07
	CV(%)	0.29	0.26	0.24	0.13	0.17	0.12	0.06	0.07	0.21	0.27
	Number	16	16	16	16	16	16	16	16	16	16

Tab.1.2-5 ANOVA analysis on the shrinkage of *E. tereticornis* wood from different heights

	SS	df	MS	F	P-value	F crit
Ta	27.6145	3	9.2048	2.0678	0.1142	2.7608
Ra	1.4238	3	0.4746	0.1975	0.8977	2.7608

Tangential shrinkage showed a tendency that it decreased with the increase of tree height, this agreed with other eucalyptus. The radial shrinkage showed no regular pattern, and the basic density showed no change with the change of tree heights (Fig.1.2-2).

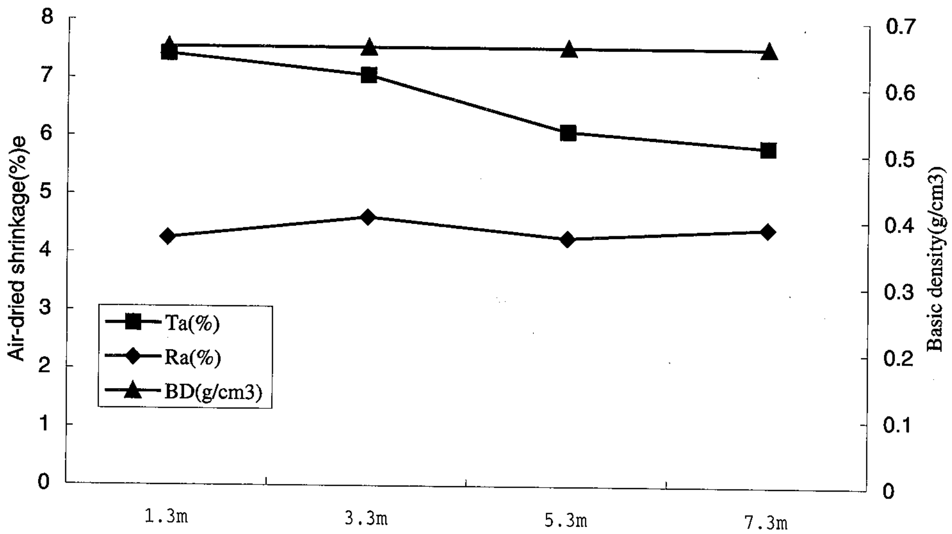

Fig.1.2-2*E.teretiocornis*: relationship between air-dried shrinkage (Ta&Ra), basic density (BD) and tree heights

1.2.2.3 Shrinkage and density of wood at different radial positions

The shrinkage, shrinkage coefficient and density from 4 different tree radial positions were listed in Tab.1.2-6. The relationship between air-dried shrinkage, basic density and tree heights were showed in Fig. 1.2- .

ANOVA analysis (Tab. 1.2-7) showed there existed significant air-dried shrinkage difference both in tangential and radial directions among different radial position.

Fig.1.2- showed that both the tangential and radial shrinkage decreased gradually from juvenile wood (near pith) to mature wood (near bark), suggesting that the mature wood has a better dimension stability than the juvenile wood. Like many other eucalyptus wood, the basis density of *E. tereticornis* presented a maximum value in transition zone.

Tab. 1.2-6 The shrinkage and density of *E.tereticornis* from different radial positions

		Ta (%)	Ra (%)	Va (%)	To (%)	Ro (%)	Vo (%)	BD (g/cm^3)	AD (g/cm^3)	Co-t (%)	Co-r (%)
近树皮 near bark	Average	5.07	3.88	8.95	9.03	6.95	15.76	0.64	0.80	0.31	0.24
	Std. dev.	1.07	0.82	1.46	0.84	1.06	1.30	0.03	0.05	0.09	0.05
	CV(%)	0.21	0.21	0.16	0.09	0.15	0.08	0.04	0.06	0.28	0.19
	Number	22	22	22	22	22	22	22	22	22	22
过渡区 transition	Average	6.68	4.23	10.73	10.58	7.56	17.65	0.70	0.89	0.29	0.25
	Std. dev.	1.71	1.52	2.42	1.42	1.74	2.23	0.02	0.04	0.05	0.06
	CV(%)	0.26	0.36	0.23	0.13	0.23	0.13	0.03	0.05	0.18	0.25
	Number	23	23	23	23	23	23	23	23	23	23
近髓心 near pith	Average	8.49	5.24	13.39	11.94	8.12	19.40	0.63	0.83	0.26	0.22
	Std.	2.26	1.86	3.40	2.34	1.73	3.10	0.04	0.06	0.04	0.04
	CV(%)	0.27	0.35	0.25	0.20	0.21	0.16	0.06	0.07	0.16	0.17
	Number	18	18	18	18	18	18	18	18	18	18

Tab.1.2-7 ANOVA analysis on the shrinkage of *E.tereticornis* wood from different radial positions

	SS	df	MS	F	P-value	F crit
Ta	115.6452	2	57.82258	19.86859	2.39E-07	3.150411
Ra	19.4184	2	9.7092	4.70528	0.012641	3.150411

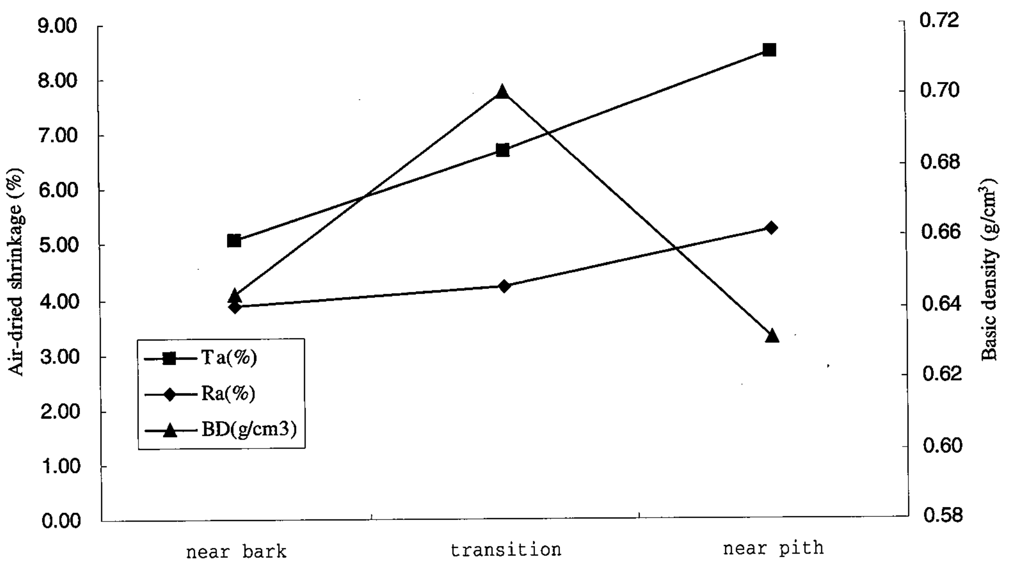

Fig.1.2-3 *E.tereticornis*: relationship between air-dried shrinkage (Ta&Ra), basic density (BD) and different radial positions

1.3 Mechanical properties

The small clear wood samples of moduli of elasticity (MOE), moduli of rupture (MOR) in static bending, compression strength parallel to grain and wood density were cut in accordance with Chinese National Standards (GB 1927~1943-91). The specimens were then stored in a conditioning chamber until it reached approximately 12% moisture content. Bending, compression and wood density test were carried out in accordance with Chinese National Standard. The air-dry density was calculated by air-dried weight and volume while oven-dry density was based on oven-dried weight and volume.

Generally *E. tereticornis* wood grain straight or oblique, texture fine to middle and even, weight middle to high, hard, shrinkage middle or large, strength highly. Nail holding power (N/mm): Radial: 70 Tangential: 78 Parallel to grain: 60.2. The mechanical properties are including tab.1.3-1.

Tab.1.3-1 Mechanical properties data of *E. Tereticornis*

Locality	Density $/g/cm^3$		DS /%		CSPG /MPa	BS /MPa	MOE /GPa	Toughness $/kJ/m^2$	Hardness /N		
	BD	ADD	R	T	CSPG/MPa	BS/MPa	MOE/GPa	Toughness/kJ/m^2	E	R	T
Guangxi Dongmen		0.872			77	146	17.39	84.8			

BD = basic density, ADD = air-dry density, DS = dry shrinkage, CSPG = compressive strength parallel to grain, BS = bending strength, MOE = modulus of elasticity, SSPG = shear strength parallel to grain(R), E = end, R = radial, T = tangential.

1.4 Chemical properties

The chemical composition was determined according to Chinese National Standards, the chemical composition results and pH values, acid and alkaline buffering capacities are listed in Tab. 1.1.4-1, and 1.1.4-2 respectively.

Tab.1.4-1 Chemical composition of *E. tereticorniss* (%)

α-Cellulose	lignin	Xylan	1% NaOH extractives	Benzene-alcohol extractives	Cold water extractives	Hot water extractives	Ash
45.04	25.54	18.49	12.50	1.69	2.79	4.01	0.33

Tab.1.4-2 Data of pH value, acid and alkaline buffering capacity of *E. tereticornis*

S	H	S	H	S	H
4.71	3.56	4.52	1.30	17.80	101.70

S- sapwood, H-heartwood

2 GROWTH STRESS

The research adopted CIRAD-Foret method to measure surface longitudinal growth strain (SLGS) of standing trees, the results at different orientations were listed in Tab.2-1.

Tab.2-1 Growth strain data for standing trees of *E. tereticornis*

Basic density (g/cm^3)	E		W		S		N	
	$\bar{x}$	δ_n	$\bar{x}$	δ_n	$\bar{x}$	δ_n	$\bar{x}$	δ_n
0.651	1572	890.6	1784	120.1	1376	525.9	1092	659.1

E=east, W=west, S=south, N=north

IX *Acacia magnium*

The information of testing materials is as Tab.1.

Tab.1 Testing materials

Tree species	Tree age (year)	Tree number	Tree height (m)		Under branch height (m)		DBH (cm)	
			Ave.	Std	Ave.	Std.	Ave.	Std
Acacia magnium	14	10	18.15	1.8981	8.55	1.8501	24.81	3.4639

1 WOOD PROPERTIES

1.1 Anatomical characteristics

Samples (2×2×1 cm) for wood anatomical section were stored in alcohol 95% : glycerine (1:1) until they sank. Transverse sections of 20μm were cut on sliding microtome, then bleached, stained with safranin, dehydrated and mounted on slides for measure anatomical properties on image analysis. Then the transverse, radial and tangential sections from each species of around 80μm were cut on the same microtome, make the samples for SEM observation and taking photos.

Prior to tracheid length measurement, the each selected growth rings were firstly separated with a chisel, then macerated in solution of acetic acid (1/3) and hydrogen peroxide 27% (2/3) for several days in 60° oven.

The measurement methods are as follows:

Measuring length and width of wood fiber and vessel element using macerated anatomical elements under fiber length measuring instrument; (2) Measuring wood fiber cell wall thickness, cell wall percentage, and tissue proportions by section method using image analysis system; (3) Measure of S_2 microfibril angle: using x-ray diffractometer.

The observation and description for macro- and micro-structure were made under the light microscope and scanning electronically microscope (SEM).

1.1.1 Tree and distribution

A tree up to 25~30 m, max 0.6 m in d.b.h trunk straight generally; but trees are small arbor or big shrub up to 7~10 m in poor site in origin producing country, Australia. Bark coarse, thicker, dark gay brown and Malaysia brown; peeling off in long strips, trunk basic with grooves. *Acacia magnium* was introduced to Malaysia, Thailand, Philippine, Bengal and India since 1966 respectively. Besides, America Hawaii, Costa Rica and Cameroon also were introducing *Acacia magnium.* It is grows very well as important plantation species. Our country is introducing this species as solid wood products in Guangdong, Guangxi and Hainan.

1.1.2 General characteristics

Sapwood light yellowish brown or yellowish brown, comparatively differs from heartwood, width 2~3 cm. ***heartwood*** blackish brown with black or dark brown stripes; glossy, wood without characteristic taste & odor. ***Growth rings*** little distinct. Wood diffuse-porous. Pores small to middle, visible to the naked eye as white dots, fairly uniformly distributed throughout the ring, radial, tyloses singularly. ***Longitudinal parenchyma*** vasicentric under a hand lens. ***Rays*** very fine to fine, clear with a hand lens. ***Ripple mark***s visible. ***Resin canals*** absent.

1.1.3 Minute anatomy (Plane V)

Vessels most solitary; in radial multiples of 2~3 few, oblique; cell wall thin; tangential average diameter 155 μm, max 269 μm. 7 (4~11) /mm^2. Helical thickness absent. Simple perforation, its plate oblique. Intervessel pits ventured, alternate, polygonal & round, pit aperture included, coalescent mostly, lenticular, linear and cranny. Ventures distributed pit aperture, canal & chamber, and full of them, most coralloid and lumpish. Vessel- ray pitting similar to intervessels pits.

Longitudinal parenchyma vasicentric, diffuse or diffuse-aggregates. Nodular end wall of parenchyma cells inconspicuous; prismatic crystals commonly in parenchyma cells.

Fiber wall thin, 1220 (886~1361) μm in length, 20μm in width with plain simple pits.

Rays part oblique, rays 8~12/mm, uniseriate rays 1~26 cells seldom, mostly multiseriate rays width 2 cells, 3 cells accidental, height 8~28 cells. Ray tissues homogeneous uniseriate and multiseriate; parenchyma cells round or oval, most with gum. Nodular end wall of parenchyma cells inconspicuous to conspicuous. Crystal and intercellular canals absent.

The data of anatomical parameter at different heights and vessel distribution frequencies and tangential diameters is including to the Tab. 1.1-1 and 1.1-2 respectively.

Tab.1.1-1 Anatomical parameter at 1.3 m for *Acacia magnium*

Fiber length (μm)		Fiber width (μm)		Fiber wall thickness (μm)		Microfibril angle (°)	
$\bar{x}$	δ_n	$\bar{x}$	δ_n	$\bar{x}$	δ_n	$\bar{x}$	δ_n
1220	13	20.1	2.4	12.83	0.902	13.62	3.579

Tab.1.1-2 Vessel distribution frequencies and tangential diameters

Vessel distribution frequency (Number/mm^2)				Vessel tangential diameter (μm)			
Ave.	Std.	Max.	Min.	Ave.	Std.	Max.	Min.
7.02	2.2505	10.60	4.20	155.16	51.3338	268.66	56.23

1.2 Physical properties

1.2.1 Moisture content of the green wood

The moisture content data of the green wood at different heights is including Tab.1.2-1 and Fig.1.2-1.

Tab.1.2-1 Moisture content of green wood for *A. magnium* at different radial sites (%)

Sites(from pit to bark)	1		2		3		4		5	
	$\bar{x}$	δ_n	$\bar{x}$	δ_n	$\bar{x}$	δ_n	$\bar{x}$	δ_n	$\bar{x}$	δ_n
	156.0	60.61	145.6	25.80	140.7	39.38	130.2	23.95	130.4	10.48

1=near pith, 2=site between 1 &3, 3=center from pith to bark, 4=site between 3 &5, 5= near bark

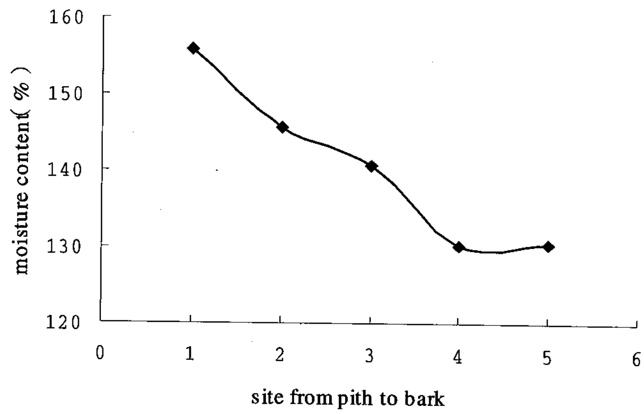

Fig.1.2-1 Moisture content of green wood for *A. magnium* at different sites

1.2.2 Shrinkage and Density

Shrinkage is the contraction of wood caused by drying the material below the fiber saturation point (William T. Simpson, 1991). It can be divided into 3 types of shrinkage according to the direction of contraction: longitudinal, radial and tangential shrinkage. The longitudinal shrinkage is the shrinkage along the grain, the radial shrinkage and the tangential shrinkage is that across the grain in a radial or in a tangential direction. Wood density, the weight of wood per unit volume, is a very important index having a close relation with wood mechanical strength. In this study, wood air-dried density and basic density were used to describe the wood density.

The shrinkage is attributed to the dimension stability and checking problem, which causes a lot of problem for the wood utilization. In another word, it causes not only the contraction of wood in size, but also the checking and deformation resulted from the different contraction in tangential, radial and longitudinal direction. Understanding the characteristics of shrinkage has no doubt to be helpful for the wood utilization for the wood industry practice. Nowadays, studying on the characteristics of shrinkage during the losing of water is becoming one of the wood science discipline[Barber NF etc.1964; Barber, 1968; Chafe, 1986; 1987; Gu H et al., 2001]。This study is intended to explore the shrinkage variation of acacia in different direction (North and south), different radial position and different tree height.

The trees studied were cut from Guangxi Zhuang Autonomous Region in the South China. Each trunk has been collected above the breast height and was cut every 2 meters. Then, four discs of each tree at different heights (about 1.3m, 3.3m, 5.3m and 7.3m respectively) were taken from the logs. All the discs were marked the south-north direction. For each disc, one specimen from the sapwood near the bark, one from the heartwood near pith and one from transition zone was made at the size of 2X2X2cm (Tangential X radial X longitudinal direction) for both north side and south side.

Two diagonal lines were drawn in three sections (i.e., T×R, T×L, R×L) of each specimen to locate the central point where the size was measured. The specimens were put into water until they were totally saturated and sunk in the water. The surface water was wiped off and the sizes in three directions (L, R, T) were measured. Specimens were set in the room for air-drying. After measuring the size and weight at the air-dried stage, the specimens were oven-dried and the same measurement was carried out. The shrinkage was determined according to Chinese National Standard. The air-dried density and was also calculated of both air-dried

The shrinkage coefficient was determined by the difference between shrinkage at air-dried and at oven-dried and divided by the MC at air-dried.

1.2.2.1 Shrinkage and density, and that of wood from south and north directions

The air-dried shrinkage in tangential direction (Ta), Radial direction (Ra) and volumetric shrinkage (Va), as well as the oven-dried shrinkage in tangential direction (To), Radial direction (Ro) and volumetric shrinkage (Vo) are listed in Tab.1.2-1 according to the categories of south direction, north direction and the overall. The basic density (B D) and air-dried density (A D), together with tangential shrinkage coefficient and radial shrinkage coefficient were also calculated and listed.

According to the IAWA (1989) method (the wood with an air-dried density smaller than 0.56 g/cm^3 is considered to be a small-density species, between 0.56 g/cm^3 and 0.75 g/cm^3 is considered to be a medium-density, between 0.75 g/cm^3 and 0.95 g/cm^3 is considered to be a large-density species, and bigger than 0.95 g/cm^3 is considered to be a extra-large-density species), *A.magnium* wood has a small density.

According to the *CHINA WOOD* method (the wood with an air-dried tangential shrinkage smaller than 5.60% is considered to be a small-shrinkage species, between 5.60% and 7.00% is considered with a medium-shrinkage species, and bigger than 7% is considered to be a big-shrinkage species), *A.magnium* is small in shrinkage, suggesting that it is good in dimension stability, which is good for solid wood utilization.

ANOVA analysis (Tab.1.2-2) showed there was no significant difference between air-dried tangential shrinkage and air-dried radial shrinkage, suggesting that the wood from north and south could be thought has the same level in shrinkage.

Tab. 1.2-2 The shrinkage and density of *A.magnium* wood from south and north side

		Ta (%)	Ra (%)	Va (%)	To (%)	Ro (%)	Vo (%)	B D (g/cm^3)	A D (g/cm^3)	Co-t (%)	Co-r (%)
South	Average	4.44	1.26	5.72	7.70	2.65	10.50	0.40	0.48	0.28	0.12
	Std.dev.	0.72	0.36	0.84	0.79	0.58	0.98	0.03	0.04	0.08	0.02
	CV(%)	0.16	0.28	0.15	0.10	0.22	0.09	0.08	0.08	0.28	0.20
	Number	15	15	15	15	15	15	15	15	15	15
North	Average	4.32	1.37	5.73	7.66	2.86	10.64	0.42	0.50	0.26	0.12
	Std. dev.	0.63	0.34	0.68	0.78	0.55	0.89	0.03	0.04	0.02	0.02
	CV(%)	0.15	0.25	0.12	0.10	0.19	0.08	0.08	0.08	0.08	0.16
	Number	15	15	15	15	15	15	15	15	15	15
Total	Average	4.38	1.32	5.72	7.68	2.75	10.57	0.41	0.49	0.27	0.12
	Std. dev.	0.67	0.35	0.75	0.77	0.57	0.92	0.03	0.04	0.06	0.02
	CV(%)	0.15	0.26	0.13	0.10	0.21	0.09	0.08	0.08	0.21	0.18
	Number	30	30	30	30	30	30	30	30	30	30

Tab.1.2-3 ANOVA analysis on the shrinkage of *A.magnium* wood from north and south

	SS	df	MS	F	P-value	F crit
Ta	0.1087	1	0.1087	0.2376	0.6298	4.1960
Ra	0.0828	1	0.0828	0.6837	0.4153	4.1960

1.2.2.2 Shrinkage and density of wood at different radial positions

The shrinkage, shrinkage coefficient and density from 4 different tree radial positions were listed in . The relationship between air-dried shrinkage, basic density and tree heights were showed in Fig. 1.2-4.

ANOVA analysis (Tab.1.2-5) showed there existed significant air-dried shrinkage difference both in tangential and radial directions among different radial position.

Fig.1.2- showed that both the tangential and radial shrinkage decreased gradually from juvenile wood (near

pith) to mature wood (near bark), suggesting that the mature wood has a better dimension stability than the juvenile wood. The basis density of *E. tereticornis* increased from pith to transition zone, then became steadily.

Tab. 1.2-4 The shrinkage and density of *A.magnium* from different radial positions

		Ta (%)	Ra (%)	Va (%)	To (%)	Ro (%)	Vo (%)	B D (g/cm³)	A D (g/cm³)	Co-t (%)	Co-r (%)
near bark	Average	3.99	1.55	5.56	7.37	3.20	10.67	0.42	0.50	0.27	0.13
	Std. dev.	0.66	0.43	0.99	0.84	0.60	1.25	0.03	0.03	0.02	0.02
	CV(%)	0.17	0.28	0.18	0.11	0.19	0.12	0.07	0.06	0.07	0.12
	Number	10	10	10	10	10	10	10	10	10	10
transition	Average	4.39	1.23	5.65	7.67	2.61	10.42	0.42	0.50	0.26	0.11
	Std. dev.	0.59	0.19	0.73	0.73	0.35	0.97	0.03	0.03	0.02	0.01
	CV(%)	0.13	0.15	0.13	0.10	0.13	0.09	0.07	0.07	0.07	0.13
	Number	10	10	10	10	10	10	10	10	10	10
near pith	Average	4.75	1.17	5.96	8.00	2.45	10.62	0.39	0.47	0.28	0.11
	Std. dev.	0.57	0.28	0.47	0.67	0.46	0.48	0.04	0.05	0.10	0.02
	CV(%)	0.12	0.24	0.08	0.08	0.19	0.04	0.10	0.10	0.34	0.21
	Number	10	10	10	10	10	10	10	10	10	10

Tab.1.2-5 ANOVA analysis on the shrinkage of *A.magnium* wood from different radial positions

	SS	df	MS	F	P-value	F crit
Ta	2.908711	2	1.454355	3.922417	0.031955	3.354131
Ra	0.812157	2	0.406078	4.117836	0.027488	3.354131

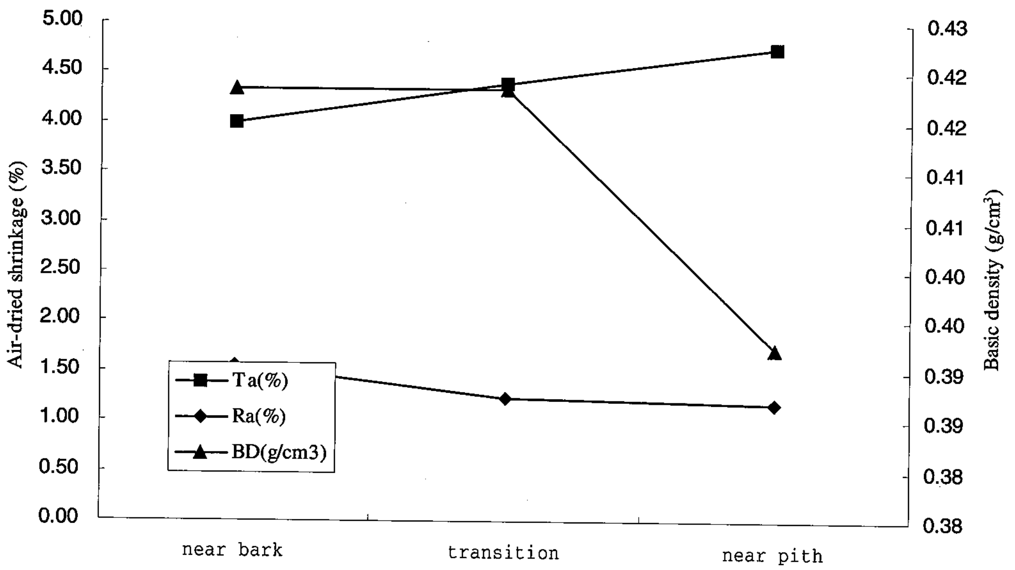

Fig.1.2-2 *A.magnium*: relationship between air-dried shrinkage (Ta&Ra), basic density (BD) and different radial positions

1.3 Mechanical properties

The small clear wood samples of moduli of elasticity (MOE), moduli of rupture (MOR) in static bending, compression strength parallel to grain and wood density were cut in accordance with Chinese National Standards (GB 1927~1943-91). The specimens were then stored in a conditioning chamber until it reached approximately 12% moisture content. Bending, compression and wood density test were carried out in accordance with Chinese National Standard. The air-dry density was calculated by air-dried weight and volume while oven-dry density was based on oven-dried weight and volume.

Generally *A. magnium* wood grain straight or oblique, texture middle and even, weight middle, hard, shrinkage middle, strength middle or highly. Nail holding power (N/mm): 15.1 Radial: 18.1 Tangential: Parallel to grain: 10.8. The mechanical properties are including tab.1.3-1.

Tab.1.3-1 Mechanical properties data of *A. magnium*

Locality	Density /g/cm^3		DS /%		CSPG /MPa	BS /MPa	MOE /GPa	Toughness /kJ/m^2	Hardness /N		
	BD	ADD	R	T	CSPG/MPa	BS/MPa	MOE/GPa	Toughness/kJ/m^2	E	R	T
Guangxi Dongmen		0.506			42	84	11.33	42.3			

BD = basic density, ADD = air-dry density, DS = dry shrinkage, CSPG = compressive strength parallel to grain, BS = bending strength, MOE = modulus of elasticity, SSPG = shear strength parallel to grain(R), E = end, R = radial, T = tangential.

1.4 Chemical properties

The chemical composition was determined according to Chinese National Standards, the chemical composition results and pH values, acid and alkaline buffering capacities are listed in Tab. 1.4-1 and 1.4-2 respectively.

Tab.1.4-1 Chemical composition of *A. magnium*

Holocellulose	α-Cellulose	Relative crystallinity	Lignin	1%NaOH extractives	Xylan	ɩenzene-alcoho extractives	Cold water extractives	Hot water extractives	Ash
72.38	46.48	39.74	21.98	22.00	23.20	6.20	4.83	7.04	0.06

Tab.1.4-2 Data of pH value, acid and alkaline buffering capacity of *A. magnium*

S	H	S	H	S	H
5.72	5.53	6.22	4.66	9.10	14.45

S- sapwood, H-heartwood

2 GROWTH STRESS

The research adopted CIRAD-Foret method to measure surface longitudinal growth strain (SLGS) of standing trees, the results at different orientations were listed in Tab.2-1.

Tab.2-1 Growth strain data for standing trees of *A. magnium*

Basic density (g/cm^3)	E		W		S		N	
	$\bar{x}$	δ_n	$\bar{x}$	δ_n	$\bar{x}$	δ_n	$\bar{x}$	δ_n
0.454	504	10.708	1346	67.609	792	31.584	649	26.352

E=east, W=west, S=south, N=north

3 DRYING TECHNIQUES

3.1 Air drying

Air drying is a traditional and economical drying method which mainly uses sun energy. To save kiln drying time and cost, and to improve kiln drying quality at the mean time, it is suggested to use Air drying as a pre-drying method, and then conventional kiln drying to target final MC (moisture content). Because of the uncontrolled drying conditions, the drying time, final MC and drying quality may be quite difference with the changes of season and drying arrangements. Air drying test focus on analysing wood Air drying properties and try to find its optimum Air drying technique and parameters.

3.1.1 Material and method

The size of sample for air drying is 700 mm (length) x 120-150 mm (width) x 25 mm (thickness). Two MC slices were cut in the two ends of each sample to calculate its initial MC (Fig.3.1-1).

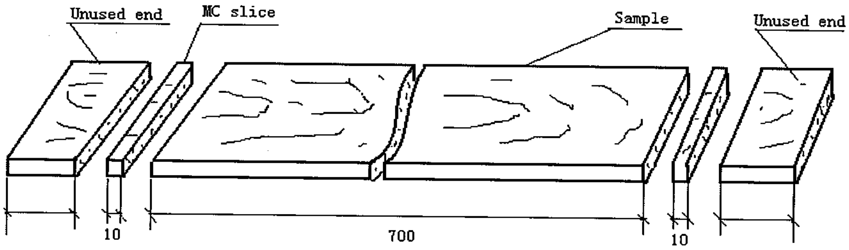

Fig.3.1-1 Drying sample making of *Acacia magium*

The samples were end-sealed with silicon, and then stacked in air-drying shed to start drying. The dry-bulb and wet-bulb temperatures in shed were recorded every day, and the weights and all visible drying defects of samples were recorded once a week at the first month, then once every two weeks till the air drying ended. When the test finished, three final MC slices and one layer MC slice for each sample were cut (Fig.3.1-2). After oven drying these slices, the final MC for each sample were be gained, and then the oven-dry weight (written as G_0) for each sample could be calculated with the equation listed below. And so, corresponding to the recorded weights of each sample in different drying times, the air-drying MC curve could be drawn.

$$G_0 = 100G_w/(100+ MC_0)$$

G_0 - oven-dry weight

G_w - initial weight

MC_0 - oven-dry MC (%)

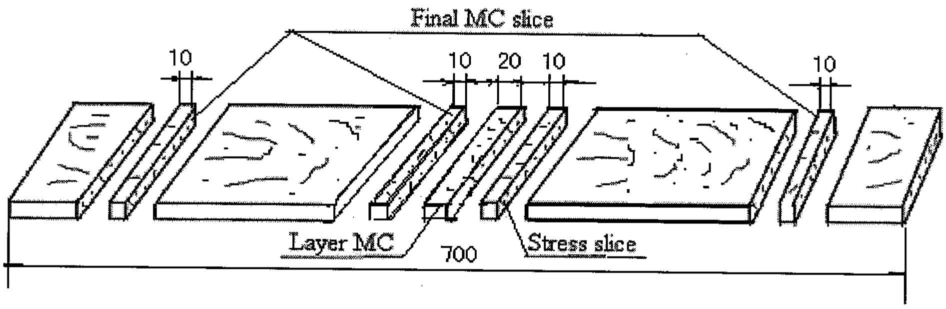

Fig.3.1-2 MC slices making of *Acacia magium*

3.1.2 Result and suggestion

The air-drying test results of *Acacia magium* are listed in Tab.3.1-1, and the air-drying MC curves in different seasons were shown in Fig.3.1-3.

Tab.3.1-1 Air-drying test results of *Acacia magium*

Season	MCw (%)	MCo (%)	Air-drying rate (%day)			Air-drying rate in early stage (%/day)		Defect grade ##
			60-30%	30-20%	Below 20% #	1st week	2nd week	
2002.8-11 Autumn	100.4	13.9	1.88	0.77	0.55 (17.8%)	5.4	2.2	1
	113	14	1.76	0.43	0.36 (15.0%)	4.1	2.8	3
	128.9	13.3	1.97	0.85	0.34 (15.2%)	4.6	3.2	3
2002.12-2003.3 Winter	134.3	18	0.52	0.4	0.25 (18.0%)	4.2	1.9	1
	143.1	16.2	0.71	0.29	0.07 (19.2%)	5.2	2.2	1
	137.5	13.9	0.71	0.23	0.33 (16.4%)	5.2	2.8	1
2003.3-2003.7 Spring	146.4	14.1	1.5	0.83	0.38 (16.2%)	3.5	1.6	1
	153.2	13.6	1.71	0.67	0.58 (14.2%)	4	1.8	2
	139.4	13.6	1.67	0.67	0.42 (15.8%)	3	1.6	2
2003.6-2003.9 Summer	113.5	14.3	1.43	0.43	0.27 (15.2%)	5.1	2.6	2
	89	14.4	2	0.77	0.15 (13.9%)	4.4	2.4	2
	107.4	16.4	1.2	0.3	0.19 (16.4%)	4.1	2.6	2

Note: # - The data in brackets are the final MC when test ended.

##- The standards for drying defects grade division: grade 1 – having no check, warp and cup deformations or just having end checks; grade 2 - having no more than five short end-surface checks or short-narrow surface checks, and the value of warp and cup deformations are smaller than 2mm; grade 3 - having five to ten short-narrow surface checks, and the value of warp and cup deformations are smaller than 4mm; grade 4 - having more than ten short-narrow surface checks and long-narrow or wide surface checks no more than five, or the value of warp and cup deformation are more than 4mm.

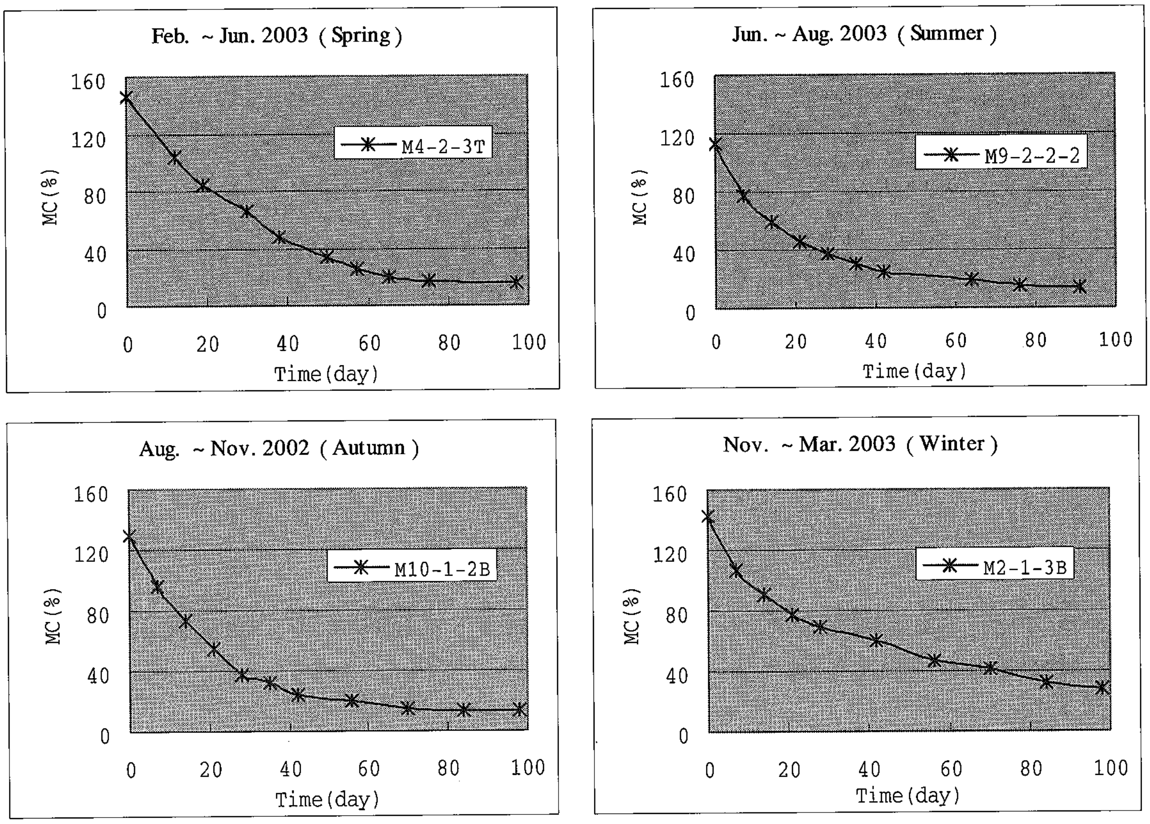

Fig.3.1-3 The air-drying MC curve of *Acacia magium*

Result showed that the air-drying rate of *Acacia magium* in summer was the fastest and that in winter in the slowest. But drying defects were very serious (grade 3 mostly), and the main drying defects were many small surface checks. So it is recommended that using controlled air-drying method to pre-dry *Acacia magium* wood before kiln drying.

3.2 Drying characteristics

3.2.1 Material and method

The sample dimension: plane-sawn lumber with 200mm x 100mm x 20mm

Other requirements of sample: planed lumber with normal colour, knot-free and straight grain, and initial moisture content is above 45%.

Equipment: Electric oven with air circulation.

100℃-test method is a fast drying test which is used to study on drying characteristics and prediction of drying schedule of plantation wood. Before test, the following data of the samples should be gained: the sample's weight, all visible surface defects, and dimension measurement data as showing in Fig.3.2-1. Then the samples were put into the electric oven with constant temperature at 100℃, and letting the samples stand erectly in the oven so that they will obtain same quantity of heat. Once the test begin, weighing the samples, observing and recording all initial defects including end checks, end-to-surface checks and surface checks at a fixed time through all the drying process. The test ended when MC was estimated below to 1%. All the samples were taken out, and then measuring cross-section deformation (Fig.3.2-2). Finally cutting moisture content slice and recording internal checks of each sample.

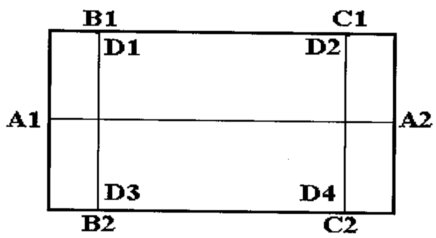

A1-A2 is length
B1-B2 and C1-C2 are width
D1,D2,D3,D4 are thickness

Fig.3.2-1 The dimension measure in 100℃-test of *Acacia magium*

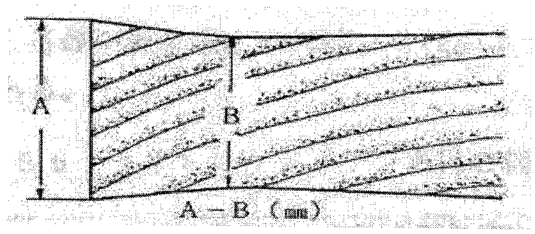

Fig.3.2-2 The cross-section measure in 100℃-tes of *Acacia magium*

To make all these defects digitalization and comparable, the grades of different drying defects are shown in Tab.3.2-1 to Tab.3.2-3.

Tab.3.2-1 The grade division of initial checks

Grade	No.1	No.2	No.3	No.4	No.5
Degree of initial check	No checks or only have end checks	Short end-to-surface checks and short-narrow surface checks	Long end-to-surface checks and long-narrow surface checks no more than two or short-narrow surface checks no more than fifteen	short-narrow surface checks more than fifteen or long-narrow and wide surface checks no more than five	short-narrow surface checks more than five or wide surface checks more than five

Note: long check -- check length ≥ 50mm; short check -- check length <50 mm; narrow check -- check width <2 mm; wide check -- check width ≥ 2mm

Tab.3.2-2 The grade division of internal checks

Grade	No.1	No.2	No.3	No.4	No.5	No.6
Degree of internal check	No :hecks	1 wide or 2 narrow checks	2-3 wide checks; 4-5 narrow checks; 1 wide and 3 narrow	4-5 wide; 7-9 narrow; 1 wide and 4-6 narrow	6-8 wide; 15 narrow; 4 wide and 6-8 narrow	15-17 wide or continuous checks

Tab.3.2-3 The grade division of cross-section deformation

Grade	No.1	No.2	No.3	No.4	No.5	No.6	No.7	No.8
A-B (mm)	0-0.3	0.3-0.5	0.5-0.8	0.8-1.2	1.2-1.8	1.8-2.5	2.5-3.5	over 3.5

Based on these drying characteristics in 100℃-test, the drying condition of this species could be gained by the relationships of drying characteristics and drying conditions showed Tab.3.2-4, which are very helpful to predict the drying schedules.

Tab.3.2-4 Drying condition based on degree of drying defects

Name	Drying condition (℃)	Grade of effects							
		No.1	No.2	No.3	No.4	No.5	No.6	No7	No8
Initial checks	Initial temperature	70	65	60	55	53	50	47	45
	Temperature depression	6.5	5.5	4.3	3.6	3.0	2.3	2.0	1.8
	Finial temperature	95	90	85	83	82	81	80	79
Cross section deformation	Initial temperature	70	66	58	54	50	49	48	47
	Temperature depression	6.5	6.0	4.7	4.0	3.6	3.3	2.8	2.5
	Finial temperature	95	88	83	80	77	75	73	70
Internal checks	Initial temperature	70	55	50	49	48	45	43	40
	Temperature depression	6.5	4.5	3.8	3.3	3.0	2.5	2.2	2.0
	Finial temperature	95	83	77	73	71	70	68	67

3.2.2 Result and suggestion

From the results of 100℃-test, the detailed data of drying defects results of *Acacia magium* were shown in Tab.3.2-5, and the consideration of all 8 test samples, the comprehensive drying defects grades of *Acacia magium* were shown in Tab.3.2-6. Corresponding to the drying condition based on degree of drying defects (Tab.3.2-4), and then the drying condition of *Acacia magium* was show in Tab.3.2-7, which would be used to determine the kiln schedule in the follow-up test. And the MC curve during 100℃-test was showed in drying Fig.3.2-3.

Tab.3.2-5 The drying defects data and grades of *Acacia magium*

No	Surface checks			End –surface checks			End checks		Grade	Internal checks			Cross section deformation	
	Long -narrow	Short -narrow	Wide	Long -narrow	Short -narrow	Wide	Wide	Short -narrow		Narrow	Wide	Grade	A-B (mm)	Grade
1	0	0	0	0	0	0	0	Many	1	9	7	5	2.46	6
2	0	0	0	0	0	0	0	Many	1	8	14	6	3.19	7
3	0	1	0	0	1	0	0	Many	2	6	10	6	2.87	7
4	0	0	0	0	0	0	0	Many	1	4	16	6	5.07	8
5	0	0	0	0	0	0	0	14	1	3	12	6	3.10	7
6	0	2	0	0	2	0	0	Many	2	3	8	5	3.01	7

Tab.3.2-6 The comprehensive drying defects grades of *Acacia magium*

Drying defects	Initial checks	Internal checks	Cross section deformation
Grade	No.2	No.6	No.7

Tab.3.2-7 The kiln drying condition of *Acacia magium*

Item	The initial temperature	The initial wet-bulb depression (Δt)	Final temperature)
Temperature (℃)	40	2	67

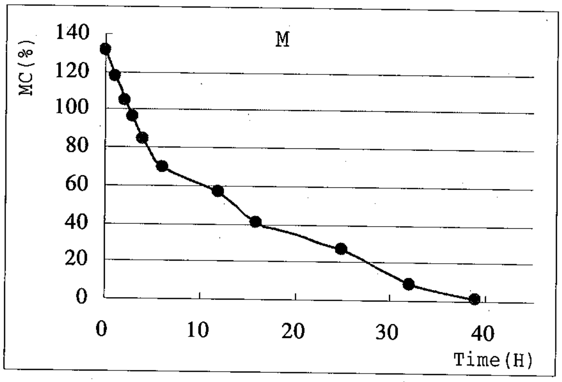

Fig.3.2-3 MC curve in 100℃-test of *Acacia magium*

3.3 Drying schedule

The sample dimension was with 500mm x 110mm x 25mm, double end-sealed with silicon sealing glue. The capacity for the stack was 500x400x300 mm, so 15 pieces of samples could by dried each time. To make it easy to fetch every sample for measurement and observation, all these 15 pieces of samples were put on a special made frame, so no heavy load on top on stack during test.

The test dryer was electric heating with 3 group of heater, which could be used independently of simultaneously according to the drying test need, the maximum of 3 group of heater was 6 kW. There was an electronic heated small boiler to afford steam during conditioning. The control system of the test dryer was semi-automatic.

Other equipment: Electric oven with air circulation, electronic balance, thermo-electronic couple temperature measuring system.

Based on the results of drying characteristics test, a schedule of *Acacia magium* wood with thickness of 25 mm was drafted, seeing in Tab.3.3-1.

Tab.3.3-1 The predicted drying schedules of *Acacia magium* (25mm)

MC stage	Dry-bulb temperature (t℃)	Wet-bulb temperature depression (Δt℃)
Above 40	40	2
40-35	44	3
35-30	48	5
30-25	52	9
25-20	56	12
20-15	60	16
Below 15	67	22

Beginning with this schedule, a series of kiln drying test had been done till the optimized schedule was gained.

3.3.2 Result and suggestion

The *Acacia magium* plantation wood belongs to low density species, and could be fast drying with less check defects, but it is easy to occur serious deformation and even collapse, so the drying temperature of *Acacia magium* plantation wood drying is not suitable such high comparing with other similar density species. To prevent and reduce the deformation and collapse of *Acacia magium* plantation wood during drying, the air-drying had been used to pre-dry *Acacia magium* plantation wood to MC around 30%, and then kiln drying. Results showed that using this combination drying method, the drying times of *Acacia magium* plantation wood reduced about 40%, and collapse reduced about 80%.

Because all 15 pieces of samples were put on a special made frame to make it easy to fetch every sample for measurement and observation, so no weight load on top on stack during lab testing. And this maybe one of the main reasons to occur serious deformation. So in practice drying, it is strongly recommended that putting heavy load on top of the stack to prevent and reduce deformation occurring during drying.

The optimised kiln drying schedule for *Acacia magium* wood with thickness of 25 mm was listed in Tab.3.3-2.

Tab.3.3-2 Drying schedule for *Acacia magium* wood with thickness of 25 mm

MC (%)	Dry-bulb T(℃)	Wet-bulb T(℃)	Notes
Pre-heating	50	49-50	Pre-heating, 3 hours
Above 35	40	37	
35 ~ 30	45	41	
=30%	55	54	Conditioning, 3 hours
30 ~ 25	50	45	
25 ~ 20	55	45	
=20%	65	63	Conditioning, 3 hours
20 ~ 15	60	45	
15 ~ 10	65	45	
Below 10	70	45	
=8%	75	69	End-treatment, 3-5 hours

The lab test results showed that using this schedule to dry *Acacia magium* plantation wood with thickness of 25mm, the drying quality could meet the National Sawn-timber Drying Quality Standard (GB/T 6491-1999) 2nd grade requirement.

X Acacia auriculiformis

The information of testing materials is as Tab.1.

Tab.1 Testing materials

Tree species	Tree age (year)	Tree number	Tree height (m)		Under branch height (m)		DBH (cm)	
			Ave.	Std	Ave.	Std.	Ave.	Std
Acacia auriculiformis		6	20.50	1.2247			23.37	1.3033

1 WOOD PROPERTIES

1.1 Anatomical characteristics

Samples (2x2x1 cm) for wood anatomical section were stored in alcohol 95% : glycerine (1:1) until they sank. Transverse sections of 20μm were cut on sliding microtome, then bleached, stained with safranin, dehydrated and mounted on slides for measure anatomical properties on image analysis. Then the transverse, radial and tangential sections from each species of around 80μm were cut on the same microtome, make the samples for SEM observation and taking photos.

Prior to tracheid length measurement, the each selected growth rings were firstly separated with a chisel, then macerated in solution of acetic acid (1/3) and hydrogen peroxide 27% (2/3) for several days in 60° oven.

The measurement methods are as follows:

Measuring length and width of wood fiber and vessel element using macerated anatomical elements under fiber length measuring instrument; (2) Measuring wood fiber cell wall thickness, cell wall percentage, and tissue proportions by section method using image analysis system; (3) Measure of S_2 microfibril angle: using x-ray diffractometer.

The observation and description for macro- and micro-structure were made under the light microscope and scanning electronically microscope (SEM).

1.1.1 Tree and distribution

A tree up to 8~20 m, trunk has two types: straight and curly generally; but tree up to 30 m in good site in origin producing country, Australia, Papua New Guinea and Indonesia. Bark dark gay or brown, the bark of young tree smooth, when old tree with rimous and coarse bark. *Acacia magnium* is introduced to Malaysia, India, Thailand, Burma, Bengal, Nigeria and Tanzania as an important plantation species to plant respectively on large scale. China is introducing this species as solid wood products in Guangxi, Fujian and Yunnan etc.

1.1.2 General characteristics

Sapwood light yellowish brown or yellowish brown, differs from heartwood, width 2~3 cm. ***heartwood*** dark reddish brown or blackish brown with black or dark brown stripes; glossy, wood without characteristic taste & odor. ***Growth rings*** little distinct. Wood diffuse-porous. Pores small to middle, visible to the naked eye as white dots, fairly uniformly distributed throughout the ring, oblique, tyloses singularly. ***Longitudinal parenchyma*** vasicentric under a hand lens. ***Rays*** very fine to fine, clear with a hand lens. ***Ripple mark***s visible.

Resin canals absent.

1.1.3 Minute anatomy (Plane V)

Vessels most solitary; in radial multiples of 2~3 few, oblique; cell wall thin; tangential average diameter 128 μm, max 216 μm. 9 (5~14) /mm^2. Helical thickness absent. Simple perforation, its plate oblique. Intervessel pits ventured, alternate, polygonal & round, pit aperture included, coalescent mostly, lenticular, linear and cranny. Ventures distributed pit aperture, canal & chamber, and full of them, most lumpish and coralloid. Vessel- ray pitting similar to intervessels pits.

Longitudinal parenchyma vasicentric, diffuse or diffuse-aggregates. Nodular end wall of parenchyma cells inconspicuous; crystals absent.

Fiber wall thin, 1185 (823~1321) μm in length, 17 μm in width with plain simple pits.

Rays part oblique, rays 8~11/mm, uniseriate rays 2~19 cells seldom, mostly multiseriate rays width 2 cells, 3 cells accidental, height 9~28 cells. Ray tissues homogeneous uniseriate and multiseriate; parenchyma cells round or oval, most with gum. Nodular end wall of parenchyma cells inconspicuous to conspicuous. Crystal and intercellular canals absent.

The data of anatomical parameter and tissue proportion at different heights and the Tab. 1.1-1 and 1.1-2 respectively. The vessel distribution frequencies and tangential diameters is including to in 1.1-3.

Tab.1.1-1 Anatomical parameter and basic density at different heights for *A. auriculiformis*

Item	1.3m		3.3m		5.3m		7.3m	
	$\bar{x}$	δ_n	$\bar{x}$	δ_n	$\bar{x}$	δ_n	$\bar{x}$	δ_n
Fiber length (μm)	1185	53	1206	82	1145	55	1162	79
Fiber width (μm)	16.9	1.1	16.4	0.8	16.2	1.1	17.1	2.0
Fiber wall thickness	8.78	1.098	9.74	0.377	8.88	1.152	9.19	1.168

Tab.1.1-2 Tissue proportion of *A. auriculiformis* at different heights for (%)

Item	1.3m		3.3m		5.3m		7.3m	
	$\bar{x}$	δ_n	$\bar{x}$	δ_n	$\bar{x}$	δ_n	$\bar{x}$	δ_n
Fiber	81.38	3.147	82.42	2.770	81.74	2.127	81.33	2.744
Vessels	11.27	2.134	9.60	1.895	9.99	1.542	11.17	1.454
Rays	6.25	0.795	7.06	2.255	7.34	1.063	6.62	1.132
Longitudinal parenchyma	1.11	0.619	0.92	0.321	0.93	0.295	0.88	0.273
Cell wall	71.79	4.872	69.89	3.083	71.62	2.997	72.72	2.473

Tab.1.1-3 Vessel distribution frequencies and tangential diameters

Vessel distribution frequency (Number/mm^2)				Vessel tangential diameter (μm)			
Ave.	Std.	Max.	Min.	Ave.	Std.	Max.	Min.
9.40	3.0026	14.32	5.47	128.09	39.0521	216.44	35.28

1.2 Shrinkage and Density

Shrinkage is the contraction of wood caused by drying the material below the fiber saturation point (William T. Simpson, 1991). It can be divided into 3 types of shrinkage according to the direction of contraction: longitudinal, radial and tangential shrinkage. The longitudinal shrinkage is the shrinkage along the grain, the radial shrinkage and the tangential shrinkage is that across the grain in a radial or in a tangential direction. Wood density, the weight of wood per unit volume, is a very important index having a close relation with wood mechanical strength. In this study, wood air-dried density and basic density were used to describe the wood density.

The shrinkage is attributed to the dimension stability and checking problem, which causes a lot of problem for the wood utilization. In another word, it causes not only the contraction of wood in size, but also the checking and deformation resulted from the different contraction in tangential, radial and longitudinal direction. Understanding the characteristics of shrinkage has no doubt to be helpful for the wood utilization for the wood industry practice. Nowadays, studying on the characteristics of shrinkage during the losing of water is becoming one of the wood science discipline[Barber NF etc.1964; Barber, 1968; Chafe, 1986; 1987; Gu H et al., 2001]。 This study is intended to explore the shrinkage variation of acacia in different direction (North and south), different radial position and different tree height.

The trees studied were cut from Guangxi Zhuang Autonomous Region in the South China. Each trunk has been collected above the breast height and was cut every 2 meters. Then, four discs of each tree at different heights (about 1.3m, 3.3m, 5.3m and 7.3m respectively) were taken from the logs. All the discs were marked the south-north direction. For each disc, one specimen from the sapwood near the bark, one from the heartwood near pith and one from transition zone was made at the size of 2X2X2cm (Tangential X radial X longitudinal direction) for both north side and south side.

Two diagonal lines were drawn in three sections (i.e., T×R, T×L, R×L) of each specimen to locate the central point where the size was measured. The specimens were put into water until they were totally saturated and sunk in the water. The surface water was wiped off and the sizes in three directions (L, R, T) were measured. Specimens were set in the room for air-drying. After measuring the size and weight at the air-dried stage, the specimens were oven-dried and the same measurement was carried out. The shrinkage was determined according to Chinese National Standard. The air-dried density and was also calculated of both air-dried

The shrinkage coefficient was determined by the difference between shrinkage at air-dried and at oven-dried and divided by the MC at air-dried.

1.2.1 Shrinkage and density, and that of wood from south and north directions

The air-dried shrinkage in tangential direction (Ta), Radial direction (Ra) and volumetric shrinkage (Va), as well as the oven-dried shrinkage in tangential direction (To), Radial direction (Ro) and volumetric shrinkage (Vo) are listed in Tab.1.2-1 according to the categories of south direction, north direction and the overall. The basic density (B D) and air-dried density (A D), together with tangential shrinkage coefficient and radial shrinkage coefficient were also calculated and listed.

According to the IAWA (1989) method (the wood with an air-dried density smaller than 0.56 g/cm^3 is considered to be a small-density species, between 0.56 g/cm^3 and 0.75 g/cm^3 is considered to be a medium-density, between 0.75 g/cm^3 and 0.95 g/cm^3 is considered to be a large-density species, and bigger than 0.95 g/cm^3 is considered to be a extra-large-density species), *A. auriculiformis* wood has a medium density.

According to the *CHINA WOOD* method (the wood with an air-dried tangential shrinkage smaller than 5.60% is considered to be a small-shrinkage species, between 5.60% and 7.00% is considered with a medium-shrinkage species, and bigger than 7% is considered to be a big-shrinkage species), *A. auriculiformis* is small in shrinkage, suggesting that it is good in wood dimension stability.

ANOVA analysis (Tab.1.2-2) showed there was no significant difference between air-dried tangential shrinkage and air-dried radial shrinkage, suggesting that the wood from north and south could be thought has the same level in shrinkage.

Tab. 1.2-1 The shrinkage and density of *A.auriculiformis* wood from south and north side

		Ta (%)	Ra (%)	Va (%)	To (%)	Ro (%)	Vo (%)	B D (g/cm^3)	A D (g/cm^3)	Co-t (%)	Co-r (%)
South	Average	4.38	1.59	6.03	7.37	3.00	10.50	0.51	0.62	0.26	0.12
	Std.dev.	0.75	0.49	1.01	1.12	0.81	1.47	0.07	0.06	0.05	0.03
	CV(%)	0.17	0.31	0.17	0.15	0.27	0.14	0.13	0.09	0.19	0.27
	Number	53	53	53	53	53	53	53	53	53	53
North	Average	4.31	1.61	6.18	7.26	2.96	10.55	0.54	0.64	0.27	0.12
	Std. dev.	0.98	0.68	1.51	1.01	1.02	1.91	0.07	0.09	0.06	0.03
	CV(%)	0.23	0.42	0.24	0.14	0.34	0.18	0.13	0.14	0.24	0.27
	Number	57	57	57	57	57	57	57	57	57	57
Total	Average	4.35	1.60	6.11	7.31	2.98	10.52	0.53	0.63	0.26	0.12
	Std. dev.	0.87	0.60	1.29	1.06	0.92	1.70	0.07	0.08	0.06	0.03
	CV(%)	0.20	0.37	0.21	0.14	0.31	0.16	0.13	0.12	0.21	0.27
	Number	110	110	110	110	110	110	110	110	110	110

Tab.1.2-2 ANOVA analysis on the shrinkage of *A.auriculiformis* wood from north and south

	SS	df	MS	F	P-value	F crit
Ta	0.1314	1	0.1314	0.1724	0.6789	3.9290
Ra	0.0103	1	0.0103	0.0288	0.8656	3.9290

1.2.2 Shrinkage and density of wood from 4 different tree heights

The shrinkage, shrinkage coefficient and density from 4 different tree heights were listed in Tab. 1.2-3. The relationship between air-dried shrinkage, basic density and tree heights were showed in Fig. 1.2-2.

ANOVA analysis (Tab.1.2-3) showed there did not exist significant air-dried shrinkage difference both in tangential and radial directions among 4 different tree heights.

Tangential shrinkage showed a tendency that it decreased with the increase of tree height, while the radial shrinkage showed a tendency that it increased with the increase of tree height, and the basic density showed no regular pattern (Fig.1.2-2).

Tab. 1.2-3 The shrinkage and density of *A.auriculiformis* s wood from different heights

		Ta (%)	Ra (%)	Va (%)	To (%)	Ro (%)	Vo (%)	B D (g/cm^3)	A D (g/cm^3)	Co-t (%)	Co-r (%)
1.3m	Average	4.45	1.45	6.12	7.48	2.64	10.47	0.56	0.66	0.27	0.11
	Std. dev.	0.52	0.25	0.63	0.75	0.41	0.86	0.03	0.04	0.03	0.02
	CV(%)	0.12	0.17	0.10	0.10	0.16	0.08	0.06	0.06	0.10	0.15
	Number	24	24	24	24	24	24	24	24	24	24
3.3m	Average	4.38	1.54	6.01	7.50	2.89	10.60	0.51	0.62	0.27	0.12
	Std. dev.	1.10	0.54	1.27	1.04	0.81	1.63	0.09	0.07	0.10	0.03
	CV(%)	0.25	0.35	0.21	0.14	0.28	0.15	0.17	0.11	0.36	0.29
	Number	30	30	30	30	30	30	30	30	30	30
5.3m	Average	4.39	1.75	6.25	7.30	3.23	10.71	0.53	0.63	0.26	0.13
	Std. dev.	0.87	0.89	1.67	1.15	1.34	2.23	0.06	0.08	0.03	0.04
	CV(%)	0.20	0.51	0.27	0.16	0.42	0.21	0.11	0.12	0.12	0.32
	Number	30	30	30	30	30	30	30	30	30	30
7.3m	Average	4.16	1.65	6.03	6.96	3.10	10.27	0.51	0.61	0.25	0.13
	Std.	0.86	0.42	1.31	1.17	0.67	1.73	0.08	0.10	0.03	0.02
	CV(%)	0.21	0.25	0.22	0.17	0.22	0.17	0.16	0.17	0.13	0.19
	Number	26	26	26	26	26	26	26	26	26	26

Tab.1.2-4 ANOVA analysis on the shrinkage of *A.auriculiformis* wood from different heights

	SS	df	MS	F	P-value	F crit
Ta	1.2301	3	0.4100	0.5350	0.6593	2.6903
Ra	1.4107	3	0.4702	1.3352	0.2669	2.6903

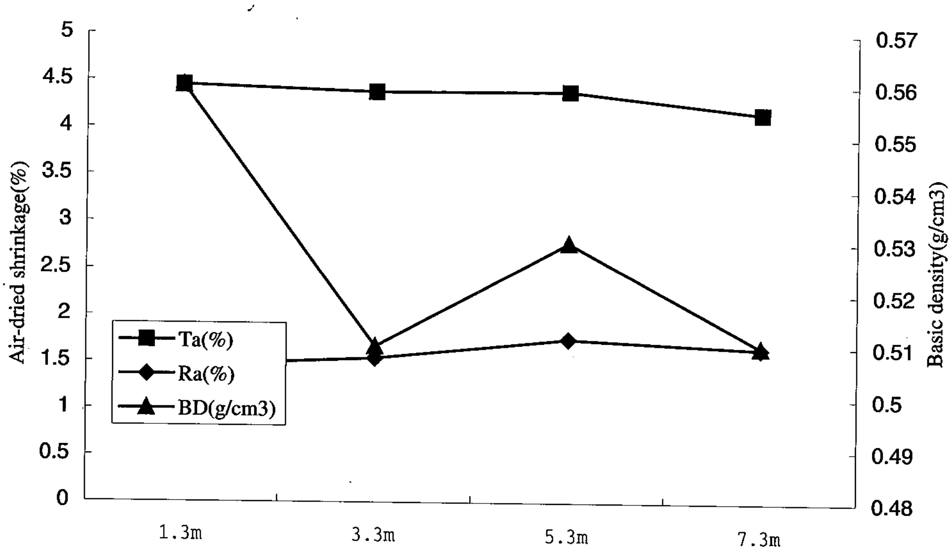

Fig.1.2-2 *A.auriculiformis*: relationship between air-dried shrinkage, basic density and tree heights

1.2.3 Shrinkage and density of wood at different radial positions

The shrinkage, shrinkage coefficient and density from 4 different tree radial positions were listed in Tab.1.2-5. The relationship between air-dried shrinkage, basic density and tree heights were showed in Fig. 1.2-5.

ANOVA analysis (Tab.1.2-6) showed there did not exist significant air-dried shrinkage difference both in tangential and radial directions among different radial position.

Fig.1.2-3 showed that both the tangential and radial shrinkage decreased gradually from mature wood (near bark) to juvenile wood (near pith), and the basic density showed a same pattern.

Tab. 1.2-5 The shrinkage and density of *A.auriculiformis* from different radial positions

		Ta (%)	Ra (%)	Va (%)	To (%)	Ro (%)	Vo (%)	B D (g/cm^3)	A D (g/cm^3)	Co-t (%)	Co-r (%)
Near bark	Average	4.57	1.71	6.49	7.59	3.17	10.98	0.54	0.66	0.27	0.13
	Std. dev.	0.68	0.49	1.09	0.93	0.77	1.47	0.08	0.06	0.05	0.03
	CV(%)	0.15	0.28	0.17	0.12	0.24	0.13	0.15	0.10	0.19	0.27
	Number	37	37	37	37	37	37	37	37	37	37
Transition	Average	4.31	1.58	5.99	7.23	2.95	10.37	0.53	0.63	0.26	0.12
	Std. dev.	0.80	0.61	1.38	1.07	0.95	1.83	0.06	0.08	0.03	0.03
	CV(%)	0.18	0.39	0.23	0.15	0.32	0.18	0.12	0.13	0.12	0.27
	Number	38	38	38	38	38	38	38	38	38	38
Near pith	Average	4.14	1.51	5.83	7.12	2.81	10.20	0.50	0.59	0.27	0.12
	Std.	1.07	0.68	1.32	1.14	1.01	1.74	0.06	0.07	0.08	0.03
	CV(%)	0.26	0.45	0.23	0.16	0.36	0.17	0.11	0.12	0.31	0.28
	Number	35	35	35	35	35	35	35	35	35	35

Tab.1.2-6 ANOVA analysis on the shrinkage of wood from different radial positions

	SS	df	MS	F	P-value	F crit
Ta	3.336384	2	1.668192	2.255528	0.10978	3.081198
Ra	0.732363	2	0.366181	1.030836	0.360224	3.081198

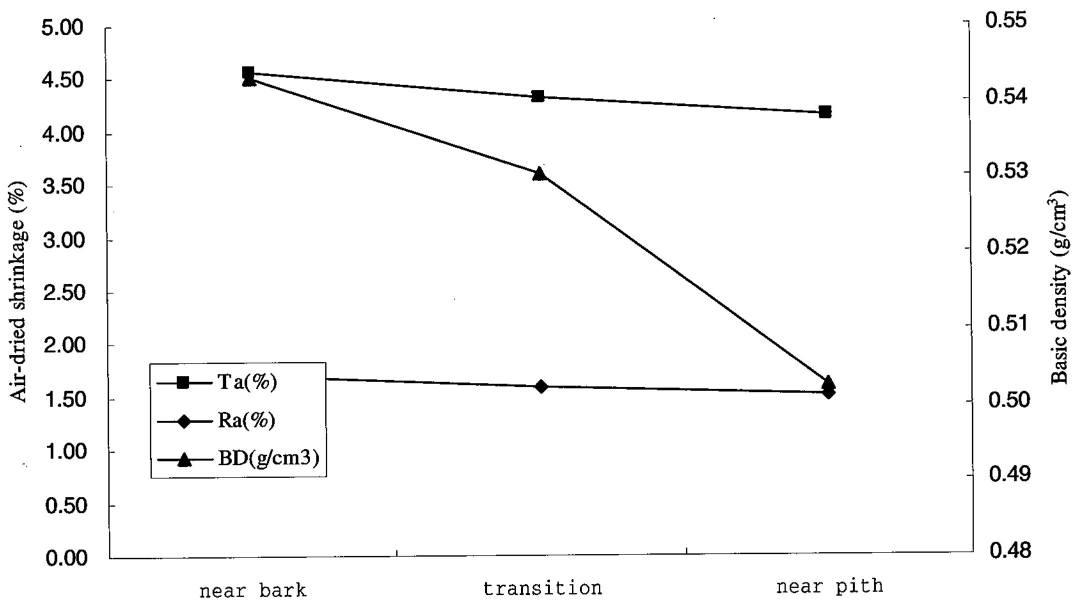

Fig.1.2-3 *A.auriculiformis*: relations between air-dried shrinkage, basic density and different radial positions

1.3 Mechanical properties

The small clear wood samples of moduli of elasticity (MOE), moduli of rupture (MOR) in static bending, compression strength parallel to grain and wood density were cut in accordance with Chinese National Standards (GB 1927~1943-91). The specimens were then stored in a conditioning chamber until it reached approximately 12% moisture content. Bending, compression and wood density test were carried out in accordance with Chinese National Standard. The air-dry density was calculated by air-dried weight and volume while oven-dry density was based on oven-dried weight and volume.

Generally *A. auriculiformis* wood grain straight or oblique, texture middle and even, weight middle, hard, shrinkage middle, strength middle or highly. The mechanical properties are including tab.1.2-1.

Tab.1.2-1 Mechanical properties data of *A. auriculiformis*

Locality	Density /g/cm^3		DS /%		CSPG /MPa	BS /MPa	MOE /GPa	Toughness /kJ/m^2	Hardness /N		
	BD	ADD	R	T	CSPG/MPa	BS/MPa	MOE/GPa	Toughness/kJ/m^2	E	R	T
Guangdong Longyandong	0.663				545	104	14.41	65.0			

BD = basic density, ADD = air-dry density, DS = dry shrinkage, CSPG = compressive strength parallel to grain, BS = bending strength, MOE = modulus of elasticity, SSPG = shear strength parallel to grain(R), E = end, R = radial, T = tangential.

1.4 Chemical properties

The chemical composition was determined according to Chinese National Standards, the chemical composition results and pH values, acid and alkaline buffering capacities are listed in Tab. 1.3-1, and 1.3-2 respectively.

Tab.1.3-1 Chemical composition of *A. auriculiformis*

Holocellulose	α-Cellulose	Relative crystallinity	Lignin	1%NaOH extractives	Xylan	Benzene-alcohol extractives	Cold water extractives	Hot water extractives	Ash
71.25	45.30	58.74	22.83	22.02	22.98	5.78	4.64	6.05	0.68

Tab.1.3-2 Data of pH value, acid and alkaline buffering capacity of *A. auriculiformis*

S	H	S	H	S	H
5.27	5.15	4.62	3.90	14.42	49.16

S- sapwood, H-heartwood

References

Armstrong Matt. 2005. Queensland regrowth spotted gum (*Corymbia citriodora*), The impact of Harvesting Age/Tree size on sawing, drying and solid wood properties of key regrowth Eucalypt species. Forest & Wood Products Research & Development Corporation, Australia: 45~53.

Barber NF 1968 A theoretical model of shrinking wood. Holzforschung 22:97-103

Barber NF,Meylan BA 1964 The anisotropic shrinkage of wood. A theoretical model. Holzforschung 18:146-156

Bariska M. 1992. Collapse Phenomena in Eucalyptus. Wood Science & Technology: 165-179

Bosman M T M, Kort I D *et al.*, 1994. Radial variation in wood properties of naturally and plantation grown light red meranti (*Shorea Dipterocarpaceae*), IAWA Journal, 15 (2):111-120

Chafe SC 1986 Collapse,volumetric shrinkage,specific gravity and extractives in Eucalyptus and other species Part1:The shrinkage/specific gravity ratio. Wood Sci Technol 20:293-307

Chafe SC 1987 Collapse,volumetric shrinkage,specific gravity and extractives in Eucalyptus and other species Part2:The influence of wood extractives. Wood Sci Technol 21:27-41

Chen Taian etc Effect of steaming process on the shrinkage and air permeability of oak. Journal of Nanjing Forestry University (Natural Science). 2003,27 (in Chinese)

Cheng J Q. 1985. Wood sciences. Beijing: Chinese forestry publishing house

Cheng J Q. 1985. Wood sciences. China Forestry Press House.

Crompton H.R. and Turnbull J.W. 2000. Eucalypt research for products to benefit small business enterprises. The Future of Eucalypts for Wood Products Proceedings, Tasmania Australia: 124-131.

D1666-64 (Reapproved 1976). 1980. Annual book of ASTM standards. Part22: Wood; Adhesives.

D1666-87 (Reapproved 1999). 2000. Annual book of ASTM standards. Section Four Construction. Vol. 04. 10

Derek W, Roman M. 1998. Machining and related mechanical properties of 15 B C wood species. Forintek Canada Corp. 1-4

Donaldson L A. 2002. Abnormal lignin distribution in wood from severely drought stressed *Pinus radiata* trees. IAWA Journal, 23(2): 161-178

Edvard Kardelj University LJUBLJANA Biotechnical Faculty. 1983. Machining and related characteristics of five wood species from Bayanga region (Central African Republic). LJUBLJANA, 5-16

Evans R & J Ilic. 2001. Rapid prediction of wood stiffness from microfibril angle and density. For. Prod. J, 51(3): 53-57

Evans R J, Ilic & A C Matheson. 2000. Rapid estimation of solid wood stiffness using SilivScan. Proceedings of 26th For. Prod. Res. Conf., CSIRO, Forestry and Forest Products, 49-50

Fang Wenbin etc. Shrinkage of loblolly pine wood in different tree heights. Journal of Central South Forestry College, 1996, 16(3):15-21 (in Chinese)

Forest Research of New Zealand. 1998. The comparative research between *Pinus radita* of New Zealand and 13 wood species of Northern-America. New Zealand. 1-8

Fu-cheng Bao, Ze-hui Jiang, Xiao-mei Jiang. 2001. Differences in wood properties between juvenile wood and mature wood in 10 species grown in China. Wood Science and Technology. 35: 363-375

Gao R Q, Teng T L, Li X L. 200. Drying Tests on Improved-preservatives Treated Rubberwood. Chinese Forestry Science and Technology. Chinese Academy of Forestry. 4(3): 45-52

Garcia J N. 1999. Theory and practice on the high quality Eucalyptus lumber production on forest improvement and sawmill techniques. In Proceedings of XII SilivScan Eucalypt in Chile: Present and Future. Corma Concepción 1-22

Gerard J, Bailleres H, Fournier M and Thibaut B. 1995. Wood quality in plantation Eucalyptus - a study of variation in three reference properties. Bois et Forêts des Tropiques. 245(3): 101-110.

Gu H,Zink-Sharp A,Sell J 2001 Hypothesis on the role of cell wall structure in differential transverse shrinkage of wood. Holz Roh-Werkstoff 59:436-442

He D H. 1987. The drying characteristics and drying schedules for twenty-four kinds of southern hardwoods. China Wood Industry.

He D H. 1991. The test on air-conventional combined timber drying. Wood drying symposium V(18).

Huang Y R. 1987. The methods to determine wood drying schedule--100℃-test. Tianjin Funiture Journel V(8): 5-9

Ivan Tomaselli. 2000: Processing Young Eucalyptus. The Future of Eucalypts for Wood Products Proceedings, Tasmania Australia: 167-174

Jakub S, Chiaki T. 2003. Evaluation of wood surface smoothness by laser displacement sensor. IUFRO Proceedings: Forest Products Research Providing For Sustainable Choice. Rotorua, New Zealand

Jiang Xiaomei, Liu Xiaoli, Yin Yafang, Nakai Takashi. 2003. Variation within Tree of Wood Anatomical Properties in Chinese Fir Plantation and Their Relationship Modeling Equations. Chinese Forestry Science and Technology, 2 (2): 1-11

Jiang Xiaomei, Yin Yafang, Lu Jianxiong, Hiroyuki Urakami. 2002. The Influence of S_2 Microfibril Angle on Longitudinal and Tangential Shrinkage in Chinese-fir *(Cunninghamia lanceolata)* Plantation Woods. Chinese Forestry Science and Technology, 1 (4): 1-7

Jiang Xiaomei. 2000: The future of eucalyptus for wood products. Situation of the resources and wood utilization of tropical plantations in the southern part of China technical report. Beijing: 57-74

Jose N.G. and Isarael L.D.L. 2000: Log end splitting and improvement in sawing *Eucalyptus grandis*. The Future of Eucalypts for Wood Products Proceedings, Tasmania Australia: 113-123

Jose N.G Isarael L D. 2000. Log end splitting and improvement in sawing Eucalyptus grandis. The Future of Eucalypts for Wood Products Proceedings, Tasmania Australia: 113-123.

Li B-K 2002: Analysis on bonding process factors for integrated materials Technology on adhesion & sealing 2; 34-35

Li Y-K 2001: Some views on developing domestic adhesive industry for wood based panel Forestry Industry 3; 3-5

Liu J-P 1998: Simple studies on the factors to affect the quality of laminated lumber China Wood Ind, 2; 28-31

Lu J. 2000. Situation of the resources and utilization of wood of tropical plantations in the southern part of China. Situation of the resources and wood utilization of tropical plantations in the southern part of China technical report. Beijing: 39-47

Lu Jianxiong. 2000: Situation of the resources and utilization of wood of tropical plantations in the southern part of China. Situation of the resources and wood utilization of tropical plantations in the southern part of China technical report. Beijing: 39-47

Micael S, Soren O. 2000. An investigation of the crack tendency on wood surfaces after different machining operations. Holzforschung. (4): 427 – 436

Nanjing Forestry University. 1991. The textbook of wood drying for forestry university. China Forestry Press House.

National Quality and Technique Inspection Bureau. 2000. Drying Quality of Sawn Timber. China Standard Press.

Nepveu G *et al.,* 1999. The third workshop "Connection between silviculture and wood quality through modeling approaches and simulation software", December INPA- Nancy France

Newlin JA,Wilson TRC 1919 The relationship of the shrinkage and strength properties of wood to its specific gravity. US For Serv Bull FPL-676,35 pp

Northway R. 1997, Evaluation of drying methods for plantation-grown Eucalypt timber, Part B: Sawing, Accelerated drying and Utilisation Characteristics of *Eucalyptus grandis*, Forest & Wood Products Research & Development Corporation, Australia.

Okuyama T, H Yamamoto & H Watanabe. 1999. Growth stresses and other wood qualities related to the growth rate in tropical man-made forest species. IUFRO WP S5.01-04. Biological improvement of wood properties proceeding, 113-122

Pashin A J, De Zeeuw C. 1980. Textbook of wood technology, New York: McGraw-Hill Book Company

Pizzi. Wood Adhesive Chemistry and Technology, MARCEL DEKKER, Inc. 1883

Sassus F. 1998. Déformations de maturation et propriétés du bois de tension chez le hêtre et le peuplier:Mesures er modèles. Ph. D Thesis. ENGREF, Montpellier

Saurat J & P Gueneau. 1976. Growth stresses in beech. Wood Sci. Technol, 10(2): 111-123

Sugiyama K, T Okuyama, H Yamamoto & M Yoshida. 1993. Generation process of growth stresses in cell walls: Relation between longitudinal released strain and chemical composition. Wood Science Technology, 27: 257-262

Thomas E. Mclain. Performance of nailed-bolted

Tomaselli I. 2000. Processing Young Eucalyptus. The Future of Eucalypts for Wood Products Proceedings, Tasmania Australia: 167-174.

Vermaas H F. 2000. A review of drying technology for young fast-grown Eucalypts. Proceedings of IUFRO Conference—'The future of eucalypts for wood products'. Launceston, Tasmania: 225-226

Vermaas H F. 2001. A review of drying technology for young fast-grown Eucalypts. Department of Wood Science University of Stellenbosch. South Africa.

Waugh G. 2000. Use of twin saw system for young, fast-grown Eucalypts. The Future of Eucalypts for Wood Products Proceedings, Tasmania Australia: 175-183

William T. Simpson. 1991. Dry Kiln Operator's Manual. United States Department of Agriculture, Forest Service, Forest Products Laboratory.Madison, Wisconsin (ISBN 0-16-035819-1)

Wimmer R. 1992. Multivariate structure property relations for pinewood. IAWA Bull 13: 265

Yamamoto H. 1998. Generation mechanism of growth stresses in wood cell walls: roles of lignin deposition and cellulose microfibril during cell wall maturation. Wood Science and Technology, 32: 171-182

Yang J.L, David Fife; Gary Waugh, Geoff Downes; Philip Backwell. 2001. The effect of growth strain and other defects on the sawn timber quality of 10-year-old *Eucalyptus globules* Labill. Australian Forestry, 65(1): 24-30

Yang J.L. 2005. The impact of log-end splits and spring on sawn recovery of 32-year-old plantation *Eucalyptus globulus* Labill. Holz als Roh-und Werkstoff, 63: 442-448

Yoshida M, Y Hosoo & T Okuyama. 2000a. Periodicity as a factor in the generation of isotropic compressive growth stress between microfbrils in cell wall formation during a twenty-four hour period. Holzforschung, 54: 469-473

Yoshida M., Okuyama T. 2002: Techniques for Measuring Growth Stress on the Xylem Surface Using Strain and Dial Gauges, Holzforschung, 56: 461~467

Zhang X-L 2000: A new white emulsion Chinese Adhesive 5; 19-21

Zhao C R, Dong Y K. 1989. The fast way to determine the wood drying schedules. Forestry Industry. Northeast Forestry University Journal. V(2): 1-4

Zhu Z X. 1999. Wood Drying. China Forestry Press House. Beijing China.

Zobel B J, Van Buijtenen J P. 1989. Wood variation --its cause and contral. New Your, London: Spring Verlag.

PLANE

Plane I

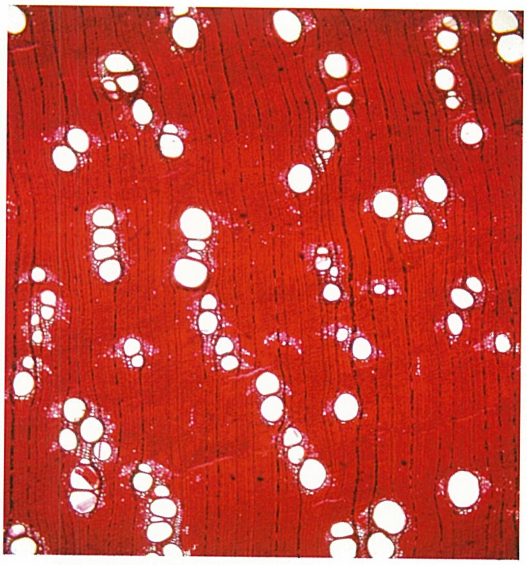

Eucalyptus citriodora （*X*）

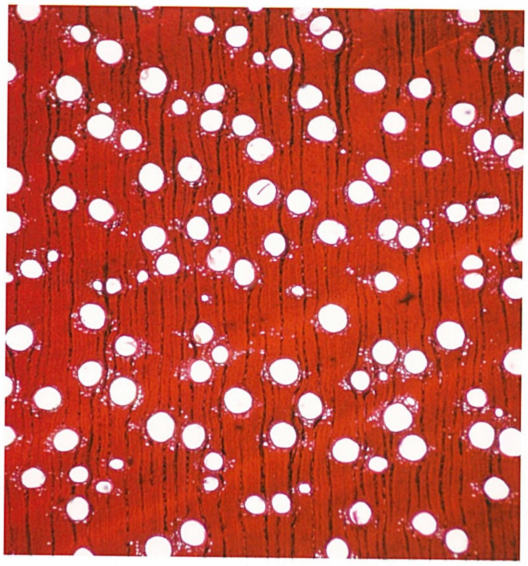

E. exserta （*X*）

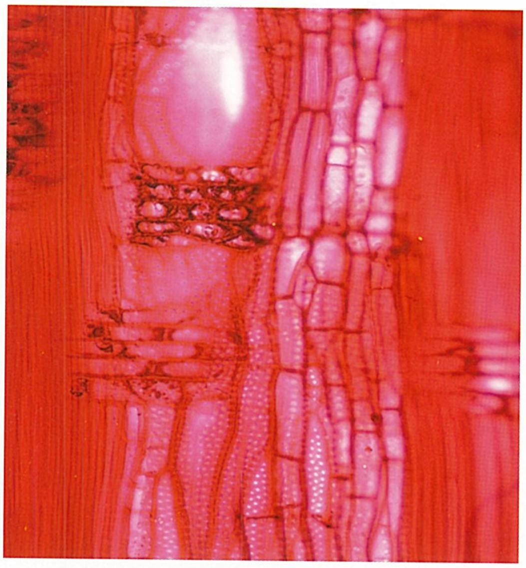

Eucalyptus citriodora （*R*）

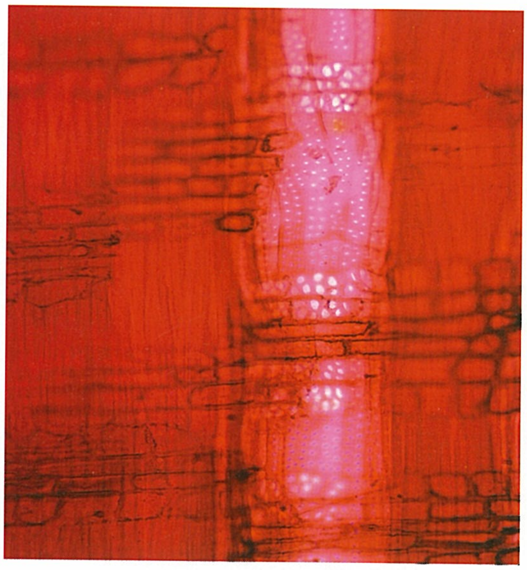

E. exserta （*R*）

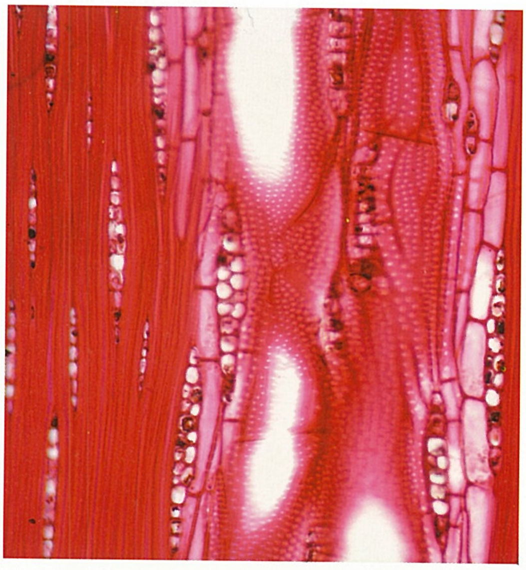

Eucalyptus citriodora （*T*）

E. exserta （*T*）

Plane II


E. urophylla x grandis （*X*）

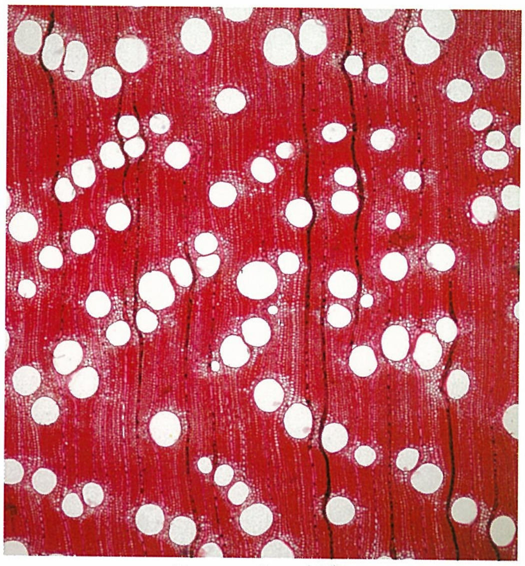
E. grandis （*X*）


E. urophylla x grandis （*R*）

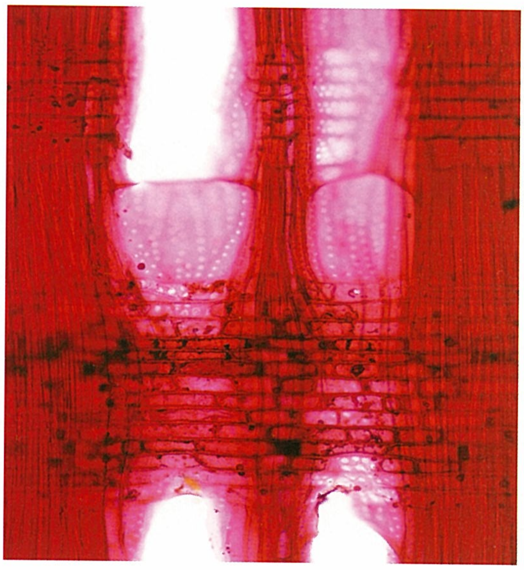
E. grandis （*R*）

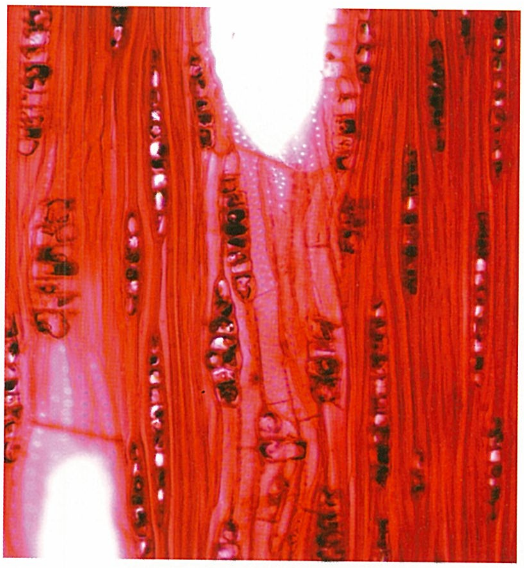
E. urophylla x grandis （*T*）

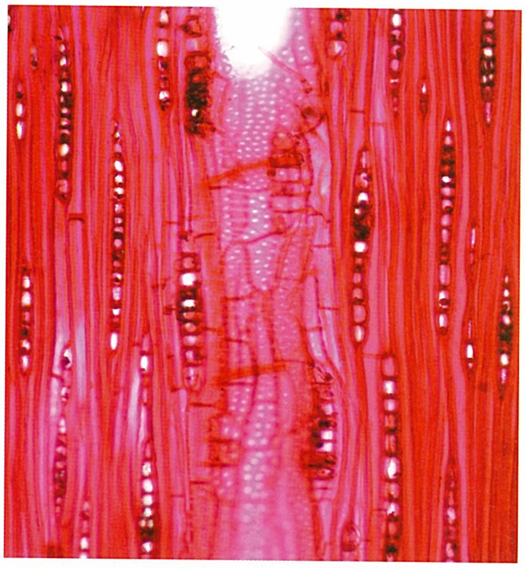
E. grandis （*T*）

Plane III

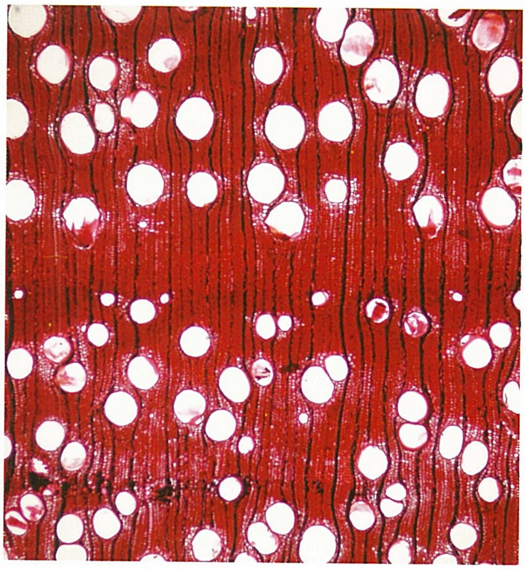

E. urophylla （*X*）

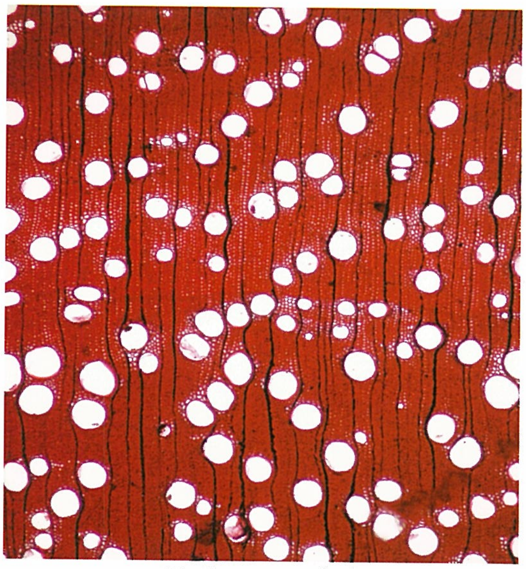

E. cloeziana （*X*）

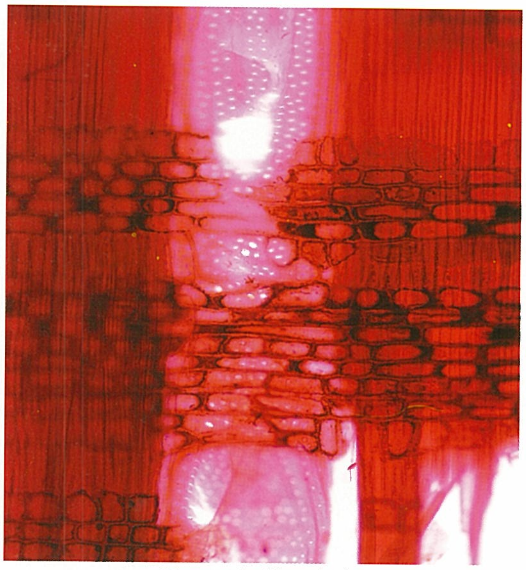

E. urophylla （*R*）

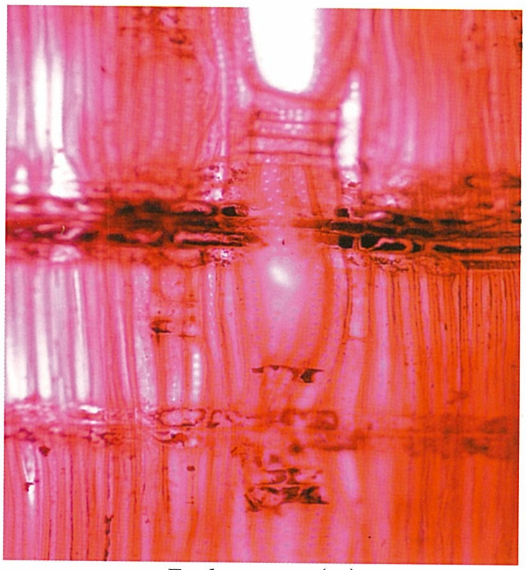

E. cloeziana （*R*）

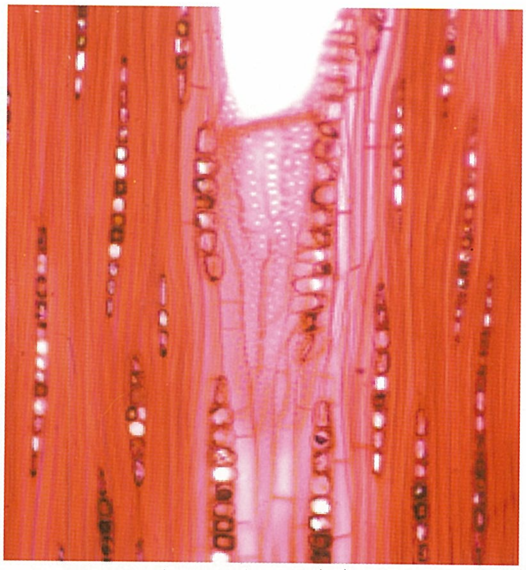

E. urophylla （*T*）

E. cloeziana （*T*）

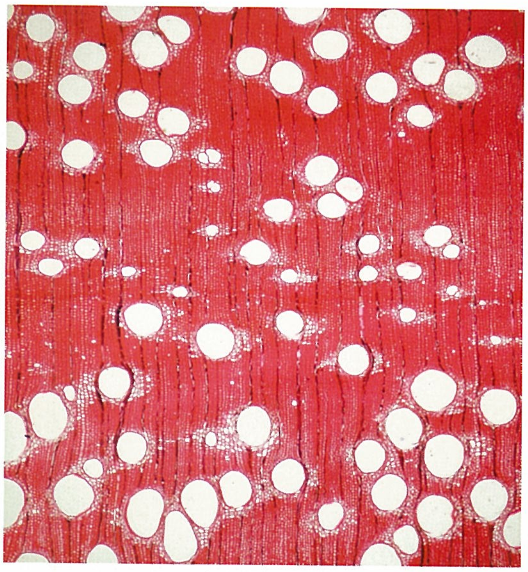

E. pellita (*X*)

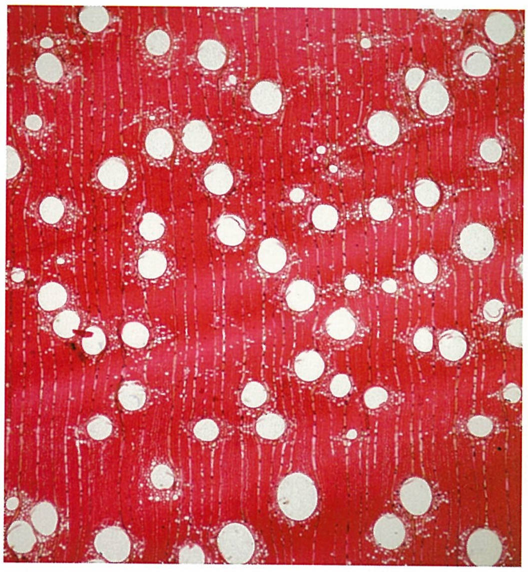

E. Tereticornis (*X*)

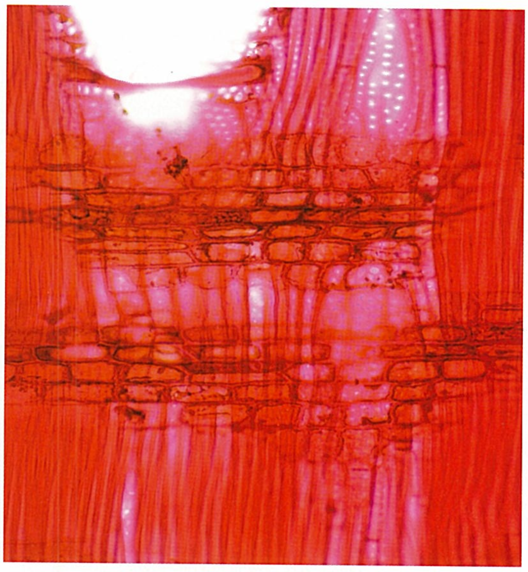

E. pellita (*R*)

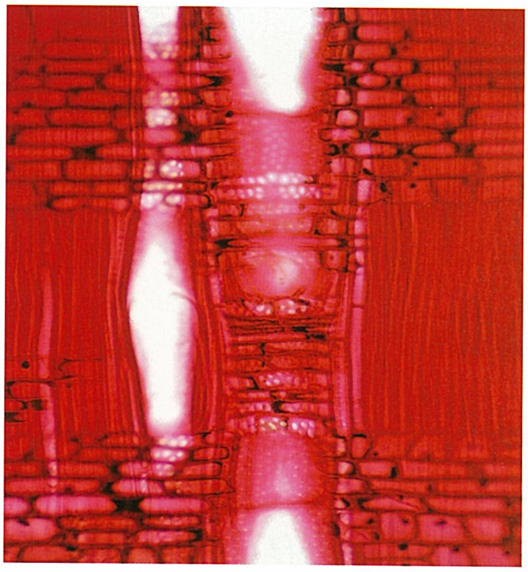

E. Tereticornis (*R*)

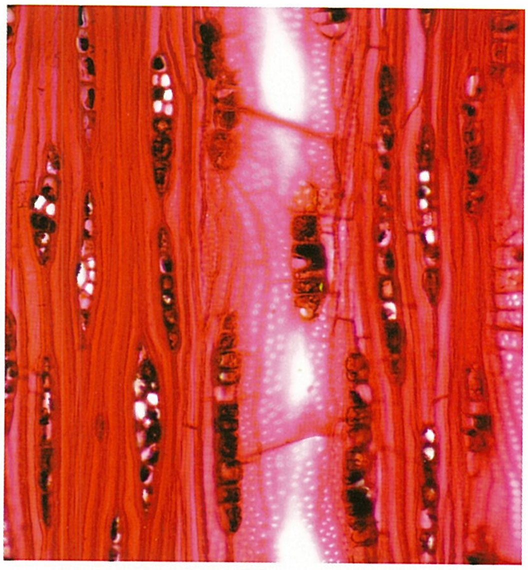

E. pellita (*T*)

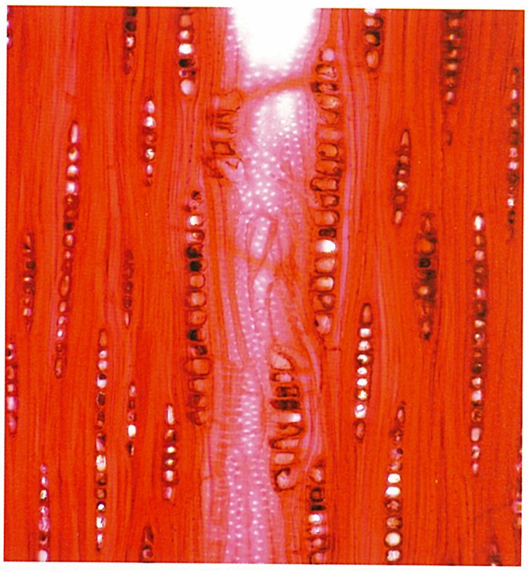

E. Tereticornis (*T*)

Plane V

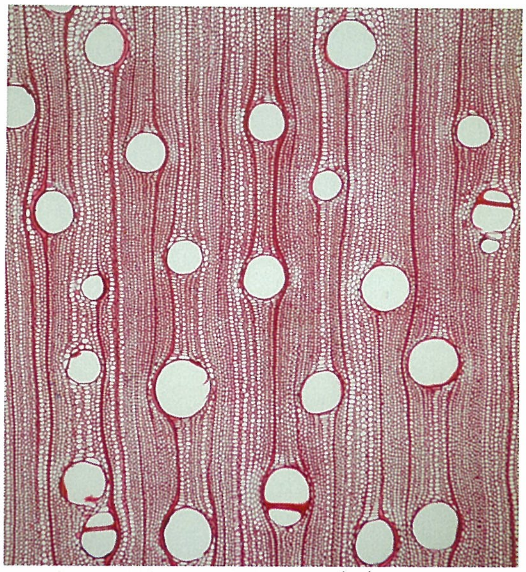

Acacia mangium （*X*）

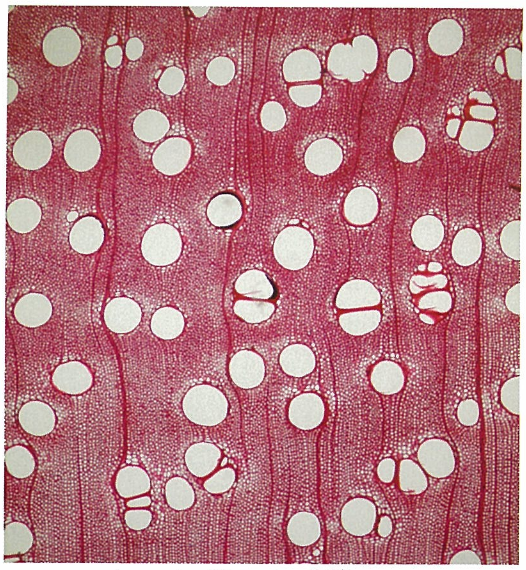

A. auriculiformis （*X*）

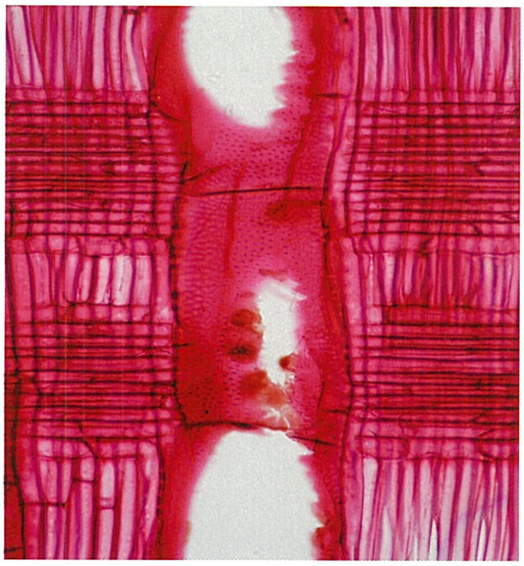

Acacia mangium （*R*）

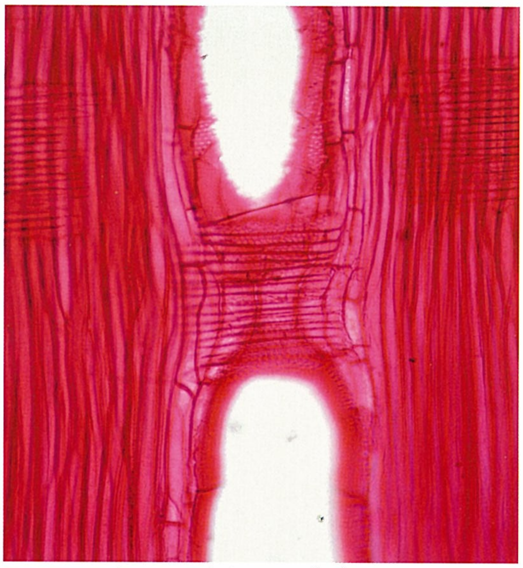

A. auriculiformis （*R*）

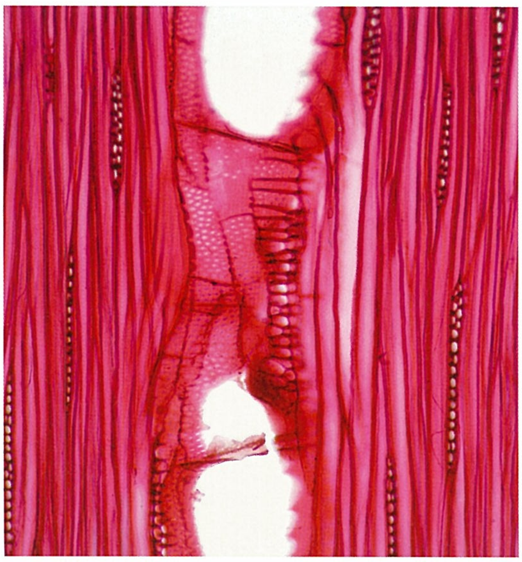

Acacia mangium （*T*）

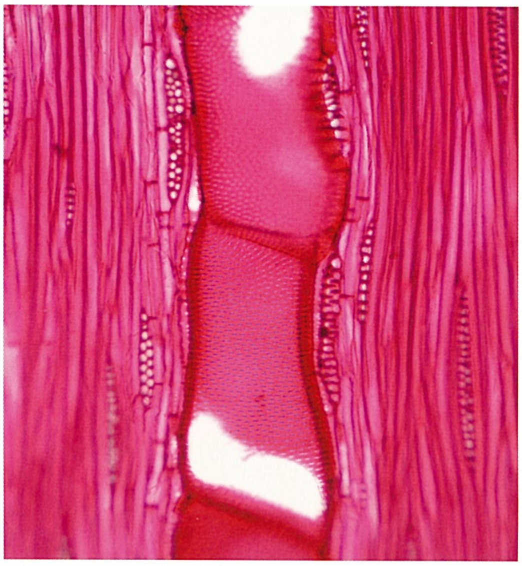

A. auriculiformis （*T*）

Project Leader: Ye Kelin, Professor, Director of CRIWI
Project Technical Leader: Jiang Xiaomei, Professor
Lu Jianxiong, Professor

Executing Agency: Research Institute of Wood Industry
Chinese Academy of Forestry
Wan Shou Shan, Beijing, 100091
P. R. China
Tel.: 86-10-62888843
Fax: 86-10-62881937
E-mail: xiaomei@forestry.ac.cn